Throughput Models and Performance Evaluation for Multi-Deep Automated Storage Systems

Zur Erlangung des akademischen Grades eines

Doktors der Ingenieurwissenschaften (Dr.-Ing.)

von der KIT-Fakultät für Maschinenbau des
Karlsruher Instituts für Technologie (KIT)

genehmigte

DISSERTATION

von

M.Sc. Timo Lehmann
geb. in Achern

Tag der mündlichen Prüfung:	14.11.2024
Hauptreferent:	Prof. Dr.-Ing. Kai Furmans
Korreferent:	Prof. Dr.Ir. René de Koster

Kurzfassung

Automatisierte Lagersysteme werden als einfach- oder mehrfachtiefe Lagersysteme in der Industrie eingesetzt. In mehrfachtiefen Lagersystemen werden mehrere Ladungsträger hintereinander in einem Lagerkanal oder übereinander in einem Stapel gelagert. Dadurch kann im Vergleich zu einfachtiefen Lagersystemen ein höherer Raumnutzungsgrad erreicht werden. Die Lastaufnahmemittel können jedoch auch nicht auf alle Ladungsträger direkt zugreifen und blockierende Ladungsträger müssen umgelagert werden. Der Vorteil des höheren Raumnutzungsgrads steht dadurch dem Nachteil benötigter Umlagerungen gegenüber.

Für die Planung neuer mehrfachtiefer Lagersysteme muss der erreichbare Durchsatz während des Betriebs abgeschätzt werden, um die Lagersysteme richtig auslegen zu können. Der Durchsatz hängt von der Betriebsstrategie ab, welche wiederrum aus den folgenden fünf Lagerpolitiken besteht: Kanalstrukturpolitik, Lagerplatzvergabepolitik, Umlagerpolitik, Lagergutauswahlpolitik und Bewegungspolitik des Regalbediengeräts bzw. Roboters. Diese Thesis präsentiert analytische Modelle zur Berechnung des Durchsatzes für mehrfachtiefe automatische Hochregallager und roboterbasierte Lagersysteme für insgesamt 13 verschiedene Betriebsstrategien. Die 13 Betriebsstrategien werden analysiert, um einerseits am Markt befindliche Lagersysteme und deren Betriebsstrategien abbilden zu können und andererseits Betriebsstrategien zu identifizieren, die einen möglichst hohen Durchsatz ermöglichen. Dadurch kann die Effizienz mehrfachtiefer Lagersysteme gesteigert werden. Bei der Erstellung der Modelle wird von einem Gleichgewichtszustand im Lager ausgegangen, bei dem es gleich viele Ein- wie Auslagerungen gibt. Dadurch wird ein Systemzustand erreicht, der repräsentativ für den Betrieb in der Praxis ist.

Acht Betriebsstrategien basieren auf der Annahme, dass es nur homogene Produkte gibt, die alle die gleiche Zugriffswahrscheinlichkeit haben. Fünf weitere Betriebsstrategien basieren auf der Annahme heterogener Produkte. Heterogene Produkte unterschieden sich in ihren Zugriffswahrscheinlichkeiten und der Anzahl gelagerter Ladungsträger im Lagersystem. Der Gleichgewichtszustand in den Lagersystemen wird mithilfe von Markov Ketten bestimmt und der Durchsatz der Lagersysteme wird durch geschlossene Wartesystemnetzwerk berechnet.

Die analytischen Modelle werden per Simulation validiert und weisen weniger als $3\,\%$ Abweichung zwischen analytischen Modellen und Simulation auf. Für die validierten Modelle wird eine Vergleichsstudie durchgeführt, um bewerten zu können, welche Druchsätze mit verschiedenen Lagerparametern erzielt werden. Dadurch kann bestimmt werden, welche Betriebsstrategien die höchsten Durchsätze erreichen. Der Vergleich der Betriebsstrategien zeigt, dass die Nutzung der Informationen heterogener Produkte verglichen zur Nutzung homogener Produkte zu signifikant höheren Durchsätzen führt. Dabei führt insbesondere eine klassenbasierte Lagerplatzvergabepolitik zu den höchsten Durchsätzen aller Betriebsstrategien.

Abstract

Automated storage systems are available as single-deep or multiple-deep storage systems. In multi-deep storage systems, several unit loads are stored behind each other in a storage channel or on top of each other in a stack. This leads to a higher space utilisation compared to single-deep storage systems. However, load handling devices cannot access all unit loads directly, and blocking unit loads must be reshuffled. The advantage of the higher space utilisation is thus offset by the disadvantage of the need for reshuffles.

When planning new multi-deep storage systems, the throughput during operation must be estimated in order to design the storage systems. The throughput depends on the operating strategy, which consists of the following five policies: allocation structure policy, storage assignment policy, reshuffle policy, retrieval unit load selection policy, and movement policy of the load handling device. This thesis presents analytical models to calculate the throughput for multi-deep automated storage and retrieval and robotic compact storage and retrieval systems for a total of 13 different operating strategies. The 13 operating strategies are analysed to be able to map storage systems on the market and their operating strategies on the one hand and to identify operating strategies that enable high throughput capacities on the other. This can increase the efficiency of multi-deep storage systems. When creating the models, a steady state is assumed in the storage system in which there are the same number of storage and retrieval jobs. This achieves a system state that is representative of operation in practice.

Eight of these operating strategies are based on the assumption that there are only homogeneous products that all have the same access frequency. Five further

operating strategies are based on the assumption that there are heterogeneous products. Heterogeneous products differ in their access frequencies and the number of stored unit loads in the storage system. The steady state in the storage systems is determined using Markov chains, and the throughput of the storage systems is calculated using closed queuing networks.

The analytical models are validated by simulation and show less than $3\,\%$ deviation between analytical models and simulation. A comparative study is performed for the validated models to evaluate which throughput capacities can be achieved for different storage system parameters. This makes it possible to determine which operating strategies achieve the highest throughput. The comparison of operating strategies shows that the utilisation of information from heterogeneous products leads to significantly higher throughput compared to the utilisation of homogeneous products. In particular, a class-based storage assignment policy leads to the highest throughput of all operating strategies.

Contents

1 Introduction and Overview

The e-commerce market was growing in the last decades and is expected to grow further in the coming years (Insider Intelligence and eMarketer 2024). The switch to e-commerce makes it necessary for producers to build their own warehouses and fulfilment centres. These warehouses can be operated by manual labour or work with automated storage systems which are operated by automatic load handling devices and manual labour is reduced. Therefore, also the market for automated storage systems is increasing and is expected to continue to grow in the next years as well (Interact Analysis 2023). Research in the field of warehouse automation can contribute to more cost and resource efficient operation of warehouses and storage systems.

Automated storage systems were introduced in the 1960s and are further developed ever since (Günthner and Heptner 2007). Multi-deep automated storage systems are one field of interest of manufacturers and warehouse operators. They yield significant advantages over single-deep storage systems: Several unit loads are stored behind or above each other in a storage channel to increase the space efficiency for multi-deep systems compared to single-deep systems. Another advantage is that fewer material handling devices are needed to operate multi-deep storage systems.

There are many different versions of multi-deep storage systems on the market ranging from multi-deep automated storage and retrieval (AS/R) systems over multi-deep autonomous vehicle based storage and retrieval (AVS/R) systems, flow rack systems and puzzle based systems to robotic compact storage and retrieval (RCS/R) systems (see Azadeh et al. (2019) for an overview of these systems).

The basic functionality of all these systems is the same. The storage systems have a certain storage capacity for unit loads which can be stored and retrieved. Load handling devices are used to transport requested unit loads from the storage location of a unit load to a handover point with other processes outside of the storage system (the handover point is also called input/output point for AS/R systems and pick station for RCS/R systems). From this handover point, the load handling devices also bring unit loads into the system and transport them to a storage location where they remain until requested again. These retrieval and storage jobs are executed within a command cycle of the load handling device. Multi-deep storage systems have in common that multiple unit loads are stored behind or above each other, denying direct access to some of the unit loads. Blocking unit loads must hence be reshuffled during a command cycle.

When a new multi-deep storage system is planned, storage planners rely on the calculation rules given in guidelines such as the VDI 4480 (Verein Deutscher Ingenieure 2002) and FEM 9.851 (Federation Europeenne de la Manutention 2003) or one of the many throughput models in the literature for multi-deep storage systems (the most important works can be found in Chapter 3) to estimate the throughput capacity of a planned storage system to comply with customer requirements. If suitable guidelines or analytic models are not available, storage planners rely on experience values or time-consuming and cost-intensive simulation. The throughput capacity depends on several influence factors, such as the layout of the storage system and implemented operating strategies. Operating strategies include the allocation structure policy, the storage assignment policy, the reshuffle policy, the retrieval unit load selection policy, and the movement policy.

The guidelines and literature mentioned cover only some of the operating strategies applied in the industry. There are throughput models for two types of unit loads because the available information about the products varies depending on the customer and is given in the design phase. Either there is no information concerning the product variety available and all products and unit loads are assumed to be unique, making them homogeneous unit loads (e.g. when a company

starts e-commerce and has no sales data available) or there is information concerning the access frequency and number of unit loads per product stored in the storage system available (e.g. when a new storage system is planned to merge several smaller storage systems). For example, this additional information can be exploited by the storage planners by applying class-based storage to reduce the number of reshuffles during retrieval which leads to higher throughput capacity.

Many of the operating strategies in the industry are not reflected in analytic models in the literature. Additionally, there exist numerous untested operating strategies that could potentially increase the throughput of a given AS/R or RCS/R system. This work extends the selection of throughput models for multi-deep storage systems by presenting analytical models for operating strategies for both homogeneous and heterogeneous unit loads for AS/R and RCS/R systems. These analytical models include operating strategies in application in the industry as well as new and untested operating strategies. Furthermore, this work validates the analytic models and presents a comparison and evaluation of all developed analytic throughput models. In the following, the research questions are defined and the scope of the thesis is laid out.

1.1 Problem Description and Research Questions

The research presented in this thesis is divided into three parts. The underlying research topics of these parts and related research questions are explained in the following.

Part 1: Throughput models for operating strategies assuming homogeneous unit loads

The literature offers many different throughput models for operating strategies assuming homogeneous unit loads for AS/R and RCS/R systems. However,

especially for multi-deep AS/R and RCS/R systems with reshuffles, the available throughput models have shortcomings. Common assumptions are that no reshuffles are necessary or that the system is completely full, which simplifies the calculation of necessary reshuffles. Another assumption is that the system is regarded right after the initial filling and not during a steady state during operation. In summary, it is necessary to develop application-oriented throughput models that accurately reproduce the operating strategies used in industry. The question arises how throughput models can be derived which model the storage systems during operation and enable an accurate throughput estimation.

> **Research Question 1: Assuming homogeneous unit loads, how can the throughput capacity be analytically estimated for AS/R and RCS/R systems?**

Related questions are:

- Which modelling techniques can be applied to represent the steady state of multi-deep AS/R and RCS/R systems?
- How can the cycle time and number of reshuffles per cycle be calculated in a steady state of the regarded systems?

Part 2: Throughput models for operating strategies assuming heterogeneous unit loads

Operating strategies which differentiate unit loads have the potential to significantly decrease the cycle time and increase the throughput capacity for multi-deep AS/R and RCS/R systems. However, storage assignment and retrieval unit load selection policies such as class-based storage or smart retrieval are only sparsely covered in the literature and the throughput capacity for common industry applications such as AutoStore cannot be evaluated analytically (AutoStore 2024). Furthermore, there are promising, yet untested operating strategies which could potentially improve the throughput for a given AS/R or RCS/R system for which no analytic model exists yet.

Research Question 2: Assuming heterogeneous unit loads, how can the throughput capacity be analytically estimated for AS/R and RCS/R systems?

Related questions are:

- How does the original AutoStore operating strategy perform compared to other operating strategies?
- How can a class-based storage assignment policy be analytically implemented where several classes can be stored in the same storage channel?
- Which RCS/R system layout maximises the throughput capacity for a given storage capacity?

Part 3: Operating Strategy comparison and evaluation
Storage planners have a variety of operating strategies to choose from for new storage systems. Therefore, it is important to know which operating strategies yield high throughput capacities for which storage system parameters. The identification of dominant operating strategies for homogeneous or heterogeneous unit loads is beneficial for storage planners and customers. Comparisons of existing operating strategies are hardly regarded in the literature, and for untested operating strategies there are no comparisons at all.

Research Question 3: How does the throughput capacity change for different AS/R and RCS/R system parameters when different operating strategies are applied?

Related questions are:

- Which AS/R or RCS/R parameters are beneficial for homogeneous and heterogeneous throughput models?
- Do operating strategies exist that yield superior throughput capacity?
- Which operating strategies minimise the number of reshuffles per retrieval??

1.2 Structure and Scope of this Thesis

This thesis aims to answer the previously defined research questions and mainly refers to three publications by the author of this thesis. The first is published in the *Logistics Journal* with the title "Travel time model for multi-deep automated storage and retrieval system with a homogeneous allocation structure" (Lehmann and Hussmann 2021), the second is published in the *International Journal of Production Research* with the title "Travel time model for multi-deep automated storage and retrieval systems with different storage strategies" (Lehmann and Hussmann 2023), and the third is currently under revision in *Transportation Science* with the title "Digging Deep: Finding and Maximizing the Throughput Capacity of Multi-deep Storage Systems" (Lehmann and De Koster 2024). The sections taken from each of these publications are marked and explained in the remainder of this work with grey boxes at the beginning of the corresponding sections.

This thesis starts in Chapter 2 with a presentation of the components and operating principles of AS/R (Section 2.1) and RCS/R (Section 2.2) systems, which are the two systems that are regarded in this work. This also includes the definition of command cycles and an introduction of the variables to be calculated for the cycle time t_{cycle}. Furthermore, different operating strategies, including various allocation structure policies, storage assignment policies, reshuffle policies, retrieval unit load selection policies, and movement policies are explained in Section 2.3.

The available literature for throughput capacity calculation for both multi-deep AS/R and RCS/R systems and similar multi-deep storage systems is presented in Chapter 3. Chapter 3 is split into three sections: First, Section 3.1 presents a chronological order of throughput models and focuses on the assumptions made for the models. Second, Section 3.2 analyses the policies used in the literature in more detail. Furthermore, in Section 3.3 the research gaps for all three research questions are elaborated and the operating strategies derived in this dissertation are introduced.

Chapter 4 contains the analytic derivation of throughput models for seven different operating strategies for multi-deep AS/R systems based on the assumption that only information for homogeneous unit loads is available for throughput modelling. Chapter 4 presents a common approach for throughput calculation and introduces five new operating strategies in the Sections 4.1, 4.3 and 4.5 to 4.7. Furthermore, the implementation of assumptions for two more operating strategies is improved in Sections 4.2 and 4.4. The analytic models are validated with simulation in Section 4.8.

Chapter 5 contains the analytic derivation of throughput models for six different operating strategies focusing on RCS/R systems and also multi-deep AS/R systems. It is assumed that information for heterogeneous unit loads is available for these models. Section 5.1 introduces two new class-based storage approaches, implements the original AutoStore operating strategy as well as one improvement of it and one class-based benchmark strategy from the literature. Furthermore, one new strategy for homogeneous unit loads is introduced. The six new models are validated with simulation in Section 5.2 and compared in Section 5.3. This is also done based on industry data. Section 5.4 focuses on the performance of the AutoStore strategy and in Section 5.5 it is shown how all 13 operating strategies can be applied for both multi-deep AS/R and RCS/R systems.

Chapter 6 contains the comparison and evaluation of the 13 presented operating strategies for both multi-deep AS/R and RCS/R systems. This section introduces the design of experiments in Section 6.1. Selected results for a full factorial design of experiments are discussed in Sections 6.2 and 6.3, and Section 6.4 summarises managerial insights and discusses the model limitations. The complete results for the experiments are presented in Appendix A.10

In summary, the research question 1 is mainly addressed in Chapter 4, research question 2 is addressed in Chapter 5, and the research question 3 is mainly answered in Chapter 6. Finally, Chapter 7 concludes this thesis with a summary of

the throughput models, results, and answers to the three research questions (see Section 7.1). Section 7.2 closes this dissertation with an outlook for future work.

2 Basics of multi-deep Storage Systems

In this chapter, the functionality and components of multi-deep AS/R (see Section 2.1) and RCS/R systems (see Section 2.2) are introduced. Furthermore, it is explained how command cycles are executed in the respective systems. Section 2.3 introduces the allocation structure policies, storage assignment policies, reshuffle policies, retrieval unit load selection policies, and movement policies.

2.1 Operating Principle of Automated Storage and Retrieval Systems

This section is cited from the section "Basics of travel time calculation" of the paper "Travel time model for multi-deep automated storage and retrieval systems with different storage strategies" published in the *International Journal of Production Research* (Lehmann and Hussmann 2023).

The text and visualisation in this section have been taken from the paper with changes of technical terms, numbering of figures and sections, and symbols. Furthermore, the language has been improved.

The author of this thesis was responsible for the conceptualisation, methodology, writing (original draft and review), and visualisation of the research presented in this section.

The throughput models developed in this work are suitable for the following AS/R system configuration, as sketched in Figure 2.1. To keep the components of the models simple, only one aisle of an AS/R system with one rack on one side of the aisle is considered. Furthermore, the input/output point (I/O point) is located at the lower left point of the single rack. The rack consists of L storage channels in

the x-direction and W storage channels in the y-direction. Every storage channel has H storage locations, which are organised in storage lanes in z-direction. E.g. a double-deep AS/R system ($H = 2$) has two storage lanes of which the first lane is the storage lane at the wall and the second lane is the storage lane close to the aisle. Besides the AS/R system itself, the storage and retrieval machine - S/R machine - is the second important component. It can serve the whole rack and is able to move in x- and y-direction simultaneously. Furthermore, it can only transport a single unit load at the same time. Furthermore, the S/R machine is either equipped with a telescopic arm (for AS/R systems with low H) or a satellite vehicle (for AS/R systems with high H).

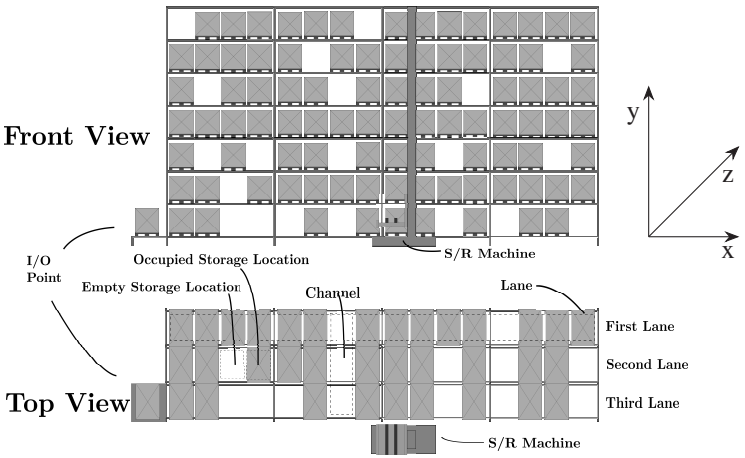

Figure 2.1: View from the Front and Top on a Rack in a triple-deep AS/R System (Lehmann and Hussmann 2022)

For such an AS/R system configuration as shown in Figure 2.1, storage and retrieval jobs can be executed in single or dual command cycles that require the cycle time t_{cycle}. In a single command storage cycle, the S/R machine picks the unit load at the I/O point (taking deterministic time t_h), drives to the storage channel (taking expected time t_{toS}), performs a channel drive to the storage location (taking expected time $t_{Ch,S}$), stores the unit load into the storage location (taking

deterministic time t_h) and moves back to the I/O point (taking expected times $t_{Ch,S}$ and t_{toHP}). For one operating strategy presented in this thesis (introduced in detail in Section 4.1), a reshuffle job can be necessary before the described storage job can be executed (taking expected time t_β). A single command retrieval cycle works analogue, but in case that the unit load is blocked by other unit loads, the blocking unit loads must be reshuffles first. For a reshuffle, a S/R machine picks the blocking unit load (taking expected time $t_{Ch,R,\beta}$ and deterministic time t_h), moves to a storage channel (taking expected time $t_{\text{Rto}\beta}$) and moves in the storage channel to a storage location (taking expected time $t_{Ch,S,\beta}$), drops the load (taking deterministic time t_h) and moves back to the original storage channel (taking expected times $t_{Ch,S,\beta}$ and $t_{\text{Rto}\beta}$). This procedure is repeated until all blocking unit loads are reshuffles.

To spare some S/R machine movements, after a storage job a retrieval job can be executed directly. The S/R machine drives from the storage channel to the retrieval channel (taking expected time t_{StoR}) without returning to the I/O point, which results in a dual command cycle.

2.2 Operating Principle of Robotic Compact Storage and Retrieval Systems

This section is cited from the section "Robotic Compact Storage and Retrieval System" of the paper "Digging Deep: Finding and Maximizing the Throughput Capacity of Multi-deep Storage Systems" currently under revision in *Transportation Science* (Lehmann and De Koster 2024).

The text and visualisation in this section have been taken from the paper with changes of technical terms and numbering of tables and sections.

The author of this thesis was responsible for the conceptualisation, methodology, writing (original draft), and visualisation of the research presented in this section.

Robotic compact storage and retrieval systems consist of a three-dimensional grid structure in which cuboid bins (unit loads) are stacked on top of each other.

Robots traverse the grid and are responsible for both storage and retrieval jobs (Figure 2.2a). Storage locations can be categorised as occupied (indicating that a unit load is stored in this location), free (no unit load is stored but the location below is occupied), or unavailable (neither a unit load in this location nor an occupied location below exists). The grid has a rectangular base with L channels in the x-direction and W channels in the y-direction. Each channel has H locations in the z-direction (Figure 2.2b). Each unit load contains one or several items of a product and a product may have multiple unit loads stored within the rack. In total, the rack accommodates $L \cdot W \cdot H \cdot \omega$ unit loads, with $\omega \in [0, 1]$ representing the stock filling level. Of the H storage locations in any given channel, $h \in \{0, ..., H\}$ locations can be occupied in an individual storage channel. Each stored unit load can be of a different class $j \in \{1, ..., J\}$ (classes are labelled alphabetically in this work). A channel with h unit loads corresponding to class-storage pattern $k \in \{1, ..., J^h\}$ is said to have channel type $c_{h,k}$ (Table 2.1 gives an example of channel types for $h = 2$ and $J = 3$). J^h is the number of channel types in a channel with h unit loads, where J^h is the size of the Cartesian product $Classes^h$ with either $J = 1$ and $Classes = \{\mathrm{A}\}$ or $J = 3$ and $Classes = \{\mathrm{A}, \mathrm{B}, \mathrm{C}\}$, depending on the operating strategies. A storage location t in a channel type $c_{h,k}$ with $t \leq h$ is denoted as $c_{h,k,t}$.

Table 2.1: All Channel Types with two Unit Loads $h = 2$ in RCS/R Systems.

Channel Type $c_{h,k}$	$c_{2,1}$	$c_{2,2}$	$c_{2,3}$	$c_{2,4}$	$c_{2,5}$	$c_{2,6}$	$c_{2,7}$	$c_{2,8}$	$c_{2,9}$
Top Unit Load	A	B	C	A	B	C	A	B	C
Bottom Unit Load	A	A	A	B	B	B	C	C	C

The robots transport unit loads to pick stations, located at the bottom of the centre of the longer side of the rectangular base of the grid (it can be shown that this is the optimal location in terms of maximal throughput capacity in case of one pick station per side, see proof in Appendix A.1). Multiple pick stations per long side of the rack are located adjacent to each other at the centre of the rack. Robots

(a) RCS/R System Application (AM Logistics Solutions 2024).

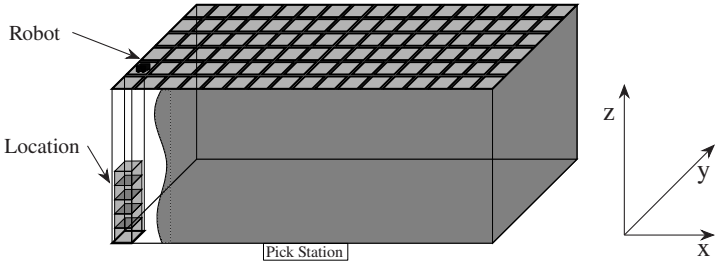

(b) Schematic View of an RCS/R System.

Figure 2.2: Application Example and Schematic View of an RCS/R System.

can move in four directions at each grid cell, adhering to a Manhattan metric. They pick up and deposit unit loads using a vertical lift mechanism integrated in their structure. Upon reaching its designated pick station and after possible queuing for preceding robots, a robot deposits its unit load into the pick station buffer and picks up a finished unit load for storage. Robots can be shared between pick stations or exclusively assigned to stations. At each pick station, an operator extracts the required quantity from the unit load and adds it to the designated customer order bins. The station can also be used to replenish inventory and add items to unit loads. After picking, the finished unit load shifts to the outbound buffer of the pick station, where it awaits the next robot to pick it up and transport it to a new storage location. Robots operate in dual command cycles, comprising the following steps. Upon completing these steps, the robot dwells at the final channel and waits for the next job.

1. To retrieve a unit load with a specific product for picking at a specific pick station, the robot drives across the grid to reach the channel (called retrieval channel) where a unit load of the requested product is stored (taking expected time t_{StoR}). If the robot must change direction on the grid, it takes additional time t_{turn}. Retrieval unit load selection policies are described in Section 2.3.4.

2. If the selected unit load is blocked, one or multiple reshuffles are necessary (taking expected time t_{β} for each blocking and reshuffled unit load). The execution of a reshuffle depends on the chosen reshuffle policy (see Section 2.3.3). The robot retrieves the blocking unit loads and either (a) places them on top of the stored unit loads of an adjacent channel (called reshuffle channels) and brings the blocking unit loads back (following a LOFI policy), after temporarily buffering the requested unit load in an adjacent channel. Or (b), relocates the blocking unit loads to any other channels like a storage job. For every retrieval or storage of unit loads, the robot takes a deterministic handling time t_h.

3. The robot retrieves the unit load (taking handling time t_h). and transports it to the designated pick station (taking expected time t_{toHP}). If the robot must change direction on the grid, it takes additional time t_{turn}.

4. The robot dwells at the pick station until all other waiting robots in front of the pick station have completed their tasks (taking time t_{wait}) and then lowers its unit load to the pick station buffer (taking handling time t_h).

5. The robot retrieves a finished unit load from the pick station for storage (taking time t_h).

6. The robot moves to the specified storage channel (taking expected time t_{toS}). If it must change direction on the grid, it takes additional time t_{turn}. The robot deposits the unit load on top of the existing stack within that channel (taking handling time t_h). The possible storage assignment policies and channel selection criteria are described in Section 2.3.2.

Additionally, every time a robot retrieves or stores a unit load, its lifting device performs a vertical movement to reach to location of the unit load. This can either occur during a storage ($t_{Ch,S}$), retrieval ($t_{Ch,R}$), or reshuffle job ($t_{Ch,R,\beta}$ at the retrieval channel and $t_{Ch,S,\beta}$ at the reshuffle channel).

2.3 Operating Strategies and Policies for multi-deep Storage Systems

Many different operating strategies for AS/R and RCS/R systems can be observed in the industry. In this work, the combination of five policies to operating strategies are considered and Table 2.2 provides an overview of all policies regarded in this thesis:

- **Allocation structure policies (see Section 2.3.1):** These policies describe how unit loads are allowed to be allocated within a storage channel.
- **Storage assignment policies (see Section 2.3.2):** These policies determine which storage location is selected for the next storage job.
- **Reshuffle policies (see Section 2.3.3):** These policies determine how reshuffles are organised when unit loads are blocking.
- **Retrieval unit load selection policies (see Section 2.3.4):** These policies determine which unit load is selected for retrieval if several unit loads of the same product are stored in the storage system.
- **Movement policies (see Section 2.3.5):** These policies determine which channel is chosen for a storage or retrieval job if two channels with the same channel type exist in the storage system.

Table 2.2: Overview of all Policies regarded in this Thesis.

Allocation Structure Policies	Homogeneous, Stack
Storage Assignment Policies	Random Storage Channel, Random Storage Location, Depth First, Stack First, Class-based Random Storage (CBRS), Class-based Storage with one Class per Channel (CBS-1), Class-based Storage with three Classes per Channel (CBS-3)
Reshuffle Policies	Homogeneous, Random Storage Channel, Random Storage Location, Depth First, Stack First, Bring-back to original Channel (BBO), Relocate-to-Best-Position (RBP)
Retrieval Unit Load Selection Policies	Random, Unit Load with Fewest Reshuffles (LFR)
Movement Policies	Random, Nearest Neighbour

2.3.1 Allocation Structure Policies

An allocation structure policy describes the allowed allocation of unit loads in a single channel. Unit loads can either be stored directly behind each other (called *stack allocation structure* (Lehmann and Hussmann 2021)) or there can be gaps between two unit loads (called *homogeneous allocation structure* (Lippolt 2003)). Figure 2.3 shows possible storage channel types with both allocation structures for a triple-deep AS/R system ($H = 3$). Both allocation structures are feasible for AS/R systems where the telescopic arm of the S/R machine can either push every new unit load back to the back wall of the rack or leave gaps. However, only the stack allocation structure is feasible for RCS/R systems due to gravity.

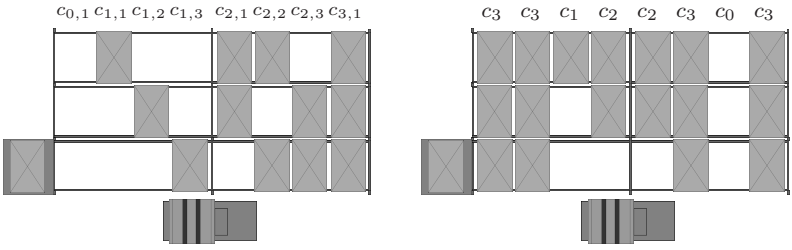

(a) Homogeneous Allocation Structure. **(b)** Stack Allocation Structure.

Figure 2.3: Possible Storage Allocation Structures for one Class ($J = 1$).

The two allocation structures can have different channel types $c_{h,k}$. For the homogeneous allocation structure it is assumed that only one class exists with $J = 1$. $k \in \{1, ..., \binom{H}{h}\}$ iterates through the Cartesian product of h unit loads and $H - h$ free storage locations. The channel types $c_{h,k}$ for the stack allocation structure with only one class and $J = 1$ are simplified to c_h. Channel types for the stack allocation structure and multiple classes are already described in Section 2.2. Figures 2.3a and 2.3b shows exemplary the channel types $c_{h,k}$ and c_h for a triple-deep AS/R system and the homogeneous allocation structure and the stack allocation structure.

2.3.2 Storage Assignment Policies

Storage assignment policies determine which channel type and storage location is selected for the next storage job. This section introduces seven storage assignment policies. Four assignment policies are for homogeneous unit loads and three for heterogeneous unit loads.

The *random storage channel policy* selects a channel type randomly of all existing channels in the rack with less than H unit loads stored. The *random storage location policy* selects a channel type randomly out of all channel types based on the number of free storage locations. Channel types with more free storage locations are preferred with the random storage location policy. The *depth first policy* assigns the unit load in the channel type with the fewest number of unit loads stored among all channels in a rack, leading to an evenly levelled rack structure. The *stack first policy* is the opposite of the depth first policy since the channel type with the most unit loads stored (maximal $H - 1$ unit loads stored) is selected for storage, leading to a rack with only two different channel types - either full channels or empty channels.
The other three storage assignment policies are based on a classification of all products (or unit loads) in classes A, B, and C based on the access frequency of the products relative to all other products. The *class-based random storage* (CBRS) policy distinguishes three product turnover classes and multiple channel

The remainder of this section is cited from the section "Storage Assignment Strategies" of the paper "Digging Deep: Finding and Maximizing the Throughput Capacity of Multi-deep Storage Systems" currently under revision in *Transportation Science* (Lehmann and De Koster 2024).
The text, formal analysis and visualisation in this section have been taken from the paper with changes of technical terms and numbering of tables and sections.
The author of this thesis was responsible for the conceptualisation, methodology, writing (original draft), and visualisation of the research presented in this section.

types $c_{h,k}$ (see Table 2.3). Each unit load of every product can be stored in each channel type on each location, and a random channel type is selected for each storage job. CBRS differs from the random storage channel policy, as the latter does not distinguish product classes. With CBRS, class A unit loads are stored with a higher frequency compared to class B and C unit loads, resulting in an increased prevalence of class A unit loads floating atop channels, compared to class B and C unit loads. *Class-based storage with one class per channel* (CBS-1) divides the rack into five zones (Figure 2.4a). Zone A (for class A products) consists of the channels in the middle of the rack with a similar distance to the closest rack side where the pick stations are located (it is assumed stations are located at both the longer rack sides). Two C zones are located near the side of the system with pick stations and two B zones are located between zone A and the C zones (Figure 2.4a). In every zone, only products of the corresponding class can be stored. For storage, a random channel type is selected from all channels in the corresponding zone. Similarly to the random storage channel policy, if there are multiple channels of the chosen channel type, the storage channel with the smallest distance from the subsequent retrieval channel is used for storage[1].

The *class-based storage with three classes per channel* (CBS-3) policy divides each channel into three zones, each corresponding to a distinct storage class (Figure 2.4b). Class C products are stored at the bottom of the rack, class B products in the middle, and class A products reside at the top. Unit loads or products of the same storage class all randomly share the space assigned to the class. While the

[1] The segmentation of the rack in five zones is only applied in RCS/R systems. For AS/R systems there are three zones with zone A being the closest to the I/O point as shown by Hausman et al. (1976).

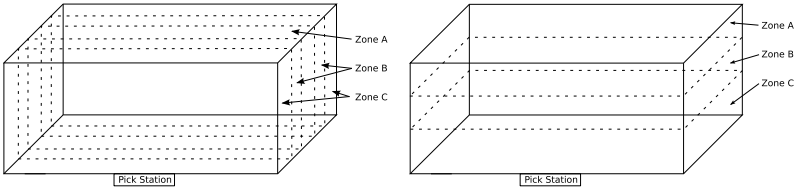

(a) CBS-1 **(b)** CBS-3

Figure 2.4: Schematic View of the Zones A, B, and C in an RCS/R System for the (a) CBS-1 and (b) CBS-3 Storage Assignment Policies.

concept is straightforward, strict segregation of unit loads into these three zones cannot always be maintained during actual operation. For instance, when a class B unit load needs to be stored but all locations in zone B are either occupied or unavailable, it will be stored in either zone C or zone A, resulting in a mix of unit loads of different classes across the three zones. The CBS-3 policy minimises the mixing as follows. To store a class A unit load, first a channel type is selected with a free location $H-1$ closest to the next following retrieval channel. If no such channel type exists, a channel type is chosen with a free $H-2$ location. If no such channel type exists, continue until one free $H-n$ location is found, prioritising channel types with higher levels h. To store a class C unit load, first a completely empty storage channel type is selected. If no such channel exists, a channel type is selected with a free second location. If no such channel exists, continue until one free n^{th} location is found, prioritising channel types with lower levels h. Class B works similarly to class C, but starts from the lowest location in zone B.

If several suitable channel types are available in the rack, the channel type with the highest priority is selected for the CBS-3 policy. Priorities are assigned in decreasing lexicographic order of the Cartesian product. Table 2.3 shows the storage priorities of channel types with two unit loads ($h=2$) and at least one free location on top of these unit loads. In this example, channel type $c_{2,9}$ is selected for storage for all three classes and only if such a channel type is not available, then a channel type $c_{2,8}$ is selected. If several free locations have the same priority, the channel with the smallest distance to the next retrieval channel, if known, is selected. Note that during a storage job, it is not essential to store

the unit load above a unit load of the same product. That means chaotic storage is preferred over clustering of unit loads of the same product. In Appendix A.2, it is shown that chaotic storage indeed leads to fewer expected reshuffles.

Table 2.3: Priorities for all Channel Types with two Unit Loads $h = 2$ in AS/R and RCS/R systems.

Channel Type $c_{h,k}$	$c_{2,1}$	$c_{2,2}$	$c_{2,3}$	$c_{2,4}$	$c_{2,5}$	$c_{2,6}$	$c_{2,7}$	$c_{2,8}$	$c_{2,9}$
Front/Top Unit Load	A	B	C	A	B	C	A	B	C
Back/Bottom Unit Load	A	A	A	B	B	B	C	C	C
Priority	9^{th}	8^{th}	7^{th}	6^{th}	5^{th}	4^{th}	3^{rd}	2^{nd}	1^{st}

2.3.3 Reshuffling Policies

Reshuffle policies determine how reshuffles work if the retrieval unit load is blocked by other unit loads and which channel type is selected for reshuffle (called reshuffle channel). The *random storage channel, random storage location, depth first* and *stack first policies* assume that every blocking unit load is a new storage unit load and a reshuffle job is like a storage job with a different starting and end. The *homogeneous reshuffle policy* aims at keeping all but one channel in the same channel type. This is achieved by choosing specific reshuffle channels for each reshuffle job. A detailed explanation of this procedure can be found in Section 4.1.3.

The remainder of this section is cited from the section “Reshuffle Strategies” of the paper “Digging Deep: Finding and Maximizing the Throughput Capacity of Multi-deep Storage Systems” currently under revision in *Transportation Science* (Lehmann and De Koster 2024).
The text in this section has been taken from the paper with changes of technical terms.
The author of this thesis was responsible for the conceptualisation, methodology, and writing (original draft) of the research presented in this section.

When selecting the channel to store a reshuffled unit load, the *random reshuffle* policy works like the random storage channel policy. The *bring-back to original channel* (BBO) policy is based on the reshuffle jobs in real AutoStore systems

as described by Meller (2023), while the *relocate-to-best position* (RBP) policy is based on the reshuffle policy used in some real AS/R systems. When a unit load must be reshuffled using the BBO policy, the unit load is transported to the closest channel with a free location at $H-1$. If no such channel exists, the closest channel with a free $H-2$ location is chosen. The unit load is buffered here until the requested unit load is retrieved from the retrieval channel, which is also temporarily stored in such a buffer location. Then, the robot moves the reshuffled unit loads back to the retrieval channel in a *Last out, First in* (LOFI) order. It then picks up the retrieval unit load and moves it to the designated pick station. Using the RBP policy, blocking unit loads are reshuffled and relocated to the storage location, following the same rules as for the CBS-3 storage policy.

2.3.4 Retrieval Unit Load Selection Policies

This section is cited from the section "Retrieval Strategies" of the paper "Digging Deep: Finding and Maximizing the Throughput Capacity of Multi-deep Storage Systems" currently under revision in *Transportation Science* (Lehmann and De Koster 2024).
The text in this section has been taken from the paper with changes of technical terms.
The author of this thesis was responsible for the conceptualisation, methodology, and writing (original draft) of the research presented in this section.

The *random retrieval* policy randomly chooses a unit load among all stored unit loads of the requested product (taking class-based access frequencies into account if class-based storage is applied). The *unit load with the fewest reshuffles retrieval* (LFR) policy selects that unit load of a product for retrieval which causes the lowest expected number of reshuffles. The affected channel is called retrieval channel.

2.3.5 Movement Policies

The movement policy describes which channel is used for storage or reshuffle if multiple channels of the same channel type are available in the rack. The *random*

policy chooses one channel of the same channel type randomly while the *nearest neighbour policy* (NN) chooses the channel which minimises the distance between the storage and retrieval channel or between the reshuffle and retrieval channel.

3 Literature Review and Research Gaps

This chapter gives an overview of previous works for operating strategies for AS/R and RCS/R systems and related storage systems. Section 3.1 presents models for calculating the throughput capacity and the cycle time for single-, double- and multi-deep AS/R systems and related storage systems in chronological order. Furthermore, the focus in Section 3.1 is on the assumptions made by some authors for operating principles of regarded storage systems and on operating strategies using homogeneous unit loads. Section 3.2 extends this to RCS/R systems and especially to operating strategies using heterogeneous unit loads and discusses the applied policies from Table 2.2. The accuracy of models in the literature is also analysed. Section 3.3 discusses the research gap in the presented literature and introduces the operating strategies analysed in this dissertation.

3.1 Chronological Literature Review for Throughput Models

This section is cited from the section "Literature review" of the paper "Travel time model for multi-deep automated storage and retrieval systems with different storage strategies" published in the *International Journal of Production Research* (Lehmann and Hussmann 2023).
The text in this section has been taken from the paper with changes of technical terms, tables for consistent style, and symbols. Furthermore, the language has been improved.
The author of this thesis was responsible for the conceptualisation, methodology, and writing (original draft and review) of the research presented in this section.

This literature review does not only focus on AS/R systems but includes different multi-deep storage systems such as AVS/R, flow rack, push-back AS/R or conveyor based AS/R systems (Azadeh et al. 2019). All of these variations can consider - depending on the AS/R system design - the necessity of reshuffles. Hence, the methods to calculate reshuffle probabilities $P(\beta)$ and number of reshuffles β for one variation of AS/R system may be transferred to other AS/R system variations. Furthermore, besides the relevant publication about analytic cycle time models, also some simulation-based publications are presented. However, the focus of this literature research is on analytic cycle time models for multi-deep AS/R systems.

The first cycle time models were developed by Gudehus (1972) and later by Bozer and White (1982) and Bozer and White (1984) for single-deep AS/R systems. They use an AS/R system with one rack, a random storage and retrieval policy, and a continuous pick face to determine the expected average cycle time for a storage or retrieval operation in closed-form expressions. The next step was the extension of this basic model to double-deep AS/R systems by Lippolt (2003), who provided an exact reshuffle probability depending on the stock filling level ω, assuming random storage assignment and retrieval policies. Lippolt (2003) shows that the reshuffle probability and the number of reshuffles can be expressed in closed-form expression only depending on the number of stored goods compared to the total capacity of the AS/R system. Lerher et al. (2010) also introduce a cycle time model for double-deep AS/R systems, but use implicitly a depth first storage assignment policy. The same principle is applied to the cycle time calculation of double-deep shuttle-based AS/R systems (Lerher 2016).

Following the models for single- and double-deep AS/R systems, cycle time models for multi-deep AS/R systems were developed. There are two categories of related literature available. The first category models the multi-deep AS/R systems with relatively simple assumptions, which eliminate the reshuffle necessity or ensure a constant number of necessary reshuffles independently from the stock filling level. The most basic works available do not regard reshuffles (Verein Deutscher Ingenieure 2002, D'Antonio and Chiabert 2019), or assume that these are not necessary at all due to batching of storage goods (Manzini et al. 2016).

The publication of Manzini et al. (2016) shows that AS/R system variations can be compared with each other. They use an AVS/R system which can be interpreted as several AS/R systems with only one storage channel in y-direction connected with a lift and therefore, the basic mechanisms as reshuffles can be compared and cycle time models can be transferred. Furthermore, several authors assume an AS/R system, which is completely filled, and therefore, whenever a storage good is blocked, the maximal number of reshuffles is required. This way, the calculation of the number of reshuffles depends only on the location of the affected storage good in the storage channel (Federation Europeenne de la Manutention 2003, Xu et al. 2019). Starting with De Koster et al. (2008), a new type of AS/R system was introduced which completes the necessary reshuffles within the rack itself. Therefore, this approach requires different methods to calculate the reshuffle probabilities, which are not useful for this thesis. However, this assumption is widely used as in e.g. Yu and de Koster (2009), Yang et al. (2015) and Yang et al. (2017).

All publications mentioned in the aforementioned first category calculate the cycle times independently from the stock filling level ω. The following second category models include the dependency from ω. Sari et al. (2005) introduce an AS/R system in which one S/R machine fills the racks and another S/R machine retrieves storage goods from the other side of the rack. Reshuffles are realised via a separate conveyor belt. Based on the stock filling level, they determine the reshuffle probability, however Sari et al. (2005) also assume a depth first storage assignment policy, which leads to a different reshuffle probability for double-deep AS/R systems compared to the analytically derived results of Lippolt (2003). Comparing simulations with analytical models, the same deviations appear as described for Lerher et al. (2010) and Lerher (2016). However, this approach has been used in the last decade by several authors, for example by Ghomri and Sari (2017). Eder (2020a) determines the reshuffle probability for a shuttle-based storage and retrieval system depending on the stock filling level and tries to determine the reshuffle probability based on an equally distributed storage channel allocation. This means that every storage location has the same probability to be occupied. The same approach is used by Eder (2020b) which approximates

the real storage channel probabilities but does not match the analytically derived probabilities from Lippolt (2003).

In addition to the analytic models, simulation models are presented in the literature. They have in common that new simulations have to be executed for new AS/R system configurations, which can be a time-consuming task. Cycle time simulations exist for different depths of racks and different AS/R system variations. Van Den Berg and Gademann (2000) present a simulation study for a single-deep AS/R system, Atz et al. (2013) analyse single- and double-deep AS/R systems, and Marolt et al. (2022a) investigate several multi-deep AVS/RS with a total of nine different operating strategies. The latter also use analytically derived closed form expressions for the movement times of vehicles, but not for the reshuffle probability and number of reshuffles unlike this work. The publications discussed in this section are summarised in Table 3.1.

3.2 Literature Review of Policies for Throughput Models

This section is cited from the section "Literature review" of the paper "Digging Deep: Finding and Maximizing the Throughput Capacity of Multi-deep Storage Systems" currently under revision in *Transportation Science* (Lehmann and De Koster 2024).
The text and visualisation in this section have been taken from the paper with changes of technical terms, tables for consistent style, and numbering of tables and sections.
The author of this thesis was responsible for the conceptualisation, methodology, writing (original draft and review), and visualisation of the research presented in this section.

This section reviews literature on throughput capacity models for multi-deep storage systems, with reshuffles. AS/R, RCS/R, AVS/R, and flow rack storage systems are included in this review (see Azadeh et al. (2019) for an overview of such systems). Throughput models for single- or double-deep storage systems and for multi-deep storage systems without reshuffles were reviewed by Roodbergen

Table 3.1: Throughput Capacity Models for multi-deep Storage Systems from Section 3.1.

CBS-1 = Class-Based Storage with one Class per Channel; CFE = Closed Form Expression; CTC = Cycle Time Calculation; CQN = Closed Queuing Network; DES = Discrete Event Simulation; DF = Depth First; FR = Flow Rack; LFR = Unit Load with Fewest Reshuffles; MC = Markov Chain; NN = Nearest Neighbour; OQN = Open Queuing Network; RLO = Rack Layout Optimisation; SC = Specified Channel; TP = Throughput Capacity.

	Storage System	System Depth	Storage Assignment Policy	Reshuffle Policy	Retrieval Unit Load Selection Policy	Method	Objective
Atz et al. (2013)	AS/R	Double	NN	NN	Random	DES	RLO
Bozer and White (1982)	AS/R	Single	Random	-	Random	CFE	CTC
Bozer and White (1984)	AS/R	Single	Random	-	Random	CFE	CTC
D'Antonio and Chiabert (2019)	AVS/R	Multi	Random; NN	-	Random	CFE	TP
Eder (2020b)	AVS/R	Multi	Random	NN	Random	OQN	RLO
Eder (2020a)	AVS/R	Multi	Random	NN	Random	OQN	TP
Federation Europeenne de la Manutention (2003)	AS/R	Double	Random	Random	Random	CFE	CTC
Ghomri and Sari (2017)	FR	Multi	DF	DF	LFR	CFE	CTC
Gudehus (1972)	AS/R	Single	Random	-	Random	CFE	CTC
Lerher et al. (2010)	AS/R	Double	DF	NN	Random	CFE	CTC
Lerher (2016)	AVS/R	Double	DF	NN	Random	CFE	TP
Lippolt (2003)	AS/R	Double	Random	Random; NN; SC	Random	MC	CTC
Marolt et al. (2022b)	AVS/R	Multi	DF	DF	Random	MC	CTC
Marolt et al. (2022a)	AVS/R	Multi	Random; NN; DF	Random; NN; DF	Random	DES	CTC
Manzini et al. (2016)	AVS/R	Multi	Random	-	LIFO	CFE	CTC
Sari et al. (2005)	FR	Multi	DF	DF	Random	CFE	CTC
Van Den Berg and Gademann (2000)	AS/R	Single	Random; CBS-1	-	Random	DES	CTC
Verein Deutscher Ingenieure (2002)	AS/R	Multi	Random	-	Random	CFE	CTC
Xu et al. (2019)	AS/R	Multi	-	SC	Random	CFE	CTC

and Vis (2009) and Azadeh et al. (2019). Another extensive overview can be found in Tutam et al. (2024).

Throughput capacity models are applied in the system design phase, which is characterised by a lack of detailed information on retrieval and storage jobs. Assumptions regarding these jobs and the number of unit loads stored per product must be made. Two model types are introduced to distinguish the levels of information used for modelling. First, models with homogeneous unit loads, which only incorporate basic information about products and their unit loads (see Section 3.2.1) and second, models with heterogeneous unit loads using comprehensive information, such as the access frequency of products or the number of unit loads per product stored in the storage system (see Section 3.2.2). Cycle times are influenced by the storage assignment, reshuffle, and retrieval unit load selection policies. The number of required reshuffles depends on the average stock filling level and the retrieval unit load selection policy. Publications differ in these two aspects to mirror operational characteristics of real storage systems. The degree of accuracy in the models presented varies, depending on how accurate and consistent the underlying policies are adopted and implemented in the throughput models (See Table 3.2). Given the inherent lack of information at the system design stage regarding the exact products that need to be stored and retrieved, most authors use probabilistic models to estimate cycle time and throughput capacity.

3.2.1 Throughput Models with Homogeneous Unit Loads

In the random storage policy and random reshuffle policy, new or reshuffled unit loads are randomly assigned to free storage locations. These policies have been evaluated by various researchers, among others by Chen et al. (2015), who use a continuous space model to describe the movement of the load handling device within a flow rack. This model is based on the cycle time estimates by Bozer and White (1984) for single-deep AS/R systems. In their study, Chen et al. (2015)

calculate the number of reshuffles by assuming that all storage channels have an equal filling level, which enables easy calculation. They use two distinct cycle time models to compare the cycle times in unidirectional and bidirectional flow racks and conclude that bidirectional flow racks outperform single-directional rack systems.

Several authors, including Eder (2020a), Hamzaoui and Zaki (2020) and Trost and Eder (2024), apply the nearest neighbour policy for reshuffles. This policy selects the nearest free channel rather than a random one. Eder (2020a) uses an open queuing network model to represent the dependencies between the lift and the shuttles in a multi-deep AVS/R system. The cycle times of the lift and shuttles are estimated by aggregating all possible movements and dividing this sum by the total number of feasible movements. The number of reshuffles is estimated based on an equal likelihood of occupation for every storage location in the rack. Eder (2020a) also optimises the rack shape based on the throughput capacity of the open queuing network. Hamzaoui and Zaki (2020) present both discrete and continuous-time models for cycle time estimation, providing a comparative analysis between the two. Their findings suggest that discrete-time models offer superior accuracy, albeit at the cost of longer computational times. Marolt et al. (2022b) apply the nearest neighbour policy also for the storage of new unit loads and evaluate it with discrete event simulation. They also use the depth first storage policy, which reduces the number of suitable storage channels compared to random storage. Potential storage channels are those with the lowest filling level among all storage channels, which leads to an evenly loaded rack configuration.

The depth first policy was initially introduced by Sari et al. (2005) for flow rack systems, although limited to rack configurations with the same number of unit loads in every channel. They base the calculation of cycle times on Bozer and White (1984) and estimate the number of reshuffles following Chen et al. (2015). Marolt et al. (2022b) also apply the depth first policy for AVS/R systems and use a Markov chain to calculate the average filling level for storage channels. They determine the movement times of robots for all jobs like Eder (2020a).

3.2.2 Throughput Models with Heterogeneous Unit Loads

Storing unit loads in predefined areas based on access frequency (i.e. class-based storage) can reduce reshuffles. Class-based storage policies can be implemented based on distance: unit loads of products with high access frequency are stored closer to the pick station. Storage channels exclusively contain unit loads of products of the same class (which are assumed to have the same access frequency), reducing cycle times without a significant effect on the number of reshuffles (Xu et al. (2019) and Eder (2022)). Eder (2022) uses an open queuing network to model the shuttles and lifts in an AVS/R system. Xu et al. (2019) focus on retrievals from a predefined static rack in perfect conditions, while placing less emphasis on detailed storage policies. Furthermore, they assume constant operation at the limit of the storage capacity of the system, simplifying the calculation of reshuffles similar to Chen et al. (2015). Zou et al. (2018) recommend storing the class of the most frequently requested products in the central region of an RCS/R system due to the distribution of pick stations on opposite sides of the RCS/R system, to achieve maximum throughput capacity. They use a semi-open queuing network to model the parallel operation of multiple robots and they temporarily buffer reshuffled unit loads on top of adjoining storage channels which are brought back to the original storage channel after the retrieval job. Yue and Smith (2023) present a simulation model which compares the policies introduced by Zou et al. (2018) with another class-based policy which allocates the products of the same class in as many different storage channels as possible, thus storing unit loads of different classes in the same channel. Cardin et al. (2012) also adopt this class-based storage policy, but mainly include channels with single classes in their simulation results.

Unit loads of the same product can be stored in the same storage channel, avoiding reshuffles during retrieval of these products using a LIFO policy as shown by Manzini et al. (2016) for AVS/R and Zou et al. (2018) for RCS/R systems. However, this approach can lead to a ‘honeycombing effect’, whereby storage locations remain unoccupied due to insufficient quantities of identical product

unit loads resulting in reduced space utilisation compared to policies in which channels are shared by different products. Another noteworthy application is to select the retrieval unit load that minimises the number of reshuffles when several unit loads of the same product are stored in the storage system. Ghomri and Sari (2017) employ this concept in the context of flow rack systems. The calculation of movements follows the method in Bozer and White (1984) incorporating the random storage policy and the random reshuffle policy. Specifically, reshuffles are calculated by assessing the likelihood of direct access of the load handling device to the desired product and extending this assessment to all subsequent number of reshuffles.

The publications presented in this section are summarised in Table 3.2.

3.3 Research Gaps and Selection of Operating Strategies

The Sections 3.1 and 3.2 present the existing literature for multi-deep storage systems with and without reshuffles. However, the existing publications and operating strategies summarised in Tables 3.1 and 3.2 show that significant research gaps exist. Either the presented throughput models do not accurately implement the underlying operating strategies or do not accurately model the throughput compared with simulation. Furthermore, the literature does not cover all operating strategies which potentially lead to higher throughput capacities of the AS/R and RCS/R systems.

This section aims to emphasise the novel contribution of this dissertation in the context of multi-deep storage systems and discusses how the research gaps can be addressed. The different policies analysed in this thesis are summarised in Table 2.2. In total 336 operating strategies are possible for AS/R systems and RCS/R systems can be operated following 168 different operating strategies. Not all operating strategies can be covered in this thesis to answer the research questions.

Table 3.2: Throughput Capacity Models for multi-deep Storage Systems from Section 3.2 (Lehmann and De Koster 2024).

BBO = Bring-Back to Original Channel; CBRS = Class-Based Random Storage; CBS-1 = Class-Based Storage with one Class per Channel; CBS-n = Class-Based Storage with n Classes per Channel; CFE = Closed Form Expression; CTC = Cycle Time Calculation; CQN = Closed Queuing Network; DES = Discrete Event Simulation; DF = Depth First; FR = Flow Rack; LFR = Unit Load with Fewest Reshuffles; MC = Markov Chain; NN = Nearest Neighbour; OQN = Open Queuing Network; RBP = Relocate Best Position; RD = Retrieval Delay; RLO = Rack Layout Optimisation; SC = Specified Channel; SOQN = Semi Open Queuing Network; TP = Throughput Capacity.

	Storage System	Storage Assignment Policy	Reshuffle Policy	Retrieval Unit Load Selection Policy	Method	Objective	Relative Error between Model and Simulation
Chen et al. (2015)	FR	Random	Random	Random	CFE	CTC	$<5\,\%$
Eder (2020a)	AVS/R	Random	NN	Random	OQN	TP	$3.15\,\%$
Hamzaoui and Zaki (2020)	FR	Random	NN	Random	CFE	CTC	$<23\,\%$
Marolt et al. (2022b)	AVS/R	DF	DF	Random	MC	CTC	$<1.5\,\%$
Sari et al. (2005)	FR	DF	DF	Random	CFE	CTC	$<14\,\%$
Trost and Eder (2024)	RCS/R	Random	BBO	Random	CFE	TP	$<2\,\%$
Cardin et al. (2012)	FR	CBS-1/n	CBS-1/n	Random	DES	RD	-
Eder (2022)	AVS/R	CBS-1	NN	Random	OQN	TP	-
Ghomri and Sari (2017)	FR	Random	Random	LFR	CFE	CTC	$<25\,\%$
Manzini et al. (2016)	AVS/R	Random	-	Random, LIFO	CFE	CTC	$<20\,\%$
Marolt et al. (2022a)	AVS/R	Random; NN; DF	Random; NN; DF	Random	DES	CTC	-
Tutam et al. (2024)	RCS/R	BBO	BBO	Random	CFE	CTC	$<1\,\%$
Xu et al. (2019)	AS/R	-	SC	Random	CFE	CTC	$<5\,\%$
Yue and Smith (2023)	RCS/R	CBS-n	BBO	Random	DES	CTC	-
Zou et al. (2018)	RCS/R	CBS-1	BBO	Random	SOQN	CTC	$<14\,\%$

However, in total 13 operating strategies (Table 3.3) are derived and analysed that contribute the most to answer the research questions. In the following, the research gaps in the literature presented in the Sections 3.1 and 3.2 are discussed and the choice of the 13 operating strategies is justified. For this, the 13 operating strategies are compared with the summary Tables 3.1 and 3.2.

Table 3.3: Overview of all Operating Strategies analysed in this Work.

	Strategy Name	Storage System	Allocation Structure	Storage Assignment Policy	Reshuffle Policy	Retrieval Unit Load Selection Policy	Number of Classes J	Movement Policy
Chapter 4	Homogeneous	AS/R	Random	Random Location	Homogeneous	Random	1	Random
	RSCS	AS/R	Stack	Random Channel	Random Channel	Random	1	Random
	RSLS	AS/R	Stack	Random Location	Random Location	Random	1	Random
	Depth First	AS/R	Stack	Depth First	Depth First	Random	1	Random
	Stack First	AS/R	Stack	Stack First	Stack First	Random	1	Random
	RSCS-NN	AS/R	Stack	Random Channel	Random Channel	Random	1	NN
	RSLS-NN	AS/R	Stack	Random Location	Random Location	Random	1	NN
Chapter 5	Random[1]	RCS/R	Stack	Random Channel	Random Channel	Random	1	NN
	Random-BBO	RCS/R	Stack	Random Channel	BBO	Random	1	NN
	CBS-1	RCS/R	Stack	CBS-1	BBO	Random	3	NN
	AutoStore	RCS/R	Stack	CBRS	BBO	Random	3	NN
	AS-LFR	RCS/R	Stack	CBRS	BBO	LFR	3	NN
	CBS-3-BBO	RCS/R	Stack	CBS-3	BBO	Random	3	NN
	CBS-3-RBP	RCS/R	Stack	CBS-3	RBP	LFR	3	NN

First, the research gap for operating strategies assuming homogeneous unit loads is discussed and it is shown how the throughput models developed in this work close the gap. The *Homogeneous* operating strategy extends the homogeneous reshuffle policy introduced by (Lippolt 2003) from double-deep to multi-deep AS/R. The *Random Storage Channel Strategy* (RSCS) and the *Random Storage Location Strategy* (RSLS) calculate the throughput for AS/R and RCS/R systems in operation with a steady state of the rack itself instead of the initial state after the first filling as in (Eder 2020a) and (Eder 2020b). Furthermore, the derived

[1] The RSCS and Random operating strategies are identical. For benchmark reasons, they are explained in Chapter 4 and in Chapter 5. However, for evaluation and comparison in Chapter 6 the operating strategy appears only with the name RSCS.

throughput models consequently apply random storage, reshuffling and retrieval as the first kind of such models. The RSLS is the first strategy in the literature to apply the random location storage and reshuffle policies. The *Depth First* strategy is modelled more accurately and with a simpler approach for depth first storage and reshuffle policies compared to (Sari et al. 2005) and (Marolt et al. 2022b). The *Stack First* strategy is new to the literature and has not been regarded so far in any throughput model for multi-deep storage systems. The *Random Storage Channel Strategy with Nearest Neighbour* policy (RSCS-NN) and the *Random Storage Location Strategy with Nearest Neighbour* policy (RSLS-NN) extend the RSCS and RSLS to apply the nearest neighbour storage and reshuffle policies. As presented in Section 3.2, this is only new to the literature in combination with the new RSCS and RSLS. The Random-BBO strategy exchanges the random reshuffle policy from the RSCS-NN with the bring-back to original channel (BBO) reshuffle policy. This operating strategy is mainly derived as a benchmark strategy. To sum up, the Homogeneous strategy, RSCS, RSLS, Depth First strategy, Stack First strategy, RSCS-NN, RSLS-NN, and Random-BBO strategy either simplify existing models, implement existing policies more accurately or introduce throughput models for uncovered policies while answering the research question 1.

Second, the research gap for operating strategies assuming heterogeneous unit loads is addressed. The throughput model for the *AutoStore* strategy is the first model that uses the same policies as the market leader for RCS/R systems as described by Meller (2023). The *AutoStore* strategy is in contrast to the existing models which are based on Autostore (Zou et al. 2018) and (Tutam et al. 2024) and which deviate from the described AutoStore operating strategy. The *AS-LFR* strategy extends the AutoStore strategy by adding the LFR unit load selection policy which was only regarded by Ghomri and Sari (2017). Compared to (Ghomri and Sari 2017), the *AS-LFR* strategy leads to a more accurate model and is applied with different policies and to AS/R and RCS/R systems instead of flow rack systems. With the *CBS-3-BBO* and *CBS-3-RBP* strategies, this thesis is the first to derive throughput models for the class-based storage policy with multiple classes per channel. To analyse the effect of different reshuffle policies, throughput models for both the *CBS-3-BBO* and *CBS-3-RBP* strategies are derived. By

deriving the throughput models for the AutoStore, AS-LFR, CBS-3-BBO, and CBS-3-RBP strategies in this work, the research question 2 will be answered.

Finally, the *CBS-1* strategy serves as a benchmark strategy and is based on the class-based storage policies implemented by Zou et al. (2018) and Eder (2022), who showed that CBS-1 performs better than the random policies.

Only few authors focused on the comparison of different operating strategies in the literature. The Tables 3.1 and 3.2 show that most authors focus on one operating strategy in their work. Generally, comparisons have been made using simulation (Van Den Berg and Gademann 2000) and (Marolt et al. 2022b). However, some authors use slightly different reshuffle policies (Zou et al. 2018) or different storage systems for one operating strategy (Chen et al. 2015) and compare them. In summary, a comprehensive comparison of different operating strategies for different multi-deep storage systems is missing in the literature. Chapter 6 closes this research gap and provides answers to Research Question 3.

4 Throughput Models for Automated Storage and Retrieval Systems for homogeneous Unit Loads

In this chapter, throughput models for AS/R systems assuming homogeneous unit loads are derived. It is shown in Section 5.5 how these models can be adapted to RCS/R systems. This chapter starts with necessary assumptions to be able to model the AS/R system behaviour and calculate the throughput capacities. It is shown how the throughput capacity and the expected travel times $t_{\text{toS}}, t_{\text{StoR}}, t_{\text{Rto}\beta}, t_{\text{toHP}}$ can be calculated independent of the operating strategies. Afterwards, the expected number of reshuffles β and the channel travel times are derived for the Homogeneous, RSCS, RSLS, Depth First, Stack First, RSCS-NN, and RSLS-NN operating strategies in the Sections 4.1 to 4.7. This chapter closes with the validation of the derived models with simulation in Section 4.8.

In order to estimate the throughput capacity for a given AS/R system and one of the seven operating strategies presented in Table 3.3, the following assumptions are made for the models in this section:

- Storage and retrieval jobs are processed exclusively in dual command cycles.
- New storage and retrieval jobs are always waiting outside of the AS/R system and therefore the S/R machine is never in an idle state. This ensures the maximal throughput.

- The throughput capacity is estimated for AS/R systems which are in a steady state which represents the characteristics of an AS/R system in application in the industry.
- Storage racks are considered to be a continuous rectangular pick face where the I/O point is located in the lower left corner of the rack (Lerher et al. 2010).
- The acceleration and deceleration of the S/R machine, the telescopic arm, the satellite vehicle, and robots is regarded in this dissertation. Another assumption it that the maximal velocity can always be achieved. This leads to a minor error for short movements, which will be addressed in Section 6.4 (Lehmann and Hussmann 2023).
- Every AS/R system is considered to be a single aisle and is operated by a single S/R machine.
- S/R machines can move using the Chebychev metric.

The throughput capacity of AS/R systems is determined by the number of command cycles that can be executed within a certain time frame. For this the average cycle time t_{cycle} is sufficient and the throughput capacity TP per hour is defined as:

$$TP = \frac{3600\,\mathrm{s}}{t_{cycle}}. \tag{4.1}$$

The calculation of t_{cycle} follows the dual command cycle description introduced in Section 2.1 and depends on the operating strategy. It differs for the Homogeneous and the other six operating strategies in this chapter with:

$$\begin{aligned} t_{cycle,hom.} &= 4t_h + t_{\text{toS}} + 2t_{Ch,S} + t_{\text{StoR}} + 2t_{Ch,R} + t_{\text{toHP}} + \beta \cdot t_\beta \\ &\quad + P(\beta > 0)(t_{\text{toHP}} + t_{\text{toS}} - t_{\text{Rto}\beta}) \end{aligned} \tag{4.2}$$

$$t_{cycle} = 4t_h + t_{\text{toS}} + 2t_{Ch,S} + t_{\text{StoR}} + 2t_{Ch,R} + t_{\text{toHP}} + \beta \cdot t_\beta \tag{4.3}$$

and

$$t_\beta = 2 \cdot (t_h + t_{\text{Rto}\beta} + t_{Ch,S,\beta} + t_{Ch,R,\beta}). \tag{4.4}$$

The handling time to pick or drop a unit load with the S/R machine t_h is a parameter and the calculation for t_{toHP} and t_{toS} for all strategies as well as the calculation of the variables t_{StoR} and $t_{\text{Rto}\beta}$ for the Homogeneous, RSCS, RSLS, Depth First, and Stack First strategies will be presented in this section. The calculation of all other variables in the Equations (4.2) to (4.4) for all operating strategies is shown in the respective subsections in this section.

The travel times from the I/O point to a storage channel and from a retrieval channel to the I/O point are defined as t_{toS} and t_{toHP}. Since the retrieval channel is chosen randomly, the travel time for t_{toHP} is the time between the S/R machine needs to cover the Chebychev distance between the I/O point and a random channel. The storage channel is either randomly distributed as well because all channel types for the operating strategies in this section are either randomly distributed or as close as possible to the random retrieval channel (for RSCS-NN and RSLS-NN) which results in t_{toS} also being the travel time between the I/O point and a random storage channel. According to Arnold and Furmans (2019), t_{toHP} and t_{toS} are calculated as:

$$t_{\text{toHP}} = t_{\text{toS}} = \begin{cases} (1 - \frac{b}{2})\frac{v_x}{a_x} + \frac{b}{2}\frac{v_y}{a_y} + \frac{l_x L}{v_x}(\frac{1}{2} + \frac{1}{6}b^2) & b \leq 1 \\ \frac{1}{2b}\frac{v_x}{a_x} + (1 - \frac{1}{2b})\frac{v_y}{a_y} + \frac{l_x L}{v_x}(\frac{b}{2} + \frac{1}{6b}) & b > 1, \end{cases} \tag{4.5}$$

where b is the wall parameter (Arnold and Furmans 2019) with

$$b = \frac{v_x}{v_y} \cdot \frac{l_y W}{l_x L}. \tag{4.6}$$

For the Homogeneous, RSCS, RSLS, Depth First, and Stack First strategies, t_{StoR} and $t_{\text{Rto}\beta}$ are the travel time of the S/R machine between two random channels in the AS/R system. Following Bozer and White (1984), the distance between two

randomly selected channels is a random variable X with the pdf $g(X)$ and the cdf $G(X)$[1]:

$$g(X) = \begin{cases} (2-2X)\cdot(2\frac{X}{b} - (\frac{X}{b})^2) + (2X - X^2)\cdot(\frac{2}{b} - \frac{2X}{b^2}) & 0 \leq X < b \\ 2\cdot(1-X) & b \leq X \leq 1 \end{cases} \tag{4.7}$$

$$G(X) = \begin{cases} (2X - X^2)\cdot(2\frac{X}{b} - (\frac{X}{b})^2) & 0 \leq X < b \\ 2X - X^2 & b \leq X \leq 1 \end{cases}. \tag{4.8}$$

The expected distance is $E(X) = \int_0^1 X \cdot g(X)\mathrm{d}X$ and the travel times t_{StoR} and $t_{\text{Rto}\beta}$ are:

$$t_{\text{StoR}} = t_{\text{Rto}\beta} = \frac{E(X)\cdot l_x L}{v_x} + \frac{1}{2}\cdot\left(\frac{v_x}{a_x} + \frac{v_y}{a_y}\right). \tag{4.9}$$

The calculation of the time needed for acceleration and deceleration of the S/R machine is based on the work of Arnold and Furmans (2019) and is used throughout the remainder of this thesis.

For further calculations in this chapter of especially the number of reshuffles, it is important to define the stock filling level ω as the share of occupied storage locations in the AS/R system. For the Homogeneous strategy, ω can be calculated with

$$\omega = \sum_{h=1}^{H} \frac{h}{H} \cdot \sum_{k=1}^{\binom{H}{h}} \pi(c_{h,k}) \tag{4.10}$$

[1] For $b > 1$ it is assumed that the rack is turned by 90° to adjust the given b for Equations (4.7) and (4.8)

and for all other strategies in this chapter, ω can be calculated with

$$\omega = \sum_{h=1}^{H} \frac{h}{H} \cdot \pi(c_h). \tag{4.11}$$

The following sections are structured as follows: First the channel type probabilities $\pi(c_{h,k})$ for the AS/R systems in the steady state with the respective operating strategies are derived. Based on that, the number of reshuffles and the travel times of the telescopic arm or shuttle vehicle can be calculated. The Sections 4.6 and 4.7 build on Sections 4.2 and 4.3 an alter the calculation of t_{StoR} and $t_{\text{Rto}\beta}$ compared to Equation (4.9). The calculation for t_{StoR}, $t_{\text{Rto}\beta}$, t_{toHP}, and t_{toS} for RCS/R systems is shown in Section 5.5. All other variables are the same for AS/R and RCS/R systems.

4.1 Homogeneous Strategy

The Homogeneous strategy aims at storing, reshuffling and retrieving unit loads in a manner that leads to a homogeneous allocation structure where every storage location has the same probability to be free or occupied only depending on the stock filling level ω. With such a homogeneous allocation structure, the calculation of the relevant system parameters becomes relatively easy. The channel type probability is calculated as

$$\pi(c_{h,k}) = (1-\omega)^{H-h} \cdot \omega^h. \tag{4.12}$$

The calculations for number of reshuffles and the channel times are shown in Sections 4.1.1 and 4.1.2. However, to achieve such a homogeneous allocation structure, special reshuffle jobs must be carried out (see Section 4.1.3). Section 4.1.4 closes this section and proves that with the explained storage, reshuffle and retrieval jobs, AS/R systems have the homogeneous allocation structure in their steady state during operation.

The Sections 4.1.1 to 4.1.4 are cited from the sections "Relocation Probabilities and Number of Relocations", "Channel Travel Times", "Storage and Retrieval Operations in a multi-deep AS/RS", and "Stable System State Proof" of the paper "Travel time model for multi-deep automated storage and retrieval system with a homogeneous allocation structure" in *Logistics Research* (Lehmann and Hussmann 2021).
The text, formal analysis and visualisation in this section have been taken from the paper with changes of technical terms, figures for consistent style, numbering of figures, equations, and sections, extension of channel time formulas with acceleration, and symbols. Furthermore, the language has been improved.
The author of this thesis was responsible for the conceptualisation, methodology, formal analysis, writing (original draft and review), and visualisation of the research presented in these sections.

4.1.1 Reshuffle Probability and Number of Reshuffles

The reshuffle probability can be determined by calculating the average number of blocking unit loads for storage lane h. This is identical to the number of occupied storage locations $h^{'}$ in the $H-h$ storage locations in front of the storage lane h. Since the probability that during a storage job a new unit load is stored in any of the H lanes is the same, due to the homogeneous allocation structure, the outer sum is divided by H. This procedure is the same for storage and retrieval jobs and therefore $P(\beta > 0)$ is the same for storage and retrieval jobs.

$$P(\beta > 0) = \frac{1}{H} \sum_{h=1}^{H} \sum_{h'=1}^{H-h} \binom{H-h}{h'} \cdot \omega^{h'} \cdot (1-\omega)^{H-h-h'} \tag{4.13}$$

For an easier calculation, the counter probability - $1-P($no blocking unit load in front of the regarded $h)$ - can be determined as well.

$$P(\beta > 0) = 1 - \frac{1}{H} \cdot \sum_{h=1}^{H} (1-\omega)^{H-h} = \frac{(1-\omega)^{H} + \omega \cdot H - 1}{\omega \cdot H} \tag{4.14}$$

For all AS/R systems with $H > 2$ it holds that the probability that at least one reshuffle is necessary is different from the number of reshuffles. β can be

determined similar to $P(\beta > 0)$ and the multiplication with $h^{'}$. The homogeneous allocation structure ensures that $\beta = \beta_S + \beta_R$ is the same for storage and retrieval jobs ($\beta_S = \beta_R$):

$$\beta_S = \frac{1}{H} \sum_{h=1}^{H} \sum_{h'=1}^{H-h} h^{'} \cdot \binom{H-h}{h'} \cdot \omega^{h'} \cdot (1-\omega)^{H-h-h'} = \frac{(H-1) \cdot \omega}{2} \tag{4.15}$$

4.1.2 Channel Travel Times

The deeper the racks of an AS/R system are designed, the longer the telescopic arm of a S/R machine needs to reach to the storage locations. $t_{Ch,S}$ can be determined relatively easy:

$$t_{Ch,S} = t_{Ch,R} = \frac{1+H}{2} \cdot \frac{l_z}{v_z} + \frac{v_z}{a_z} \tag{4.16}$$

This means that the S/R machine must move halfway into the storage channel during a storage or retrieval job. Once again, the homogeneous allocation structure allows this simple definition. It also enables that $t_{Ch,S,\beta} = t_{Ch,R,\beta}$. However, $t_{Ch,S,\beta}$ can be determined by analysing every storage lane h and all storage locations in front of each lane and calculating the channel time for each storage location in front of the regarded lane. This sum divided by β is the number of storage locations the telescopic arm or shuttle vehicle have to cross during a reshuffle:

$$\begin{aligned} t_{Ch,S,\beta} &= \frac{\frac{1}{H} \sum_{h=1}^{H} \sum_{h'=1}^{H-h} h' \cdot \frac{1+H-h}{2} \cdot \binom{H-h}{h'} \cdot \omega^{h\prime} \cdot (1-\omega)^{H-h-h'}}{\beta} \cdot \frac{l_z}{v_z} + \frac{v_z}{a_z} \\ &= \frac{H+1}{3} \cdot \frac{l_z}{v_z} + \frac{v_z}{a_z} \end{aligned} \tag{4.17}$$

4.1.3 Storage, Reshuffle, and Retrieval Jobs

Both storage and retrieval jobs can be understood as a transition between two channel types $c_{h,k}$ and $c_{h',k'}$. A storage job S and a retrieval job R can be defined as:

$$S : c_{h,k} \rightarrow c_{h',k'}, \qquad R : c_{h',k'} \rightarrow c_{h,k} \tag{4.18}$$

Retrieval jobs can be understood as an inversion of a storage job. For each storage job, there exists exactly one retrieval job that does the opposite, by just reverting the channel type transition. To achieve the homogeneous allocation structure, a storage or retrieval job needs to satisfy two principles:

1. Only one storage location in the channel type $c_{h,k}$ is allowed to change.
2. This change must be either from a free to an occupied storage location at a storage job or from an occupied to a free storage location at a retrieval job.

In total, there are $\sum_{h=0}^{H} \binom{H}{h} \cdot (H-h) = 2^{H-1} \cdot H$ different storage jobs and the same number of retrieval jobs possible. For further considerations, it is important to know the probability that a storage or retrieval job affects a certain channel type. The conditional probabilities of a storage or retrieval job taking place in a channel type $c_{h,k}$ are:

$$P(c_{h,k}|S) = \frac{\pi(c_{h,k})}{\sum_{i=0}^{H}(H-i) \cdot \sum_{j=1}^{\binom{H}{i}} \pi(c_{i,j})} \tag{4.19}$$

$$P(c_{h,k}|R) = \frac{\pi(c_{h,k})}{\sum_{i=0}^{H} i \cdot \sum_{j=1}^{\binom{H}{i}} \pi(c_{i,j})}. \tag{4.20}$$

Not all jobs S and R for any $c_{h,k}$ can be executed directly, due to blocking unit loads. The necessary number of reshuffles is then the numbers of unit loads stored in front of the storage or retrieval location in $c_{h,k}$.

The basic idea of reshuffles is that the blocking unit loads are not reassigned randomly, but to a storage channel in a predetermined channel type. The reshuffle job is exemplary shown by the Figures 4.1 to 4.3. When the unit load i must be retrieved, the ii and iii unit loads must be relocated first.

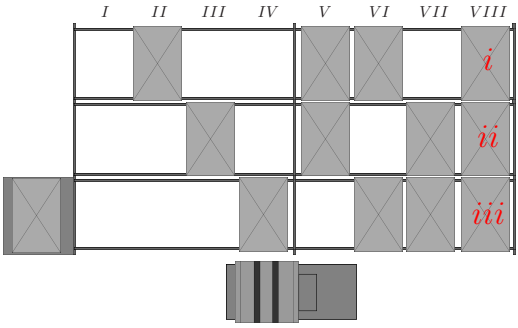

Figure 4.1: Triple-deep AS/R System. Unit Load i shall be retrieved out of Channel $VIII$.

A storage channel type $c_{h,k}$ for the reshuffle of a blocking unit load has to be found which satisfies the following conditions:

1. During a retrieval job, the lane (see Figure 2.1 for definition of a lane) of the unit load to be retrieved must be free. In a storage job it must be occupied.

2. All other storage locations in channel type $c_{h,k}$ with a lower lane number than the relevant storage or retrieval location (unit load i in Figure 4.1) must be the same as in the original channel

3. All storage locations in channel type $c_{h,k}$ with the same or a higher lane than the relevant storage or retrieval location must be free

Only one storage channel type fulfills these conditions, which is channel III (type $c_{1,2}$) for the first reshuffle. After the first reshuffle the AS/R system changed to Figure 4.2. The second reshuffle follows the same three rules and the result is shown in Figure 4.3. After this reshuffle, the unit load i can be retrieved. It is also noticeable that the S/R machine has to perform the same number of steps

inside the original and the reshuffle channel for every reshuffle as assumed in Section 4.1.2.

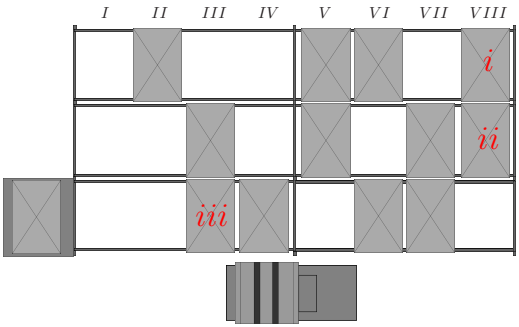

Figure 4.2: Triple-deep AS/R System after the first Reshuffle.

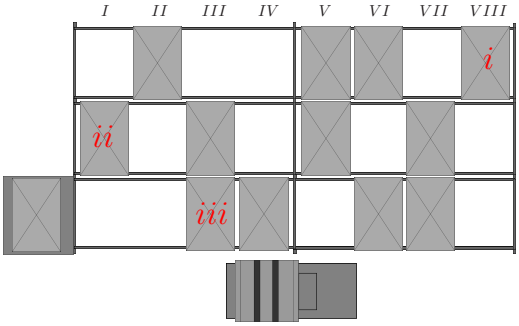

Figure 4.3: Triple-deep AS/R System after the second Reshuffle.

It should be emphasized that the described procedure for a reshuffle aims at keeping the number of channels from every type stable, except from the original channel. In total only one channel changed its type and this type transition is illustrated in Figure 4.4.

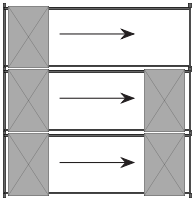

Figure 4.4: Channel Type Transition of a triple-deep AS/R System after the second Reshuffle.

4.1.4 Steady State Proof

The hypothesis in this section is that the channel type probabilities $\pi(c_{h,k}) = (1-\omega)^{H-h} \cdot \omega^h$ and the storage, retrieval and reshuffle jobs explained in Section 4.1.3 describe a steady state for a multi-deep AS/R system.

This steady state requires that every $c_{h,k}$ can be transformed into any other $c_{h',k'}$ with one more or one less unit load by only one storage or retrieval job. Furthermore, every storage or retrieval job must be directly reversible. This means that for every storage job $c_{h,k} \rightarrow c_{h',k'}$, there is exactly one retrieval job which reverses the storage job with $c_{h',k'} \rightarrow c_{h,k}$. This steady state can be described with a Markov chain.

Therefore, a finite state space and transition probabilities between these states must be defined. These states can be interpreted as the 2^H possible channel types. The transition probabilities are the conditional probabilities $P(S|c_{h,k})$ and $P(R|c_{h,k})$ that a storage or retrieval job is performed regarding a channel $c_{h,k}$. This Markov chain can be described with a $2^H \times 2^H$ transition matrix M. The entries in this matrix are the following:

- With every row h of M and, therefore, for every channel type, $(H-h)$ storage and h retrieval jobs can be performed. These are expressed with the conditional probabilities $P(S|c_{h,k})$ and $P(R|c_{h',k'})$.
- The entries of the main diagonal is $1-h \cdot P(R|c_{h',k'}) - (H-h) \cdot P(S|c_{h,k})$.
- All remaining entries are 0.

This transition matrix can be resolved to:

$$\begin{pmatrix} \pi(c_{0,1}) \\ ... \\ \pi(c_{H,1}) \end{pmatrix} = \begin{pmatrix} \pi(c_{0,1}) \\ ... \\ \pi(c_{H,1}) \end{pmatrix}^{\top} \cdot M$$

Generally it has to be shown that:

$$\pi(c_{h,k}) \cdot P(S|c_{h,k}) = \pi(c_{h',k'}) \cdot P(R|c_{h',k'}). \tag{4.21}$$

If this is achievable with the so far derived channel type probabilities and storage and retrieval probabilities, these probabilities make up a stable multi-deep AS/R system together. In the following, the hypothesis will be proven for all storage jobs. The prove for retrieval jobs is then trivial.

$$\pi(c_{h,k}) = (1-\omega)^{H-h} \cdot \omega^{h} \tag{4.22}$$

$$\pi(c_{h',k'}) = (1-\omega)^{H-h-1} \cdot \omega^{h+1} \tag{4.23}$$

$$P(S|c_{h,k}) = \frac{P(c_{h,k}|S) \cdot P(S)}{\pi(c_{h,k})} = \frac{P(S)}{(1-\omega) \cdot H} \tag{4.24}$$

$$P(R|c_{h',k'}) = \frac{P(c_{h',k'}|R) \cdot P(R)}{\pi(c_{h',k'})} = \frac{P(R)}{\omega \cdot H} \tag{4.25}$$

Filling Equations (4.19) and (4.20) and Equations (4.22) to (4.25) into Equation (4.21) results in:

$$(1-\omega)^{H-h} \cdot \omega^{h} \cdot \frac{P(S)}{(1-\omega) \cdot H} = (1-\omega)^{H-h-1} \cdot \omega^{h+1} \cdot \frac{P(R)}{\omega \cdot H}$$

and

$$(1-\omega)^{H-h-1} \cdot \omega^{h} \cdot \frac{P(S)}{H} = (1-\omega)^{H-h-1} \cdot \omega^{h} \cdot \frac{P(R)}{H}$$

Following the assumption that $P(S) = P(R)$, it is shown that Equation (4.21) is true and the Hypothesis can be confirmed.

The Sections 4.2 to 4.5 are cited from the sections “Random storage channel strategy – RSCS”, “Random storage location strategy – RSLS”, “Minimal variance strategy”, and “Maximal variance strategy” of the paper “Travel time model for multi-deep automated storage and retrieval systems with different storage strategies” published in the *International Journal of Production Research* (Lehmann and Hussmann 2023).
The text, formal analysis and visualisation in this section have been taken from the paper with changes of technical terms, numbering of figures, equations, and sections, and symbols. Furthermore, the language has been improved.
The author of this thesis was responsible for the conceptualisation, methodology, formal analysis, writing (original draft and review), and visualisation of the research presented in these sections.

4.2 Random Storage Channel Strategy

To determine the number of reshuffles and the channel times, the steady state of the rack, meaning the equilibrium probability distribution after a sufficient number of storage and retrieval jobs, is required. The basis for this are the single storage and retrieval jobs which lead to the steady state of the rack. In general, H different storage jobs can occur, and Figure 4.5 shows exemplary the 3 storage jobs for a triple-deep AS/R system.

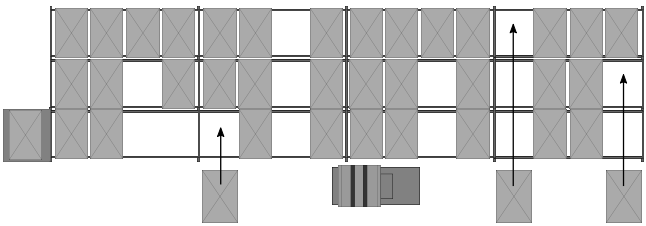

Figure 4.5: The three possible Storage Jobs in a triple-deep AS/R System (Lehmann and Hussmann 2022).

The probability which storage job is chosen depends on the probabilities of the storage channel types $c_{h,k}$. The probability of choosing the middle storage job in Figure 4.5 can be determined by dividing the probability for an empty channel $\pi(c_0)$ by the probability of all valid storage channel types for a storage

job $\sum_{h=0}^{H-1} \pi(c_h)$. Equation (4.26) shows the generalised calculation for the storage probabilities $P(S_h)$, where S_h is a storage job into a channel type c_h.

$$P(S_h) = \frac{\pi(c_h)}{\sum_{h=0}^{H-1} \pi(c_h)} \tag{4.26}$$

During the retrieval jobs reshuffles may occur. Therefore, the retrieval jobs are divided into a pure retrieval component - that includes the retrieval of the desired unit load itself - a reshuffle-retrieval component - that includes the retrieval of the reshuffle unit loads - and a reshuffle-storage component, meaning the transfer of the reshuffle unit load to other storage channels. There are $\sum_{h=1}^{H} h = \frac{H(H+1)}{2}$ potential retrieval components. Figure 4.6 shows the six different retrieval components for a triple-deep AS/R system.

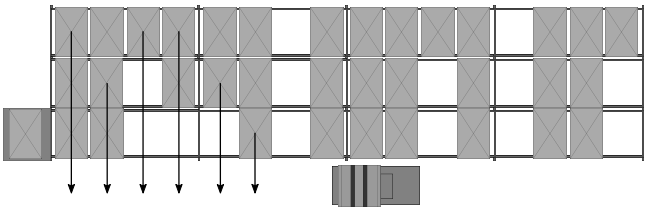

Figure 4.6: The six possible Retrieval Jobs in a triple-deep AS/R System (Lehmann and Hussmann 2022).

It is apparent that from a storage channel with a higher h, more different retrievals are possible and therefore the denominator in Equation (4.27) must account for this.

$$P(R_h) = \frac{\pi(c_{h,1})}{\sum_{h=1}^{H} h \cdot \pi(c_{h,1})} = P(c_{h,1}|R) \tag{4.27}$$

The reshuffle-retrieval component can consist out of a single reshuffle, but it is also possible that several reshuffles must be completed - as one can see in Figure 4.6 at the left side. This means that over all $\frac{H(H+1)}{2}$ different retrieval components, $\sum_{i=2}^{H}\sum_{j=i}^{H}(i-1) = \frac{H^3-H}{6}$ reshuffle components in the original storage channel are possible. Every reshuffle job can combine one of these reshuffle-retrieval components with n reshuffle-storage components - similar to regular storage jobs with a different starting point, resulting in the probability for every c_h to be chosen during a reshuffle: $P(S_h) \cdot \sum_{i=2}^{H}\sum_{j=i}^{H}(i-1) \cdot P(R_j)$.

$P(S_h)$ displays the regular storage jobs. $P(c_h|S)$ is the conditional probability that a channel of type c_h is chosen for a storage job as well as a reshuffle-storage component and is calculated in Equation (4.28). With Bayes' theorem Equation (4.29) and Equation (4.30) follow.

$$P(c_h|S) = P(S_h) \cdot (1 + \sum_{i=2}^{H}\sum_{j=i}^{H}(i-1) \cdot P(R_j)) \tag{4.28}$$

$$P(S|c_h) = \frac{(1 + \sum_{i=2}^{H}\sum_{j=i}^{H}(i-1) \cdot P(R_j)) \cdot P(S)}{\sum_{i=0}^{H-1}\pi(c_{i,1})} \tag{4.29}$$

$$P(R|c_h) = \frac{P(R)}{\sum_{i=1}^{H} i \cdot \pi(c_{i,1})} \tag{4.30}$$

$P(S|c_h)$ - the probability for a storage job when the system is in the channel of type c_h - and $P(R|c_h)$ are necessary, to model the AS/R system with a Markov chain. Since the rack does not remember the order of former storage and retrieval jobs and the next storage or retrieval job is only depending on the current state of the rack, a Markov chain can be used to determine the channel type probabilities.

The state space of the Markov chain consists of the $H+1$ channel types. The channel type transitions during storage and retrieval jobs can be described with the conditional probabilities $P(S|c_h)$ and $P(R|c_h)$. The Markov chain is represented by the $(H+1) \times (H+1)$ transition matrix M:

$$M_{i,j} = \begin{cases} 0 & i < j-1 \\ P(S|c_{i,1}) & i < j \\ P(S|c_{i,1}) & j < i \\ 1 - H \cdot P(R|c_{i,1}) & i = j \text{ and } j = H+1 \\ 1 - P(S|c_{i,1}) - (i-1)P(R|c_{i,1}) & i = j \end{cases} \tag{4.31}$$

For example for $H = 3$, the transition matrix is the matrix in Equation (4.32). α in Equation (4.32) is 1 minus the sum of all other entries in the same row, because the sum of each row in a transition matrix must equal 1. α represents the conditional probability that neither a storage nor reshuffle job affects the channel type of the row in M. For example the empty channel c_0 has the conditional probability $P(S|c_0)$ that a storage job occurs into a channel of type c_0 when all channels c_0 are regarded. And α is the conditional probability that c_0 is not affected when storage or retrieval jobs are carried out which only concern other c_h than c_0.

$$M = \begin{pmatrix} \alpha & P(S|c_0) & 0 & 0 \\ P(R|c_1) & \alpha & P(S|c_1) & 0 \\ P(R|c_2) & P(R|c_2) & \alpha & P(S|c_2) \\ P(R|c_3) & P(R|c_3) & P(R|c_3) & \alpha \end{pmatrix} \tag{4.32}$$

To get the desired channel type probabilities $\pi(c_h)$, it is necessary to resolve the transition matrix M to

$$\begin{pmatrix} \pi(c_0) \\ \dots \\ \pi(c_h) \end{pmatrix}^T = \begin{pmatrix} \pi(c_0) \\ \dots \\ \pi(c_h) \end{pmatrix}^T \cdot M. \tag{4.33}$$

Together with $\sum_{h=0}^{H} \pi(c_h) = 1$, the solution for the system of equations (4.33) can be given by Equation (4.34). It is only possible to display $\pi(c_h)$ in closed form dependent on the probability of the empty channel type $\pi(c_0)$.

$$\pi(c_h) = \begin{cases} \dfrac{(h+1) \cdot \pi(c_0)^{1-h} \cdot (\pi(c_0)-1)^h \cdot \Gamma\left(1+\dfrac{1}{\pi(c_0)}\right)}{(-1)^h \cdot \Gamma\left(1+h+\dfrac{1}{\pi(c_0)}\right)} & ,0 \leq h < H \\ \dfrac{\pi(c_0)^{1-h} \cdot (\pi(c_0)-1)^h \cdot \Gamma\left(1+\dfrac{1}{\pi(c_0)}\right)}{(-1)^h \cdot \Gamma\left(h+\dfrac{1}{\pi(c_0)}\right)} & ,h = H \end{cases} \tag{4.34}$$

Γ in Equation (4.34) is the Gamma function with $\Gamma(x+1) = \int_0^\infty t^x e^{-t} dt$.

4.2.1 Number of Reshuffles

With the knowledge about $\pi(c_h)$ and ω it is now possible to determine $P(\beta > 0)$ and β.

$$P(\beta > 0) = \sum_{i=1}^{H-1} \sum_{h=1+i}^{H} P(R_h) \tag{4.35}$$

$$\beta = \sum_{i=1}^{H-1} \left(i \cdot \sum_{h=1+i}^{H} P(R_h) \right) \tag{4.36}$$

4.2.2 Channel Travel Times

Finally, it is possible to determine the average times the S/R machine needs to perform storage jobs - $t_{Ch,S}$, the retrieval component - $t_{Ch,R}$, the reshuffle-retrieval component - $t_{Ch,R,\beta}$ - and the reshuffle-storage component $t_{Ch,S,\beta}$. Since storage jobs always follow the stack allocation structure, the movement distance correspond to the difference between the maximum channel depth H

and the storage location h given by the channel type c_h weighted by the channel probability $\pi(c_h)$, divided by the cumulative channel probability of the channels into which storage jobs are possible. The same principal applies for the reshuffle-storage component.

$$t_{Ch,S} = t_{Ch,S,\beta} = \frac{\sum_{h=0}^{H-1} \pi(c_h) \cdot (H-h)}{\sum_{h=0}^{H-1} \pi(c_h)} \cdot \frac{l_z}{v_z} + \frac{v_z}{a_z} \tag{4.37}$$

The expected retrieval time $t_{Ch,R}$ is the average retrieval time of channel c_h weighted by channel probability $\pi(c_h)$. Since for channel c_h the retrieval of all h unit loads has the same probability, the average retrieval time of channel c_h is given by the average of the distances associated with the h unit loads. The aggregated sum in the numerator is finally divided by a weighted sum of the channel probabilities; the weighting considers that for a channel c_h the retrieval probability is h times larger, because when randomly selecting a unit load in the rack, the probability of selecting a unit load in a filled channel is higher.

$$t_{Ch,R} = \frac{\sum_{h=1}^{H} \pi(c_h) \Big(\sum_{i=1}^{h} H - h + i \Big)}{\sum_{h=1}^{H} h \cdot \pi(c_h)} \cdot \frac{l_z}{v_z} + \frac{v_z}{a_z} \tag{4.38}$$

The expression of the expected time of the reshuffle-retrieval component is closely related with Equation (4.38), the inner sum iterating overall unit loads of any channel type starts at $i = 2$, in contrast to $t_{Ch,R}$, since $i = 1$ corresponds to the pure retrieval job. Moreover, the expression $\frac{i(i-1)}{2}$ occurs in the sum - a Gaussian sum - which depicts that in a channel with h unit loads, for the i-th unit load to be

removed, all unit loads in front of it must also be removed; this additional inner sum can be simplified to the Gaussian expression.

$$t_{C,R,\beta} = \frac{\sum_{h=2}^{H}\left(\sum_{i=2}^{h}(i-1)\cdot\pi(c_h)\cdot\frac{\sum_{j=2}^{h}(h-1)\cdot(H-h)+\frac{j(j-1)}{2}}{\sum_{j=1}^{h-1}j}\right)}{\sum_{h=2}^{H}\left(\sum_{i=2}^{h}(i-1)\cdot\pi(c_h)\right)}\cdot\frac{l_z}{v_z}+\frac{v_z}{a_z} \tag{4.39}$$

4.3 Random Storage Location Strategy

When a storage channel is chosen in consideration of all free storage locations, storage channels with few unit loads are preferred. This can be expressed by multiplying the probability for the choice of a certain storage channel by the number of free storage locations in a channel c_h in the numerator and also the denominator in $P(S_h)$.

$$P(S_h) = \frac{(H-h)\cdot\pi(c_h)}{\sum_{i=0}^{H-1}(H-i)\cdot\pi(c_{i,1})} \tag{4.40}$$

This also leads to a new conditional probability for storage jobs.

$$P(S|c_h) = \frac{(1+\sum_{i=2}^{H}\sum_{j=i}^{H}(i-1)\cdot P(R_j))\cdot P(S)\cdot(H-j)}{\sum_{i=0}^{H-1}(H-i)\cdot\pi(c_{i,1})} \tag{4.41}$$

The calculation of $P(R_h)$ and $P(R|c_h)$ stays the same as in Equations (4.27) and (4.30) and also the transition matrix M stays the same as in Equation (4.31).

The transition matrix M can be resolved and the storage channel probabilities are obtained.

$$\pi(c_h) = \begin{cases} \dfrac{(\pi(c_0)-1)^h \cdot (-1)^{h-1} \cdot \pi(c_0) \cdot H \cdot (h+1)}{(h-H) \cdot \prod_{i=1}^{h} (\frac{i \cdot \pi(c_0) \cdot (H+1)}{H-i} + 1)} & ,0 \leq h < H \\ \dfrac{(\pi(c_0)-1)^h \cdot (-1)^h}{\prod_{i=1}^{h-1} (\frac{i \cdot \pi(c_0) \cdot (H+1)}{H-i} + 1)} & ,h = H \end{cases} \tag{4.42}$$

Since only the probabilities during storage and reshuffle jobs are calculated differently compared to Section 4.2, the calculation of $P(\beta > 0)$, β, $t_{Ch,R}$, and $t_{Ch,R,\beta}$ is the same as in Equations (4.35), (4.36), (4.38) and (4.39). The channel times during storage jobs and reshuffle-storage components do also differ from the RSCS strategy. For the RSLS strategy they are:

$$t_{Ch,S} = t_{Ch,S,\beta} = \frac{\sum_{h=0}^{H-1} (H-h) \cdot \pi(c_h) \cdot (H-h)}{\sum_{h=0}^{H-1} (H-h) \cdot \pi(c_h)} \cdot \frac{l_z}{v_z} + \frac{v_z}{a_z}. \tag{4.43}$$

4.4 Depth First Strategy

In Sections 4.2 and 4.3, the channel type probabilities were derived from an underlying Markov chain. This procedure is not applicable for the Depth First and Stack First strategies, because only the retrieval jobs follow a random policy, and the storage jobs must store in a certain storage channel. Instead, the Depth First strategy stores a new unit load into a storage channel c_h with the smallest $h = \lfloor H \cdot \omega \rfloor$ and chooses randomly from all unit loads for a retrieval job. This way it is possible to reduce the fill level variance of all storage channels. In the perfect state of an AS/R system, there are always at most two storage channel

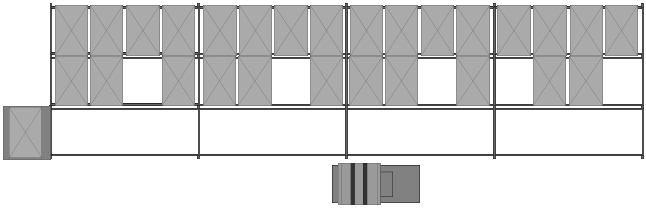

Figure 4.7: Example of the top View of a Rack in a triple-deep AS/R System with a Depth First Strategy (Lehmann and Hussmann 2022).

types (c_h and c_{h+1}), as it is shown in Figure 4.7 for a triple-deep AS/R system with $\omega = 0.5625$.

This basic idea of the Depth First strategy is used ad-hoc when deriving the channel type probabilities, the number of reshuffles as well as the channel travel times, although the perfect AS/R system as shown in Figure 4.7 is not always satisfied, especially after retrieval jobs with reshuffles. To compensate for this, a correction term will be used while deriving the storage and reshuffle-storage channel times.

The channel type probabilities $\pi(c_h)$ of a storage channel correspond to a piece-wise linear function, where the probability for a channel type c_h rises until all storage channels are of this type, every further unit load reduces the probability linearly. The piece-wise linear probability function then corresponds to Equation (4.44) for all H and ω.

$$\pi(c_h) = \begin{cases} 0 & , \omega < \dfrac{h-1}{H} \\ H \cdot \omega + 1 - h & , \dfrac{h-1}{H} \leq \omega < \dfrac{h}{H} \\ h + 1 - H \cdot \omega & , \dfrac{h}{H} \leq \omega \leq \dfrac{h+1}{H} \\ 0 & , \dfrac{h+1}{H} < \omega \end{cases} \tag{4.44}$$

It is now possible to determine the reshuffle probability and number of reshuffles.

$$P(\beta > 0) = \begin{cases} \dfrac{H \cdot \omega - 1}{H \cdot \omega} & , H \cdot \omega \geq 1 \\ 0 & , H \cdot \omega < 1 \end{cases} \tag{4.45}$$

$$\beta = \frac{\sum_{i=1}^{h} \sum_{j=1}^{i} \pi(c_{h+1,1}) + \sum_{i=2}^{h} \sum_{j=2}^{i} \pi(c_h)}{H \cdot \omega} = \frac{h \cdot (2 \cdot H \cdot \omega - h - 1)}{2 \cdot H \cdot \omega} \tag{4.46}$$

The channel time for a retrieval job is shown in Equation (4.47). The reshuffle-retrieval channel time $t_{C,R,\beta}$ sums the channel times up for every possible reshuffle, which is divided by all possible reshuffles.

$$\begin{aligned} t_{Ch,R} =& \frac{\sum_{i=1}^{h} (H - h + i) + (H \cdot \omega - h) \cdot (H - h)}{H \cdot \omega} \cdot \frac{l_z}{v_z} + \frac{v_z}{a_z} \\ =& \frac{h + h^2 + 2H^2 \cdot \omega - 2H \cdot \omega \cdot h}{2H \cdot \omega} \cdot \frac{l_z}{v_z} + \frac{v_z}{a_z} \end{aligned} \tag{4.47}$$

$$\begin{aligned} t_{Ch,R,\beta} =& \frac{\pi(c_{h+1,1}) \sum_{i=1}^{h} \sum_{j=1}^{i} (H - h + j - 1) + \pi(c_h) \sum_{i=2}^{h} (i-1)(H - i + 1)}{\sum_{i=1}^{h} \sum_{j=1}^{i} \pi(c_{h+1,1}) + \sum_{i=2}^{h} \sum_{j=2}^{i} \pi(c_h)} \\ & \cdot \frac{l_z}{v_z} + \frac{v_z}{a_z} \\ =& \frac{4h^2 + (3 + (-3 - 6z)H)h + 6H^2\omega - 3H - 1}{6H \cdot \omega - 3h - 3} \cdot \frac{l_z}{v_z} + \frac{v_z}{a_z} \end{aligned} \tag{4.48}$$

In the perfect AS/R system from Figure 4.7 only two channel types c_h and $c_{h+1,1}$ are observed and therefore, a S/R machine must drive over $H - h$ storage locations to reach the channel of type c_h. However, such a perfect AS/R system may be obsolete for example after retrieving out of the first lane in Figure 4.7. If such

a retrieval happens, the next storage job must drive over more storage locations than $H - h$. The correction term of the channel time is added in Equation (4.49).

$$\begin{aligned} t_{Ch,S} = t_{Ch,S,\beta} &= \frac{(H-h)\cdot(1+\beta) + \frac{\sum_{i=1}^{h}\sum_{j=1}^{i} j}{H\cdot\omega}}{1+\beta} \cdot \frac{l_z}{v_z} + \frac{v_z}{a_z} \\ &= \frac{4h^2 + (2+(-3-6z)\cdot H)\cdot h + 6H^2\cdot\omega}{6H\cdot\omega - 3h} \cdot \frac{l_z}{v_z} + \frac{v_z}{a_z} \end{aligned} \tag{4.49}$$

4.5 Stack First Strategy

The Stack First strategy pursues the goal that all storage channels are either completely filled or empty. Additionally, storage channels can have other channel types after storage or retrieval jobs. However, the next storage or reshuffle jobs seek to eliminate these temporary channel types. For the determination of the channel type probabilities the other channel types are not relevant since the rack is continuous and the deviating channel types are very scarce compared to c_0 and c_H. It follows that the channel type probabilities only depend on ω:

$$\pi(c_h) = \begin{cases} 1-\omega & h = 0 \\ 0 & 0 < h < H \\ \omega & h = H \end{cases} \tag{4.50}$$

For retrieval jobs, only channels c_H are relevant and following the Equations (4.35) and (4.36), $P(\beta > 0) = 1 - \frac{1}{H}$ and

$$\beta = \frac{H-1}{2}. \tag{4.51}$$

The channel time for a retrieval job is only depending on the depth of the AS/R system:

$$t_{Ch,R} = \frac{1}{H} \cdot \sum_{h=1}^{H} (H+1-h) \cdot \frac{l_z}{v_z} + \frac{v_z}{a_z} = \frac{H+1}{2} \cdot \frac{l_z}{v_z} + \frac{v_z}{a_z} \tag{4.52}$$

When reshuffle jobs are necessary, the S/R machine must relocate 1 up to $H-1$ unit loads - depending on the location of the designated retrieval unit load - and therefore:

$$t_{C,R,\beta} = \frac{\sum_{h=1}^{H-1} \sum_{i=1}^{H-h} i}{\sum_{h=1}^{H-1} h} \cdot \frac{l_z}{v_z} + \frac{v_z}{a_z} = \frac{H+1}{3} \cdot \frac{l_z}{v_z} + \frac{v_z}{a_z} \tag{4.53}$$

Each dual command cycle contains at least one storage job. In an empty storage channel, the S/R machine must perform H steps. However, retrieval jobs may leave a storage channel, which is neither from type c_0 nor c_H. Therefore, the average channel distance for storage jobs are lower than H. The same applies for the reshuffle-storage component and thus $t_{Ch,S} = t_{Ch,S,\beta}$.

$$t_{Ch,S} = H - \frac{\sum_{h=1}^{H} \sum_{i=1}^{H-h+1} i - H}{\sum_{h=1}^{H} h} \cdot \frac{l_z}{v_z} + \frac{v_z}{a_z} = \frac{H+2}{3} \cdot \frac{l_z}{v_z} + \frac{v_z}{a_z} \tag{4.54}$$

4.6 Random Storage Channel Strategy with Nearest Neighbour Policy

The cycle time calculation is similar to Section 4.2 with difference in calculation of t_{StoR} and $t_{\text{Rto}\beta}$ because these movement times are not calculated following a random policy but the nearest neighbour policy. This means that for a storage job a storage channel as close as possible to the subsequent retrieval channel is chosen

and the same applies for a reshuffle job. t_{StoR} and $t_{\text{Rto}\beta}$ depend on the number of available storage channels with less than H unit loads stored (denoted as d) with $d = C \cdot \sum_{h=0}^{H-1} \pi(c_h)$. Following Han et al. (1987) together with the Equations (4.7) and (4.8), the times $t_{\text{StoR}} = t_{\text{Rto}\beta}$ are:

$$t_{\text{StoR}} = \frac{\int_0^1 X \cdot d(1 - G(X))^{d-1} \cdot g(X) \mathrm{d}X \cdot l_x L}{v_x} + \frac{1}{2} \cdot (\frac{v_x}{a_x} + \frac{v_y}{a_y}). \quad (4.55)$$

4.7 Random Storage Location Strategy with Nearest Neighbour Policy

The cycle time calculation is similar to the calculation in Section 4.3 and only the calculation of t_{StoR} and $t_{\text{Rto}\beta}$ is different than in Section 4.3. The calculation of t_{StoR} and $t_{\text{Rto}\beta}$ can be found in Equation (4.55).

4.8 Validation of Analytic Models for Automated Storage and Retrieval Systems

To validate the throughput models presented in the Sections 4.1 to 4.7, simulations are performed to compare the cycle times obtained in the simulations with the analytic models (the functionality of the simulation can be found in Appendix A.3). Since the calculation of the throughput with given cycle time t_{cycle} following Equation (4.1) is trivial, it is sufficient to validate the cycle time. The simulation consists of a warm-up phase to bring the AS/R system into a steady state of operation and the evaluation phase. The warm-up phase ends when the average cycle time of two consecutive blocks of $10,000$ dual command cycles changes less than $1\,\%$. The evaluation phase consists of $100,000$ dual command cycles. This ensures a half width of the $95\,\%$ confidence interval of the cycle times of less than $0.5\,\%$ of the cycle time t_{cycle}. Afterwards the mean and the $95\,\%$ confidence

interval (with lower bound CI_L and upper bound CI_U) for the cycle time t_{cycle} and the number of reshuffles per command cycle β are calculated. The relative errors compared to the mean δ and confidence interval δ_{CI} for t_{cycle} and β are:

$$\delta_X = \frac{\text{Analytic value X} - \overline{\text{Simulated value X}}}{\overline{\text{Simulated value X}}}$$

For validation, a baseline AS/R system is defined and varied afterwards for the most important influence factors on the cycle time. These are the depth of the system H, the number of channels in x- and y-direction (L and W) as well as the stock filling level ω. The baseline AS/R system is presented in Table 4.1 and the different configurations in Table 4.2. The homogeneous strategy leads to 256 channel types for $H = 8$ which makes a larger rack necessary to validate the model. L is set to 100 and W is set to 30 for configuration V and the homogeneous strategy.

Table 4.1: Parameters of the AS/R System for Validation of the Models in Chapter 4. Values are based on (Lehmann and Hussmann 2023).

l	w	ht	v_x	v_y	v_z	a_x	a_y	a_z	t_h	t_d
0.5	0.4	0.6	3	1	1.5	2	1.5	1	1	5

Table 4.2: Validation Configurations for the used AS/R System.

Configuration ID	L	W	H	ω
I	33	11	4	0.75
II	15	5	4	0.75
III	100	30	4	0.75
IV	33	11	2	0.75
V	33	11	8	0.75
VI	33	11	4	0.6
VII	33	11	4	0.9

Figures 4.8 and 4.9 show the validation results and the detailed results can be found in Appendix A.4. For all models $\delta \leq 3\,\%$ and thus the throughput models perform relatively accurate compared with models in the literature as can be observed when comparing with Table 3.2. The largest δ for the Homogeneous, RSCS, RSLS, Depth First, Stack First, and RSCS-NN strategies can be observed for configuration II with up to $\delta = 3\,\%$. This can be explained due to the relatively small AS/R system in configuration II with only 75 storage channels and thus the continuous rack face approach leads to these δ between analytic model and simulation. For the RSLS-NN strategy, the number of reshuffles are underestimated by up to $3\,\%$ in the analytic model (for configuration V) which is still in an acceptable range compared to literature.

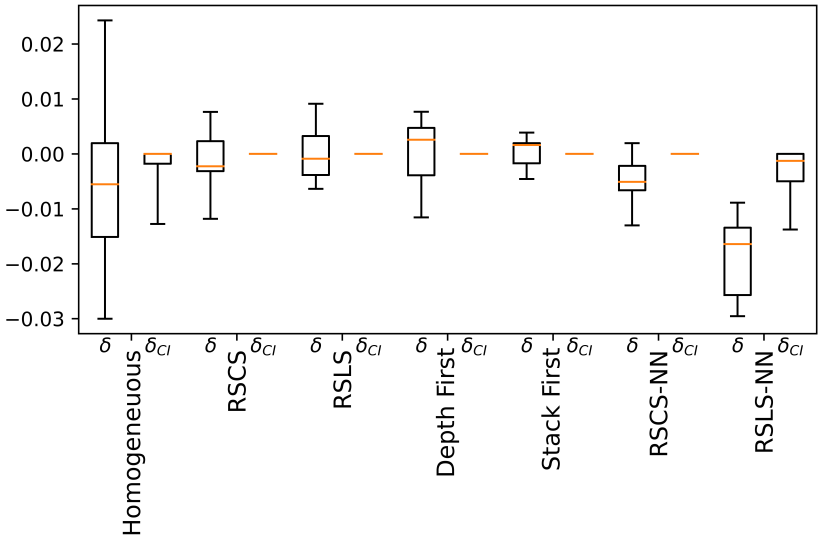

Figure 4.8: Validation Results for the Number of Reshuffles for all Configurations.

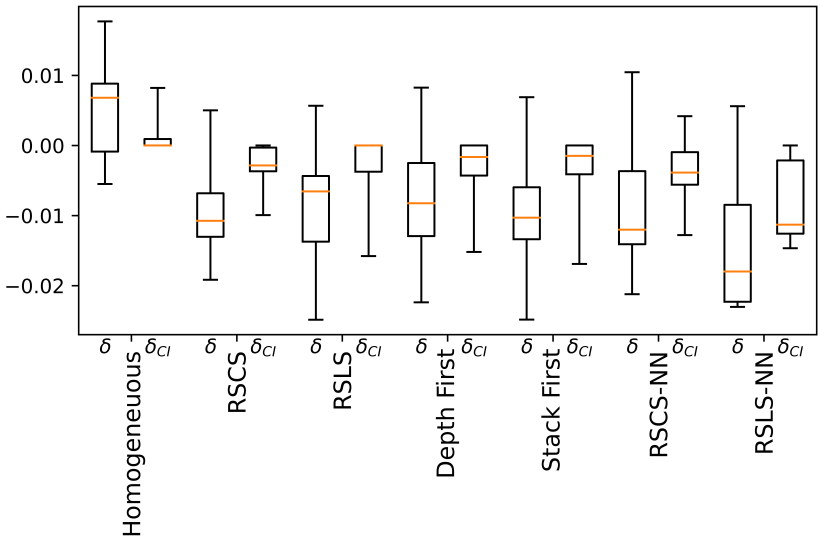

Figure 4.9: Validation Results for the Cycle Time for all Configurations.

5 Throughput Models for Robotic Compact Storage and Retrieval Systems for heterogeneous Unit Loads

The throughput models for the Random, Random-BBO, CBS-1, AutoStore, AS-LFR, CBS-3-BBO, ad CBS-3-RBP strategies will be derived in Section 5.1 and validated in Section 5.2. Based on industry data, a comparison and validation of operating strategies is shown in Section 5.3. Section 5.4 mainly discusses the performance of the AutoStore strategy compared with the other strategies and provides some managerial insights. Finally, Section 5.5 presents how all 13 operating strategies can be applied for AS/R and RCS/R systems.

The Sections 5.1 to 5.4 are cited from the sections "Throughput Models for RCS/R Systems", "Analytical Model Validation", "Results", and "Managerial Insights" of the paper "Digging Deep: Finding and Maximizing the Throughput Capacity of Multi-deep Storage Systems" currently under revision in *Transportation Science* (Lehmann and De Koster 2024).
The text, formal analysis and visualisation in this section have been taken from the paper with changes of technical terms, numbering of figures, equations, and sections, and symbols.
The author of this thesis was responsible for the conceptualisation, methodology, software, validation, formal analysis, investigation, writing (original draft), and visualisation of the research presented in these sections.

5.1 Throughput Model Derivation for Robotic Compact Storage and Retrieval Systems

The throughput estimation is based on the operating principle and strategies described in Sections 2.2 and 2.3. Furthermore, the following model assumptions are made:

1. The RCS/R system operates with one pick station located at position $(\frac{L}{2}, 0, 0)$ as shown in Figure 2.2b. It is assumed that K robots are exclusively assigned to one pick station and are either moving in the rack and transporting unit loads or waiting on top of the pick station. With these assumptions, it is straightforward to extend the models to more than one pick station.

2. One robot is assigned to a full command cycle consisting of a retrieval with corresponding reshuffle and return storage tasks. Robots do not collaborate but instead execute their command cycles in parallel.

3. Robot congestion on top of the rack grid does not occur. Only queuing on top of the pick station is considered. Note, that this assumption is reasonable if the robot density on the grid is not too large, as multiple shortest paths between locations exist, which can all be chosen by a robot.

4. The robot's drop-off and pick-up process at a pick station is synchronised with the time an operator needs to process a unit load. This implies that after dropping off a unit load, the robot can continue picking up a unit load previously picked at the pick station without additional waiting.

5. At the pick station, robots are served following an FCFS policy.

6. Products of the same class have the same access frequency, number of stored unit loads, and replenishment frequency.

7. The throughput model only considers the retrieval and subsequent storage of existing unit loads in the rack.

To estimate the throughput capacity of a given RCS/R system, it is modelled as a CQN with two server nodes (see Figure 5.1). In a CQN, retrieval jobs are always available and robots do not have to wait for new command cycles. The time needed for storage, reshuffles, and retrieval of a command cycle is assumed to be an exponentially distributed delay process (an infinite server, denoted by IS), with mean value $\frac{1}{\mu_{cycle}} = t_{cycle}$. In Appendix A.5, the distribution of the cycle time is analysed and it is showed that it indeed can be well approximated with a discrete exponential distribution. The service time of the pick station is assumed to be exponentially distributed with a mean value $\frac{1}{\mu_{pick}} = t_{pick}$ and the queuing discipline is FCFS. Note that, with these assumptions, the inter-arrival time at the pick station is also exponentially distributed. Robots may have to queue at the pick station while the operator is still handling a previous unit load and there are K robots in the network per pick station.

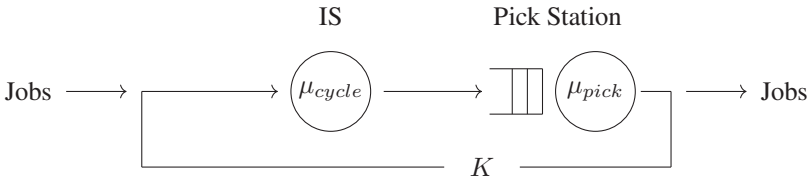

Figure 5.1: Closed Queuing Network with K Robots and two Server Nodes.

Section 5.1.1 derives the calculation of t_{cycle}. The proposed solution method is explained in Section 5.1.2 and based on these results, the throughput capacity (TP) can be calculated in retrieved unit loads per hour. The throughput capacity depends on the number of pick stations (PS) which is set to 1 in this work.

$$TP = \frac{3600\,\mathrm{s} \cdot PS \cdot K}{t_{cycle} + t_{wait} + t_{pick}}, \tag{5.1}$$

where t_{wait} represents the mean robot waiting time for service at the pick station. For RCS/R systems with $H > 12$ levels (such systems are quite common in practice), the calculation of t_{cycle} becomes too computation-time intensive. For

this reason, a regression approach is presented in Section 5.1.3 to estimate t_{cycle} for large values of H.

5.1.1 Cycle Time Calculation

The time t_{cycle} consists of three components: the time to take the requested unit load to the pick station, the time to return a finished unit load to a storage location, and the reshuffle movements of the robot on the grid. This last component depends on the number of reshuffles which in turn depends on the channel type from which the retrieval unit load is to be retrieved. If only the retrieval unit load is stored in the channel, no reshuffles occur. However, if the channel is fully occupied and the retrieval unit load is located at the bottom of the channel, then $H - 1$ reshuffles must be executed. Therefore, it is necessary to know the probability distribution of channel types in the steady state of the rack. Based on these channel type probabilities $\pi(c_{h,k})$ (Section 5.1.1.1), the number of reshuffles is calculated (Section 5.1.1.2) and the cycle time of the robots in the rack (Section 5.1.1.3) can be calculated. The calculation in all three subsections is strategy-dependent. Table 5.1 groups the seven strategies with identical calculations for each of the three sections. Calculations of strategies in the same group are identical for each section.

Table 5.1: Groups of Strategies with similar Calculation for Sections 5.1.1.1 to 5.1.1.3.

Section 5.1.1.1: Channel Type Probabilities $\pi(c_{h,k})$	Group 1	Random
	Group 2	Random-BBO, CBS-1
	Group 3	AutoStore, AS-LFR
	Group 4	CBS-3-BBO
	Group 5	CBS-3-RBP
Section 5.1.1.2: Number of Reshuffles β	Group 1	AS-LFR, CBS-3-RBP
	Group 2	Random, Random-BBO, CBS-1, AutoStore, CBS-3-BBO
Section 5.1.1.3: Robot Travel Times t_{cycle}	Group 1	Random, CBS-3-RBP
	Group 2	Random-BBO, AutoStore, AS-LFR, CBS-3-BBO
	Group 3	CBS-1

5.1.1.1 Calculation of Channel Type Probabilities

For the strategy in group 1, the steady state probabilities $\pi(c_{h,k})$ that channels are of type $c_{h,k}$ are provided by Lehmann and Hussmann (2022). In order to determine the probabilities that channels are of type $c_{h,k}$ in the steady state of the storage system for strategies of groups $2, 3, 4$, and 5, the system is modelled as a Markov chain and derive the steady state probabilities $\pi(c_{h,k})$. The state space of the Markov chain is determined by the channel types. Transitions between states are determined by the conditional probabilities $P(S_j|c_{h,k})$, that a storage job S_j of a unit load of class j occurs when channel type $c_{h,k}$ is considered and the conditional probabilities $P(R_j|c_{h,k,t})$, that a unit load of class j is requested (R_j), which is stored at location t when a channel type $c_{h,k}$ is considered with $\sum_{t=1}^{h} \pi(c_{h,k,t}) = \pi(c_{h,k})$. Note that $P(S_j) = f_j \cdot P(S)$, where f_j is the access probability of class j and $P(R_j) = f_j \cdot P(R)$. To ensure that the different classes and the total rack operate in a steady state, it is assumed that $P(S_j) = P(R_j)$, $\forall j$, and $P(S) = \sum_{i \in \{A,B,C\}} P(S_i) = 0.5$. Figure 5.2 shows the Markov chain for group 2 strategies of an RCS/R system with $H = 3$. In this simple case, only one product class (A) needs to be distinguished and the number of channel types equals 1 for every $h \in H$.

To solve for $\pi(c_{h,k})$ for all strategies of groups 2, 3, 4, and 5 from the equation $\pi \cdot M = \pi$ (with M the transition matrix of the Markov process), first $P(S_j|c_{h,k})$ and $P(R_j|c_{h,k,t})$ have to be expressed in terms of $\pi(c_{h,k})$. The sparse transition matrix M with positions (row and column indices) of $P(S_j|c_{h,k})$ and $P(R_j|c_{h,k,t})$ for all h, k and t, is described in Appendix A.6 for groups 2, 3, 4, and 5. With these, the balance equations, $\pi \cdot M = \pi$, can be drawn up for the Markov chain. With the additional constraints that $\sum_{h=0}^{H} \sum_{k=1}^{J^h} \pi(c_{h,k}) = 1$ and $\sum_{h=0}^{H} \sum_{k=1}^{J^h} \frac{h}{H} \cdot \pi(c_{h,k}) = \omega$, the equilibrium probabilities $\pi(c_{h,k})$ can be derived. It is now elaborated on how to calculate the transition probabilities $P(S_j|c_{h,k})$ and $P(R_j|c_{h,k,t})$ of the strategies in the groups.

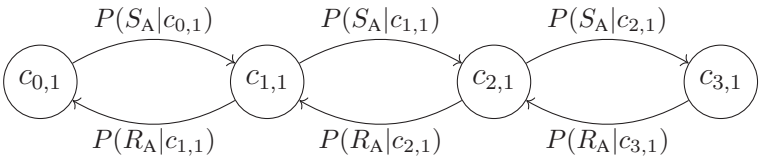

Figure 5.2: Markov Chain for Group 2 Strategies for an RCS/R System with $H = 3$ and $J = 1$.

The strategies in group 2 have in common that $J = 1$ and therefore $k = 1$ for all stack heights h, resulting in possible channel types $c_{0,1}, c_{1,1}, ..., c_{H,1}$ (for CBS-1, this is the case for every individual zone). Also, the BBO reshuffle policy is applied. To calculate the transition probabilities, Bayes' theorem is applied. It follows that $P(S_\mathrm{A}|c_{h,1}) = \frac{P(c_{h,1}|S_\mathrm{A}) \cdot P(S_\mathrm{A})}{\pi(c_{h,1})}$, where $P(c_{h,1}|S_\mathrm{A})$ is the probability that the channel type $c_{h,1}$ is selected for storage of a unit load of class $j =$A. This probability of selecting channel type $c_{h,1}$ is the probability of a channel type $c_{h,1}$ divided by the sum of probabilities of all channel types eligible for storage (i.e., with at least one free storage location). In analogy to this, $P(c_{h,1,t}|R_\mathrm{A})$ is the probability that a retrieval unit load is selected from $c_{h,1}$ at location t. It can be calculated as the quotient of $\pi(c_{h,1})$ and the sum of probabilities of all channel types with $h \geq 1$. From this, $P(S_\mathrm{A}|c_{h,1})$ for $h \leq H - 1$ and $P(R_\mathrm{A}|c_{h,1,t})$ for $h \geq 1$ and $t \leq h$ can be calculated as follows.

$$P(S_\mathrm{A}|c_{h,1}) = \frac{\pi(c_{h,1})}{\sum_{i=0}^{H-1} \pi(c_{i,1})} \cdot \frac{P(S_\mathrm{A})}{\pi(c_{h,1})} = \frac{P(S_\mathrm{A})}{\sum_{i=0}^{H-1} \pi(c_{i,1})} \quad , h \leq H-1 \tag{5.2}$$

$$P(R_\mathrm{A}|c_{h,1,t}) = \frac{\pi(c_{h,1})}{\sum_{i=1}^{H} i \cdot \pi(c_{i,1})} \cdot \frac{P(R_\mathrm{A})}{\pi(c_{h,1})} = \frac{P(R_\mathrm{A})}{\sum_{i=1}^{H} i \cdot \pi(c_{i,1})} \quad , h \geq 1, t \leq h. \tag{5.3}$$

The calculation of the transition probabilities for operating strategies of group 3 is similar to that of group 2. The difference is that the access frequencies f_j of the three classes $j \in \{\mathrm{A}, \mathrm{B}, \mathrm{C}\}$ are used to weigh the storage and retrieval

probabilities $P(S)$ and $P(R)$. Furthermore, the denominator in Equation (5.5) is the sum of the probabilities of all retrieval jobs where a unit load from class j is retrieved. Therefore, for all classes j, $P(S_j|c_{h,k})$ for $h \leq H-1$ and $P(R_j|c_{h,k,t})$ for $h \geq 1$ and $t \leq h$ is:

$$P(S_j|c_{h,k}) = \frac{f_j \cdot P(S)}{\sum_{i=0}^{H-1} \sum_{g=1}^{3^i} \pi(c_{i,g})} \tag{5.4}$$

$$P(R_j|c_{h,k,t}) = \begin{cases} \frac{f_j \cdot P(R) \cdot P(\beta_{j,h-t})}{\sum_{h'=1}^{H} \sum_{k'=1}^{3^{h'}} \sum_{t'=1}^{h'} \pi(c_{h',k'}) \cdot \mathbb{1}_{j|\text{class } j \text{ is at location } t'}} & \text{if class } j \text{ is at location } t \leq h \\ 0 & \text{else,} \end{cases} \tag{5.5}$$

where $P(\beta_{j,h-t})$ is the probability that $h-t \geq 0$ reshuffles are necessary when retrieving a product of class j from location t in a channel type $c_{h,k}$, thus weighing the probability of this specific retrieval possibility compared to all other retrieval possibilities. $P(\beta_{j,h-t})$ is derived in Equation (5.16) in Section 5.1.1.2.

For the group 4 strategy, all channel types are ranked by priority (see Section 2.3.2). The probability $P(c_{h,k}|S_j)$ that the channel type $c_{h,k}$ is selected for a storage job of a class j product is the probability that at least one channel of this channel type $c_{h,k}$ exists in the system multiplied with the probability that no channel of a type with higher priority $c_{h',k'}$ exists in the system (h' can either equal h or it can be any other level of the RCS/R system with a higher priority. Priorities of levels for products of the three classes A, B, and C are defined in Section 2.3.2). The probability that at least one channel of type $c_{h,k}$ exists is $1-\alpha(h,k)$ with $\alpha(h,k) = (1-\pi(c_{h,k}))^C$, with $C = L \cdot W$. The probability that no channel type with higher priority $c_{h',k'}$ exists is the product of $\alpha(h',k')$ over all channel types $c_{h',k'}$ with higher priority than the regarded channel type $c_{h,k}$. Channel types with higher priority than the regarded channel and the same number of stacked unit loads ($h = h'$) are channel types $c_{h,k'}$ with $k' = k+1...J^h$. Furthermore, the level h' depends on the class j of the product to be stored. As mentioned in Section 2.3.2, a different policy is applied to every class which determines which

channel types with which number of stacked unit loads h' have a higher priority than the channel types with h unit loads stacked. For example, the probability that any $c_{h,k}$ is selected for the next storage job of a class A product, is the product of the access frequency of class A products (f_{A}) and the probability that at least one channel of type $c_{h,k}$ exists in the rack ($1 - \alpha(h,k)$). This is multiplied with the probability that no channel type exists in the rack with the same h but higher priority ($\prod_{m=k+1}^{3^h} \alpha(h,m)$) and with the probability that also no channel type exists with $h' > h$ (thus higher priority for class A products) ($\prod_{m=1}^{H-h} \prod_{n=1}^{3^{h+m}} \alpha(h+m,n)$). For $h < H$ this results in:

$$P(c_{h,k}|S_{\mathrm{A}}) = f_{\mathrm{A}} \cdot (1 - \alpha(h,k)) \cdot \prod_{m=k+1}^{3^h} \alpha(h,m) \cdot \prod_{m=1}^{H-h} \prod_{n=1}^{3^{h+m}} \alpha(h+m,n). \tag{5.6}$$

In a similar fashion, $P(c_{h,k}|S_j)$ for the classes B and C of the group 4 strategy for $h < H$ can be obtained as:

$$P(c_{h,k}|S_{\mathrm{B}}) = f_{\mathrm{B}} \cdot (1 - \alpha(h,k)) \cdot \prod_{m=k+1}^{3^h} \alpha(h,m) \cdot \begin{cases} \prod_{m=\underline{B}}^{h-1} \prod_{n=1}^{3^{h-m}} \alpha(h-m,n) & \underline{B} \le h \le \overline{B} \\ \prod_{m=h+1}^{\overline{B}+\underline{B}-h-1} \prod_{n=1}^{3^{h-m}} \alpha(h-m,n) & h < \underline{B} \\ \prod_{m=\underline{B}+\overline{B}-h}^{h-1} \prod_{n=1}^{3^{h-m}} \alpha(h-m,n) & h > \overline{B} \end{cases} \tag{5.7}$$

$$P(c_{h,k}|S_{\mathrm{C}}) = f_{\mathrm{C}} \cdot (1-\alpha(h,k)) \cdot \prod_{m=k+1}^{3^h} \alpha(h,m) \cdot \prod_{m=1}^{h} \prod_{n=1}^{3^{h-m}} \alpha(h-m,n). \tag{5.8}$$

With Bayes' theorem, the conditional probability that a storage job S_j occurs when channel type $c_{h,k}$ is regarded is $P(S_j|c_{h,k}) = \frac{P(c_{h,k}|S_j) \cdot P(S_j)}{\pi(c_{h,k})}$. The probability $P(R_j|c_{h,k,t})$ is the same as for group 3 in Equation (5.5).

The only difference between the group 4 and group 5 strategy is the calculation of $P(c_{h,k}|S_j)$. In addition to the Equations (5.6) to (5.8)), the reshuffled unit loads are included in the storage probabilities, because a reshuffle in the CBS-3-RBP strategy can be regarded as an additional storage job for $h < H$:

$$P(c_{h,k}|S_{\mathrm{A}}) = (f_{\mathrm{A}} + \zeta_{\mathrm{A}})(1-\alpha(h,k)) \cdot \prod_{m=k+1}^{3^h} \alpha(h,m) \cdot \prod_{m=1}^{H-h} \prod_{n=1}^{3^{h+m}} \alpha(h+m,n) \tag{5.9}$$

$$P(c_{h,k}|S_{\mathrm{B}}) = (f_{\mathrm{B}} + \zeta_{\mathrm{B}})(1-\alpha(h,k)) \cdot \prod_{m=k+1}^{3^h} \alpha(h,m) \cdot \begin{cases} \prod_{m=\underline{B}}^{h-1} \prod_{n=1}^{3^{h-m}} \alpha(h-m,n) & \underline{B} \le h \le \overline{B} \\ \prod_{m=h+1}^{\overline{B}+\underline{B}-h-1} \prod_{n=1}^{3^{h-m}} \alpha(h-m,n) & h < \underline{B} \\ \prod_{m=\underline{B}+\overline{B}-h}^{h-1} \prod_{n=1}^{3^{h-m}} \alpha(h-m,n) & h > \overline{B} \end{cases} \tag{5.10}$$

$$P(c_{h,k}|S_{\mathrm{C}}) = (f_{\mathrm{C}} + \zeta_{\mathrm{C}})(1 - \alpha(h,k)) \cdot \prod_{m=k+1}^{3^h} \alpha(h,m) \cdot \prod_{m=1}^{h} \prod_{n=1}^{3^{h-m}} \alpha(h-m,n). \tag{5.11}$$

In these expressions ζ_j is the expected number of blocking unit loads of class j with

$$\zeta_j = \sum_{h=1}^{H} \sum_{k=1}^{3^h} \sum_{t=1}^{h} P(c_{h,k,t}|R_j) \cdot (h-t)).$$

Although the calculations of the Markov chain solutions of group 2 strategies are straightforward due to the small state space, the large state space and high exponents for the strategies of group 3, 4, and 5 require an iterative method to numerically obtain the channel type probabilities. Our iterative algorithm uses the power method (Bolch et al. 2006) and starts with a given state probability distribution that complies with the given stock filling levels $\omega_{\mathrm{A}}, \omega_{\mathrm{B}}$ and ω_{C}. The iterative algorithm converges towards the steady state because the Markov chain is positive recurrent and thus possesses only one steady state. This follows directly from the countable state space and the irreducibility of the Markov chain and transition matrix.

5.1.1.2 Calculation of Number of Reshuffles

The presented approach for calculating the number of reshuffles can be applied for both group 1 and group 2 strategies. However, the number of stored unit loads per product of class j (ξ_j) is set to 1 for group 2 strategies because the random retrieval unit load selection policy is used. This policy randomly selects a unit load of a given product and thus can be treated as if only one unit load of each product exists.

It is assumed that all unit loads of class j are equally distributed over all locations t in all channel types $c_{h,k}$ in which class j unit loads are stored. It is

also assumed that all unit loads of a single product ξ_j are equally distributed over all locations t in all channel types $c_{h,k}$ in which class j unit loads are stored. A combinatorial approach is chosen to calculate the probability that s reshuffles are necessary during the retrieval of a class j product. Therefore, the number of possible allocations is calculated of the ξ_j unit loads of a single product in the system that cause s reshuffles when the unit load that causes the fewest reshuffles is retrieved. This is then divided through all possible allocations of the ξ_j unit loads of a single product in the system.

Let γ_j be the total number of class j unit loads stored in the RCS/R system. Let $\rho_{j,s}$ be the total number of class j unit loads in the system causing $0 \leq s \leq H-1$ reshuffles when being retrieved. Then $\lambda_{j,0}$ is the total number of class j unit loads in the system causing more than 0 reshuffles when being retrieved which equals $\gamma_j - \rho_{j,0}$. The expressions $\rho_{j,s}$ and $\lambda_{j,s}$ can be calculated as:

$$\lambda_{j,0} = \gamma_j - \rho_{j,0} \tag{5.12}$$

$$\lambda_{j,s} = \lambda_{j,s-1} - \rho_{j,s} \tag{5.13}$$

$$\rho_{j,s} = \sum_{h=1}^{H} \sum_{k=1}^{J^h} \pi(c_{h,k}) \cdot C \cdot \tau_{j,s,h,k}, \tag{5.14}$$

$$\text{where} \quad \tau_{j,s,h,k} = \begin{cases} 1, & \text{if the unit load at } c_{h,k,h-s} \text{ is from class } j \\ 0, & \text{else} \end{cases}. \tag{5.15}$$

Note that $\rho_{j,s}$ can be calculated because $\pi(c_{h,k})$ is known and with $\pi(c_{h,k}) \cdot C$ it is known how many channels with type $c_{h,k}$ exist in the RCS/R system. To calculate the number of allocations of the ξ_j unit loads of a single product which cause s reshuffles, first all allocations are calculated in which one unit load causes s reshuffles and all remaining $\xi_j - 1$ unit loads cause more than s reshuffles with $\binom{\rho_{j,s}}{1} \cdot \binom{\lambda_{j,s}}{\xi_j - 1}$. This calculation is repeated for all $m \in \{1, ..., \xi_j\}$ unit loads causing the s reshuffles and $\xi_j - m$ unit loads causing more than s reshuffles. Only allocations in which at least s reshuffles are necessary are regarded because all other allocations lead to fewer than s reshuffles and are irrelevant for calculating the probability that s reshuffles are necessary. All calculated allocations are

summed up and divided by all possible allocations of the ξ_j unit loads of a single product in the system:

$$P(\beta_{j,s}) = \frac{\sum_{m=1}^{\xi_j} \left(\binom{\rho_{j,s}}{m} \cdot \binom{\lambda_{j,s}}{\xi_j - m} \right)}{\binom{\gamma_j}{\xi_j}}. \tag{5.16}$$

The expected number of reshuffles during a unit load retrieval for group 1 and 2 strategies can now be calculated as:

$$\beta = \sum_{j=1}^{J} \Big(f_j \cdot \sum_{s=0}^{H-1} \Big(s \cdot P(\beta_{j,s}) \Big) \Big). \tag{5.17}$$

5.1.1.3 Robot Travel Times

Section 2.2 describes all steps in the dual command cycle of a robot. The mean cycle time t_{cycle} (see Appendix A.7 for an estimate of the variance of the cycle time) for a dual-command cycle of a robot consists of the following movement and handling times for all seven strategies:

$$t_{cycle} = t_{\text{StoR}} + t_{\text{toHP}} + t_{\text{toS}} + 4 \cdot t_h + 2(t_{Ch,S} + t_{Ch,R}) + 3 \cdot t_{turn} + \beta \cdot t_\beta. \tag{5.18}$$

For group 1 strategies, t_{StoR} is the time a robot needs to drive from the last storage channel to the next retrieval channel and depends on the expected number d of all channels of type $c_{h,k}$ in the rack, which is given by $d = \pi(c_{h,k}) \cdot C$. The nearest neighbour movement policy is applied whenever possible. The smallest distance between a random retrieval channel of type $c_{h,k}$ and d randomly distributed storage channels is a random variable X_d with pdf:

$$g(X_d) = d \cdot (1 - G(x))^{d-1} \cdot g(x). \tag{5.19}$$

The expected distance $E(X_d)$ is

$$E(X_d) = \int_0^{l_x L + l_y W} (x \cdot g(X_d)) \mathrm{d}x, \tag{5.20}$$

where $G(x)$ and $g(x)$ are the probability distribution and density function, respectively, of the distance between two randomly selected channels in the grid. Both $g(x)$ and $G(x)$ are derived in Appendix A.7. $E(X_d)$ has to be calculated for every possible storage job and is then weighted with all other possible storage jobs, as indicated in Equation (5.21). This method of individual calculation and weighting with all other storage or retrieval job probabilities can be found throughout the remainder of this section. The resulting average travel time t_{StoR} is:

$$t_{\text{StoR}} = \frac{\sum_{h=0}^{H-1} \sum_{k=1}^{J^{h+1}} P(c_{h,k}|S) \cdot E(X_d)}{\sum_{h=0}^{H-1} \sum_{k=1}^{J^{h+1}} P(c_{h,k}|S) \cdot v_x} + 2 \cdot \frac{v_x}{a_x}. \tag{5.21}$$

$\frac{v_x}{a_x}$ is the approximate time for acceleration and deceleration of a single movement of the robot, based on Arnold and Furmans (2019). The robot drives in two directions for the vast majority of movements. Therefore, $\frac{v_x}{a_x}$ is taken twice in Equation (5.21)). Regardless of the unit load retrieval policy, the retrieval channel is randomly positioned in the rack. Therefore, the next storage channel with minimal distance to the retrieval channel is also randomly distributed in the rack, thus the travel times from the retrieval channel to the pick station (t_{toHP}) and the travel time from the pick station to the next storage channel (t_{toS}) are:

$$t_{\text{toHP}} = t_{\text{toS}} = \frac{l_x \cdot L + 2 \cdot l_y \cdot W}{4 \cdot v_x} + 2 \cdot \frac{v_x}{a_x}. \tag{5.22}$$

The derivation of Equation (5.22) is shown in Appendix A.7. The lift times $t_{Ch,R}$ and $t_{Ch,S}$ for group 1 are:

$$t_{Ch,S} = t_{Ch,R} = \frac{\sum_{h=0}^{H-1} \sum_{k=1}^{J^{h+1}} P(c_{h,k}|S) \cdot h \cdot l_z}{\sum_{h=0}^{H-1} \sum_{k=1}^{J^{h+1}} P(c_{h,k}|S) \cdot v_z} + \frac{v_z}{a_z}. \tag{5.23}$$

The robot only has to change direction on the grid of the RCSR system when the next channel is on another row and column as the previous one, which occurs with probability $\frac{L \cdot W}{L \cdot W - L - W}$. This leads to:

$$t_{turn} = \frac{L \cdot W}{L \cdot W - L - W} \cdot t_u \tag{5.24}$$

Furthermore, the time for one reshuffle t_β for group 1 consists of the following travel and handling times. The robot lowers the lift in the retrieval channel (taking time $t_{Ch,R,\beta}$), picks up the unit load (t_h), retrieves the lifting device ($t_{Ch,R,\beta}$), drives to a new storage channel ($t_{\text{Rto}\beta}$ and, if the robot changes direction, followed by t_{turn}), lowers the lifting device with the unit load ($t_{Ch,S,\beta}$), drops the unit load (t_h), retrieves the lifting device ($t_{Ch,S,\beta}$), and drives back to the retrieval channel ($t_{\text{Rto}\beta}$ + t_{turn}). This leads to:

$$t_\beta = 2 \cdot (t_2 + t_{Ch,R,\beta} + t_{Ch,S,\beta} + t_h + t_{turn}), \tag{5.25}$$

with t_2 being the same as t_{StoR} in Equation (5.21), $t_{Ch,R,\beta} = t_{Ch,R}$ and $t_{Ch,S,\beta} = t_{Ch,S}$ from Equation (5.23) and t_{turn} is obtained from Equation (5.24).

For group 2 strategies, t_{StoR}, t_{toHP}, t_{toS}, $t_{Ch,S}$ and t_{turn} are the same as in group 1 in Equations (5.21) to (5.24). However, the values t_β and the lift times $t_{Ch,R}$, $t_{Ch,R,\beta}$ and $t_{Ch,S,\beta}$ are calculated differently by considering that the blocking unit loads are taken back to the retrieval channel. The reshuffle time t_β for group 2 strategies is:

$$t_\beta = 4 \cdot (t_2 + t_{Ch,R,\beta} + t_{Ch,S,\beta} + t_h + t_{turn}). \tag{5.26}$$

The time a robot needs to travel from the retrieval channel to the reshuffle channel (t_2) for group 2 strategies does not regard all possible channel types but only those with $h = H - 1$ unit loads stored. Since the unit loads are only buffered temporarily, the exact channel type of channels with $H - 1$ unit loads is not relevant. Therefore, the expected number d, of channels of type $c_{H-1,k}$ is given by $d = \sum_{k=1}^{J^{H-1}} \pi(c_{H-1,k}) \cdot C$, and

$$t_2 = \frac{E(X_d)}{v_x} + 2 \cdot \frac{v_x}{a_x}, \tag{5.27}$$

with $E(X_d)$ from Equation (5.20). The lift times for group 2 are:

$$t_{Ch,R} = \frac{\sum_{h=1}^{H} \sum_{k=1}^{J^h} \sum_{j \in \text{A,B,C}} \sum_{t=1}^{h} P(c_{h,k,t}|R_j) \cdot h \cdot l_z}{\sum_{h=1}^{H} \sum_{k=1}^{J^h} \sum_{j \in \text{A,B,C}} \sum_{t=1}^{h} P(c_{h,k,t}|R_j) \cdot v_z} + \frac{v_z}{a_z} \tag{5.28}$$

$$t_{Ch,S,\beta} = \frac{l_z}{v_z} + \frac{v_z}{a_z} \tag{5.29}$$

$$t_{Ch,R,\beta} = \frac{\sum_{h=1}^{H} \sum_{k=1}^{J^h} \sum_{j \in \text{A,B,C}} \sum_{t=1}^{h} \sum_{s=1}^{h-t} P(c_{h,k,t}|R_j) \cdot (h-s) \cdot l_z}{\sum_{h=1}^{H} \sum_{k=1}^{J^h} \sum_{j \in \text{A,B,C}} \sum_{t=1}^{h} \sum_{s=1}^{h-t} P(c_{h,k,t}|R_j) \cdot v_z} + \frac{v_z}{a_z} \tag{5.30}$$

For the group 3 strategy, the expressions for t_{StoR} and $t_{\text{Rto}\beta}$ are similar to Equation (5.21) and Equation (5.27) with the difference, that the upper limit

of the integral of $E(X_d)$ depends on ω_j. The resulting $E(X_d)_j$ applied for calculation of t_{StoR} and $t_{\text{Rto}\beta}$ are for the three investigated classes j =A, B, and C:

$$E(X_d)_{\text{A}} = \int_0^{l_x L + \omega_A \cdot l_y W} (x \cdot g(X_d))\mathrm{d}x \tag{5.31}$$

$$E(X_d)_{\text{B}} = \int_0^{l_x L + 0.5 \cdot \omega_B \cdot l_y W} (x \cdot g(X_d))\mathrm{d}x \tag{5.32}$$

$$E(X_d)_{\text{C}} = \int_0^{l_x L + 0.5 \cdot \omega_C \cdot l_y W} (x \cdot g(X_d))\mathrm{d}x, \tag{5.33}$$

with $d = \pi(c_{h,k}) \cdot C$ for the calculation of t_{StoR} and $d = P(c_{1,H-1}) \cdot C$ for the calculation of $t_{\text{Rto}\beta}$. The values t_{toHP} and t_{toS} for the individual classes j =A, B, and C ($t_{\text{toHP,j}}$ and $t_{\text{toS,j}}$) can be calculated:

$$t_{\text{toHP,A}} = \frac{l_x L + \omega_j \cdot 2 l_y W + 0.5 \cdot l_y W(\omega_B + \omega_C)}{4 \cdot v_x} + 2 \cdot \frac{v_x}{a_x} = t_{\text{toS,A}} \tag{5.34}$$

$$t_{\text{toHP,B}} = \frac{l_x L + \omega_j \cdot 2 l_y W + 0.5 \cdot l_y W \cdot (\omega_C + \omega_A + 0.5 \cdot \omega_B)}{4 \cdot v_x} + 2 \cdot \frac{v_x}{a_x} = t_{\text{toS,B}} \tag{5.35}$$

$$t_{\text{toHP,C}} = \frac{l_x L + \omega_j \cdot 2 l_y W + 0.5 \cdot l_y W(\omega_B + \omega_A + 0.5 \cdot \omega_C)}{4 \cdot v_x} + 2 \cdot \frac{v_x}{a_x} = t_{\text{toS,C}}. \tag{5.36}$$

The combined values for t_{toHP} and t_{toS} are calculated by weight $t_{\text{toHP,j}}$ and $t_{\text{toS,j}}$ by the access frequencies of the classes f_j:

$$t_{\text{toHP}} = t_{\text{toS}} = \frac{\sum_{j=1}^{3} f_j \cdot t_{\text{toHP,j}}}{\sum_{j=1}^{3} f_j}. \tag{5.37}$$

t_{turn}, $t_{Ch,S}$, $t_{Ch,R}$, $t_{Ch,S,\beta}$ and $t_{Ch,R,\beta}$ are the same as in the Equations (5.23), (5.24) and (5.28) to (5.30).

5.1.2 Solution Approach for the Closed Queuing Network

In Section 5.2, a simulation model is introduced to validate our analytical models. This simulation model can also be used to analyse the distribution of t_{cycle} and of the interarrival time at the pick station for all seven strategies. The results are presented in Appendix A.5 and show that the interarrival time at the pick station can indeed be well approximated by an exponential distribution. Note that it is assumed that the service time at the pick station is exponentially distributed. Therefore, the Mean Value Analysis (MVA) can be applied to calculate the waiting times of the robots in front of the pick stations with $t_{wait} = T - t_{pick}$, where T is the mean response time at the pick station (see Bolch et al. (2006), Section 8.2.1, on how to calculate this). With t_{wait} the throughput capacity can be estimated using Equation (5.1).

5.1.3 Regression Models

For the AutoStore, AS-LFR, CBS-3-BBO, and CBS-3-RBP strategies, $\sum_{h=0}^{H} 3^h$ channel types result in a $O(3^H)$ complexity to solve the Markov chain. This cannot be done in reasonable time for large state spaces with $H > 12$. Therefore, regression models are introduced which can estimate the behaviour of systems with $H > 12$. The regressions are for the travel and reshuffle terms in Equation (5.18), based on expressions calculated in this section. The regression models are fit for various system configurations, all with height $H \leq 12$. For the AutoStore, AS-LFR, and CBS-3-BBO strategies, only t_{StoR}, $t_{\text{Rto}\beta}$, $t_{Ch,S}$, $t_{Ch,R}$, $t_{Ch,R,\beta}$ and β in Equations (5.18) and (5.26) depend on the result of the Markov chain. The travel time t_{StoR} converges towards the distance between two random channels in the rack which is:

$$\int_0^{l_x L} \int_0^{l_y W} \int_0^{l_x L} \int_0^{l_y W} (|i - i'| + |j - j'|) \mathrm{d}i \mathrm{d}j \mathrm{d}i' \mathrm{d}j' = \frac{l_x L + l_y W}{3} \quad (5.38)$$

and thus $t_{\text{StoR}} = \frac{l_x \cdot L + w_y \cdot W}{3 \cdot v_x} + 2 \cdot \frac{v_x}{a_x}$, for all $H > 12$. To obtain $t_{\text{Rto}\beta}$, $t_{Ch,R}$, $t_{Ch,S,\beta}$, $t_{Ch,R,\beta}$, and β linear regression can be applied. For the CBS-3-RBP strategy only t_{StoR}, $t_{\text{Rto}\beta}$, $t_{Ch,S}$, $t_{Ch,R}$ and β in the Equations (5.18) and (5.25) depend on the Markov chain. Both t_{StoR} and $t_{\text{Rto}\beta}$ converge towards the distance between two random channels and therefore $t_{\text{StoR}} = t_{\text{Rto}\beta} = \frac{l_x \cdot L + w_y \cdot W}{3 \cdot v_x} + \frac{v_x}{a_x}$. Quadratic regression can be used to estimate β, $t_{Ch,S}$, and $t_{Ch,R}$. Appendix A.8 presents the regression models and shows their fit, for $H \leq 12$, for one example layout.

5.2 Validation of Analytic Models for Robotic Compact Storage and Retrieval Systems

To validate the throughput model, an RCS/R system with a single pick station is simulated. The RCS/R system consisting of the rack, the robots, and the pick station are described in Section 2.2 and follow the same assumptions as introduced in Section 5.1. The flow diagrams of the simulation model for all the strategies and a description of how the unit loads and products are generated can be found in Appendix A.3. The model is implemented in Python. The simulation is divided into a warm-up and an operating phase. The warm-up phase ends when the rack has reached a steady state, which is characterised by a relative difference of less than $0.1\,\%$ for t_{cycle} of two consecutive blocks of $10,000$ command cycles each. After the warm-up phase, further dual command cycles are executed to evaluate the analytic models. $100,000$ command cycles are randomly generated after the warm-up phase following the corresponding strategies as described in Appendix A.3, leading to a $95\,\%$ confidence interval of the cycle times t_{cycle} where the half-width is less than $1\,\%$ of the average. Then, 100 blocks are randomly selected, each consisting of B command cycles from the total $100,000$ command cycles and calculate the mean and $95\,\%$ confidence interval (with lower bound CI_L and upper bound CI_U) for the most important performance indicators: the throughput capacity TP obtained from the CQN, the cycle time of a robot in the rack t_{cycle}, and the number of reshuffles per command cycle β. Then, the results

of the analytical model are compared with the mean and confidence intervals obtained from simulation. The relative errors compared to the mean δ for TP, t_{cycle} and β are:

$$\delta_X = \frac{\text{Analytic value X} - \overline{\text{Simulated value X}}}{\overline{\text{Simulated value X}}}$$

A baseline instance of the RCS/R system is set and subsequently alter the parameters (see Table 5.2). By sequentially fixing one variable at the base level and varying the others at the two alternative levels, 11 instances are evaluated (see Table 5.3). All other parameters of the RCS/R system are listed in Table 5.4.

Table 5.2: Values for the Variables of different Instances for Validation.

Variable	Alternative 1	Baseline	Alternative 2
C	1641	2500	5041
H	4	8	12
K	2	5	10
ω	0.6	0.75	0.9
B	10	50	100
$a_{\mathrm{A}}, a_{\mathrm{B}}, a_{\mathrm{C}}$	(1,1,1)	(6,3,3)	(20,10,5)

Table 5.3: Validation Instances.

ID	C	H	K	ω	B	a	ID	C	H	K	ω	B	a
I	2500	8	5	0.75	50	6,3,3	VII	2500	8	5	0.90	50	6,3,3
II	2500	8	5	0.75	50	1,1,1	VIII	2500	8	2	0.75	50	6,3,3
III	2500	8	5	0.75	50	20,10,5	IX	2500	8	10	0.75	50	6,3,3
IV	2500	8	5	0.75	10	6,3,3	X	5041	4	5	0.75	50	6,3,3
V	2500	8	5	0.75	100	6,3,3	XI	1681	12	5	0.75	50	6,3,3
VI	2500	8	5	0.60	50	6,3,3							

Table 5.4: Validation Parameters of the RCS/R System.

Variable	Values
l_x, l_y, l_z	0.7, 0.5, 0.25
v_x, v_z	4, 1.6
a_x, a_z	1.4, 1.4
f_A, f_B, f_C	$6, 2, 1$
ω_A,ω_B,ω_C	$15\,\%$, $20\,\%$, $40\,\%$
t_{pick}, t_h, t_u	20, 2, 1.2

Figure 5.3 shows the relative errors δ for the throughput capacity for all instances and the seven operating strategies. Detailed results per instance and strategy can be found in Tables A.5 and A.6 in Appendix A.9. Figure 5.3 shows that the absolute relative error for the throughput capacity is less than $3\,\%$, for all instances and strategies. However, not all estimation models perform equally accurately. The absolute relative error δ for t_{cycle} is less than $7\,\%$ for all strategies and instances. The error for β is also less than $7\,\%$ for all instances of the Random, Random-BBO, CBS-1, AutoStore, CBS-3-BBO, and CBS-3-RBP strategies. The relative error for β for instance III of the AS-LFR strategy is quite large: up to $43\,\%$. However, this large relative error is related to a small absolute error of this instance, since $\beta = 0.12$ in the analytical model and $\beta = 0.21$ in the simulation (see Table A.5 in Appendix A.9). It is the smallest number of reshuffles over all experiments and therefore does not cause a large error in the throughput capacity of instance III for AS-LFR ($TP = 163.66$ for the analytical model and $TP = 163.03$ for the simulation - see Table A.5 in Appendix A.9). Table 3.2 in the Literature Review section shows relative errors of related models in the literature. These range between $1\,\%$ (Lehmann and Hussmann 2021, Tutam et al. 2024) and $25\,\%$ (Ghomri and Sari 2017). We conclude that the models are sufficiently accurate and has comparable quality as other models in literature.

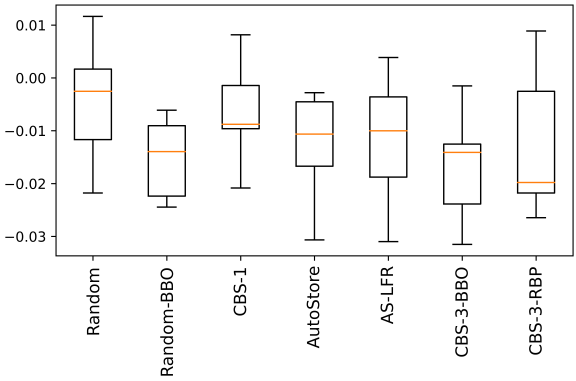

Figure 5.3: Relative Error δ for the Throughput TP over all Validation Instances for all Operating Strategies.

5.3 Results

This section compares the seven strategies to determine which yields the highest throughput. In Section 5.3.1, the dimensions of the rack (L, W and H) are varied to find the throughput maximising dimensions for every strategy. The throughput maximising ratio of length to width of the RCS/R systems is also determined for all seven strategies in Section 5.3.1. Section 5.3.2 compares the best operating strategies with the AutoStore benchmark strategy in more detail and Section 5.3.3 includes a case study with industry data and compares the two best performing strategies in a real-world application. The analytic models are used to maximise the system throughput for given system constraints.

5.3.1 Throughput Maximisation

The closed queuing network model solves rapidly (within a few seconds) for RCS/R systems. To determine t_{cycle} by solving the Markov-chain models take hours for systems with $H = 12$ (and seconds for $H = 2$). For larger heights, the regression model is used to determine t_{cycle}. The model can therefore be

used to optimise the system dimensions for throughput capacity maximisation. Assumptions are a rack capacity of about $20,000$ unit loads, $K = 5$ robots and one pick station, while the number of unit loads per product (ξ_A, ξ_B, ξ_C) equals $(6, 3, 3)$. All other characteristics are given in Table 5.4. The throughput capacity is maximised in two models, M1 and M2. M1 varies the depth of the system H and the number of channels in length L and width W direction. M2 additionally sets the $l_x L$ to $l_y W$ ratio r as an additional constraint.

M1:
$$\begin{aligned} \max \quad & TP \\ \text{s.t.} \quad & H \leq 24 \\ & L \cdot W \cdot H \geq 20,000 \\ & L, W, H \in \mathbb{N} \end{aligned}$$

M2:
$$\begin{aligned} \max \quad & TP \\ \text{s.t.} \quad & H \leq 24 \\ & L \cdot W \cdot H \geq 20,000 \\ & L, W, H \in \mathbb{N} \\ & \tfrac{l \cdot L}{w \cdot W} = r \end{aligned}$$

As the solution space is limited and the CQN solves sufficiently fast, the feasible values of L, W, and H for all seven strategies can be evaluated by full enumeration. Figure 5.4 shows the maximum throughput capacities for all possible values of $H \leq 24$ (Meller (2023) indicates a maximum of 24 stacked unit loads in an AutoStore system). The maximum throughput capacity is achieved for the AS-LFR strategy for $H = 3$, $L = 94$ and $W = 71$ with 163.6 cycles per hour closely followed by the CBS-3-RBP strategy for $H = 3$, $L = 94$ and $W = 71$ with 162.6 cycles per hour. If a footprint restriction is added to the maximisation problem of e.g., $1000\,\mathrm{m}^2$, the maximum throughput capacity drops to 150.5 cycles for the AS-LFR strategy and to 157.9 cycles for CBS-3-RBP (with $H = 8$ for both strategies). All strategies have in common that the maximum throughput capacity decreases with higher values of H. The two best performing strategies (AS-LFR and CBS-3-RBP) are used together with the AutoStore strategy as benchmarks to apply M2 by full enumeration. The highest throughput can be achieved for the ratios $r = 1.92$ for AutoStore, $r = 1.85$ for AS-LFR, and $r = 1.85$ for the CBS-3-RBP strategy (see Figure 5.5a). Note that all three ratios are between 1 and 2, which is also the result of an analytical derivation of the lower and upper bounds of the throughput-maximising ratio. In Appendix A.1, the maximum

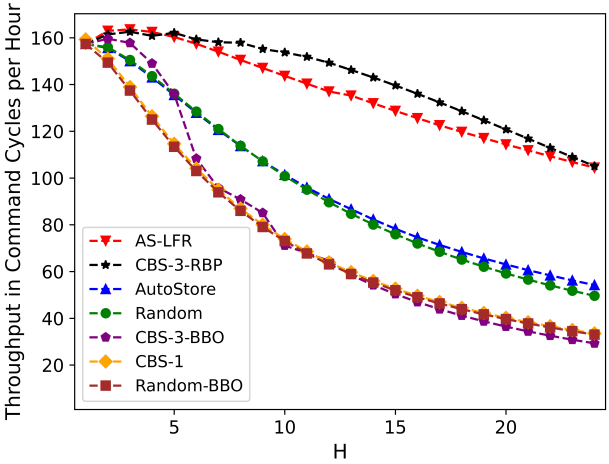

Figure 5.4: Results for Model M1: Maximum Throughput Capacity for every $H \leq 24$.

throughput capacity is achieved for a ratio r of $l_x \cdot L$ and $w_y \cdot W$ between 1 and 2 for all seven strategies. Figure 5.5a also shows that the maximum throughput is relatively insensitive to the length to width ratio of the system. Figure 5.5b shows that the throughput maximising value H does not change in the relevant area for $1 \leq r \leq 2$.

5.3.2 Operating Strategies Discussion

The CBS-3-RBP and AS-LFR strategies yield the overall highest throughput capacities because they both apply the LFR unit load selection policy, which is designed to reduce reshuffles. Although they yield comparable results regarding throughput capacity and number of reshuffles (see Table A.5 in Appendix A.9), the operating principles are different. In the CBS-3-RBP strategy, every reshuffle acts as a storage job to a specific channel type, which leads to a relatively high travel time per movement of the reshuffle. In contrast, the AS-LFR strategy requires a reshuffled unit load to be transported back to the original channel (BBO

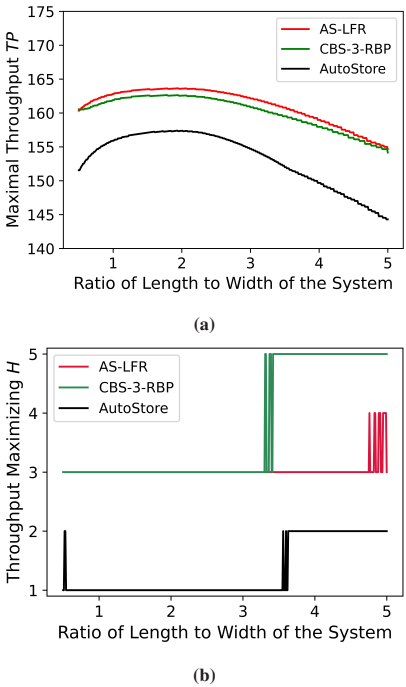

Figure 5.5: Results for Model M2: Maximum Throughput (a) and the resulting value of H (b) for Length to Width Ratios of the System between 0.5 and 5 in 0.01 Steps.

reshuffle policy), causing more robot movements, each with a relatively short travel time. As a consequence, no strategy strictly dominates the other; both yield higher throughput capacities for different model parameters.

The AutoStore strategy leads to a relatively low throughput capacity, which can be up to $48.5\,\%$ less compared to the CBS-3-RBP strategy for storage systems with $H > 8$ (see Figure 5.4). To further compare the two best performing strategies and the AutoStore strategy, the number of unit loads per product in class A is varied. In Figure 5.6 ξ_B and ξ_C are set to $\xi_B = 1$ and $\xi_C = 1$ and only vary ξ_A, and observe the impact of the number of unit loads per product on throughput capacity. It can be seen that the throughput capacity increases

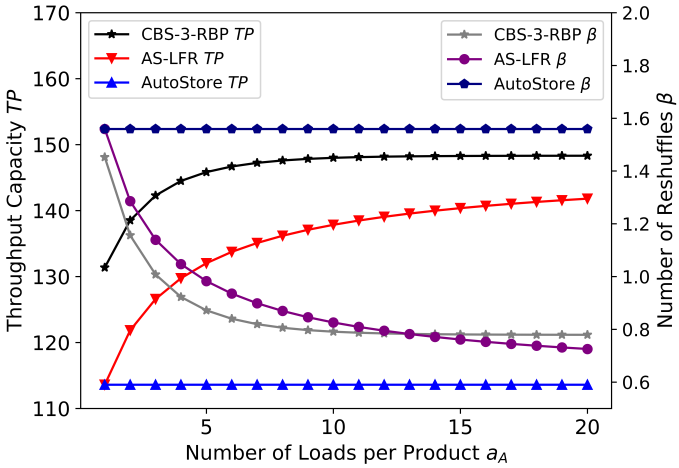

Figure 5.6: Throughput Capacity and Number of Reshuffles of the CBS-3-RBP, AS-LFR, and AutoStore Strategies for varying Number of Unit Loads per Product of Class A.

for an increasing number of unit loads per product for both the CBS-3-RBP and AS-LFR strategies, with the LFR retrieval unit load selection policy. The reason for this is the decreasing number of reshuffles per retrieval. Note that this effect is also decreasing in itself, leading to concave throughput capacity curves. However, the throughput capacity for the AutoStore strategy does not change, because the strategy cannot exploit the additional information as it draws a unit load randomly from all unit loads of the same product during retrieval.

In Table 5.5, the channel type probabilities $\pi(c_{h,k})$ are aggregated over all levels h of the RCS/R system with instance I. It shows the percentage of unit loads of class A in each level h. When comparing the newly introduced CBS-3-BBO and CBS-3-RBP strategies, it can be observed that both strategies achieve different effective allocation of unit loads to the corresponding zones. Only $75\,\%$ of class A unit loads are stored in zone A in the CBS-3-BBO strategy, compared to $100\,\%$ in the CBS-3-RBP strategy (see Table 5.5). The latter strategy thus preserves the

zones of classes better. This reduces the number of reshuffles (see Table A.5 in Appendix A.9).

Table 5.5: Share of Unit Loads of Class A stored in Level h in the Steady State.

h	Designated Zone	CBS-3-BBO	CBS-3-RBP
8	A	20.2 %	33.3 %
7	A	20.4 %	33.3 %
6	A	18.2 %	33.4 %
5	B and A	15.7 %	0.0 %
4	C and B	12.5 %	0.0 %
3	C	8.6 %	0.0 %
2	C	3.8 %	0.0 %
1	C	0.6 %	0.0 %

5.3.3 Case Study with Industry Data

A dataset was obtained from a spare parts storage system in the automotive industry, performing $181,568$ dual command retrieval and storage jobs in one year. The company considers installing an RCS/R system with an optimal layout configuration which can store the same number of unit loads and products with a maximum throughput capacity. Compared to the randomly generated data of the previous section, the data from the current storage and retrieval jobs show some differences. For each retrieval from the generated data, first a class is randomly generated according to the demand frequency and then randomly draw a product from this class. This procedure makes it unlikely that two unit loads of the same product are retrieved back to back and ensures that the retrievals of unit loads of the same product are spread evenly over the whole review period. However, the industry data contain sequences of storage and retrieval jobs of the same product back to back as well as the storage and retrieval of all unit loads of one product within one day or week. Furthermore, for the model it is assumed that all products of one class have the same number of unit loads per product and the same access

frequency. This is typically not the case for real storage systems.

The analytical models of the two best performing strategies from Section 5.3.1 (AS-LFR and CBS-3-RBP) are applied with these industry data. The products are divided in three classes based on demand frequency (Class A: Accessed once a week or more often. Class B: Accessed once a month or more often. Class C: All other products). In the industry dataset, the access frequency and the number of unit loads per product follow an empirical distribution from which the average number of unit loads per product and the access frequency for each class can be extracted which are used in our analytic model. All specific warehouse characteristics can be found in Table 5.6.

Table 5.6: Model Parameters for Validation with Industry Data.

L, W, H	l_x,l_y,l_z	K	B	a
$50, 40, 8$	$0.7, 0.5, 0.25$	5	50	$7, 3, 2$
f	$\omega_{\mathrm{A}}, \omega_{\mathrm{B}}, \omega_{\mathrm{C}}$	v_x, a_x	v_z, a_z	t_{pick}, t_h, t_u
$6, 2, 1$	$0.21, 0.19, 0.35$	$4\,\mathrm{m/s}, 1.4\,\mathrm{m/s^2}$	$1.6\,\mathrm{m/s}, 1.4\,\mathrm{m/s^2}$	20, 2, 1.2

First the analytical models are validated for the AS-LFR and CBS-3-RBP strategies based on simulation. The same criteria are applied for the warm-up phase and command cycle evaluation for validation as in Section 5.2. The results in Table 5.7 show that both models validate well for the throughput capacity. Errors are below 6%. The CBS-3-RBP strategy produces good overall approximations, also for the number of reshuffles and t_{cycle}.

Table 5.7: Analytic Model Results for the AS-LFR and CBS-3-RBP Applied for Industry Data.

	TP			t_{cycle}			β		
	Ana	Sim	δ	Ana	Sim	δ	Ana	Sim	δ
AS-LFR	148.07	158.04 $\pm$4.19	-0.06	75.17	64.05 $\pm$2.83	0.17	0.57	0.42 $\pm$0.06	0.36
CBS-3-RBP	154.94	156.63 $\pm$3.38	-0.01	66.67	67.36 $\pm$2.02	-0.01	0.55	0.57 $\pm$0.06	-0.04

Figure 5.7 shows the maximum throughput for $1 \leq H \leq 24$ for the AS-LFR and CBS-3-RBP strategies using the industry data and the system characteristics of Table 5.6 (except for H, L, and W). It can be observed that the overall maximum throughput of 164.8 command cycles per hour can be achieved using the CBS-3-RBP strategy for a system with $H = 3$, $L = 89$, and $W = 60$. In the industry case, the available floor space is limited to $500\,\mathrm{m}^2$ which results in the maximum throughput of 146.2 command cycles for the CBS-3-RBP strategy, achieved with $H = 12$, $L = 43$, and $W = 31$.

Therefore, it is recommended for the company to use an RCS/R system with $H = 12$, $L = 43$, and $W = 31$ which results in a length to width ratio of 1.94:1 and to use the CBS-3-RBP strategy.

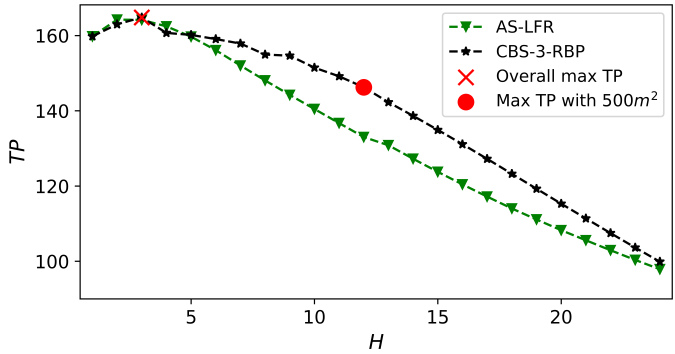

Figure 5.7: Results for Model M1 and the Industry Data: Maximum Throughput Capacity for every $H \leq 24$

5.4 Managerial Insights

The results obtained from the models and numerical results lead to some interesting managerial insights for RCS/R (and, in extension, for multi-deep AS/R) systems. These are summarised first. Following that, four research questions are

addresses which have been raised by Meller (2023).

Well-performing operating strategies. These strategies focus on reducing the number of reshuffles during operation, since our results and model comparison shows that this is the most influential factor impacting the throughput capacity (see number of reshuffles and throughput capacity for all strategies and instances in Table A.5 in Appendix A.9). The CBS-3-RBP strategy leads to the overall highest throughput capacity, also when no information about the number of stored unit loads per product is available.

Reshuffling strategies. The market leader, AutoStore, currently uses the BBO policy to reshuffle blocking unit loads (Meller 2023).However, the RBP policy can lead to fewer reshuffles, which means fewer robots are needed to achieve the same throughput. Fewer robots also lead to less congestion, which can enhance throughput capacity. These findings are also valid if the number of unit loads per article is set to 1 as shown for instance II in Table A.5 in the Appendix A.9. Another advantage of the RBP strategy is that the reshuffles lead to a continuous mixing of the unit loads of the same product which makes this policy suitable even for perishable goods.

Layout considerations. Our results in Figure 5.5 clearly show that RCS/R systems with a $l_x \cdot L : w_y \cdot W$ footprint ratio between 1:1 and 2:1 yield maximum throughput capacity. Particularly in the design phase, there is some freedom in the footprint ratio. A ratio closer to these values can increase the throughput capacity by up to $3.9\,\%$ compared to a ratio of 1:2 and up to $1.7\,\%$ compared to a ratio of 3:1 when the AutoStore strategy is applied. The results in the Figures 5.4 and 5.5 also show that systems with $H \leq 5$ should be preferred if the throughput capacity is weighted higher than space requirements.

Impact of number of unit loads per product and access frequency per class. Whenever the access frequency of products is known or can be estimated, a strategy should be used that can make use of this information (AS, AS-LFR, CBS-3-BBO, or CBS-3-RBP). Our results presented in Figure 5.4 show that these

strategies can increase the throughput capacity by up to $218.7\,\%$ compared to strategies which do not use any of this information (Random-BBO). Strategies that also can select a proper unit load of a product (CBS-3-RBP, AS-LFR) can gain up to $94.1\,\%$ throughput capacity compared to strategies that only use the access frequency (AutoStore). As shown in Section 2.2 and Appendix A.2, for the case of multiple stored unit loads per product, a chaotic storage assignment outperforms a storage assignment which clusters unit loads of the same product. Exceptions should only be made if there are enough unit loads of the same product to fill a whole channel with one product and if these are retrieved shortly after each other. In such a case, unit loads of the same product should be stored in the same channel.

In his paper, Meller (2023) states four research questions concerning the choice of operating strategies and operational information important for managers of RCS/R systems. This section aims to provide at least partial answers to these research questions.

First, Meller (2023) questions whether AutoStore's BBO reshuffle policy should be used and suggests to critically question the fact that blocking unit loads are returned in the same order as they are retrieved. The throughput models show that the BBO reshuffle policy can lead to fewer reshuffles compared to the random reshuffle and RBP reshuffle policies (see Table A.5 in Appendix A.9). However, the reshuffling process for the BBO policy is time-consuming because the blocking unit loads are taken back and thus a robot has to perform two movements for a blocking unit load. This time-consuming reshuffling nullifies the lower number of reshuffles, yielding a similar throughput capacity for the AutoStore and the benchmark Random strategy. It is concluded that the RBP policy should replaced the BBO policy so that unit loads are not returned to their channel after the reshuffle.

Second, Meller (2023) asks how storage channels for new and returning unit loads should be selected, thereby addressing the storage location selection problem. Therefore, it is important to store a unit load close to a next retrieval channel, if known. Furthermore, any strategy that employs class-based storage should be

preferred.

Third, Meller (2023) questions the AutoStore claim that $80\,\%$ of unit loads are retrieved from the top $20\,\%$ levels if a 20/80 distribution for class A, B and C articles is assumed. Taking into account a rack-filling level of $z = 0.75$, this is translated to a claim that $80\,\%$ of unit loads cause fewer than two reshuffles for a $H = 10$ system. Table 5.8 shows that for an example system only $60.9\,\%$ of retrievals cause fewer than two reshuffles. Our results are therefore more pessimistic than AutoStore's claim.

Fourth, Meller (2023) asks how long it takes until a rack reaches the steady state, after starting the operation of the rack. Table 5.9 presents simulation results for the seven strategies and the baseline instance I of the validation. It shows the number of command cycles and operating time the RCS/R system needs to reach less than either $0.1\,\%$ or $1\,\%$ deviation from the steady state. It is concluded that the CBS-3-RBP strategy achieves a steady state (with 0.1% deviation) within 24 working days, assuming 16 hours of operation of the storage system per day.

Table 5.8: Distribution of Number of Reshuffles for Unit Loads of Classes A, B, C, and Overall System with $H = 10$, $C = 2000$, $K = 5$, $a = (1, 1, 1)$, $f = (8, 1, 1)$, $z = (0.15, 0.2, 0.4)$, AutoStore Strategy. Characteristics are from Table 5.4.

s	0	1	2	3	4	5	6	7	8	9
$P(\beta_{A,s})$	0.428	0.290	0.164	0.076	0.029	0.009	0.002	0.000	0.000	0.000
$P(\beta_{B,s})$	0.085	0.127	0.157	0.165	0.152	0.125	0.091	0.058	0.030	0.010
$P(\beta_{C,s})$	0.047	0.077	0.108	0.132	0.144	0.144	0.131	0.107	0.074	0.037
$P(\beta_s)$	0.356	0.253	0.158	0.091	0.053	0.034	0.024	0.017	0.010	0.005

Table 5.9: Number of Command Cycles and Time for the Strategies to reach the Steady State.

Threshold		Random	Random-BBO	CBS-1	AutoStore	AS-LFR	CBS-3-BBO	CBS-3-RBP
0.1 %	Command Cycles	130,000	20,000	50,000	40,000	440,000	120,000	60,000
	Time [h]	1139	229	549	348	2940	1287	375
1 %	Command Cycles	10,000	20,000	10,000	40,000	30,000	50,000	10,000
	Time [h]	88	229	110	348	200	536	63

5.5 Transfer of Throughput Models to other Storage Systems

Multi-deep AS/R systems and RCS/R systems are similar systems and the models developed for the one system can be adapted for the other system. An RCS/R system can be regarded as 90 rotated AS/R system with the I/O point or pick station located at a different location. Therefore, this section shows how all 13 developed models can be adapted to the respective other storage system. For both AS/R and RCS/R systems the throughput capacity depends on the cycle time t_{cycle} with:

$$TP_{AS/R} = \frac{3600\,\mathrm{s}}{t_{cycle}} \tag{5.40}$$

$$TP_{RCS/R} = \frac{3600\,\mathrm{s} \cdot PS \cdot K}{t_{cycle} + t_{wait} + t_{pick}}. \tag{5.41}$$

The formulas for t_{cycle} for the 13 operating strategies (Equations (4.2), (4.3) and (5.18)) can be taken for both AS/R and RCS/R systems. The variables $t_{Ch,S}$, $t_{Ch,R}$, $t_{Ch,S,\beta}$, $t_{Ch,R,\beta}$, β, and $P(\beta_{j,s})$ are the same for all operating strategies for AS/R and RCS/R systems. Only t_{StoR}, $t_{\mathrm{Rto}\beta}$, t_{toHP}, and t_{toS} depend on the system because the I/O point or pick station is at a different location and the S/R machine in an AS/R system uses the Chebychev metric and robots in an RCS/R system use the Manhattan metric.

t_{StoR} and $t_{\text{Rto}\beta}$ depend on the pdf and cdf of a random variable X which is the distance between two random channels in an AS/R or RCS/R system. pdf and cdf for an AS/R system are defined in Equations (4.7) and (4.8), pdf and cdf for an RCS/R system are defined in Equations (A.5) and (A.6). t_{toHP} and t_{toS} are defined in Equation (4.5) for AS/R systems and in Equation (5.22) for RCS/R systems. For all models the formulas for t_{StoR}, $t_{\text{Rto}\beta}$, t_{toHP}, and t_{toS} can be exchanged to make a model for the other storage system.

One exception is the calculation of t_{toHP} and t_{toS} for the CBS-1 strategy due to the different zone allocation for AS/R and RCS/R systems. t_3 and t_{toS} for the CBS-1 strategy and for AS/R systems can be found in Hausman et al. (1976).

With t_{cycle} it is directly possible to calculate TP in Equation (5.40). For TP in Equation (5.41), the same CQN as shown in Figure 5.1 must be solved. The same solution approach as shown in Section 5.1.2 can be used.

6 Comparison and Evaluation of Operating Strategies

The Chapters 4 and 5 have introduced 13 operating strategies for AS/R and RCS/R systems. As summarised in Table 3.3, these operating strategies apply different allocation structure policies, storage assignment policies, reshuffle policies, retrieval unit load selection policies, and movement policies. In this chapter, the effect of the operating strategies on the cycle time and throughput capacity of different AS/R and RCS/R systems is evaluated. As shown in Equations (4.1) and (5.1), the throughput depends mainly on the cycle time, and hence this chapter focuses on it. As discussed in the previous chapters, the cycle time for each operating strategy depends on a variety of parameters. The interesting parameters for storage planers are: The number of storage locations, the depth of the system, the access frequency and number of unit loads per product, the velocity and acceleration of the load handling devices, and the size of the unit loads. Experiments are conducted to gain insights on the effects of changing operating strategies and parameters. With knowledge about the effect of an increase or decrease of these parameters, the storage planners can preselect operating strategies and do not have to evaluate new AS/R or RCS/R systems with all available operating strategies to find the throughput maximising operating strategy.

The design of experiments is introduced in Section 6.1. This is followed by the evaluation of AS/R systems in Section 6.2 and RCS/R systems in Section 6.3. In each section operating strategies are analysed for both homogeneous and heterogeneous unit loads. The insights are summarised in Section 6.4 and further

managerial implications are given in this section. This also includes limitations of the developed models.

6.1 Design of Experiments

The parameters[1] and steps of the parameters for the experiments are explained in this section.

Number of storage locations $L \cdot W \cdot H$: The number of storage locations and thus storage capacity in common multi-deep storage systems range from a few thousand to hundreds of thousands unit loads. The steps $10000, 50000, 100000$ are chosen for this design of experiments to represent this range.

Access frequency f and number of unit loads per product ξ: Products with a high access frequency usually also have more unit loads stored in the system. Therefore, both parameters are summarised in one factor. The relevant steps reach from the same access frequency of all products and only one unit load per product (basically homogeneous unit loads) to clear distinction between the classes. The chosen steps are:

- $f = (1, 1, 1), \xi = (1, 1, 1)$
- $f = (10, 2, 1), \xi = (5, 2, 1)$
- $f = (100, 10, 1), \xi = (20, 10, 5)$

Depth of the AS/R or RCS/R system H: AS/R systems are usually single to quadruple-deep but it is also possible to design AS/R systems with depth up to $H = 12$ and therefore, relevant depths for AS/R systems are $H \in 1, ..., 12$. According to Meller (2023) RCS/R systems are build with $H \leq 24$ and the steps in this section are $H \in 1, ..., 24$ for RCS/R systems.

[1] Also called factors according to Siebertz et al. (2017).

Handling-to-driving-ratio θ: The size of the unit loads and storage locations, velocity and acceleration of the S/R machine or robot, and handling times to pick and drop unit loads can be summarised as one factor. This can be achieved by normalising the driving time and the handling time of the S/R machine or robot. The driving time of an S/R machine or robot from one corner of the rack to the diagonally opposite corner of the rack is used for normalisation of the driving time. Normalisation of the handling time of the telescopic arm or lifting device of the robot is realised by dividing the time needed for all handling operations during a dual command cycle by the time needed for one drive to the rear/bottom, handling of a unit load and driving back.

With Equations (4.2), (4.3) and (5.18), the normalised driving time t_{dg} and handling time t_{hg} can be calculated for AS/R and RCS/R systems as follows:

$$t_{dg,AS/R} = \frac{t_{\text{StoR}} + t_{\text{toHP}} + t_{\text{toS}} + 2 \cdot \beta \cdot t_{\text{Rto}\beta}}{\max(\frac{L \cdot l_x}{v_x} + \frac{v_x}{a_x}, \frac{W \cdot w_y}{v_y} + \frac{v_y}{a_y})} \tag{6.1}$$

$$t_{dg,RCS/R} = \frac{t_{\text{StoR}} + t_{\text{toHP}} + t_{\text{toS}} + 2 \cdot \beta \cdot t_{\text{Rto}\beta}}{\frac{L \cdot l_x}{v_x} + \frac{v_x}{a_x} + \frac{W \cdot w_y}{v_y} + \frac{v_y}{a_y} + t_{turn}} \tag{6.2}$$

$$t_{hg} = \frac{4t_h + 2t_{Ch,S} + 2t_{Ch,R} + 2\beta(t_h + t_{Ch,R,\beta} + t_{Ch,S,\beta})}{t_h + 2 \cdot (\frac{l_z \cdot H}{v_z} + \frac{v_z}{a_z})}. \tag{6.3}$$

For the Homogeneous strategy and the operating strategies applying the BBO reshuffle policy, the normalised driving and handling times are:

$$t_{dg,AS/R,Hom.} = \frac{t_{\text{StoR}} + t_{\text{toHP}} + t_{\text{toS}} + 2\beta t_{\text{Rto}\beta} + P(\beta)(t_{\text{toHP}} + t_{\text{toS}} - t_{\text{Rto}\beta})}{\max(\frac{L \cdot l_x}{v_x} + \frac{v_x}{a_x}, \frac{W \cdot w_y}{v_y} + \frac{v_y}{a_y})} \tag{6.4}$$

$$t_{dg,RCS/R,Hom.} = \frac{t_{\text{StoR}} + t_{\text{toHP}} + t_{\text{toS}} + 2\beta t_{\text{Rto}\beta} + P(\beta)(t_{\text{toHP}} + t_{\text{toS}} - t_{\text{Rto}\beta})}{\frac{L \cdot l_x}{v_x} + \frac{v_x}{a_x} + \frac{W \cdot w_y}{v_y} + \frac{v_y}{a_y} + t_{turn}} \tag{6.5}$$

$$t_{hg,Hom.} = \frac{4t_h + 2t_{Ch,S} + 2t_{Ch,R} + 4\beta(t_h + t_{Ch,R,\beta} + t_{Ch,S,\beta})}{t_h + 2 \cdot (\frac{l_z \cdot H}{v_z} + \frac{v_z}{a_z})} \tag{6.6}$$

$$t_{dg,AS/R,BBO} = \frac{t_{\text{StoR}} + t_{\text{toHP}} + t_{\text{toS}} + 4 \cdot \beta \cdot t_{\text{Rto}\beta}}{\max(\frac{L \cdot l_x}{v_x} + \frac{v_x}{a_x}, \frac{W \cdot w_y}{v_y} + \frac{v_y}{a_y})} \tag{6.7}$$

$$t_{dg,RCS/R,BBO} = \frac{t_{\text{StoR}} + t_{\text{toHP}} + t_{\text{toS}} + 4 \cdot \beta \cdot t_{\text{Rto}\beta}}{\frac{L \cdot l_x}{v_x} + \frac{v_x}{a_x} + \frac{W \cdot w_y}{v_y} + \frac{v_y}{a_y} + t_{turn}} \tag{6.8}$$

$$t_{hg,BBO} = \frac{4t_h + 2t_{Ch,S} + 2t_{Ch,R} + 4\beta(t_h + t_{Ch,R,\beta} + t_{Ch,S,\beta})}{t_h + 2 \cdot (\frac{l_z \cdot H}{v_z} + \frac{v_z}{a_z})}. \tag{6.9}$$

With $\theta \in (0, 1)$, the normalised cycle time $t_{cycle,n}$ can be calculated with:

$$t_{cycle,n} = \theta \cdot t_{hg} + (1 - \theta) \cdot t_{dg} \tag{6.10}$$

Low values for θ imply that the underlying AS/R or RCS/R system have telescopic arms or lifts with high velocity and acceleration and small H and/or S/R machines and robots with small velocity and acceleration and high L, W. Respectively, large θ represent AS/R or RCS/R systems with slow telescopic arms or lifts and high H values and/or fast S/R machines or robots and small unit loads.

Storage systems: Both AS/R and RCS/R systems are included in the design of experiments.

Operating strategies: All 13 operating strategies are regarded for AS/R systems. Only the Homogeneous strategy is not regarded for the RCS/R systems.

Length to Width ratio $L : W$: Both AS/R and RCS/R systems are fixed to a 2:1 ratio of storage channels in x- to y-direction.

Stock filling level ω: Usually, storage planners in the industry assume a storage filling level of $\omega = 0.75$ during the planning phase of a new storage system. This is the only step regraded in the design of experiments.

The experiments are designed as a full factorial design which leads to $3 \cdot 3 \cdot 12 \cdot 13 \cdot 1 \cdot 1 = 1404$ experiments for AS/R systems and $3 \cdot 3 \cdot 24 \cdot 12 \cdot 1 \cdot 1 = 2592$ experiments for RCS/R systems and 3996 experiments in total. The 3996 results of experiments are shown in Tables A.7 to A.23 in Appendix A.10 in dependency of θ. The following Sections 6.2 and 6.3 analyse the most interesting results for AS/R and RCS/R systems and Section 6.4 summarise the insights gained.

6.2 Cycle Time Evaluation for Automated Storage and Retrieval Systems

The effect of changing parameters are analysed in this section by selected results. First, the effect of the depth H is analysed for an AS/R system with system parameters presented in Table 6.1. To enable a comparison of different depths of an AS/R system with the same S/R machine (this leads to different θ), the cycle time t_{cycle} is not normalised for the analysis of the effect of the depths on the cycle time which is shown in Figure 6.1. The same is applied to the results presented in Figures 6.2 to 6.7 to analyse the effect of the depth and number of storage locations or access frequencies and number of unit loads per product together.

Table 6.1: AS/R System Parameters.

Parameter	Values
Number of Storage Locations $L \cdot W \cdot H$	50000
Length, Width, and Height of a Location l_x, l_y, l_z	0.5, 0.4, 0.6
Stock Filling Level $\omega_A, \omega_B, \omega_C$	0.15, 0.2, 0.4
Number of Unit Loads per Product ξ	5, 2, 1
Access Frequency f	10, 2, 1
Velocity of S/R Machine v	3, 1, 1.5
Acceleration of S/R Machine a	2, 1.5, 1
Handling Time t_h	2

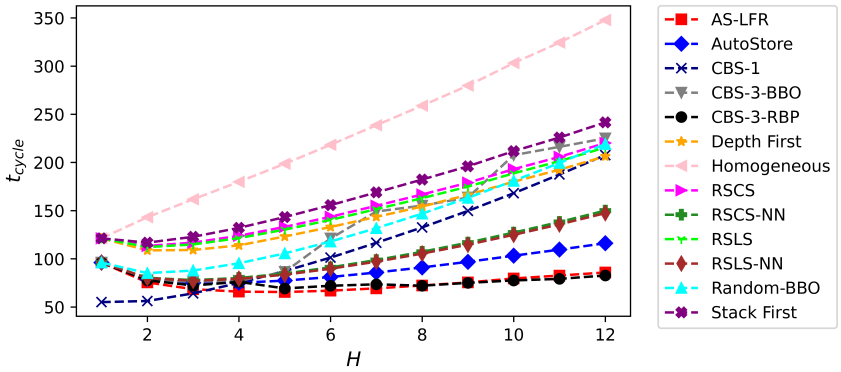

Figure 6.1: Cycle Times for all Strategies for the AS/R System with Table 6.1 Parameters.

Effect of Depth: Figure 6.1 shows that the CBS-1 strategy achieves the lowest cycle time for $H \leq 3$ and for deeper systems with $H \geq 4$ the AS-LFR and CBS-3-RBP strategies perform best because these two strategies use the information about access frequencies and number of unit loads per product. For $H \leq 3$, the short movements of the S/R machine due to the placement of class A products close to the I/O point are the reason for the good performance of the CBS-1 strategy. For a single-deep AS/R system ($H = 1$), there are only three different values: The mentioned CBS-1 strategy, all other operating strategies employing a nearest neighbour movement policy and all operating strategies employing a random movement policy. Figure 6.1 shows that operating strategies with nearest neighbour movement policy perform better compared to their counterparts with

random movement policy. This can be observed when comparing the RSCS or RSLS strategy with the RSCS-NN or RSLS-NN strategy. However, there are two exceptions, the CBS-3-BBO and Random-BBO strategy achieve higher cycle times than the Depth First, Stack First, RSCS and RSLS strategies, because the number of reshuffles and time per reshuffle are relatively high. Number of reshuffles β and the time required for each reshuffle determine the cycle time beginning with double-deep systems.

Figures 6.2 and 6.3 show how the operating strategies perform for these performance indicators. Figure 6.1 shows that increasing depths of AS/R systems does not necessarily lead to higher cycle times. In fact, for the AS-LFR and CBS-3-RBP strategies the cycle time stays constant between $H = 4$ and $H = 10$ and for the most strategies the cycle time decreases from $H = 1$ to $H = 2$ because the number of channels is halved for a double-deep system compared to a single-deep system. One notable strategy is the Homogeneous strategy which has the highest cycle times due to the random movement policy and the necessity of reshuffles during storage and with this also the highest number of reshuffles per cycle.

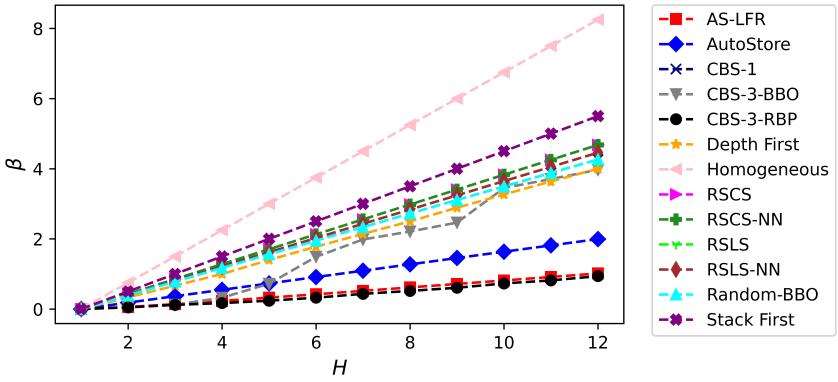

Figure 6.2: Number of Reshuffles per Command Cycle for all Strategies for the AS/R Systems with Table 6.1 Parameters.

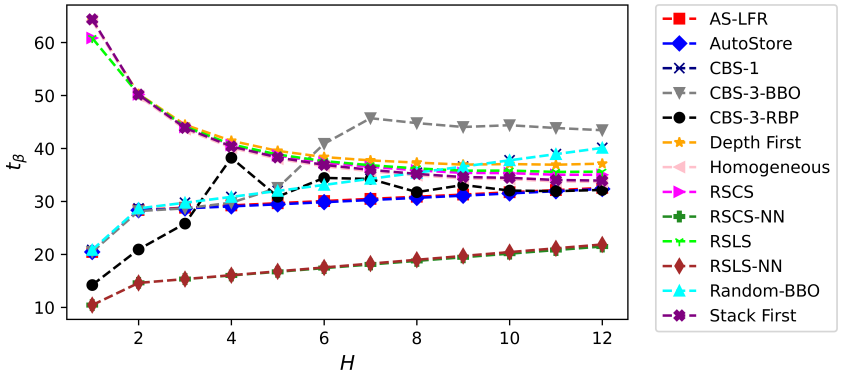

Figure 6.3: Time per Reshuffle for all Strategies for the AS/R Systems with Table 6.1 Parameters.

Figure 6.2 shows the difference in the number of reshuffles between strategies that only incorporate homogeneous unit loads (e.g., RSCS, Depth First) and the strategies that use heterogeneous unit loads (e.g. AutoStore, AS-LFR, CBS-3-RBP). It also shows that using class-based storage with unsuitable storage assignment or reshuffle strategies does not improve the cycle time (e.g. CBS-3-BBO or CBS-1 for $H \geq 4$). Overall, the RSCS and RSLS have the lowest times per reshuffle because they place the blocking unit loads in any storage channel adjacent to the retrieval channel

Effect of Number of Storage Locations: AS/R systems with only few storage locations yield smaller movement times of the S/R machine compared to AS/R systems with many storage locations. Therefore, the number of reshuffles and the handling time per reshuffle gain relevance for smaller systems. Figures 6.4 and 6.5 show the cycle times for fewer and more storage locations compared to the AS/R system with Table 6.1 parameters. Figure 6.4 shows that the CBS-1 strategy is the best strategy only for $H = 1$ and that all strategies employing a random movement policy perform relatively better compared to the nearest neighbour movement policy when fewer storage locations exist. However, this changes when the AS/R system consists out of more storage locations as shown in Figure 6.5. In the latter case movement strategies with nearest neighbour perform better. All

other observations described before are the same.

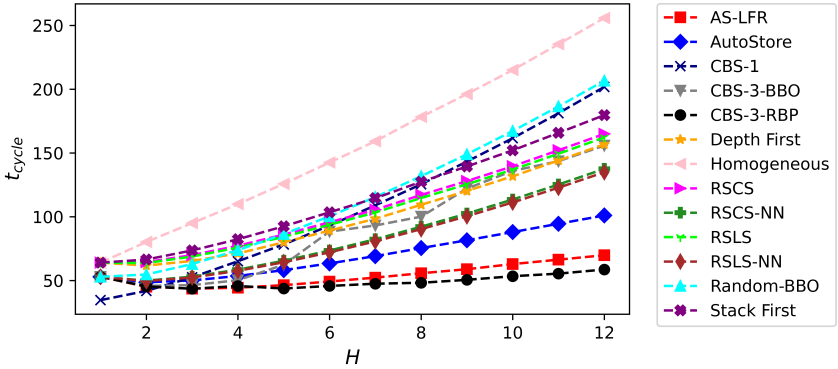

Figure 6.4: Cycle Time for all Strategies for AS/R Systems with Table 6.1 Parameters and 10000 Storage Locations.

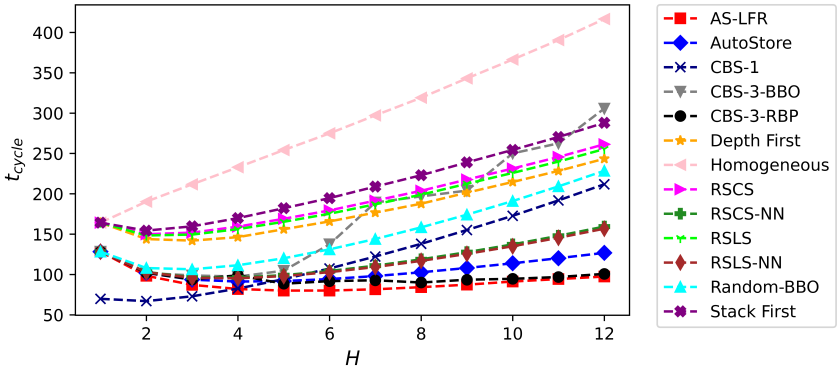

Figure 6.5: Cycle Time for all Strategies for AS/R Systems with Table 6.1 Parameters and 100000 Storage Locations.

Effect of Access Frequency and Number of Unit Loads per Product: When the access frequency and number of unit loads are set to $f = (1, 1, 1)$ and $\xi = (1, 1, 1)$, the AutoStore, AS-LFR, CBS-3-BBO and CBS-3-RBP strategies

cannot exploit this information and therefore the RSCS-NN and RSLS-NN strategies yield the lowest cycle times (see Figure 6.6). On the other hand, the AutoSore, AS-LFR, CBS-3-BBO and CBS-3-RBP strategies can exploit higher access frequencies and number of unit loads per product compared to the strategies for homogeneous unit loads, achieving lower cycle times (see Figure 6.7). In fact, the CBS-3-RBP strategy has monotonous decreasing cycle times with increasing H.

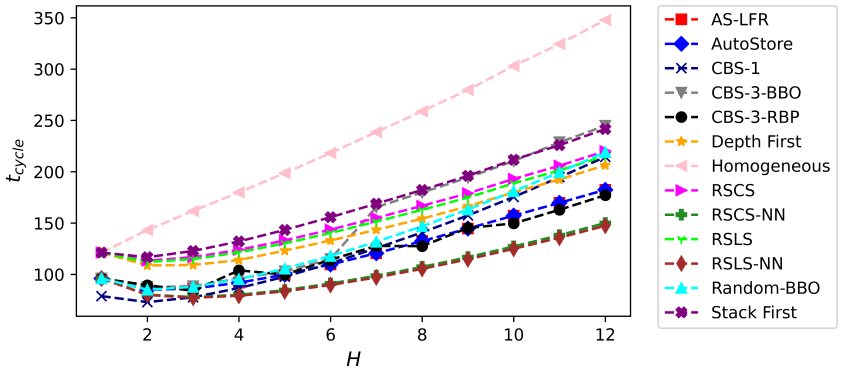

Figure 6.6: Cycle Times for all Strategies for the AS/R Systems with Table 6.1 Parameters and $\xi = (1, 1, 1)$ and $f = (1, 1, 1)$.

Ratios Handling-to-Driving-Ratio: The Figures 6.8 and 6.9 show the normalised cycle times $t_{cycle,n}$ for the AS/R system with system parameters presented in Table 6.2 for $H = 4$ and $H = 8$ and different handling-to-driving-ratios θ.

Table 6.2: AS/R System Parameters.

Parameter	Values
Number of Storage Locations $L \cdot W \cdot H$	50000
Stock Filling Level $\omega_A, \omega_B, \omega_C$	0.15, 0.2, 0.4
Number of Unit Loads per Product ξ	5, 2, 1
Access Frequency f	10, 2, 1

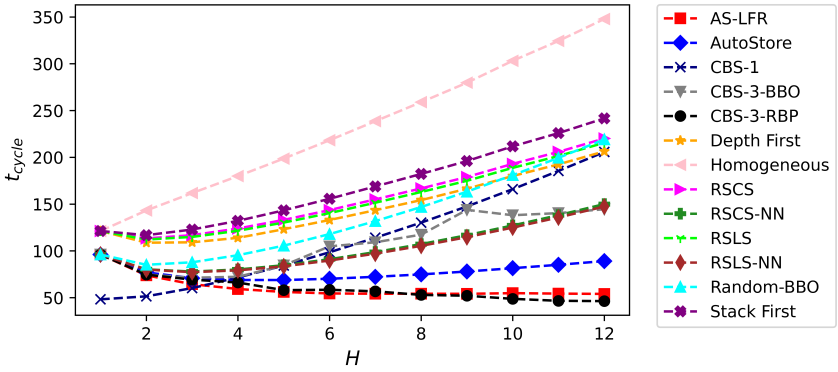

Figure 6.7: Cycle Times for all Strategies for the AS/R Systems with Table 6.1 Parameters and $\xi = (20, 10, 5)$ and $f = (100, 10, 1)$.

For small θ, operating strategies yield lower cycle times which focus on reducing the driving time of the S/R machine such as the CBS-1 strategy and strategies which focus on reducing the number of reshuffles and thus the driving time for reshuffles such as the AS-LFR and CBS-3-RBP strategies. However, if the handling time is the main component of the cycle time (high θ), strategies which reduce the handling time are dominant strategies. Such strategies are the AS-LFR and CBS-3-RBP strategies for heterogeneous unit loads and the depth first strategy for homogeneous unit loads.

To analyse the depth, number of storage locations, access frequencies and number of unit loads per product and handling-to-driving-ratio together, Table 6.3 shows an extract of the complete results for the best performing strategies for AS/R systems (RSLS-NN, Depth First, CBS-1, AS-LFR and CBS-3-RBP) presented in Tables A.7 to A.11 in Appendix A.10. Since $t_{cycle,n}$ are linear equations for all strategies depending on θ, it is interesting to evaluate the effect of driving-heavy and handling-heavy storage systems on the cycle time. This is realised by presenting the normalised cycle times for $\theta = 0.1$ and $\theta = 0.9$ in Table 6.3.
Depending on the parameters of a given AS/R systems and thus θ of a system,

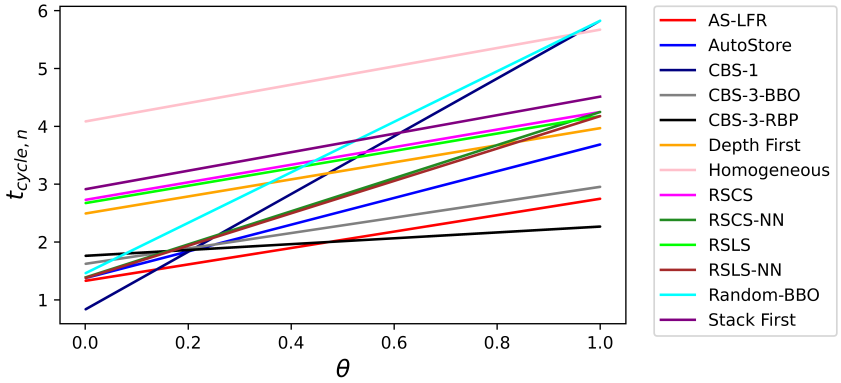

Figure 6.8: The normalised Cycle Time $t_{cycle,n}$ for each handling-to-driving-ratio θ for the AS/R Systems with Table 6.2 Parameters and $H = 4$.

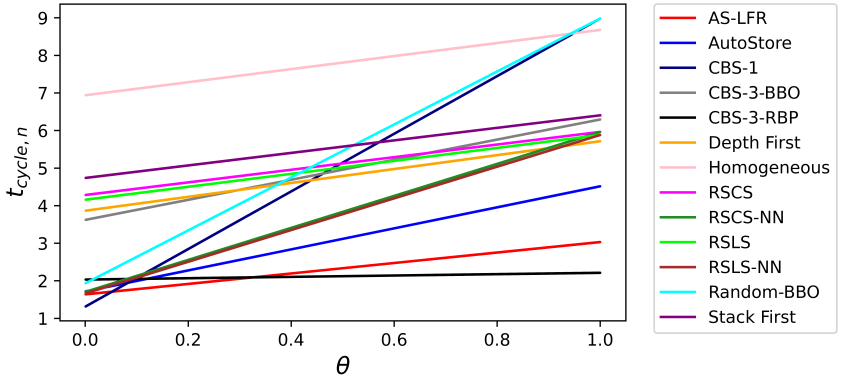

Figure 6.9: The normalised Cycle Time $t_{cycle,n}$ for each handling-to-driving-ratio θ for the AS/R Systems with Table 6.2 Parameters and $H = 8$.

Table 6.3 gives an assessment which operating strategies should be applied for which parameter combination. Some general insights are:

- The CBS-1 strategy is dominant over all other operating strategies for $H = 1$ for any combination of access frequency, number of unit loads per product and number of storage channels. And most importantly, the CBS-1

Table 6.3: Normalised Cycle Times for different exemplary AS/R System Configurations. $\underline{\theta} = 0.1$, $\overline{\theta} = 0.9$, $\gamma_1 = \{\xi = (1,1,1), f = (1,1,1)\}$, $\gamma_2 = \{\xi = (5,2,1), f = (10,2,1)\}$, $\gamma_3 = \{\xi = (20,10,5), f = (100,10,1)\}$

		$L \cdot W \cdot H = 10000$						$L \cdot W \cdot H = 50000$						$L \cdot W \cdot H = 100000$					
	H	γ_1		γ_2		γ_3		γ_1		γ_2		γ_3		γ_1		γ_2		γ_3	
		$\underline{\theta}$	$\overline{\theta}$	$\underline{\theta}$	$\overline{\theta}$	$\underline{\theta}$	$\overline{\theta}$	$\underline{\theta}$	$\overline{\theta}$	$\underline{\theta}$	$\overline{\theta}$	$\underline{\theta}$	$\overline{\theta}$	$\underline{\theta}$	$\overline{\theta}$	$\underline{\theta}$	$\overline{\theta}$	$\underline{\theta}$	$\overline{\theta}$
AS-LFR	1	1.42	2.55	1.42	2.55	1.42	2.55	1.40	2.55	1.40	2.55	1.40	2.55	1.39	2.55	1.39	2.55	1.39	2.55
	4	2.14	4.93	1.63	2.62	1.49	2.01	1.87	4.90	1.49	2.61	1.39	2.00	1.81	4.90	1.48	2.60	1.38	2.00
	8	3.44	6.92	2.15	2.93	1.77	1.67	2.63	6.83	1.81	2.89	1.58	1.65	2.40	6.80	1.70	2.88	1.50	1.64
	12	4.63	8.33	2.49	3.20	1.79	1.49	3.43	8.16	2.11	3.16	1.69	1.48	3.10	8.16	1.99	3.15	1.65	1.48
CBS-1	1	1.18	2.52	0.85	2.49	0.77	2.48	1.15	2.52	0.82	2.48	0.73	2.47	1.14	2.52	0.81	2.48	0.71	2.47
	4	1.94	5.39	1.62	5.36	1.53	5.35	1.66	5.36	1.33	5.33	1.24	5.31	1.60	5.36	1.27	5.32	1.18	5.31
	8	3.15	8.33	2.85	8.30	2.76	8.29	2.40	8.25	2.08	8.21	1.98	8.20	2.20	8.23	1.88	8.19	1.79	8.18
	12	4.56	10.90	4.26	10.86	4.17	10.86	3.23	10.75	2.91	10.72	2.82	10.70	2.88	10.71	2.56	10.68	2.46	10.67
CBS-3-RBP	1	1.42	2.55	1.42	2.55	1.42	2.55	1.40	2.55	1.40	2.55	1.40	2.55	1.39	2.55	1.39	2.55	1.39	2.55
	4	2.51	3.39	1.89	2.22	1.67	1.92	2.42	3.38	1.83	2.22	1.60	1.92	2.42	3.38	1.83	2.22	1.60	1.92
	8	3.62	4.65	2.23	2.21	1.71	1.48	3.33	4.62	2.08	2.20	1.60	1.46	3.22	4.60	2.03	2.19	1.60	1.46
	12	5.11	5.85	2.62	2.40	1.83	1.25	4.86	5.82	2.51	2.39	1.48	1.22	4.78	5.81	2.47	2.38	1.38	1.20
Depth First	1	1.77	2.59	1.77	2.59	1.77	2.59	1.75	2.59	1.75	2.59	1.75	2.59	1.75	2.59	1.75	2.59	1.75	2.59
	4	2.71	3.83	2.71	3.83	2.71	3.83	2.64	3.82	2.64	3.82	2.64	3.82	2.65	3.82	2.65	3.82	2.65	3.82
	8	4.30	5.56	4.30	5.56	4.30	5.56	4.05	5.53	4.05	5.53	4.05	5.53	3.95	5.52	3.95	5.52	3.95	5.52
	12	5.64	7.16	5.64	7.16	5.64	7.16	5.41	7.14	5.41	7.16	5.41	7.14	5.33	7.13	5.33	7.13	5.33	7.13
RSLS-NN	1	1.42	2.55	1.42	2.55	1.42	2.55	1.40	2.55	1.40	2.55	1.40	2.55	1.39	2.55	1.39	2.55	1.39	2.55
	4	1.81	3.91	1.81	3.91	1.81	3.91	1.65	3.90	1.65	3.90	1.65	3.90	1.62	3.90	1.62	3.90	1.62	3.90
	8	2.55	5.51	2.55	5.51	2.55	5.51	2.08	5.46	2.08	5.46	2.08	5.46	1.96	5.44	1.96	5.44	1.96	5.44
	12	3.33	7.00	3.33	7.00	3.33	7.00	2.56	6.91	2.56	6.91	2.56	6.91	2.36	6.89	2.36	6.89	2.36	6.89

strategy is also dominant for all θ. The reason for this is the location of class A unit loads adjacent to the I/O point and the absence of reshuffles for single-deep AS/R systems. For other AS/R system with small $H > 1$, the CBS-1 strategy is still competitive, but it depends on θ and the other AS/R parameters if the CBS-1 strategy or another strategy should be preferred. This must be analysed for each AS/R system in detail individually.

- The AS-LFR, CBS-3-RBP, and RSLS-NN strategies yield the same normalised cycle times for $H = 1$ and all system parameters. The differences increase with increasing H.

- The RSLS-NN which assumes only homogeneous unit loads yields smaller cycle times compared with the AS-LFR and CBS-3-RBP strategies for small θ, small H, and small access frequencies and number of unit loads per product.
- The AS-LFR strategy performs better for small θ compared to the CBS-3-RBP strategy. This applies for small AS/R systems for all combinations of access frequencies and number of unit loads per products. For medium and large AS/R systems with many storage locations, this applies only for small access frequencies and number of unit loads per product.
- If only information about homogeneous unit loads is available, RSLS-NN yields smaller cycle times compared to the Depth First strategy, especially for small θ. For large θ both strategies perform comparable.

6.3 Cycle Time Evaluation for Robotic Compact Storage and Retrieval Systems

As in Section 6.2, selected results are presented in this section and the first results are presented without the normalised cycle times. The cycle times are calculated using the RCS/R system parameters shown in Table 6.4. The cycle times and number of reshuffles for all operating strategies are shown in Figures 6.10 and 6.11. In general, the same observations as for AS/R systems can be made (due to the Manhattan metric, all cycle times are higher for RCS/R systems compared to AS/R systems with same parameters) with the exception that the CBS-1 strategy yields higher cycle times. Because the channels of class A are not located closer to the pick station in RCS/R systems but are located in the middle of the rack, leading to same cycle times as for the Random-BBO strategy.
RCS/R systems with $H > 12$ yield higher cycle times compared to RCS/R systems with $H \leq 12$ for all strategies except the AS-LFR and CBS-3-RBP strategies. Figure 6.12 shows that these strategies can even reduce the cycle time with increasing H when the access frequency and number of unit loads per product are

Table 6.4: RCS/R System Parameters.

Parameter	Values
Number of Storage Locations $L \cdot W \cdot H$	50000
Length, Width, and Height of a Location l_x, l_y, l_z	0.7, 0.5, 0.25
Stock Filling Level $\omega_A, \omega_B, \omega_C$	0.15, 0.2, 0.4
Number of Unit Loads per Product ξ	5, 2, 1
Access Frequency f	10, 2, 1
Velocity of S/R Machine v	4, 4, 1.6
Acceleration of S/R Machine a	1.4, 1.4, 1.4
Handling Time t_h	2
Turn Time of a Robot t_u	1.2

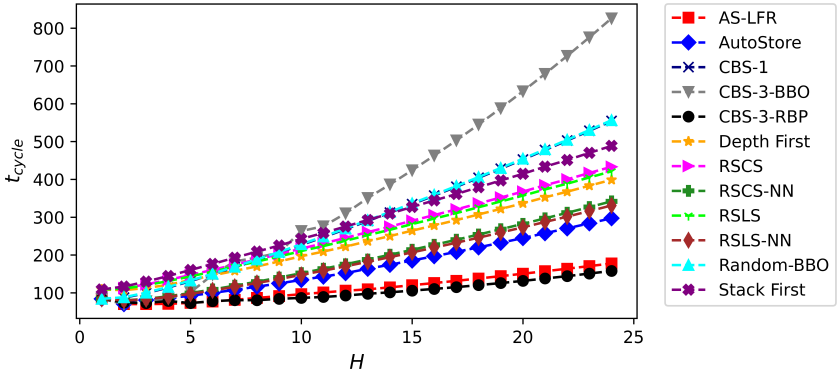

Figure 6.10: Cycle Times for all Strategies for the RCS/R Systems with Table 6.4 Parameters.

high. In this case the number of reshuffles is low for all H because the LFR retrieval policy mostly finds a suitable unit load for retrieval on top of the RCS/R system (see Figure 6.13).

Table 6.5 sums up the results for the RCS/R systems and shows that the same conclusions can be drawn as for AS/R systems in Table 6.3. One exception is the CBS-1 strategy because the zone allocation for classes A, B, and C is different and less favourable for RCS/R systems compared to AS/R systems.

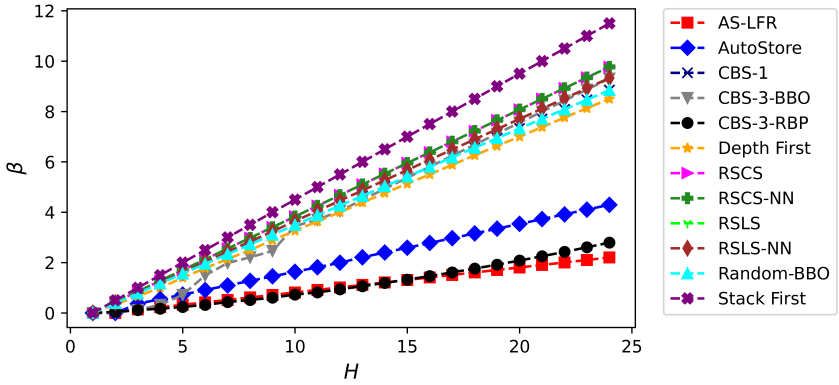

Figure 6.11: Number of Reshuffles for all Strategies for the RCS/R Systems with Table 6.4 Parameters.

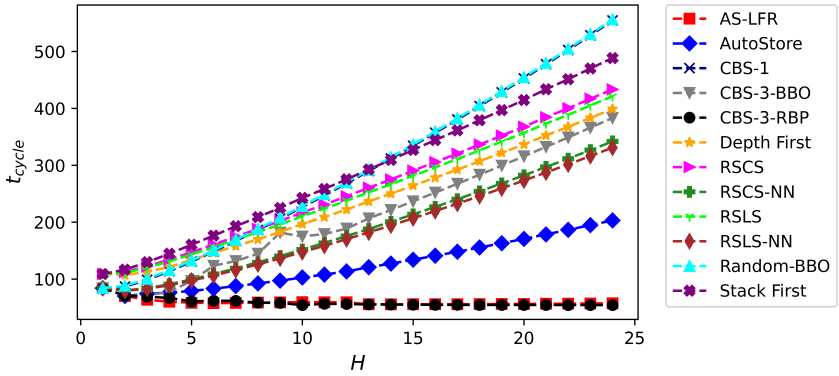

Figure 6.12: Cycle Times for all Strategies for the RCS/R Systems with Table 6.4 Parameters and $\xi = (20, 10, 5)$ and $f = (100, 10, 1)$.

6.4 Managerial Insights

Sections 6.2 and 6.3 show that it is not possible to identify operating strategies which are always superior over all other operating strategies and that storage planers have to apply several operating strategies for a new AS/R or RCS/R system to find the cycle time minimising or throughput maximising operating strategy. This

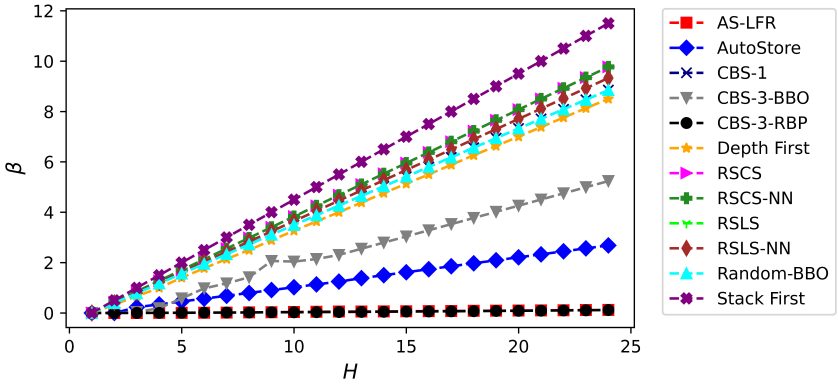

Figure 6.13: Number of Reshuffles for all Strategies for the RCS/R Systems with Table 6.4 Parameters and $\xi = (20, 10, 5)$ and $f = (100, 10, 1)$.

section summarises the most important insights of the cycle time and throughput models developed in Chapters 4 and 5 and discusses the model limitations.

Only the AS-LFR, CBS-1, CBS-3-RBP, Depth First and RSLS-NN strategies perform best under any parameter for AS/R system as shown in Section 6.2 and only the AS-LFR, CBS-3-RBP, Depth First and RSLS-NN strategies perform best for RCS/R systems (see Section 6.3). This means that all other operating strategies do not have to be regarded in the storage planning process. Furthermore, while for small H systems the CBS-1 strategy can be applied, this strategy should not be used for large H systems.

Storage planners should be aware that the increase in number of reshuffles as one of the most important performance indicators can be assumed as linear for all operating strategies but the CBS-3-RBP strategy (quadratic for CBS-3-RBP strategy as shown in Appendix A.8). Either the assumption of linearity can be supported by Appendix A.8 for the AutoStore, AS-LFR and CBS-3-BBO strategy or can be observed in Figures 6.2 and 6.11.

Table 6.5: Normalised Cycle Times for different RCS/R System Configurations. $\underline{\theta} = 0.1$, $\overline{\theta} = 0.9$, $\gamma_1 = \xi = (1,1,1), f = (1,1,1)$, $\gamma_2 = \xi = (5,2,1), f = (10,2,1)$, $\gamma_3 = \xi = (20,10,5), f = (100,10,1)$

	H	$C = 10000$						$C = 50000$						$C = 100000$					
		γ_1		γ_2		γ_3		γ_1		γ_2		γ_3		γ_1		γ_2		γ_3	
		$\underline{\theta}$	$\overline{\theta}$	$\underline{\theta}$	$\overline{\theta}$	$\underline{\theta}$	$\overline{\theta}$	$\underline{\theta}$	$\overline{\theta}$	$\underline{\theta}$	$\overline{\theta}$	$\underline{\theta}$	$\overline{\theta}$	$\underline{\theta}$	$\overline{\theta}$	$\underline{\theta}$	$\overline{\theta}$	$\underline{\theta}$	$\overline{\theta}$
AS-LFR	1	1.25	2.69	1.25	2.69	1.25	2.69	1.07	2.67	1.07	2.67	1.07	2.67	1.02	2.66	1.02	2.66	1.02	2.66
	8	5.81	8.92	2.73	3.75	1.77	2.12	2.01	8.71	2.01	3.67	1.40	2.08	3.39	8.65	1.76	3.65	1.27	2.06
	16	12.44	15.40	4.57	5.23	1.98	1.85	3.22	14.95	3.22	5.08	1.55	1.80	6.92	14.79	2.76	5.03	1.39	1.78
	24	19.98	21.90	6.64	6.80	2.19	1.73	4.64	21.17	4.64	6.58	1.70	1.68	11.14	20.91	3.92	6.50	1.52	1.65
CBS-3-RBP	1	1.25	2.69	1.25	2.69	1.25	2.69	1.07	2.67	1.07	2.67	1.07	2.67	1.02	2.66	1.02	2.66	1.02	2.66
	8	4.16	5.51	2.34	2.80	1.72	1.98	1.93	5.43	1.93	2.75	1.41	1.94	3.16	5.40	1.81	7.24	1.34	1.93
	16	8.08	8.48	3.72	3.54	1.92	1.59	3.08	8.32	3.08	3.47	1.57	1.57	6.30	8.35	2.87	3.45	1.44	1.53
	24	12.08	11.35	5.61	4.82	2.04	1.37	4.64	11.12	4.64	4.71	1.70	1.38	9.66	11.48	4.30	4.67	1.55	1.30
Depth First	1	1.50	2.72	1.50	272	1.50	2.72	1.34	2.67	1.34	2.67	1.34	2.67	1.30	2.70	1.30	2.70	1.30	2.70
	8	4.79	6.32	4.79	6.32	4.79	6.32	4.04	6.24	4.04	6.24	4.04	6.24	3.80	6.21	3.80	6.21	3.80	6.21
	16	8.98	10.18	8.98	10.18	8.98	10.18	7.47	9.92	7.47	9.92	7.47	9.92	6.95	9.86	6.95	9.86	6.95	9.86
	24	13.60	13.34	13.60	13.34	13.60	13.34	11.08	13.35	11.08	13.35	11.08	13.35	10.26	13.25	10.26	13.25	10.26	13.25
RSLS-NN	1	1.25	2.69	1.25	2.69	1.25	2.69	1.07	2.70	1.07	2.70	1.07	2.70	1.02	2.66	1.02	2.66	1.02	2.66
	8	4.00	6.54	4.00	6.54	4.00	6.54	2.83	6.41	2.83	6.41	2.83	6.41	2.45	6.37	2.45	6.37	2.45	6.37
	16	7.84	10.24	7.84	10.24	7.84	10.24	5.34	9.96	5.34	9.96	5.34	9.96	4.48	9.87	4.48	9.87	4.48	9.87
	24	12.08	13.66	12.08	13.66	12.08	13.66	8.22	13.23	8.22	13.23	8.22	13.23	6.84	20.91	6.84	20.91	6.84	20.91

This work also shows that storage planners should use and exploit any information or assumption about the access frequency or number of unit loads per product in the system. Figures 6.8 and 6.9 as well as Tables 6.3 and 6.5 show that as soon as such information is available, the CBS-1, AS-LFR and CBS-3-RBP strategies yield lower cycle times compared to the Depth First or RSLS-NN strategies. Furthermore, the models or parts of the models developed in this can be applied by the interested reader to a variety of other storage systems such as container terminals, flow racks, AVS/R systems or crane based bloc systems as presented in Bolender et al. (2018).

As all models, also the throughput models introduced in the Chapters 4 and 5 have some shortcomings and use assumptions leading to deviations from industry applications. Storage planners should be aware of these shortcomings, which will be discussed in the following:

- For both S/R machines and robots a simplified acceleration model presented by Arnold and Furmans (2019) is used. This leads to deviations between the model and application when the maximal velocity is not reached. Especially for small systems, this can lead to a significant error between model and application. Storage planners should try to use other acceleration models such as by Hwang and Lee (1990) when they want to apply the models for small systems.
- The models in this thesis all assume a steady state during operation. This might not be the case in low demand times. If single command cycles are executed and storage or retrieval jobs are not waiting, the system leaves the steady state, and the models cannot be applied accurately anymore. It is also possible to perform any kind of premarshalling during low demand times, which is also not regarded in the models. Single command cycles can decrease the throughput while premarshalling can increase the throughput compared to the results of this thesis.
- For the heterogeneous unit loads, average values for the access frequency and number of unit loads per product are assumed. Section 5.3.3 shows that this is a good assumption for the available industry data. This is not necessarily the case for every use case.
- The robots for the RCS/R system in Chapter 5 uses two simplified assumptions. First it is assumed that robots perform every job by their own, in application robots can collaborate and for example share reshuffles. Second, robots can block each other on the grid during movement. This congestion is also not regarded but has the potential to reduce the throughput of an RCS/R system as shown by Zou et al. (2018).
- Except for the Depth First and Stack First strategies, no closed form expressions for the number of reshuffles, cycle times or throughput capacity were derived in this work. The number of reshuffles, cycle times and throughput capacity must be calculated numerically for all other operating strategies. This also means that the optimality of throughput maximising system layouts as introduced in Section 5.3 cannot be guaranteed or shown.

- Due to runtime limitations, regressions are needed for the calculation of cycle times for the AutoStore, AS-LFR, CBS-3-BBO, and CBS-3-RBP strategies for $H > 12$.

7 Conclusion and Outlook

Multi-deep AS/R and RCS/R systems are automated storage systems in which the unit loads are stored behind or above each other. In these systems, S/R machines and robots do not have direct access to all unit loads and must reshuffle unit loads first in case these unit loads are blocking unit loads. These systems can be operated following a variety of operating strategies which depend on the level of information the customer can provide to the storage planner. Depending on this level, either operating strategies for homogeneous unit loads or heterogeneous unit loads can be designed. These different operating strategies lead to different throughput capacities for given AS/R or RCS/R systems.

7.1 Conclusion

This thesis was written to answer three major research questions:

1. Assuming homogeneous unit loads, how can the throughput capacity be analytically estimated for AS/R and RCS/R systems?
2. Assuming heterogeneous unit loads, how can the throughput capacity be analytically estimated for AS/R and RCS/R systems?
3. How does the throughput capacity change for different AS/R and RCS/R system parameters when different operating strategies are applied??

In total, throughput models for 13 different operating strategies were developed, analysed and compared with each other to answer these three research questions. These 13 operating strategies use two different allocation structure policies, seven

storage assignment policies, six reshuffle policies, two retrieval unit load selection policies and two movement policies. Eight strategies are designed for homogeneous unit loads, and five operating strategies are suitable for heterogeneous unit loads. For model development, the steady states of the AS/R and RCS/R systems are mainly derived with Markov chains, and the throughput is determined using closed queuing networks which can be solved accurately with the MVA. The analytic models are validated with simulations and show $\leq 3\,\%$ deviation between the analytic model and simulation. Furthermore, the AS-LFR and the CBS-3-RBP strategies are validated with industry data and also show small deviation between the model and simulation. Experiments are conducted to compare all operating strategies for different multi-deep AS/R and RCS/R systems.

To answer the first two research questions, throughput models for 13 operating strategies were derived in Chapters 4 and 5. The steady states were derived to accurately estimate the throughput during operation of storage systems. This work shows that this can be done with two modelling techniques. For homogeneous unit loads, the steady state can be derived either with Markov chains or directly with some assumptions concerning the stock filling level as for the Depth First or Stack First strategies. If heterogeneous unit loads are available, the steady state can only be determined using Markov chains. For this purpose, the state transitions are modelled with the probabilities of different possible storage, reshuffle, and retrieval jobs. Two different Markov chain frameworks are presented, and it is shown that both yield accurate results compared with simulation. Markov chains for operating strategies assuming homogeneous unit loads solve relatively fast compared to the calculation-intensive Markov chains for heterogeneous unit loads due to the larger state space.

The most important results of the research conducted to answer the first two research questions are: Accurate throughput models have been developed, enabling storage planners to estimate the throughput of multi-deep AS/R and RCS/R systems in application with real operating strategies. For the first time, it is possible to analytically determine the throughput capacity of the AutoStore system

assuming the same operating strategy as the market leader. Especially the development of accurate throughput models for class-based storage with three classes per storage channel policies for multi-deep AS/R and RCS/R systems closes another important research gap. It is also shown that throughput and especially cycle time models can be applied to other storage systems with minor adaptions.

The thesis concludes with an extensive comparison of the 13 operating strategies for AS/R and RCS/R systems, which answers the third research question. The systems are evaluated using a full factorial design of experiments. Furthermore, the handling and driving times of the S/R machine and robots are normalised to be able to draw general insights from the models. The most important insights are that the CBS-1 and RSLS-NN strategies yield the highest throughput capacities for homogeneous unit loads (CBS-1 for systems with only few unit loads stored behind or above each other, RSLS-NN for systems with many unit loads), and the AS-LFR and CBS-3-RBP strategies yield the highest throughput capacities for heterogeneous unit loads and large H, outperforming the original AutoStore strategy.

7.2 Outlook

Based on the work presented in this thesis, several further work can be carried out. The assumption that the I/O point is always on the left bottom corner of the AS/R system and the pick station is in the middle of the longer side of the RCS/R system can be extended by regarding different locations for I/O point and pick station. Furthermore, the analytic models can be extended to capture more details of the functionality of the AS/R and RCS/R systems. The congestion on top of RCS/R systems between robots can be included too. Furthermore, the more accurate acceleration models from Hwang and Lee (1990) can be used.

The 13 implemented operating strategies do not exhaust the potential for further strategies. For example, a full turnover-based storage policy is not regarded

yet for multi-deep AS/R or RCS/R systems. Furthermore, details in the implementations of policies in this work can be altered which leads to a potential increase in throughput. For example, the priorities for the CBS-3-BBO and CBS-3-RBP strategies can be changed, and the resulting cycle times can be analysed.

This thesis shows that the models can be adapted relatively easy from AS/R to RCS/R systems and the other way around. A potential topic is to even extend this to flow rack, AVS/R systems or variants of RCS/R systems (Jungheinrich 2024). It is also interesting to analyse the gap between the potential throughput capacity and the realised throughput in application in more detail, similar to the case study in this thesis. This can be realised with a comparison of the models in this thesis with a deep reinforcement learning agent for scheduling of tasks applied to the same systems. Another direction of future research is an extensive regression analysis including all system parameters and all possible factor steps of the parameters. This enables storage planners to avoid calculation effort for every new customer. This can be implemented with the help of AI and for example with a multi layer perceptron.

Acronyms and symbols

Acronyms

AS	AutoStore
AS/R	Automated Storage and Retrieval
AVS/R	Autonomous Vehicle Based Storage and Retrieval
BBO	Bring-Back to Original Channel
CBRS	Class-Based Random Storage
CBS – 1	Class-Based Storage with 1 Class per Channel
CBS – n	Class-Based Storage with n Classes per Channel
CFE	Closed Form Expression
CTC	Cycle Time Calculation
CQN	Closed Queuing Network
DES	Discrete Event Simulation
DF	Depth First
FR	Flow Rack
I/O Point	Input and Output Point
LFR	Load with Fewest Reshuffles
LIFO	Last In First Out
LOFI	Last Out First In
MC	Markov Chain

NN	Nearest Neighbour
OQN	Open Queuing Network
RBP	Relocate to Best Position
RCS/R	Robotic Compact Storage and Retrieval
RD	Retrieval Delay
RLO	Rack Layout Optimisation
RSCS	Random Storage Channel Strategy
RSLS	Random Storage Location Strategy
S/R Machine	Storage and Retrieval Machine
SC	Specified Channel
SF	Stack First
SOQN	Semi-Open Queuing Network

AS/R and RCS/R System Parameters

a_x, a_y, a_z	Acceleration and Deceleration of S/R machines and robots in the x-, y-, and z-direction in m/s^2
C	Number of all channels of a rack $L \cdot W$
h	The H levels of the rack with $h \in 0, ..., H$
K	Number of robots assigned to each pick station
L, W, H	Number of storage locations in x, y, and z-direction
l_x, l_y, l_z	Length, width, and height of a storage location in meter
PS	Number of pick stations
t_h	Determinisitc handling time to pick and drop a unit load with a S/R machine or robot in seconds
t_{pick}	Operator time for a pick in seconds
t_u	Time a robot needs to change direction once in seconds

t_{wait}	Waiting time of a robot in front of a pick station in seconds
v_x, v_y, v_z	Velocity of S/R machines and robots in the x-, y-, and z-direction in m/s

Product Parameters

f_j	Access frequencies for class j
J	Number of classes
$\underline{j}$, $\overline{j}$	The lowest and highest h assigned to class j
γ_j, ξ_j	Number of unit loads per class j, and unit loads per product of class j
ω, ω_j	Overall stock filling level, and stock filling level per class j

Result Variables

$t_{Ch,R}$	Expected travel time in the z-direction in seconds during a retrieval job
$t_{Ch,S}$	Expected travel time in the z-direction in seconds during a storage job
$t_{Ch,R,\beta}$	Expected travel time in the z-direction in seconds during a retrieval of blocking unit load
$t_{Ch,S,\beta}$	Expected travel time in the z-direction in seconds during a storage of blocking unit load
t_{cycle}	Cycle time for one command cycle in the rack in seconds
$t_{cycle,n}$	Normalised cycle time
$t_{driving}$	Normalised driving time
$t_{handling}$	Normalised handling time
$t_{\text{Rto}\beta}$	Expected travel time from a retrieval channel to a reshuffle channel in seconds
t_{StoR}	Expected travel time from a storage channel to a retrieval channel in seconds
t_{toHP}	Expected travel time from a retrieval channel to a handover point in seconds
t_{toS}	Expected travel time from a handover point to a storage channel in seconds
t_{turn}	Time a robot needs to change direction during a travel in seconds

t_β	Expected travel time for one reshuffle job in seconds
TP	Throughput capacity
β, $P(\beta_{j,s})$	Expected number of reshuffles for a storage or retrieval job; and probability that s reshuffles are necessary for a retrieval of a unit load of class j
$P(\beta > 0$	Probability that more than 0 reshuffles are necessary for a retrieval job

Auxiliary Variables

$c_{h,k}$	k^{th} channel type with h stored unit loads
$c_{h,k,t}$	The location t in a channel type $c_{h,k}$
S_j, $R_{j,t}$	Storage job of class j, and retrieval jobs of class j from location t. If there is only one class this is simplified to S and R
ζ_j	The expected number of blocking unit loads of class j
μ_{cycle}	Service rate of the infinite server in the queuing system
μ_{pick}	Service rate of the pick station in the queuing system
θ	Handling-to-driving-ratio

Bibliography

AM Logistics Solutions. Am logistics solutions - AutoStore, 2024. URL `https://www.amlogisticsolutions.de/autostore/`. Accessed on: 13.08.2024.

Dieter Arnold and Kai Furmans. *Materialfluss in Logistiksystemen*, volume 7. Springer-Verlag, Heidelberg, 2019.

Thomas Atz, Daniel Lantschner, and Willibald A. Günthner. Simulative throughput calculation for storage planning. In *The International Workshop on Applied Modelling and Simulation WAMS 2013*, 2013.

AutoStore. Autostore - company homepage, 2024. URL `https://www.autostoresystem.com/de/company`. Accessed on: 13.08.2024.

Kaveh Azadeh, René De Koster, and Debjit Roy. Robotized and automated warehouse systems: Review and recent developments. *Transportation Science*, 53(4):917–945, 2019.

Gunter Bolch, Stefan Greiner, Hermann De Meer, and Kishor S. Trivedi. *Queueing networks and Markov chains: modeling and performance evaluation with computer science applications*. John Wiley & Sons, Hoboken, 2006.

Steffen Bolender, Jan Oellerich, Meike Braun, Markus Golder, and Kai Furmans. System zur reproduzierbaren, automatischen und sicheren Stapelung von Gitterboxen mit einem Brückenkran - KrasS. *Logistics Journal: Proceedings*, 2018(01), 2018.

Yavuz A. Bozer and John A. White. Travel time models for automated storage/retrieval systems. Technical report, Georgia Institute of Technology, 1982.

Yavuz A. Bozer and John A. White. Travel-time models for automated storage/retrieval systems. *IIE transactions*, 16(4):329–338, 1984.

Olivier Cardin, Pierre Castagna, Zaki Sari, and Nihad Meghelli. Performance evaluation of in-deep class storage for flow-rack AS/RS. *International Journal of Production Research*, 50(23):6775–6791, 2012.

Zhuxi Chen, Xiaoping Li, and Jatinder N.D. Gupta. A bi-directional flow-rack automated storage and retrieval system for unit-load warehouses. *International Journal of Production Research*, 53(14): 4176–4188, 2015.

René De Koster, Tho Le-Duc, and Yu Yugang. Optimal storage rack design for a 3-dimensional compact AS/RS. *International journal of production research*, 46(6):1495–1514, 2008.

Gianluca D'Antonio and Paolo Chiabert. Analytical models for cycle time and throughput evaluation of multi-shuttle deep-lane AVS/RS. *The International Journal of Advanced Manufacturing Technology*, 104(5-8):1919–1936, 2019.

Michael Eder. An approach for a performance calculation of shuttle-based storage and retrieval systems with multiple-deep storage. *The International Journal of Advanced Manufacturing Technology*, 107(1):859–873, 2020a.

Michael Eder. An approach for performance evaluation of sbs/rs with shuttle vehicles serving multiple tiers of multiple-deep storage rack. *The International Journal of Advanced Manufacturing Technology*, 110(11):3241–3256, 2020b.

Michael Eder. An analytical approach for a performance calculation of shuttle-based storage and retrieval systems with multiple-deep and class-based storage. *Production & Manufacturing Research*, 10(1):321–336, 2022.

Federation Europeenne de la Manutention. FEM 9.851: Performance Data of S/R Machines - Cycle Times, 2003.

Latéfa Ghomri and Zaki Sari. Mathematical modeling of the average retrieval time for flow-rack automated storage and retrieval systems. *Journal Of Manufacturing Systems*, 44:165–178, 2017.

Timm Gudehus. Grundlagen der Spielzeitberechnung für automatische Hochregallager. *Deutsche Hebe-und Fördertechnik*, 18:63–68, 1972.

Willibald A. Günthner and Klaus Heptner. *Technische Innovationen für die Logistik*, volume 1. Huss-Verlag, München, 2007.

Mohammed A Hamzaoui and Sari Zaki. Cycle time models for the bidirectional flow-rack AS/RS. *FME Transactions*, 48(1):211–226, 2020.

Min-Hong Han, Leon F. McGinnis, Jin Shen Shieh, and John A. White. On sequencing retrievals in an automated storage/retrieval system. *IIE transactions*, 19(1):56–66, 1987.

Warren H. Hausman, Leroy B. Schwarz, and Stephen C. Graves. Optimal storage assignment in automatic warehousing systems. *Management Science*, 22(6):629–638, 1976.

Hark Hwang and Seong Beak Lee. Travel-time models considering the operating characteristics of the storage and retrieval machine. *The International Journal of Production Research*, 28(10): 1779–1789, 1990.

Insider Intelligence and eMarketer. Worldwide retail ecommerce forecast 2024, 2024. URL https://www.emarketer.com/content/worldwide-retail-ecommerce-forecast-2024. Accessed on: 13.08.2024.

Interact Analysis. Global revenue and order intake forecast, 2023. URL https://interactanalysis.com/warehouse-automation-market-to-return-to-growth-in-2024/. Accessed on: 13.08.2024.

Jungheinrich. Jungheinrich - powerstore powercube, 2024. URL https://www.jungheinrich.de/systeme/automatische-lagersysteme/powercube. Accessed on: 13.08.2024.

Timo Lehmann and René De Koster. Digging deep: Finding and maximizing the throughput capacity of multi-deep storage systems. *Transportation Science*, 2024. Major Revision.

Timo Lehmann and Jakob Hussmann. Travel time model for multi-deep automated storage and retrieval system with a homogeneous allocation structure. *Logistics Research*, 2021.

Timo Lehmann and Jakob Hussmann. Travel time model for multi-deep automated storage and retrieval systems with different storage strategies. Repository KITopen, 2022.

Timo Lehmann and Jakob Hussmann. Travel time model for multi-deep automated storage and retrieval systems with different storage strategies. *International Journal of Production Research*, 61(16):5676–5691, 2023.

Tone Lerher. Travel time model for double-deep shuttle-based storage and retrieval systems. *International Journal of Production Research*, 54(9):2519–2540, 2016.

Tone Lerher, Matjaz Sraml, Iztok Potrc, and Tomaz Tollazzi. Travel time models for double-deep automated storage and retrieval systems. *International Journal of Production Research*, 48(11): 3151–3172, 2010.

Christian R. Lippolt. *Spielzeiten in Hochregallagern mit doppeltiefer Lagerung*. PhD thesis, Institute for Material Handling and Logistics; Karlsruhe Institut of Technology, 2003.

Riccardo Manzini, Riccardo Accorsi, Giulia Baruffaldi, Teresa Cennerazzo, and Mauro Gamberi. Travel time models for deep-lane unit-load autonomous vehicle storage and retrieval system (AVS/RS). *International Journal of Production Research*, 54(14):4286–4304, 2016.

Jakob Marolt, Nenad Kosanić, and Tone Lerher. Relocation and storage assignment strategy evaluation in a multiple-deep tier captive automated vehicle storage and retrieval system with undetermined retrieval sequence. *The International Journal of Advanced Manufacturing Technology*, 118(9): 3403–3420, 2022a.

Jakob Marolt, Simona Šinko, and Tone Lerher. Model of a multiple-deep automated vehicles storage and retrieval system following the combination of depth-first storage and depth-first relocation strategies. *International Journal of Production Research*, pages 1–18, 2022b.

Russell D. Meller. Considerations when designing an autostoretm system. *PMHR: 16th Proceedings (Dresden, Germany- 2023)*, (12), 2023.

Kees Jan Roodbergen and Iris F.A. Vis. A survey of literature on automated storage and retrieval systems. *European journal of operational research*, 194(2):343–362, 2009.

Zaki Sari, Can Saygin, and Noureddine Ghouali. Travel-time models for flow-rack automated storage and retrieval systems. *The International Journal of Advanced Manufacturing Technology*, 25 (9-10):979–987, 2005.

Kai Siebertz, David van Bebber, and Thomas Hochkirchen. *Statistische Versuchsplanung. Design of Experiments (DoE)*, volume 2. Springer Vieweg Berlin, Heidelberg, 2017.

Philipp Trost and Michael Eder. A performance calculation approach for a robotic compact storage and retrieval system (RCS/RS) serving one picking station. *Production & Manufacturing Research*, 12 (1):2336056, 2024.

Mahmut Tutam, Jingming Liu, and John A White. Consideration of skewness in designing robotic compact storage and retrieval systems. *Expert Systems with Applications*, 248:123361, 2024.

Jeroen P. Van Den Berg and A.J.R.M. Gademann. Simulation study of an automated storage/retrieval system. *International Journal of Production Research*, 38(6):1339–1356, 2000.

Verein Deutscher Ingenieure. VDI 4480/4: Durchsatz von automatischen Lagern mit mehrfachtiefer Lagerung, 2002.

Xianhao Xu, Xiaozhen Zhao, Bipan Zou, and Mingze Li. Optimal dimensions for multi-deep storage systems under class-based storage policies. *Cluster Computing*, 22(3):861–875, 2019.

Peng Yang, Lixin Miao, Zhaojie Xue, and Lei Qin. Optimal storage rack design for a multi-deep compact AS/RS considering the acceleration/deceleration of the storage and retrieval machine. *International Journal of Production Research*, 53(3):929–943, 2015.

Peng Yang, Kaidong Yang, Mingyao Qi, Lixin Miao, and Bin Ye. Designing the optimal multi-deep as/rs storage rack under full turnover-based storage policy based on non-approximate speed model of s/r machine. *Transportation Research Part E: Logistics and Transportation Review*, 104: 113–130, 2017.

Yugang Yu and René BM de Koster. Optimal zone boundaries for two-class-based compact three-dimensional automated storage and retrieval systems. *IIE Transactions*, 41(3):194–208, 2009.

Anni Yue and Stephen L Smith. Minimizing robot digging times to retrieve bins in robotic-based compact storage and retrieval systems. *arXiv preprint arXiv:2312.05338*, 2023.

Bipan Zou, René De Koster, and Xianhao Xu. Operating policies in robotic compact storage and retrieval systems. *Transportation Science*, 52(4):788–811, 2018.

List of own Publications

Fernando Arranz, T. Lehmann, F. Rauscher, G. Fischer, S. Koehler, J. Garrido, M. Rouret, and D. Sanchez-Herranz. Logistics and maintenance research activities for dones facility. *Fusion Engineering and Design*, 192:113630, 2023.

Oliver Crofts, A. Loving, M. Torrance, S. Budden, B. Drumm, T. Tremethick, D. Chauvin, M. Siuko, W. Brace, V. Milushev, T. Lehmann, et al. EU DEMO remote maintenance system development during the pre-concept design phase. *Fusion Engineering and Design*, 179:113121, 2022.

Samuel Hall, M. Hora, G. Fischer, S. Köhler, F. Rauscher, T. Lehmann, J. Oellerich, O. Crofts, M. Torrance, and B. Drumm. Creation of a development platform for remote maintenance solutions in fusion power plants. *IEEE Transactions on Plasma Science*, 2024.

Timo Lehmann and R. De Koster. Digging deep: Finding and maximizing the throughput capacity of multi-deep storage systems. *Transportation Science*, 2024. Major Revision.

Timo Lehmann and J. Hussmann. Travel time model for multi-deep automated storage and retrieval system with a homogeneous allocation structure. *Logistics Research*, 2021.

Timo Lehmann and J. Hussmann. Travel time model for multi-deep automated storage and retrieval systems with different storage strategies. *International Journal of Production Research*, 61(16): 5676–5691, 2023.

Timo Lehmann and P. Knötgen. Betriebspunktuntersuchung des Lagerfüllgrads eines doppeltiefen automatischen Hochregallagers. *Logistics Journal: Proceedings*, 2020(12), 2020.

Timo Lehmann, F. Rauscher, J. Oellerich, G. Fischer, and J. Zapata. Modular transportation concept for application in DEMO Oriented Neutron Source (DONES). *Fusion Engineering and Design*, 164:112199, 2021.

Timo Lehmann, G. Fischer, F. Rauscher, S. Köhler, and F. Arranz. Material flow planning in fusion test facilities. *Fusion Engineering and Design*, 202:114412, 2024.

Martin Mittwollen, G. Fischer, P. Pagani, C. Kunert, J. Oellerich, T. Lehmann, G. Micciche, and A. Ibarra. Maintenance logistics for IFMIF-DONES. *Fusion Engineering and Design*, 146: 2743–2747, 2019.

Ivan Podadera, A. Ibarra, M. Weber, B. Bolzon, N. Chauvin, S. Chel, A. Madur, T. Dézsi, F. Arranz, C. de la Morena, T. Lehmann, et al. Commissioning plan of the IFMIF-DONES accelerator. *Proc. LINAC'22*, pages 330–333, 2022.

Felix Rauscher, G. Fischer, T. Lehmann, J.J. Zapata, P. Pagani, and A. Loving. A digital twin concept for the development of a demo maintenance logistics modelling tool. *Fusion Engineering and Design*, 168:112399, 2021.

List of Figures

List of Tables

A Appendix

The Appendices A.1 to A.3 and A.5 to A.9 are the appendix of the paper "Digging Deep: Finding and Maximizing the Throughput Capacity of Multi-deep Storage Systems" currently under revision in *Transportation Science* (Lehmann and De Koster 2024).
The text, formal analysis and visualisation in these sections have been taken from the paper with minor changes.
The author of this thesis was responsible for the conceptualisation, methodology, software, validation, formal analysis, investigation, writing (original draft), and visualisation of the research presented in these sections.

A.1 Optimal Pick Station Location and Length to Width Ratio

In this section it is shown for all strategies: 1) The optimal allocation of a single pick station and 2) the optimal length to width ($l_x \cdot L$ to $l_y \cdot W$) ratio of a RCS/R system with given number of channels. The location of the pick station only influences t_{toHP} and t_{toS} of t_{cycle}. We first assume that the pick station is allocated somewhere on the $l_x \cdot L$ long side of the RCS/R system. Depending on the distance d of the pick station from the one corner (normalised to $d \in (0, 1)$) the average travel distance for t_{toHP} and t_{toS} is:

$$\frac{\int_0^{l_x \cdot L \cdot d} \int_0^{l_y \cdot W} (i+j) \mathrm{d}i \mathrm{d}j + \int_0^{l_x \cdot L \cdot (1-d)} \int_0^{l_y \cdot W} (i+j) \mathrm{d}i \mathrm{d}j}{l_x \cdot L + l_y \cdot W} = l_x \cdot L(d^2 - d + \frac{1}{2}) + \frac{l_y \cdot W}{2}$$

This expression can be minimised for $d = 0.5$. The same can be done for pick station allocated at the $l_y \cdot W$ long side of the rack. We get the two possibilities for travel distance:

$$dist_L = \frac{l_x \cdot L + 2 \cdot l_y \cdot W}{4}$$
$$dist_W = \frac{2 \cdot l_x \cdot L + l_y \cdot W}{4}$$

Assuming that $l_x \cdot L = l_y \cdot W \cdot \epsilon$ with $\epsilon > 0$ we get:

$$dist_L = \frac{(3+\epsilon) l_y W}{4} < \frac{(3+2\epsilon) l_y W}{4} = dist_W$$

This means that allocating the pick station in the middle of the longer side of the RCSR system minimises the travel distance and thus travel time of t_{toHP} and t_{toS} and therefore also for t_{cycle} for any $l_x L \geq l_y W$.

For 2) the problem is split to get an upper and lower bound for the $l_x L : l_y W$ ratio. First, we want to find the optimal rack layout L and W which minimises the travel distance of t_{StoR} and $t_{\text{Rto}\beta}$. We analyse t_{StoR} and $t_{\text{Rto}\beta}$ for $d = 1$, but this can be done for all d analogue. The average distance is:

$$\frac{\int_0^{l_x L} \int_0^{l_y W} \int_0^{l_x L} \int_0^{l_y W} (|i - i'| + |j - j'|) \mathrm{d}i \mathrm{d}j \mathrm{d}i' \mathrm{d}j'}{{l_x}^2 L^2 {l_y}^2 W^2} = \frac{l_x L + l_y W}{3}$$

which can be minimised for $l_x L = l_y W$ and thus a $l_x L : l_y W$ ratio of 1:1. Second, the optimal rack layout to minimise t_{toHP} and t_{toS} is a $l_x L : l_y W$ ratio which minimises $\frac{l_x \cdot L + 2 \cdot l_y \cdot W}{4}$. Minimal t_{toHP} and t_{toS} are achieved for $l_x L = 2 l_y W$ and thus the $l_x L : l_y W$ ratio is 2:1. Since t_{StoR} and $t_{\text{Rto}\beta}$ depend on d which is individually calculated for all strategies and rack parameters, the lower bound of a t_{cycle} minimising and therefore throughput maximising rack layout for the $l_x L : l_y W$ ratio is 1:1 and the upper bound is 2:1.

Throughout the work, nearest neighbour policy is used to reduce the cycle time, but if the random policy is used, the optimal rack layout ratio can be determined

even more precisely. A random policy equals to $d = 1$ for all $t_{\text{Rto}\beta}$ and t_{toS}. Since the summands $t_{\text{StoR}}, t_{\text{toHP}}$ and t_{toS} appear once in t_{cycle}, a new upper limit for the $l_xL : l_yW$ ratio is $\frac{8}{5} : 1$ with:

$$t_{\text{StoR}} + t_{\text{toHP}} + t_{\text{toS}} = \frac{l_xL + l_yW}{3} + \frac{l_x \cdot L + 2 \cdot l_y \cdot W}{2} = \frac{5l_xL + 8l_yW}{6}$$

and the minimum for $l_xL = \frac{8}{5}l_yW$.

By incorporating the number of reshuffles β, the optimal rack layout ratio $l_xL : l_yW$ can be determined exactly. The relevant distance is:

$$\begin{aligned} t_{\text{StoR}} + t_{\text{toHP}} + t_{\text{toS}} + \beta \cdot t_{\text{Rto}\beta} &= \frac{5l_xL + 8l_yW}{6} + \beta \cdot \frac{l_xL + l_yW}{3} \\ &= \frac{(5 + 2\beta)l_xL + (8 + 2\beta)l_yW}{6} \end{aligned} \tag{A.1}$$

and the optimal rack layout ratio $l_xL : l_yW$ is $\frac{8+2\beta}{5+2\beta} : 1$.

A.2 Proof: Loads of the Same Product - Clustered or Random Storage?

We assume:

- Without loss of generality, only unit loads of products of one class are regarded
- The rack is aggregated to one representative channel
- At the initial state, the unit loads of the same product are randomly distributed across the representative channel
- The unit load of the product which causes the fewest reshuffles is chosen for retrieval

During any storage job, the system can decide whether the unit load should be stored above a unit load with the same product if this location is free or whether it should be stored above a unit load of a random product. For any fill level $\omega \cdot H \in \mathbb{N}$ of the regarded representative channel and any number of unit loads per product $\xi \leq H$ already stored in this channel either randomly or clustered, the resulting number of reshuffles can be calculated for the next retrieval of such a product after sufficiently many command cycles between the last storage and the next retrieval job:

$$\begin{aligned}
\beta_{Clustered} &= \frac{\sum_{i=0}^{H-\xi} i}{h-\xi+1} = \frac{H-\xi}{2} \\
\beta_{Random} &= \frac{\sum_{i=1}^{H-\xi+1} \binom{h-i}{\xi-1} \cdot (i-1)}{\binom{H}{\xi}} = \frac{\binom{H}{\xi+1}}{\binom{H}{\xi}} = \frac{H-\xi}{\xi+1} \\
\frac{\beta_{Random}}{\beta_{Clustered}} &= \frac{\frac{H-\xi}{\xi+1}}{\frac{H-\xi}{2}} = \frac{2}{\xi+1}
\end{aligned} \tag{A.2}$$

For $\xi = 1$ it is trivial that number of reshuffles is equal. For all $\xi > 1$ the fraction in Equation (A.2) is < 1 and thus the number of reshuffles for β_{Random} is smaller than for $\beta_{Clustered}$.

A.3 Simulation for Validation of the Throughput Models

Figure A.1 shows the procedure of the simulations for all strategies. The reshuffle strategies are shown in detail in Figures A.2 and A.3 and the storage assignment strategies in Figure A.4.

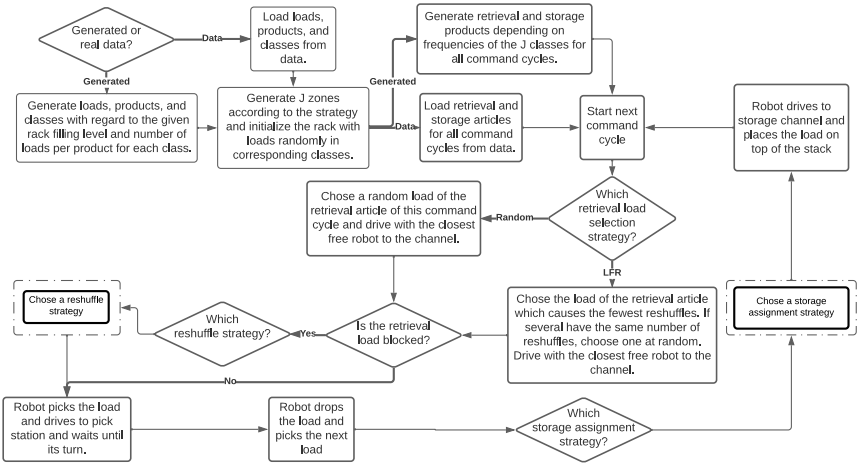

Figure A.1: Flowchart of the Procedure of the Simulation.

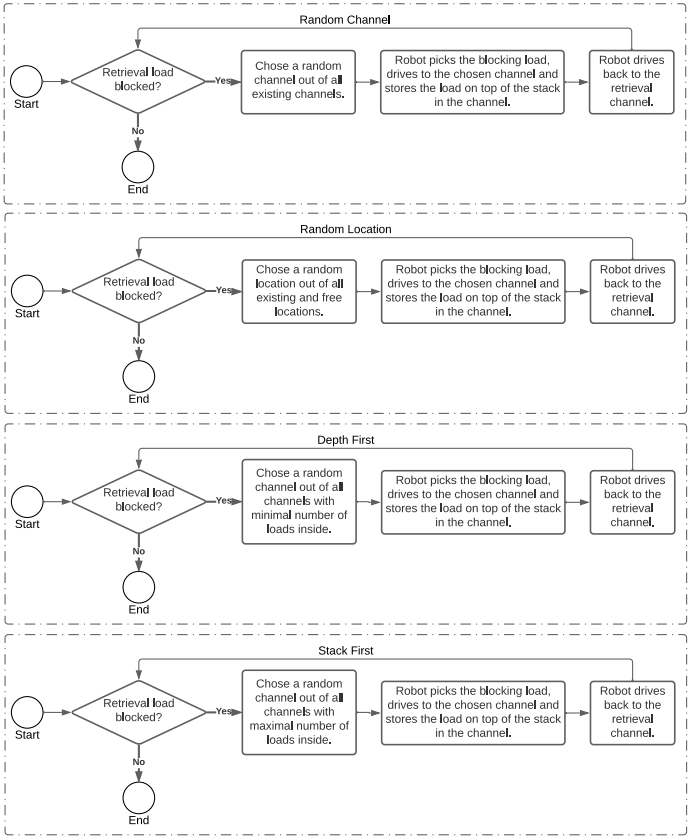

Figure A.2: Flowchart for the Simulation of Reshuffle Strategies.

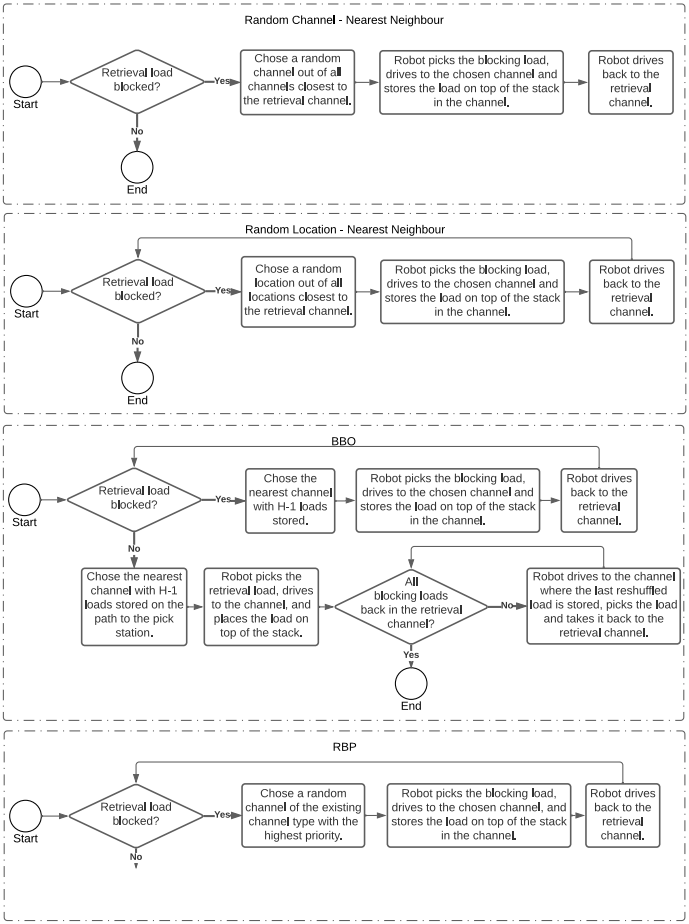

Figure A.3: Flowchart for the Simulation of Reshuffle Strategies.

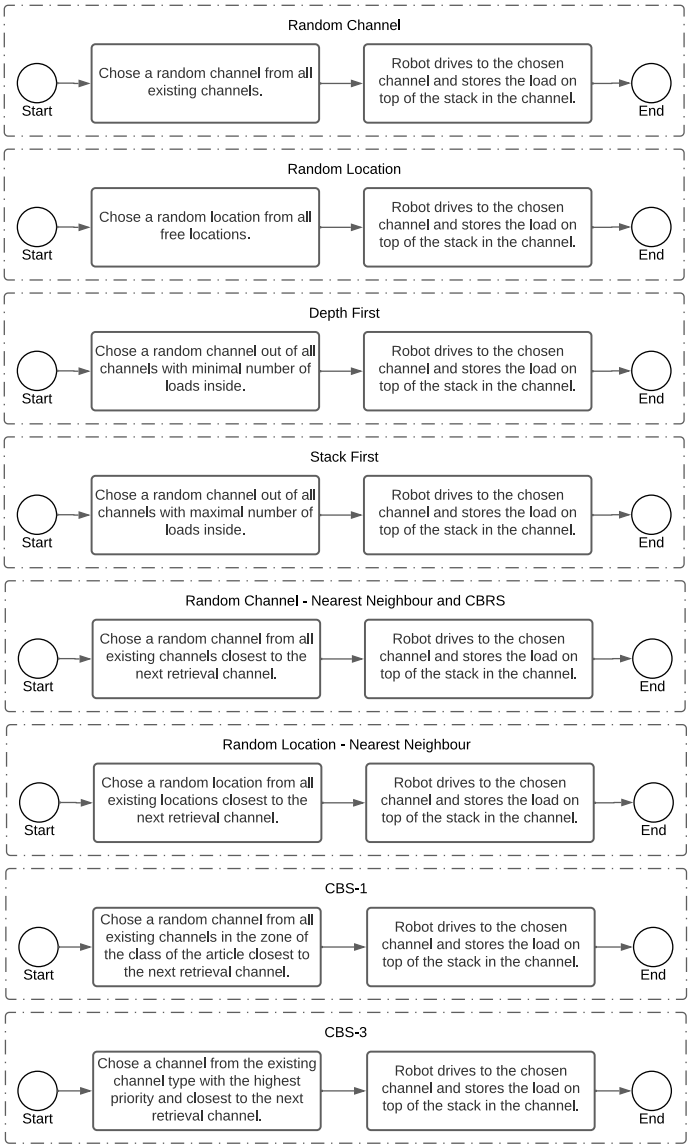

Figure A.4: Flowchart for the Simulation of Storage Allocation Strategies.

A.4 Validation Results for Automated Storage and Retrieval Systems

Table A.1: Validation Results.

	ID	t_{cycle} [s]				β			
		Ana	Sim	δ	δ_{CI}	Ana	Sim	δ	δ_{CI}
Homogeneous	I	69.46	69.41 ± 0.62	0.0	0.0	1.12	1.12 ± 0.02	0.0	0.0
	II	57.21	56.22 ± 0.53	0.02	0.01	1.12	1.16 ± 0.02	-0.03	-0.01
	III	113.99	113.22 ± 0.95	0.01	0.0	1.12	1.14 ± 0.02	-0.02	0.0
	IV	39.35	39.45 ± 0.29	-0.0	0.0	0.38	0.37 ± 0.01	0.02	0.0
	V	209.7	208.2 ± 1.75	0.01	0.0	2.62	2.67 ± 0.04	-0.02	-0.0
	VI	61.23	61.57 ± 0.52	-0.01	0.0	0.9	0.91 ± 0.02	-0.01	0.0
	VII	77.58	76.78 ± 0.66	0.01	0.0	1.35	1.36 ± 0.03	-0.01	0.0
RSCS	I	49.34	49.87 ± 0.39	-0.01	-0.0	1.28	1.28 ± 0.02	0.0	0.0
	ÍI	41.16	41.97 ± 0.4	-0.02	-0.01	1.28	1.27 ± 0.02	0.01	0.0
	III	79.01	78.61 ± 0.62	0.01	0.0	1.28	1.28 ± 0.02	0.0	0.0
	IV	32.03	32.26 ± 0.21	-0.01	-0.0	0.43	0.43 ± 0.01	0.0	0.0
	V	90.39	91.7 ± 0.95	-0.01	-0.0	2.98	2.98 ± 0.04	0.0	0.0
	VI	46.81	47.11 ± 0.4	-0.01	0.0	1.11	1.1 ± 0.02	0.01	0.0
	VII	51.38	51.99 ± 0.44	-0.01	-0.0	1.42	1.43 ± 0.03	-0.01	0.0
RSLS	I	48.44	48.75 ± 0.45	-0.01	0.0	1.21	1.21 ± 0.02	0.0	0.0
	II	40.43	41.46 ± 0.38	-0.02	-0.02	1.21	1.22 ± 0.02	-0.01	0.0
	III	77.51	77.08 ± 0.58	0.01	0.0	1.21	1.21 ± 0.02	0.0	0.0
	IV	31.67	31.75 ± 0.18	-0.0	0.0	0.4	0.4 ± 0.0	0.0	0.0
	V	88.78	90.12 ± 1.01	-0.01	-0.0	2.84	2.84 ± 0.05	0.0	0.0
	VI	45.37	45.67 ± 0.4	-0.01	0.0	1.01	1.0 ± 0.02	0.01	0.0
	VII	51.04	51.68 ± 0.45	-0.01	-0.0	1.39	1.4 ± 0.02	-0.01	0.0
Depth First	I	45.74	46.12 ± 0.31	-0.01	-0.0	1.0	1.0 ± 0.02	0.0	0.0
	II	38.26	39.14 ± 0.29	-0.02	-0.02	1.0	1.01 ± 0.01	-0.01	0.0
	III	72.9	72.3 ± 0.66	0.01	0.0	1.0	1.0 ± 0.02	0.0	0.0
	IV	30.64	30.62 ± 0.17	0.0	0.0	0.33	0.33 ± 0.01	0.0	0.0
	V	85.32	86.49 ± 0.82	-0.01	-0.0	2.5	2.49 ± 0.03	0.0	0.0
	VI	41.81	42.04 ± 0.29	-0.01	0.0	0.75	0.75 ± 0.02	0.0	0.0
	VII	50.27	50.9 ± 0.41	-0.01	-0.0	1.33	1.34 ± 0.02	-0.01	0.0
Stack First	I	52.53	53.08 ± 0.47	-0.01	-0.0	1.5	1.5 ± 0.02	0.0	0.0
	II	43.81	44.92 ± 0.36	-0.02	-0.02	1.5	1.5 ± 0.02	0.0	0.0
	III	84.16	83.59 ± 0.7	0.01	0.0	1.5	1.5 ± 0.03	0.0	0.0
	IV	33.08	33.23 ± 0.18	-0.0	0.0	0.5	0.5 ± 0.01	0.0	0.0
	V	97.84	99.21 ± 0.98	-0.01	-0.0	3.5	3.49 ± 0.04	0.0	0.0
	VI	52.53	52.93 ± 0.44	-0.01	0.0	1.5	1.49 ± 0.02	0.01	0.0
	VII	52.53	53.22 ± 0.46	-0.01	-0.0	1.5	1.5 ± 0.02	0.0	0.0
RSCS-NN	I	42.52	43.04 ± 0.35	-0.01	-0.0	1.28	1.29 ± 0.03	-0.01	0.0
	II	38.79	39.64 ± 0.34	-0.02	-0.01	1.28	1.29 ± 0.02	-0.01	0.0
	III	56.27	55.69 ± 0.35	0.01	0.0	1.28	1.28 ± 0.02	0.0	0.0
	V	77.81	78.81 ± 0.85	-0.01	-0.0	2.98	3.02 ± 0.05	-0.01	0.0
	VI	40.46	41.09 ± 0.33	-0.02	-0.01	1.11	1.12 ± 0.03	-0.01	0.0

	VII	44.73	44.67 ± 0.36	0.0	0.0	1.42	1.42 ± 0.02	0.0	0.0
RSLS-NN	I	41.73	42.5 ± 0.29	-0.02	-0.01	1.21	1.23 ± 0.01	-0.02	-0.01
	II	37.99	38.88 ± 0.37	-0.02	-0.01	1.21	1.23 ± 0.03	-0.02	0.0
	III	55.48	55.17 ± 0.34	0.01	0.0	1.21	1.23 ± 0.02	-0.02	0.0
	IV	28.06	28.32 ± 0.14	-0.01	-0.0	0.4	0.41 ± 0.01	-0.02	0.0
	V	76.17	77.93 ± 0.86	-0.02	-0.01	2.84	2.92 ± 0.04	-0.03	-0.01
	VI	39.36	40.25 ± 0.31	-0.02	-0.01	1.01	1.03 ± 0.02	-0.02	0.0
	VII	44.14	44.48 ± 0.36	-0.01	0.0	1.39	1.41 ± 0.02	-0.01	0.0

Table A.2: Aggregated δ and δ_{CI} for all 11 Instances.

	t_{cycle}						β					
	$\overline{\delta}$	δ^{max}	δ^{min}	$\overline{\delta_{CI}}$	δ_{CI}^{min}	δ_{CI}^{max}	$\overline{\delta}$	δ^{max}	δ^{min}	$\overline{\delta_{CI}}$	δ_{CI}^{min}	δ_{CI}^{max}
Homogeneous	0.00	-0.01	0.02	0.00	0.00	0.01	-0.01	-0.03	0.02	-0.00	-0.01	0.00
RSCS	-0.01	-0.02	0.01	-0.00	-0.01	0.00	0.00	-0.01	0.01	0.00	0.00	0.00
RSLS	-0.01	-0.02	0.01	-0.00	-0.02	0.00	-0.00	-0.01	0.01	0.00	0.00	0.00
Depth First	-0.01	-0.02	0.01	-0.00	-0.02	0.00	-0.00	-0.01	0.00	0.00	0.00	0.00
Stack First	-0.01	-0.02	0.01	-0.00	-0.02	0.00	0.00	0.00	0.01	0.00	0.00	0.00
RSCS-NN	-0.01	-0.02	0.01	-0.00	-0.01	0.00	-0.01	-0.01	0.00	0.00	0.00	0.00
RSLS-NN	-0.01	-0.02	0.01	-0.01	-0.01	0.00	-0.02	-0.03	-0.01	-0.00	-0.01	0.00

A.5 Cycle Time Distribution

Figures A.5 and A.6 show the histograms of t_{cycle} and the resulting interarrival time of robots at a pick station taken from the steady state evaluations of the simulation. We conclude that especially for the CBS-1, AutoStore, AS-LFR, CBS-3-BBO, and CBS-3-RBP strategies, an exponential distribution for t_{cycle} is a good assumption. However, due to the number of robots ($K = 5$), also the histogram of the Random and Random-BBO strategies lead to exponentially distributed interarrival times at pick stations.

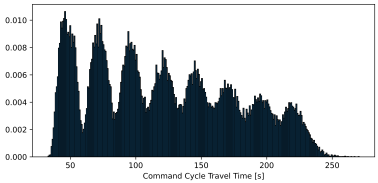

(a) Random

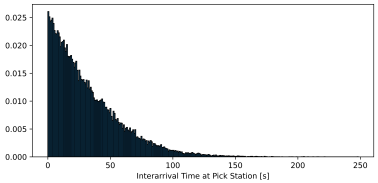

(b) Random

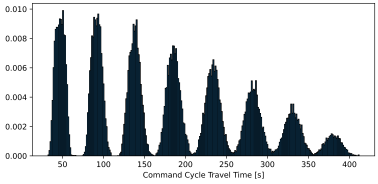

(c) Random-BBO

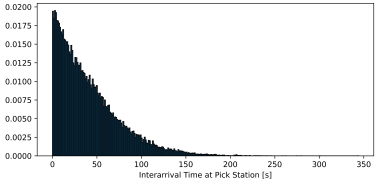

(d) Random-BBO

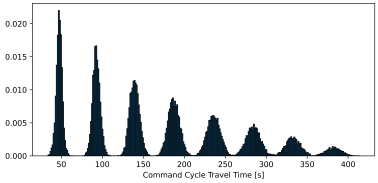

(e) CBS-1

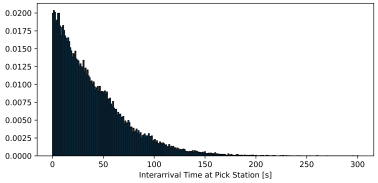

(f) CBS-1

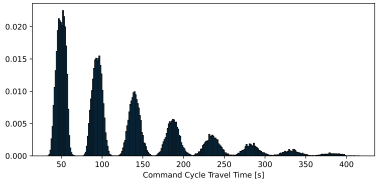

(g) AutoStore

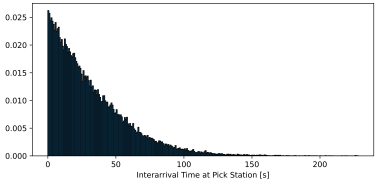

(h) AutoStore

Figure A.5: Histogram of the Cycle Time t_{cycle} and the Interarrival Time at the Pick Station for the Random, Random-BBO, CBS-1, and AutoStore Strategies and the Baseline Configuration I.

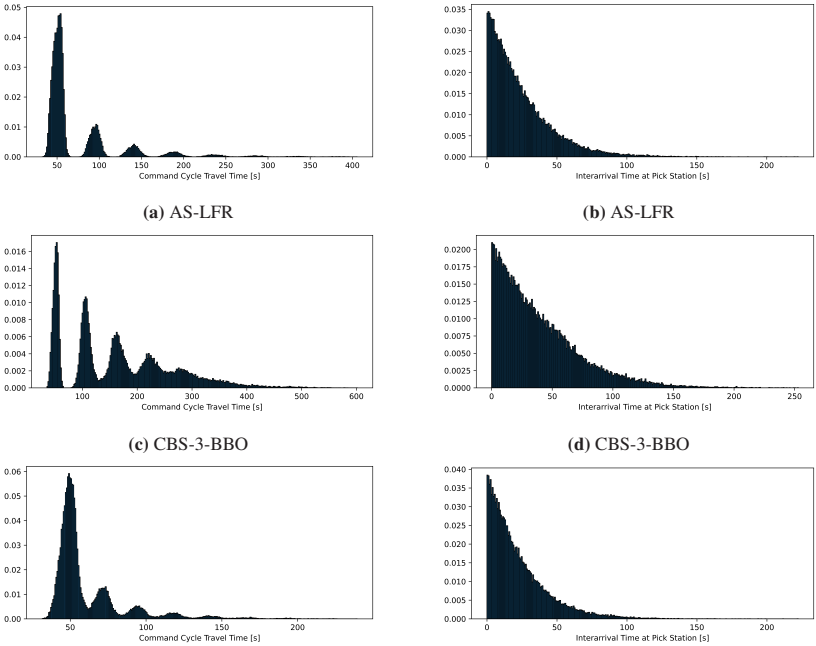

(a) AS-LFR **(b)** AS-LFR

(c) CBS-3-BBO **(d)** CBS-3-BBO

(e) CBS-3-RBP **(f)** CBS-3-RBP

Figure A.6: Histogram of the Cycle Time t_{cycle} and the Interarrival Time at the Pick Station for the AS-LFR, CBS-3-BBO, and CBS-3-RBP Strategies and the Baseline Configuration I.

A.6 Transition Matrix

The state space $\pi_{h,k}$ depends on the strategy considered. This section presents the positions (row and column indices) of the transition probabilities $P(S_j|c_{h,k})$ and $P(R_j|c_{h,k,t})$ in the transition matrix M. Algorithm 1 shows the allocation for all $P(S_j|c_{h,k})$ of all strategies. The transition matrix for an RCS/R system with $h = 2$ for the CBS-3-RBP strategy is shown in Equation (A.3):

(A.3)

$$
\begin{array}{c|cccccccccccc}
 & M_{[0,0]} & P(S_A|c_{0,1}) & P(S_B|c_{0,1}) & P(S_C|c_{0,1}) & 0 & 0 & 0 & 0 & 0 & 0 & 0 & 0 \\
P(R_A|c_{1,1,1}) & P(S_A|c_{0,1}) & M_{[1,1]} & 0 & 0 & 0 & 0 & 0 & 0 & 0 & 0 & 0 & 0 \\
P(R_B|c_{1,2,1}) & P(S_B|c_{0,1}) & 0 & M_{[2,2]} & 0 & 0 & 0 & 0 & 0 & 0 & 0 & 0 & 0 \\
P(R_C|c_{1,3,1}) & P(S_C|c_{0,1}) & 0 & 0 & M_{[3,3]} & 0 & 0 & 0 & 0 & 0 & 0 & 0 & 0 \\
P(R_A|c_{2,1,1}) & 0 & P(R_A|c_{2,1,2}) & 0 & 0 & M_{[4,4]} & 0 & 0 & 0 & 0 & 0 & 0 & 0 \\
P(R_A|c_{2,2,1}) & 0 & P(R_B|c_{2,2,2}) & 0 & 0 & 0 & M_{[5,5]} & 0 & 0 & 0 & 0 & 0 & 0 \\
P(R_A|c_{2,3,1}) & 0 & P(R_C|c_{2,3,2}) & 0 & 0 & 0 & 0 & M_{[6,6]} & 0 & 0 & 0 & 0 & 0 \\
P(R_B|c_{2,4,1}) & 0 & 0 & P(R_A|c_{2,4,2}) & 0 & 0 & 0 & 0 & M_{[7,7]} & 0 & 0 & 0 & 0 \\
P(R_B|c_{2,5,1}) & 0 & 0 & P(R_B|c_{2,5,2}) & 0 & 0 & 0 & 0 & 0 & M_{[8,8]} & 0 & 0 & 0 \\
P(R_B|c_{2,6,1}) & 0 & 0 & P(R_C|c_{2,6,2}) & 0 & 0 & 0 & 0 & 0 & 0 & M_{[9,9]} & 0 & 0 \\
P(R_C|c_{2,7,1}) & 0 & 0 & 0 & P(R_A|c_{2,7,2}) & 0 & 0 & 0 & 0 & 0 & 0 & M_{[10,10]} & 0 \\
P(R_C|c_{2,8,1}) & 0 & 0 & 0 & P(R_B|c_{2,8,2}) & 0 & 0 & 0 & 0 & 0 & 0 & 0 & M_{[11,11]} \\
P(R_C|c_{2,9,1}) & 0 & 0 & 0 & P(R_C|c_{2,9,2}) & 0 & 0 & 0 & 0 & 0 & 0 & 0 & 0
\end{array}
\begin{array}{c|cccccccccccc}
 & 0 & 0 & 0 & 0 & 0 & 0 & 0 & 0 & 0 & 0 & 0 & 0 \\
P(R_A|c_{1,1,1}) & 0 & 0 & 0 & 0 & 0 & 0 & 0 & 0 & 0 & 0 & 0 & 0 \\
P(R_B|c_{1,2,1}) & 0 & 0 & 0 & 0 & 0 & 0 & 0 & 0 & 0 & 0 & 0 & 0 \\
P(R_C|c_{1,3,1}) & 0 & 0 & 0 & 0 & 0 & 0 & 0 & 0 & 0 & 0 & 0 & 0 \\
P(R_A|c_{2,1,1}) & P(S_A|c_{1,1}) & 0 & 0 & 0 & 0 & 0 & 0 & 0 & 0 & 0 & 0 & 0 \\
P(R_A|c_{2,2,1}) & 0 & P(S_B|c_{1,1}) & 0 & 0 & 0 & 0 & 0 & 0 & 0 & 0 & 0 & 0 \\
P(R_A|c_{2,3,1}) & 0 & 0 & P(S_C|c_{1,1}) & 0 & 0 & 0 & 0 & 0 & 0 & 0 & 0 & 0 \\
P(R_B|c_{2,4,1}) & P(S_A|c_{1,2}) & 0 & 0 & 0 & 0 & 0 & 0 & 0 & 0 & 0 & 0 & 0 \\
P(R_B|c_{2,5,1}) & 0 & P(S_B|c_{1,2}) & 0 & 0 & 0 & 0 & 0 & 0 & 0 & 0 & 0 & 0 \\
P(R_B|c_{2,6,1}) & 0 & 0 & P(S_C|c_{1,2}) & 0 & 0 & 0 & 0 & 0 & 0 & 0 & 0 & 0 \\
P(R_C|c_{2,7,1}) & P(S_A|c_{1,3}) & 0 & 0 & 0 & 0 & 0 & 0 & 0 & 0 & 0 & 0 & 0 \\
P(R_C|c_{2,8,1}) & 0 & P(S_B|c_{1,3}) & 0 & 0 & 0 & 0 & 0 & 0 & 0 & 0 & 0 & 0 \\
P(R_C|c_{2,9,1}) & 0 & 0 & P(S_C|c_{1,3}) & 0 & 0 & 0 & 0 & 0 & 0 & 0 & 0 & 0
\end{array}
$$

Algorithm 2 shows the allocation for all $P(R_j|c_{h,k,t})$ of the Random-BBO, CBS-1, AutoStore, AS-LFR, and CBS-3-BBO strategy. Algorithm 3 shows the allocation for all $P(R_j|c_{h,k,t})$ for the CBS-3-RBP strategy. To complete the transition matrix, the entries in the diagonal of the matrix are:

$$M[i,i] = 1 - \sum_{m=0}^{i-1}(M[i,m]) - \sum_{m=i+1}^{\sum_{h=0}^{H} J^h}(M[i,m]) \tag{A.4}$$

Algorithm 1 Transition Matrix Entries - Storage Probabilities

```
1: class = 1
2: for j ∈ J do
3:     counter = 0
4:     for h ∈ H do
5:         for k ∈ J^h do
6:             M[counter, J · counter + class] = P(S_j|c_{h,k})
7:             counter = counter +1
8:     class = class +1
```

Algorithm 2 Transition Matrix Entries - Retrieval Probabilities BBO

counter$_1$, counter$_2$, counter$_3$, counter$_4$, counter$_5$, counter$_6$ $= 0, 1, 0, 0, 0, 0$
for $h \in H$ **do**
  for $i \in J^h$ **do**
    for $t \in h$ **do**
      class = 1
      for $j \in J$ **do**
        if $c_{i,h,t}$ = class **then**
          Probability$[counter] = P(R_j|p_{h,k,t})$
          counter$_1$ = counter$_1$ +1
        class = class +1
for i from 1 to $H + 1$ **do**
  for j from 0 to J^{i-1} **do**
    counters$[i - 1, j]$ = counter$_2$
    counter$_2$ = counter$_2$ +1
for i from 0 to H **do**
  lower = $\frac{J^{i+1}-1}{2}$
  upper = $\frac{J^{i+2}-1}{2}$
  result = result.append(repeat([lower...upper],$i + 1$)
Position$[0]$ = result
for i from 0 to H **do**
  for j from 0 to nonzero_entries(counters$[i]$) **do**
    for $l \in J$ **do**
      for k from 0 to $i + 1$ **do**
        Position$[1$,counter$_6]$ = counters$[k, \lfloor \frac{j}{J^{i-k}} \rfloor] - 1$
        counter$_6$ = counter$_6$ + 1
  original_value = $\frac{J^{i-1}}{2}$
  value = original_value
  for j from 1 to $\frac{J^{H+1}}{2} - \frac{J^{j+1}}{2} + 1$ **do**
    result_values$[i, j - 1]$ =value
    if j modulo $J^{i+1} = 0$ **then**
      original_value = value +1
      value = original_value
    else if i modulo $J^j = 0$ **then**
      value = original_value
    else
      value = value +1
for i from 1 to $H + 1$ **do**
  for j from 0 to J^i **do**
    for k from $i - 1$ to -1 **do**
      Position$[1$,counter$_4]$ = result_values$[k$,counter$_3[k]]$
      counter$_4$ = counter$_4$ +1
      counter$_3[k]$ = counter$_3[k] + 1$
for Probability.length **do**
  M[Position[counter$_5$, 1],Position[counter$_5$, 1]] = Probability[counter$_5$]
  counter$_5$ = counter$_5$ +1

Algorithm 3 Transition Matrix Entries - Retrieval Probabilities RBP

counter$_1$, counter$_2$, counter$_3$, counter$_4$ $= 0, 1, 0, 0$
for $h \in H$ **do**
  for $i \in J^h$ **do**
    for $t \in h$ **do**
      class = 1
      for $j \in J$ **do**
        if $c_{k,h,t}$ = class **then**
          Probability$[counter_1] = P(R_j|c_{h,k,t})$
          counter$_1$ = counter$_1$ +1
        class = class +1
for i from 1 to $H + 1$ **do**
  for j from 0 to J^{i-1} **do**
    counters$[i-1, j]$ = counter$_2$
    counter$_2$ = counter$_2$ +1
for i from 0 to H **do**
  lower = $\frac{J^{i+1}-1}{2}$
  upper = $\frac{J^{i+2}-1}{2}$
  result = result.append(repeat([lower...upper],i+1)
Position$[0]$ = result
for i from 0 to H **do**
  for j from 0 to nonzero_entries(counters$[i]$) **do**
    for $l \in J$ **do**
      for k from 0 to $i + 1$ **do**
        Position$[1$,counter$_3]$ = counters$[k, \lfloor \frac{j}{J^{i-k}} \rfloor] - 1$
        counter$_3$ = counter$_3$ + 1
for Probability.length **do**
  M[Position[counter$_4$, 1],Position[counter$_4$, 1]] = Probability[counter$_4$]
  counter$_4$ = counter$_4$ +1

A.7 Cycle Times

A.7.1 Derivation of t_{StoR}, $t_{\text{Rto}\beta}$, t_{toHP} and t_{toS}

For t_{StoR} and $t_{\text{Rto}\beta}$ there is a random variable x, which is the distance between two channels in the rack. This distance can be split in distance in L and W direction. The probability density functions for the distances between a random channel and all other channels in one direction are:

$$f_L(x) = \begin{cases} \frac{2 \cdot l_x L - 2 \cdot x}{(l_x L)^2} & 0 \leq x \leq l_x L \\ 0 & x > l_x L \end{cases}$$

$$f_W(x) = \begin{cases} \frac{2 \cdot l_y W - 2 \cdot x}{(l_y W)^2} & 0 \leq x \leq l_y W \\ 0 & x > l_y W \end{cases}$$

The pdf $g(x)$ and cdf $G(x)$ for the combined distance of a random channel to all other channels is then:

$$\begin{aligned} g(x) &= \int f_L(z) \cdot f_W(x-z) \mathrm{d}z \\ &= \begin{cases} \frac{2 \cdot x(x^2 - 3 \cdot (l_x L + l_y W) \cdot x + 6 \cdot l_x L l_y W)}{3 \cdot (l_x L)^2 (l_y W)^2} & x \leq l_y W \\ \frac{6 \cdot l_x L + 2 \cdot l_y W - 6 \cdot x}{3 \cdot (l_x L)^2} & x \leq l_x L \\ \frac{-2 \cdot (x - (l_x L + l_y W))^3}{3 \cdot (l_x L)^2 (l_y W)^2} & l_x L < x \end{cases} \end{aligned} \tag{A.5}$$

$$\begin{aligned} G(x) &= \int g(x) \mathrm{d}x \\ &= \begin{cases} 2 \cdot \frac{\frac{1}{4} x^4 + (-l_x L - l_y W) \cdot x^3 + 3 \cdot l_x L l_y W \cdot x^2}{3 \cdot (l_x L)^2 (l_y W)^2} & x \leq l_y W \\ \frac{2(x \cdot (3 l_x L + l_y W) - \frac{3x^2}{2} + \frac{l_y W}{4} \cdot (-3 l_y W + 8 l_x L) - \frac{l_y W}{2} \cdot (6 l_x L - l_y W))}{3 l_x L^2} & x \leq l_x L \\ \frac{2 \cdot (-\frac{(x - l_x L - l_y W)^4}{4 (l_y W)^2} + \frac{3 (l_x L)^2}{2})}{3 (l_x L)^2} & l_x L < x \end{cases} \end{aligned} \tag{A.6}$$

t_{toHP} and t_{toS} are calculated as follows:

$$t_{\text{toHP}} = \frac{\int_0^{\frac{1}{2}\cdot l_x \cdot L + l_y \cdot W} \left(x \cdot \begin{cases} \frac{2 \cdot x}{l_x \cdot L \cdot l_y \cdot W} & 0 \le x \le 0.5 \cdot l_x \cdot L \\ \frac{2}{2 \cdot l_y \cdot W} & 0.5 \cdot l_x \cdot L < x \le l_y \cdot W \\ \frac{2 \cdot (0.5 \cdot l_x \cdot L + l_y \cdot W - x)}{l_x \cdot L \cdot l_y \cdot W} & l_y \cdot W < x \le \frac{l_x \cdot L}{2} + l_y \cdot W \end{cases} \mathrm{d}x \right)}{v_{hor}} .$$

$$\frac{v_{hor}}{a_{hor}} = t_{\text{toS}}$$

A.7.2 Variance of Cycle Time of a Robot

The variance can be approximated with:

$$Var = \sqrt{\sum_{k=0}^{H-1} \Big((|(k \cdot t_\beta + t_{\text{StoR}}) - t_{cycle}|)^2 \cdot P(\beta_k) \Big)} .$$

A.8 Regression Models for Travel and Handling Times, and Reshuffles

This section presents the regression models and the results of the regression analysis. We take the RCS/R characteristics from the optimisation problem in Section 5.3.1 as an example. We take the throughput maximising rack layouts for each $H \leq 12$ for the AutoStore, AS-LFR, CBS-3-BBO, and CBS-3-RBP strategies. Based on these layouts, the values for t_{StoR}, $t_{\text{Rto}\beta}$, β, $t_{Ch,R}$, $t_{Ch,S}$ and $t_{Ch,R,\beta}$ are calculated for the four strategies according to the models presented in Section 5.1. Based on these values, linear (AutoStore, AS-LFR, CBS-3-BBO) and quadratic (CBS-3-RBP) regression models are determined for $H \leq 12$ ($7 \leq H \leq 12$ for $t_{\text{Rto}\beta}$ for the CBS-3-BBO strategy). The resulting regression models for $t_{\text{Rto}\beta}$, β, $t_{Ch,R}$, $t_{Ch,S}$ and $t_{Ch,R,\beta}$ are presented in Table A.3.

Table A.3: Regression Models for the AutoStore, AS-LFR, CBS-3-BBO, and CBS-3-RBP Strategies.

Variable	AutoStore	AS-LFR	CBS-3-BBO	CBS-3-RBP
$t_{\text{Rto}\beta}(H)$	$0.003 \cdot H + 7.046$	$0.001 \cdot H + 7.062$	$-0.025 \cdot H + 9.256$	-
$\beta(H)$	$0.222 \cdot H - 0.217$	$0.080 \cdot H - 0.144$	$0.372 \cdot H - 0.792$	$0.003 \cdot H^2 + 0.036 \cdot H - 0.046$
$t_{Ch,R}(H)$	$0.070 \cdot H + 1.228$	$0.051 \cdot H + 1.244$	$0.075 \cdot H + 1.178$	$0.001 \cdot H^2 + 0.035 \cdot H + 1.262$
$t_{Ch,S}(H)$	$0.035 \cdot H + 1.261$	$0.038 \cdot H + 1.267$	$0.017 \cdot H + 1.302$	$0.001 \cdot H^2 + 0.035 \cdot H + 1.262$
$t_{Ch,R,\beta}(H)$	$0.041 \cdot H + 1.186$	$0.045 \cdot H + 1.188$	$0.023 \cdot H + 1.242$	-

Figure A.7 shows the calculated values for t_{StoR} for the AutoStore, AS-LFR, and CBS-3-BBO strategies and t_{StoR} and $t_{\text{Rto}\beta}$ for the CBS-3-RBP strategy as well as the travel time between two random channels ($t_{\text{StoR,random}}$). The presented values for t_{StoR} and $t_{\text{Rto}\beta}$ converge to the time between two random channels for $H > 12$.

Table A.4 shows the analytic values and the corresponding regression values for $t_{\text{Rto}\beta}$, β, $t_{Ch,R}$, $t_{Ch,S}$ and $t_{Ch,R,\beta}$ for the AutoStore, AS-LFR, CBS-3-BBO, and CBS-3-BBO strategies. Table A.4 also shows the calculated Root Mean Square Error (RMSE) for all analytic and regression values. The RMSE is between 0.00 and 0.03 for the AutoStore, AS-LFR, and CBS-3-RBP strategies, from which it is concluded that the regression fit is good (Note that the unit for the times is in seconds). The RMSE is between 0.01 and 0.15 in the CBS-3-BBO strategy. The

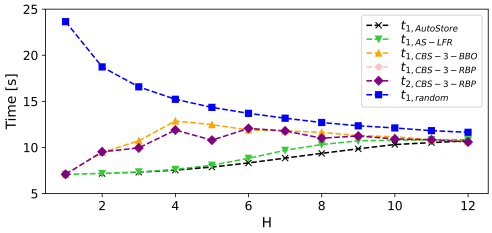

Figure A.7: Calculated Values for t_{StoR} (and $t_{\text{Rto}\beta}$ for the CBS-3-RBP Strategy) for $H \leq 12$ of the Optimisation Example. $t_{\text{StoR,random}}$ is the Travel Time Between two Random Channels.

values for R^2 differ from 0.10 to 0.33 for the regression of $t_{\text{Rto}\beta}$ (note the small RMSE of 0.01 to 0.15) and from 0.77 to 1.00 for the regression of β, $t_{Ch,R}$, $t_{Ch,S}$ and $t_{Ch,R,\beta}$.

Table A.4: Comparison of Analytic and Regression Values for $t_{\text{Rto}\beta}$, β, $t_{Ch,R}$, $t_{Ch,S}$ and $t_{Ch,R,\beta}$. Ana = Analytic Value, Reg = Regression Value, RMSE = Root Mean Square Error

		AS				AS-LFR				CBS-3-BBO				CBS-3-RBP			
Variable	H	Ana	Reg	RSME	R^2	Ana	Reg	RSME	R^2	Ana	Reg	RSME	R^2	Ana	Reg	RSME	R^2
	1	7.08	7.05			7.08	7.06										
	2	7.05	7.05			7.07	7.06										
	3	7.05	7.05			7.06	7.07										
	4	7.04	7.06			7.06	7.07										
	5	7.05	7.06			7.06	7.07										
$t_{\text{Rto}\beta}$	6	7.05	7.06	0.01	0.33	7.06	7.07	0.01	0.12			0.15	0.10				
	7	7.06	7.06			7.06	7.07			9.31	9.09						
	8	7.06	7.07			7.07	7.07			9.16	9.06						
	9	7.07	7.07			7.07	7.07			9.07	9.03						
	10	7.08	7.07			7.07	7.07			9.04	9.00						
	11	7.08	7.08			7.08	7.07			8.95	8.98						
	12	7.09	7.08			7.08	7.07			8.88	8.96						
	1	0.00	0.00			0.00	-0.06			0.00	-0.42			0.00	-0.06		
	2	0.22	0.23			0.02	0.02			0.07	-0.05			0.03	0.01		
	3	0.45	0.45			0.08	0.10			0.17	0.32			0.09	0.09		
	4	0.67	0.67			0.15	0.18			0.40	0.70			0.15	0.16		
	5	0.89	0.89			0.23	0.26			0.76	1.07			0.19	0.23		
β	6	1.12	1.11	0.00	1.00	0.31	0.34	0.03	0.99	1.47	1.44	0.21	0.97	0.26	0.30	0.01	1.00
	7	1.34	1.34			0.40	0.42			1.86	1.81			0.35	0.37		
	8	1.56	1.56			0.48	0.50			2.09	2.19			0.41	0.44		
	9	1.78	1.78			0.57	0.58			2.38	2.56			0.51	0.51		
	10	2.00	2.00			0.66	0.66			3.18	2.93			0.59	0.58		
	11	2.22	2.22			0.75	0.76			3.43	3.30			0.67	0.66		
	12	2.44	2.44			0.84	0.82			3.71	3.68			0.78	0.73		
	1	1.30	1.29			1.30	1.30			1.30	1.25			1.30	1.30		
	2	1.37	1.37			1.35	1.35			1.35	1.33			1.34	1.33		
$t_{Ch,R}$				0.00	1.00			0.00	1.00			0.03	0.99			0.01	1.00

	3	1.44	1.44			1.40	1.40			1.39	1.40			1.37	1.37	
	4	1.51	1.51			1.45	1.45			1.44	1.48			1.42	1.41	
	5	1.58	1.58			1.50	1.50			1.52	1.55			1.45	1.46	
	6	1.65	1.65			1.55	1.55			1.63	1.63			1.50	1.50	
	7	1.72	1.72			1.60	1.60			1.71	1.70			1.55	1.55	
	8	1.79	1.79			1.65	1.65			1.77	1.78			1.59	1.60	
	9	1.86	1.86			1.70	1.70			1.83	1.85			1.65	1.64	
	10	1.93	1.93			1.75	1.75			1.96	1.93			1.69	1.69	
	11	2.00	2.00			1.80	1.80			2.02	2.00			1.74	1.75	
	12	2.07	2.07			1.86	1.85			2.08	2.08			1.80	1.80	
	1	1.30	1.30			1.30	1.31			1.30	1.32			1.30	1.29	
	2	1.33	1.33			1.34	1.34			1.34	1.34			1.34	1.33	
	3	1.37	1.37			1.38	1.38			1.36	1.35			1.37	1.37	
	4	1.40	1.40			1.42	1.42			1.38	1.37			1.42	1.41	
	5	1.44	1.44			1.46	1.46			1.40	1.39			1.45	1.46	
$t_{Ch,S}$	6	1.47	1.47	0.00	1.00	1.50	1.50	0.00	1.00	1.40	1.40	0.01	0.98	1.50	1.50	0.01 1.00
	7	1.51	1.51			1.54	1.53			1.42	1.42			1.55	1.55	
	8	1.54	1.54			1.57	1.57			1.44	1.44			1.59	1.60	
	9	1.58	1.58			1.61	1.61			1.46	1.45			1.65	1.65	
	10	1.61	1.61			1.65	1.65			1.47	1.47			1.67	1.69	
	11	1.65	1.65			1.69	1.69			1.48	1.49			1.74	1.75	
	12	1.69	1.68			1.73	1.73			1.50	1.50			1.80	1.80	
	1	1.14	1.23			1.14	1.23			1.14	1.27					
	2	1.30	1.27			1.30	1.27			1.30	1.29					
	3	1.34	1.31			1.35	2.32			1.35	1.31					
	4	1.37	1.35			1.39	2.36			1.39	1.34					
	5	1.41	1.39			1.44	1.41			1.40	1.36					
$t_{Ch,R,\beta}$	6	1.44	1.43	0.03	0.96	1.48	1.46	0.03	0.96	1.40	1.38	0.04	0.77			
	7	1.48	1.47			1.52	1.50			1.42	1.40					
	8	1.52	1.51			1.56	1.55			1.44	1.43					
	9	1.55	1.56			1.59	1.59			1.45	1.45					
	10	1.59	1.60			1.63	1.64			1.46	1.47					
	11	1.63	1.64			1.67	1.69			1.48	1.50					
	12	1.66	1.68			1.71	1.73			1.50	1.52					

A.9 Validation Results for Robotic Compact Storage and Retrieval Systems

Table A.5: Validation Results.

	ID	TP				t_{cycle} [s]				β			
		Ana	Sim	δ	δ_{CI}	Ana	Sim	δ	δ_{CI}	Ana	Sim	δ	δ_{CI}
Random	I	113.74	113.55 ± 1.41	0.00	0.00	122.23	123.13 ± 1.60	-0.01	0.00	2.98	3.05 ± 0.07	-0.02	0.00
	II	113.74	113.55 ± 1.41	0.00	0.00	122.23	123.13 ± 1.60	-0.01	0.00	2.98	3.05 ± 0.07	-0.02	0.00
	III	113.74	113.55 ± 1.41	0.00	0.00	122.23	123.13 ± 1.60	-0.01	0.00	2.98	3.05 ± 0.07	-0.02	0.00
	IV	113.74	116.27 ± 2.68	-0.02	0.00	122.23	121.30 ± 3.20	0.01	0.00	2.98	2.97 ± 0.13	0.00	0.00
	V	113.74	114.38 ± 1.06	-0.01	0.00	122.23	122.01 ± 1.13	0.00	0.00	2.98	3.00 ± 0.05	-0.01	0.00
	VI	120.15	122.70 ± 1.83	-0.02	0.01	112.25	110.96 ± 1.52	0.01	0.00	2.57	2.56 ± 0.07	0.00	0.00
	VII	108.36	108.64 ± 1.49	-0.00	0.00	131.28	131.93 ± 1.72	-0.00	0.00	3.31	3.30 ± 0.06	0.00	0.00
	VIII	49.64	50.20 ± 0.60	-0.01	0.00	122.23	121.15 ± 1.53	0.01	0.00	2.98	2.96 ± 0.06	0.01	0.00
	IX	171.61	171.85 ± 0.97	-0.00	0.00	122.23	121.43 ± 0.28	0.01	0.00	2.98	2.98 ± 0.01	0.00	0.00
	X	143.35	141.70 ± 2.49	0.01	0.00	81.01	82.22 ± 0.75	-0.01	0.01	1.28	1.31 ± 0.03	-0.02	0.00
	XI	89.59	90.70 ± 1.22	-0.01	0.00	169.73	168.71 ± 2.20	0.01	0.00	4.68	4.68 ± 0.08	0.00	0.00
Random-BBO	I	85.91	87.87 ± 1.11	-0.02	0.01	178.98	175.82 ± 2.23	0.02	0.01	2.72	2.77 ± 0.04	-0.02	0.0
	II	85.91	87.87 ± 1.11	-0.02	0.01	178.98	175.82 ± 2.23	0.02	0.01	2.72	2.77 ± 0.04	-0.02	0.00
	III	85.91	87.87 ± 1.11	-0.02	0.01	178.98	175.82 ± 2.23	0.02	0.01	2.72	2.77 ± 0.04	-0.02	0.00
	IV	85.91	86.44 ± 2.27	-0.01	0.00	178.98	180.73 ± 5.25	-0.01	0.00	2.72	2.83 ± 0.11	-0.04	0.00
	V	85.91	87.58 ± 0.79	-0.02	0.01	178.98	175.59 ± 1.73	0.02	0.01	2.72	2.76 ± 0.04	-0.01	0.00
	VI	94.92	95.63 ± 1.22	-0.01	0.00	157.48	155.92 ± 2.15	0.01	0.00	2.26	2.28 ± 0.04	-0.01	0.00
	VII	78.58	79.43 ± 1.07	-0.01	0.00	199.73	198.53 ± 2.71	0.01	0.00	3.18	3.18 ± 0.06	0.00	0.00
	VIII	35.82	36.33 ± 0.53	-0.01	0.00	178.98	177.58 ± 2.80	0.01	0.00	2.72	2.81 ± 0.06	-0.03	0.01
	IX	150.20	151.82 ± 0.53	-0.01	0.01	178.98	175.72 ± 0.58	0.02	0.02	2.72	2.76 ± 0.01	-0.01	0.01
	X	124.79	127.92 ± 1.69	-0.02	0.01	105.49	103.94 ± 1.24	0.01	0.00	1.17	1.20 ± 0.03	-0.03	0.00
	XI	63.05	63.44 ± 1.00	-0.01	0.00	258.46	257.58 ± 4.68	0.00	0.00	4.26	4.31 ± 0.09	-0.01	0.00
CBS-1	I	91.13	92.02 ± 1.30	-0.01	0.00	166.05	164.69 ± 2.49	0.01	0.00	2.53	2.51 ± 0.06	0.01	0.00
	II	91.13	92.02 ± 1.30	-0.01	0.00	166.05	164.69 ± 2.49	0.01	0.00	2.53	2.51 ± 0.06	0.01	0.00
	III	91.13	92.02 ± 1.30	-0.01	0.00	166.05	164.69 ± 2.49	0.01	0.00	2.53	2.51 ± 0.06	0.01	0.00
	IV	91.13	93.07 ± 3.26	-0.02	0.00	166.05	168.53 ± 6.34	-0.01	0.00	2.53	2.56 ± 0.13	-0.01	0.00
	V	91.13	91.93 ± 1.00	-0.01	0.00	166.05	165.1 ± 2.02	0.01	0.00	2.53	2.51 ± 0.04	0.01	0.00
	VI	100.51	99.70 ± 1.42	0.01	0.00	145.86	150.36 ± 2.44	-0.03	0.01	2.09	2.13 ± 0.05	-0.02	0.00
	VII	80.27	81.11 ± 1.22	-0.01	0.00	194.61	193.36 ± 3.24	0.01	0.00	3.15	3.15 ± 0.06	0.00	0.00
	VIII	38.26	38.35 ± 0.60	-0.00	0.00	166.05	166.71 ± 2.81	-0.00	0.00	2.53	2.54 ± 0.06	-0.00	0.00
	IX	155.61	155.70 ± 0.57	-0.00	0.00	166.05	166.26 ± 0.56	-0.00	0.00	2.53	2.53 ± 0.01	0.00	0.00
	X	126.46	127.58 ± 1.77	-0.01	0.00	103.13	102.13 ± 1.15	0.01	0.00	1.15	1.15 ± 0.02	0.00	0.00
	XI	65.19	65.08 ± 1.10	0.00	0.00	248.77	251.37 ± 4.68	-0.01	0.00	4.12	4.17 ± 0.10	-0.01	0.00
AutoStore	I	113.62	114.13 ± 1.74	-0.00	0.00	122.43	121.36 ± 2.09	0.01	0.00	1.56	1.56 ± 0.04	0.00	0.00
	II	113.62	114.13 ± 1.74	-0.00	0.00	122.43	121.36 ± 2.09	0.01	0.00	1.56	1.56 ± 0.04	0.00	0.00
	III	113.62	114.13 ± 1.74	-0.00	0.00	122.43	121.36 ± 2.09	0.01	0.00	1.56	1.56 ± 0.04	0.00	0.00
	IV	113.62	117.21 ± 3.75	-0.03	0.00	122.43	120.05 ± 4.81	0.02	0.00	1.56	1.54 ± 0.10	0.01	0.00
	V	113.62	114.84 ± 1.40	-0.01	0.00	122.43	121.57 ± 1.68	0.01	0.00	1.56	1.57 ± 0.04	-0.01	0.00
	VI	121.10	122.96 ± 2.11	-0.02	0.00	110.84	110.57 ± 1.87	0.00	0.00	1.29	1.30 ± 0.04	-0.01	0.00
	VII	106.94	108.99 ± 1.61	-0.02	0.00	133.79	131.74 ± 2.21	0.02	0.00	1.82	1.81 ± 0.05	0.01	0.00
	VIII	49.57	50.05 ± 0.74	-0.01	0.00	122.43	121.71 ± 2.09	0.01	0.00	1.56	1.57 ± 0.04	-0.01	0.00
	IX	171.55	172.03 ± 0.85	-0.00	0.00	122.43	121.17 ± 0.48	0.01	0.01	1.56	1.56 ± 0.01	0.00	0.00
	X	142.81	144.69 ± 2.26	-0.01	0.00	81.69	81.02 ± 0.95	0.01	0.00	0.67	0.66 ± 0.02	0.02	0.00
	XI	91.03	92.73 ± 1.46	-0.02	0.00	166.3	164.15 ± 3.24	0.01	0.00	2.44	2.39 ± 0.07	0.02	0.00
AS-LFR	I	149.90	152.83 ± 2.85	-0.02	0.00	72.91	73.25 ± 1.25	-0.00	0.00	0.48	0.51 ± 0.03	-0.06	0.00

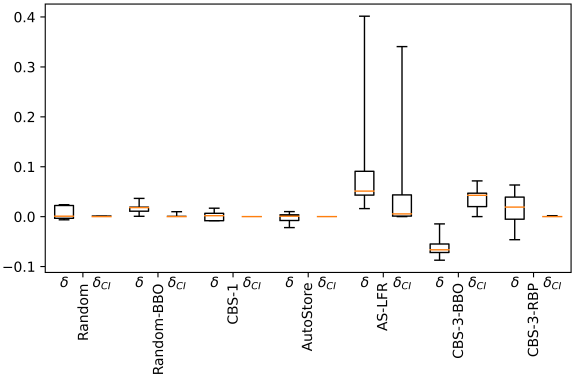

Figure A.8: δ for Number of Reshuffles β over all Validation Instances for all Operating Strategies.

	II	113.62	114.77 ± 1.65	-0.01	0.00	122.43	123.17 ± 2.04	-0.01	0.00	1.56	1.61 ± 0.05	-0.03	0.00
	III	163.66	163.03 ± 3.30	0.00	0.00	55.39	59.58 ± 0.91	-0.07	0.06	0.12	0.21 ± 0.02	-0.43	0.37
	IV	149.90	154.69 ± 4.95	-0.03	0.00	72.91	72.80 ± 3.31	0.00	0.00	0.48	0.51 ± 0.07	-0.06	0.00
	V	149.90	149.98 ± 2.24	-0.00	0.00	72.91	73.25 ± 0.99	-0.00	0.00	0.48	0.51 ± 0.02	-0.06	0.02
	VI	154.03	154.78 ± 3.11	-0.00	0.00	67.80	69.20 ± 0.94	-0.02	0.01	0.37	0.41 ± 0.02	-0.10	0.05
	VII	145.82	150.12 ± 2.82	-0.03	0.01	77.95	79.65 ± 1.54	-0.02	0.00	0.60	0.66 ± 0.04	-0.09	0.03
	VIII	74.06	75.44 ± 1.19	-0.02	0.00	72.91	72.56 ± 1.40	0.00	0.00	0.48	0.49 ± 0.03	-0.02	0.00
	IX	179.46	179.89 ± 1.16	-0.00	0.00	72.91	73.81 ± 0.34	-0.01	0.01	0.48	0.52 ± 0.01	-0.08	0.06
	X	162.17	163.09 ± 3.43	-0.01	0.00	57.39	59.72 ± 0.60	-0.04	0.03	0.15	0.17 ± 0.01	-0.12	0.06
	XI	135.49	138.01 ± 2.49	-0.02	0.00	90.99	91.82 ± 2.02	-0.01	0.00	0.84	0.89 ± 0.04	-0.06	0.01
CBS-3-BBO	I	90.52	91.81 ± 1.30	-0.01	0.00	167.5	165.92 ± 2.89	0.01	0.00	2.09	1.96 ± 0.04	0.07	0.04
	II	90.52	91.81 ± 1.30	-0.01	0.00	167.50	165.92 ± 2.89	0.01	0.00	2.09	1.96 ± 0.04	0.07	0.04
	III	90.52	91.81 ± 1.30	-0.01	0.00	167.50	165.92 ± 2.89	0.01	0.00	2.09	1.96 ± 0.04	0.07	0.04
	IV	90.52	93.02 ± 2.83	-0.03	0.00	167.50	166.84 ± 5.76	0.00	0.00	2.09	2.0 ± 0.09	0.04	0.00
	V	90.52	92.51 ± 0.84	-0.02	0.01	167.50	163.64 ± 1.86	0.02	0.01	2.09	1.93 ± 0.03	0.08	0.07
	VI	83.57	84.03 ± 1.47	-0.01	0.00	185.22	184.75 ± 3.77	0.00	0.00	2.38	2.22 ± 0.05	0.07	0.05
	VII	107.21	110.09 ± 1.77	-0.03	0.01	133.31	129.51 ± 2.27	0.03	0.01	1.77	1.74 ± 0.05	0.02	0.00
	VIII	37.97	38.39 ± 0.59	-0.01	0.00	167.50	166.28 ± 3.02	0.01	0.00	2.09	1.97 ± 0.04	0.06	0.04
	IX	155.01	160.06 ± 3.00	-0.03	0.01	167.50	165.48 ± 3.05	0.01	0.00	2.09	1.96 ± 0.05	0.07	0.04
	X	148.62	151.00 ± 3.03	-0.02	0.00	74.49	74.38 ± 0.88	0.00	0.00	0.4	0.39 ± 0.02	0.03	0.00
	XI	64.26	64.35 ± 0.93	-0.00	0.00	252.92	254.62 ± 3.93	-0.01	0.00	3.72	3.45 ± 0.06	0.08	0.06
CBS-3-RBP	I	157.87	161.06 ± 2.28	-0.02	0.01	62.98	61.08 ± 0.69	0.03	0.02	0.41	0.42 ± 0.03	-0.02	0.00
	II	131.36	131.21 ± 2.29	0.00	0.00	96.43	97.52 ± 1.48	-0.01	0.00	1.45	1.44 ± 0.04	0.01	0.00
	III	163.20	166.78 ± 3.70	-0.02	0.00	56.02	56.78 ± 0.79	-0.01	0.00	0.23	0.24 ± 0.02	-0.04	0.00
	IV	157.87	162.16 ± 3.94	-0.03	0.00	62.98	61.77 ± 1.68	0.02	0.00	0.41	0.43 ± 0.06	-0.05	0.00
	V	157.87	156.48 ± 2.09	0.01	0.00	62.98	64.19 ± 0.82	-0.02	0.01	0.41	0.44 ± 0.03	-0.07	0.00
	VI	158.97	162.56 ± 3.28	-0.02	0.00	61.57	61.67 ± 0.93	-0.00	0.00	0.36	0.36 ± 0.03	0.00	0.00
	VII	151.64	155.27 ± 2.90	-0.02	0.00	70.77	71.20 ± 1.26	-0.01	0.00	0.62	0.64 ± 0.04	-0.03	0.00
	VIII	82.00	82.20 ± 1.36	-0.00	0.00	62.98	63.91 ± 1.24	-0.01	0.00	0.41	0.43 ± 0.04	-0.05	0.00
	IX	179.80	180.28 ± 1.12	-0.00	0.00	62.98	63.55 ± 0.28	-0.01	0.00	0.41	0.42 ± 0.01	-0.02	0.00
	X	159.42	162.71 ± 3.97	-0.02	0.00	60.99	59.58 ± 0.51	0.02	0.01	0.15	0.15 ± 0.01	0.00	0.00
	XI	149.30	150.51 ± 2.87	-0.01	0.00	73.66	73.08 ± 1.41	0.01	0.00	0.78	0.74 ± 0.04	0.05	0.00

Table A.6: Aggregated δ and δ_{CI} for all 11 Instances.

	TP						t_{cycle}					
	$\overline{\delta}$	δ^{max}	δ^{min}	$\overline{\delta_{CI}}$	δ_{CI}^{min}	δ_{CI}^{max}	$\overline{\delta}$	δ^{max}	δ^{min}	$\overline{\delta_{CI}}$	δ_{CI}^{min}	δ_{CI}^{max}
Random	-0.01	0.01	-0.02	0.00	0.00	0.01	0.00	0.01	-0.01	0.00	0.00	0.01
Random-BBO	-0.02	-0.01	-0.02	0.01	0.00	0.01	0.01	0.02	-0.01	0.00	0.00	0.02
CBS-1	-0.01	0.01	-0.02	0.00	0.00	0.00	-0.00	0.01	-0.03	0.00	0.00	0.01
AutoStore	-0.01	-0.00	-0.03	0.00	0.00	0.00	0.01	0.02	0.00	0.00	0.00	0.01
AS-LFR	-0.01	0.00	-0.03	0.00	0.00	0.01	-0.02	0.00	-0.07	0.01	0.00	0.06
CBS-3-BBO	-0.02	-0.00	-0.03	0.00	0.00	0.01	0.01	0.03	-0.01	0.00	0.00	0.01
CBS-3-RBP	-0.01	0.01	-0.03	0.00	0.00	0.01	0.00	0.03	-0.02	0.00	0.00	0.02

	β					
	$\overline{\delta}$	δ^{max}	δ^{min}	$\overline{\delta_{CI}}$	δ_{CI}^{min}	δ_{CI}^{max}
Random	-0.01	0.01	-0.02	0.00	0.00	0.00
Random-BBO	-0.02	-0.00	-0.04	0.00	0.00	0.01
CBS-1	-0.00	0.01	-0.02	0.00	0.00	0.00
AutoStore	0.00	0.02	-0.01	0.00	0.00	0.00
AS-LFR	-0.10	-0.02	-0.43	0.06	0.00	0.37
CBS-3-BBO	0.06	0.08	0.02	0.03	0.00	0.07
CBS-3-RBP	-0.02	0.05	-0.06	0.00	0.00	0.00

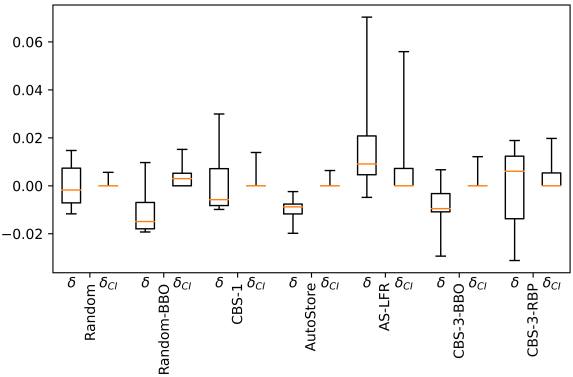

Figure A.9: δ for the Cycle Time t_{cycle} over all Validation Instances for all Operating Strategies.

A.10 Results of the Comparison Experiments

This appendix includes the results for the experiments conducted in Chapter 6 for both AS/R and RCS/R systems. The Tables A.7 to A.23 contain the linear functions for the normalised cycle time in dependency of θ with $t_{cycle,n} = c+m\cdot\theta$ for AS/R and RCS/R systems and all 13 operating strategies. In the following tables the combinations of access frequency and number of unit loads per product are $\gamma_1 = \{\xi = (1,1,1), f = (1,1,1)\}$, $\gamma_2 = \{\xi = (5,2,1), f = (10,2,1)\}$, $\gamma_3 = \{\xi = (20,10,5), f = (100,10,1)\}$.

Table A.7: Normalised Cycle Times for the AS-LFR, AutoStore and CBS-1 Strategies for AS/R Systems.

		$L \cdot W \cdot H = 10000$			$L \cdot W \cdot H = 50000$			$L \cdot W \cdot H = 100000$		
	H	γ_1	γ_2	γ_3	γ_1	γ_2	γ_3	γ_1	γ_2	γ_3
AS-LFR	1	$1.28 + 1.41\theta$	$1.28 + 1.41\theta$	$1.28 + 1.41\theta$	$1.25 + 1.44\theta$	$1.25 + 1.44\theta$	$1.25 + 1.44\theta$	$1.25 + 1.44\theta$	$1.25 + 1.44\theta$	$1.25 + 1.44\theta$
	2	$1.41 + 2.31\theta$	$1.34 + 1.31\theta$	$1.32 + 1.11\theta$	$1.31 + 2.41\theta$	$1.28 + 1.37\theta$	$1.27 + 1.17\theta$	$1.28 + 2.44\theta$	$1.26 + 1.39\theta$	$1.25 + 1.18\theta$
	3	$1.56 + 3.01\theta$	$1.39 + 1.29\theta$	$1.35 + 0.88\theta$	$1.38 + 3.19\theta$	$1.30 + 1.39\theta$	$1.28 + 0.95\theta$	$1.33 + 3.24\theta$	$1.28 + 1.41\theta$	$1.26 + 0.97\theta$
	4	$1.73 + 3.55\theta$	$1.45 + 1.30\theta$	$1.37 + 0.70\theta$	$1.46 + 3.82\theta$	$1.33 + 1.42\theta$	$1.29 + 0.78\theta$	$1.40 + 3.88\theta$	$1.31 + 1.44\theta$	$1.28 + 0.79\theta$
	5	$1.98 + 3.92\theta$	$1.56 + 1.26\theta$	$1.44 + 0.50\theta$	$1.58 + 4.32\theta$	$1.38 + 1.44\theta$	$1.33 + 0.62\theta$	$1.48 + 4.41\theta$	$1.34 + 1.47\theta$	$1.30 + 0.64\theta$
	6	$2.28 + 4.16\theta$	$1.70 + 1.19\theta$	$1.55 + 0.26\theta$	$1.71 + 4.72\theta$	$1.45 + 1.44\theta$	$1.38 + 0.44\theta$	$1.57 + 4.87\theta$	$1.38 + 1.51\theta$	$1.33 + 0.49\theta$
	7	$2.56 + 4.35\theta$	$1.82 + 1.14\theta$	$1.63 + 0.10\theta$	$1.88 + 5.04\theta$	$1.54 + 1.42\theta$	$1.45 + 0.27\theta$	$1.69 + 5.22\theta$	$1.45 + 1.51\theta$	$1.39 + 0.34\theta$
	8	$2.92 + 4.43\theta$	$1.99 + 1.04\theta$	$1.72 - 0.06\theta$	$2.07 + 5.29\theta$	$1.64 + 1.39\theta$	$1.53 + 0.12\theta$	$1.82 + 5.53\theta$	$1.52 + 1.51\theta$	$1.45 + 0.20\theta$
	9	$3.17 + 4.58\theta$	$2.05 + 1.04\theta$	$1.71 - 0.12\theta$	$2.25 + 5.50\theta$	$1.72 + 1.38\theta$	$1.58 + 0.01\theta$	$1.99 + 5.76\theta$	$1.61 + 1.48\theta$	$1.53 + 0.07\theta$
	10	$3.53 + 4.59\theta$	$2.21 + 0.96\theta$	$1.79 - 0.25\theta$	$2.50 + 5.62\theta$	$1.86 + 1.30\theta$	$1.68 - 0.14\theta$	$2.18 + 5.94\theta$	$1.72 + 1.44\theta$	$1.61 - 0.07\theta$
	11	$3.84 + 4.63\theta$	$2.30 + 0.92\theta$	$1.81 - 0.31\theta$	$2.66 + 5.81\theta$	$1.92 + 1.31\theta$	$1.69 - 0.19\theta$	$2.32 + 6.15\theta$	$1.78 + 1.44\theta$	$1.64 - 0.14\theta$
	12	$4.17 + 4.62\theta$	$2.40 + 0.89\theta$	$1.82 - 0.37\theta$	$2.83 + 5.96\theta$	$1.98 + 1.31\theta$	$1.71 - 0.26\theta$	$2.47 + 6.32\theta$	$1.85 + 1.44\theta$	$1.67 - 0.21\theta$
AutoStore	1	$1.28 + 1.41\theta$	$1.28 + 1.41\theta$	$1.28 + 1.41\theta$	$1.25 + 1.44\theta$	$1.25 + 1.44\theta$	$1.25 + 1.44\theta$	$1.25 + 1.44\theta$	$1.25 + 1.44\theta$	$1.25 + 1.44\theta$
	2	$1.41 + 2.31\theta$	$1.37 + 1.72\theta$	$1.35 + 1.48\theta$	$1.31 + 2.41\theta$	$1.29 + 1.79\theta$	$1.28 + 1.55\theta$	$1.28 + 2.44\theta$	$1.27 + 1.82\theta$	$1.26 + 1.57\theta$
	3	$1.56 + 3.01\theta$	$1.46 + 1.95\theta$	$1.41 + 1.54\theta$	$1.38 + 3.19\theta$	$1.33 + 2.08\theta$	$1.31 + 1.65\theta$	$1.33 + 3.24\theta$	$1.30 + 2.11\theta$	$1.28 + 1.67\theta$
	4	$1.73 + 3.55\theta$	$1.55 + 2.14\theta$	$1.47 + 1.59\theta$	$1.46 + 3.82\theta$	$1.37 + 2.31\theta$	$1.34 + 1.72\theta$	$1.40 + 3.88\theta$	$1.34 + 2.34\theta$	$1.32 + 1.75\theta$
	5	$1.98 + 3.92\theta$	$1.69 + 2.23\theta$	$1.57 + 1.58\theta$	$1.58 + 4.32\theta$	$1.44 + 2.48\theta$	$1.39 + 1.77\theta$	$1.48 + 4.41\theta$	$1.39 + 2.54\theta$	$1.35 + 1.81\theta$
	6	$2.28 + 4.16\theta$	$1.86 + 2.28\theta$	$1.69 + 1.56\theta$	$1.71 + 4.72\theta$	$1.52 + 2.62\theta$	$1.44 + 1.81\theta$	$1.57 + 4.87\theta$	$1.43 + 2.71\theta$	$1.38 + 1.87\theta$
	7	$2.56 + 4.35\theta$	$2.02 + 2.32\theta$	$1.79 + 1.54\theta$	$1.88 + 5.04\theta$	$1.61 + 2.72\theta$	$1.50 + 1.83\theta$	$1.69 + 5.22\theta$	$1.50 + 2.83\theta$	$1.42 + 1.91\theta$
	8	$2.92 + 4.43\theta$	$2.24 + 2.27\theta$	$1.94 + 1.47\theta$	$2.07 + 5.29\theta$	$1.71 + 2.80\theta$	$1.56 + 1.85\theta$	$1.82 + 5.53\theta$	$1.57 + 2.95\theta$	$1.46 + 1.95\theta$
	9	$3.17 + 4.58\theta$	$2.38 + 2.29\theta$	$2.02 + 1.46\theta$	$2.25 + 5.50\theta$	$1.82 + 2.86\theta$	$1.62 + 1.87\theta$	$1.99 + 5.76\theta$	$1.66 + 3.02\theta$	$1.51 + 1.97\theta$
	10	$3.44 + 4.69\theta$	$2.54 + 2.30\theta$	$2.13 + 1.42\theta$	$2.46 + 5.66\theta$	$1.95 + 2.88\theta$	$1.71 + 1.85\theta$	$2.15 + 5.98\theta$	$1.75 + 3.08\theta$	$1.57 + 1.99\theta$
	11	$3.74 + 4.73\theta$	$2.72 + 2.26\theta$	$2.25 + 1.37\theta$	$2.61 + 5.85\theta$	$2.05 + 2.93\theta$	$1.76 + 1.86\theta$	$2.29 + 6.18\theta$	$1.84 + 3.14\theta$	$1.62 + 2.01\theta$
	12	$4.06 + 4.73\theta$	$2.90 + 2.22\theta$	$2.39 + 1.30\theta$	$2.79 + 6.01\theta$	$2.17 + 2.95\theta$	$1.84 + 1.85\theta$	$2.43 + 6.36\theta$	$1.95 + 3.17\theta$	$1.68 + 2.01\theta$
CBS-1	1	$1.01 + 1.68\theta$	$0.65 + 2.04\theta$	$0.55 + 2.14\theta$	$0.98 + 1.71\theta$	$0.61 + 2.08\theta$	$0.51 + 2.18\theta$	$0.97 + 1.72\theta$	$0.60 + 2.09\theta$	$0.49 + 2.20\theta$
	2	$1.15 + 2.71\theta$	$0.79 + 3.07\theta$	$0.69 + 3.17\theta$	$1.04 + 2.82\theta$	$0.68 + 3.19\theta$	$0.57 + 3.29\theta$	$1.02 + 2.85\theta$	$0.64 + 3.22\theta$	$0.54 + 3.32\theta$
	3	$1.31 + 3.59\theta$	$0.96 + 3.94\theta$	$0.85 + 4.04\theta$	$1.11 + 3.79\theta$	$0.74 + 4.15\theta$	$0.64 + 4.25\theta$	$1.06 + 3.83\theta$	$0.70 + 4.20\theta$	$0.59 + 4.30\theta$
	4	$1.51 + 4.32\theta$	$1.15 + 4.67\theta$	$1.05 + 4.77\theta$	$1.19 + 4.63\theta$	$0.83 + 4.99\theta$	$0.73 + 5.10\theta$	$1.13 + 4.69\theta$	$0.76 + 5.06\theta$	$0.66 + 5.17\theta$
	5	$1.68 + 5.00\theta$	$1.35 + 5.33\theta$	$1.25 + 5.43\theta$	$1.29 + 5.39\theta$	$0.93 + 5.75\theta$	$0.83 + 5.85\theta$	$1.20 + 5.48\theta$	$0.84 + 5.85\theta$	$0.73 + 5.95\theta$
	6	$1.95 + 5.54\theta$	$1.60 + 5.88\theta$	$1.51 + 5.98\theta$	$1.40 + 6.09\theta$	$1.04 + 6.44\theta$	$0.94 + 6.54\theta$	$1.27 + 6.21\theta$	$0.91 + 6.58\theta$	$0.81 + 6.68\theta$
	7	$2.22 + 6.03\theta$	$1.87 + 6.38\theta$	$1.77 + 6.48\theta$	$1.54 + 6.71\theta$	$1.18 + 7.07\theta$	$1.08 + 7.17\theta$	$1.37 + 6.88\theta$	$1.00 + 7.25\theta$	$0.90 + 7.35\theta$
	8	$2.51 + 6.47\theta$	$2.17 + 6.81\theta$	$2.07 + 6.91\theta$	$1.67 + 7.31\theta$	$1.31 + 7.67\theta$	$1.21 + 7.77\theta$	$1.45 + 7.53\theta$	$1.09 + 7.89\theta$	$0.99 + 7.99\theta$
	9	$2.79 + 6.90\theta$	$2.45 + 7.24\theta$	$2.35 + 7.34\theta$	$1.79 + 7.89\theta$	$1.44 + 8.24\theta$	$1.34 + 8.34\theta$	$1.57 + 8.11\theta$	$1.20 + 8.48\theta$	$1.10 + 8.59\theta$
	10	$3.04 + 7.33\theta$	$2.71 + 7.66\theta$	$2.62 + 7.75\theta$	$1.96 + 8.41\theta$	$1.61 + 8.76\theta$	$1.51 + 8.86\theta$	$1.66 + 8.71\theta$	$1.30 + 9.06\theta$	$1.20 + 9.17\theta$
	11	$3.37 + 7.66\theta$	$3.05 + 7.99\theta$	$2.96 + 8.08\theta$	$2.13 + 8.91\theta$	$1.77 + 9.27\theta$	$1.67 + 9.37\theta$	$1.77 + 9.26\theta$	$1.42 + 9.62\theta$	$1.31 + 9.72\theta$
	12	$3.77 + 7.92\theta$	$3.43 + 8.26\theta$	$3.34 + 8.35\theta$	$2.29 + 9.40\theta$	$1.94 + 9.75\theta$	$1.84 + 9.86\theta$	$1.90 + 9.79\theta$	$1.54 + 10.15\theta$	$1.44 + 10.25\theta$

Table A.8: Normalised Cycle Times for the CBS-3-BBO, CBS-3-RBP and Depth First Strategies for AS/R Systems.

		$L \cdot W \cdot H = 10000$			$L \cdot W \cdot H = 50000$			$L \cdot W \cdot H = 100000$		
	H	γ_1	γ_2	γ_3	γ_1	γ_2	γ_3	γ_1	γ_2	γ_3
CBS-3-BBO	1	$1.28 + 1.41\theta$	$1.28 + 1.41\theta$	$1.28 + 1.41\theta$	$1.25 + 1.44\theta$	$1.25 + 1.44\theta$	$1.25 + 1.44\theta$	$1.25 + 1.44\theta$	$1.25 + 1.44\theta$	$1.25 + 1.44\theta$
	2	$1.52 + 1.70\theta$	$1.39 + 1.19\theta$	$1.35 + 1.05\theta$	$1.44 + 1.77\theta$	$1.34 + 1.24\theta$	$1.30 + 1.11\theta$	$1.42 + 1.80\theta$	$1.32 + 1.26\theta$	$1.28 + 1.12\theta$
	3	$1.69 + 2.29\theta$	$1.60 + 0.97\theta$	$1.51 + 0.75\theta$	$1.55 + 2.42\theta$	$1.53 + 1.05\theta$	$1.45 + 0.81\theta$	$1.52 + 2.45\theta$	$1.51 + 1.06\theta$	$1.44 + 0.83\theta$
	4	$1.92 + 2.78\theta$	$1.73 + 1.23\theta$	$1.68 + 0.81\theta$	$1.73 + 2.97\theta$	$1.62 + 1.33\theta$	$1.59 + 0.91\theta$	$1.70 + 3.00\theta$	$1.61 + 1.34\theta$	$1.58 + 0.92\theta$
	5	$2.15 + 3.20\theta$	$2.09 + 1.70\theta$	$2.20 + 1.11\theta$	$1.86 + 3.49\theta$	$1.80 + 1.99\theta$	$1.88 + 1.45\theta$	$1.79 + 3.56\theta$	$1.73 + 2.06\theta$	$1.79 + 1.53\theta$
	6	$2.61 + 3.41\theta$	$3.17 + 1.88\theta$	$2.52 + 1.17\theta$	$2.07 + 3.95\theta$	$2.55 + 2.88\theta$	$2.44 + 1.61\theta$	$1.93 + 4.08\theta$	$2.25 + 3.17\theta$	$2.44 + 1.93\theta$
	7	$4.13 + 2.86\theta$	$3.38 + 1.76\theta$	$2.78 + 1.04\theta$	$3.57 + 3.56\theta$	$3.38 + 2.82\theta$	$2.62 + 1.60\theta$	$3.38 + 3.78\theta$	$3.39 + 3.36\theta$	$2.65 + 1.84\theta$
	8	$4.70 + 2.71\theta$	$3.75 + 1.52\theta$	$3.22 + 1.05\theta$	$3.96 + 3.63\theta$	$3.62 + 2.67\theta$	$2.89 + 1.56\theta$	$3.70 + 3.92\theta$	$3.63 + 3.23\theta$	$2.79 + 1.84\theta$
	9	$5.09 + 2.69\theta$	$4.50 + 1.73\theta$	$3.59 + 1.02\theta$	$4.33 + 3.67\theta$	$3.89 + 2.55\theta$	$3.53 + 1.92\theta$	$4.08 + 3.96\theta$	$3.88 + 3.07\theta$	$3.51 + 2.36\theta$
	10	$5.91 + 2.42\theta$	$5.16 + 1.39\theta$	$4.03 + 0.72\theta$	$4.89 + 3.52\theta$	$5.04 + 2.90\theta$	$3.49 + 1.59\theta$	$4.53 + 3.93\theta$	$4.83 + 3.60\theta$	$3.78 + 2.11\theta$
	11	$6.58 + 2.16\theta$	$5.52 + 1.10\theta$	$4.44 + 0.57\theta$	$5.36 + 3.50\theta$	$5.32 + 2.68\theta$	$3.60 + 1.38\theta$	$4.96 + 3.92\theta$	$5.17 + 3.42\theta$	$3.45 + 0.38\theta$
	12	$7.16 + 1.89\theta$	$6.07 + 0.84\theta$	$4.97 + 0.37\theta$	$5.80 + 3.40\theta$	$5.63 + 2.43\theta$	$3.75 + 1.26\theta$	$5.36 + 3.86\theta$	$6.63 + 2.20\theta$	$4.63 + 0.79\theta$
CBS-3-RBP	1	$1.28 + 1.41\theta$	$1.28 + 1.41\theta$	$1.28 + 1.41\theta$	$1.25 + 1.44\theta$	$1.25 + 1.44\theta$	$1.25 + 1.44\theta$	$1.25 + 1.44\theta$	$1.25 + 1.44\theta$	$1.25 + 1.44\theta$
	2	$1.59 + 1.27\theta$	$1.40 + 1.09\theta$	$1.35 + 1.04\theta$	$1.53 + 1.33\theta$	$1.35 + 1.15\theta$	$1.30 + 1.09\theta$	$1.51 + 1.35\theta$	$1.33 + 1.16\theta$	$1.28 + 1.10\theta$
	3	$1.68 + 1.53\theta$	$1.52 + 0.85\theta$	$1.48 + 0.66\theta$	$1.59 + 1.62\theta$	$1.46 + 0.91\theta$	$1.43 + 0.71\theta$	$1.57 + 1.64\theta$	$1.45 + 0.92\theta$	$1.41 + 0.72\theta$
	4	$2.35 + 1.15\theta$	$1.80 + 0.47\theta$	$1.57 + 0.38\theta$	$2.27 + 1.23\theta$	$1.76 + 0.51\theta$	$1.53 + 0.42\theta$	$2.28 + 1.22\theta$	$1.77 + 0.50\theta$	$1.54 + 0.42\theta$
	5	$2.42 + 1.42\theta$	$1.77 + 0.43\theta$	$1.54 + 0.25\theta$	$2.21 + 1.63\theta$	$1.70 + 0.51\theta$	$1.44 + 0.35\theta$	$2.19 + 1.66\theta$	$1.69 + 0.52\theta$	$1.42 + 0.36\theta$
	6	$2.90 + 1.27\theta$	$1.98 + 0.21\theta$	$1.64 + 0.02\theta$	$2.72 + 1.44\theta$	$1.90 + 0.29\theta$	$1.58 + 0.08\theta$	$2.68 + 1.49\theta$	$1.88 + 0.31\theta$	$1.56 + 0.10\theta$
	7	$3.35 + 1.13\theta$	$2.08 + 0.14\theta$	$1.69 - 0.14\theta$	$3.22 + 1.27\theta$	$2.02 + 0.21\theta$	$1.64 - 0.09\theta$	$3.16 + 1.32\theta$	$2.00 + 0.23\theta$	$1.61 - 0.06\theta$
	8	$3.42 + 1.36\theta$	$2.16 + 0.05\theta$	$1.67 - 0.22\theta$	$3.13 + 1.65\theta$	$2.03 + 0.18\theta$	$1.58 - 0.13\theta$	$3.03 + 1.75\theta$	$1.98 + 0.23\theta$	$1.59 - 0.14\theta$
	9	$4.02 + 1.02\theta$	$2.28 - 0.05\theta$	$1.62 - 0.24\theta$	$3.79 + 1.25\theta$	$2.19 + 0.04\theta$	$1.59 - 0.19\theta$	$2.56 + 2.16\theta$	$2.16 + 0.06\theta$	$1.54 - 0.17\theta$
	10	$4.12 + 1.23\theta$	$2.41 - 0.13\theta$	$1.69 - 0.39\theta$	$3.87 + 1.49\theta$	$2.32 - 0.04\theta$	$1.54 - 0.25\theta$	$3.67 + 1.69\theta$	$2.23 + 0.05\theta$	$1.50 - 0.21\theta$
	11	$4.55 + 1.09\theta$	$2.50 - 0.21\theta$	$1.85 - 0.61\theta$	$4.29 + 1.34\theta$	$2.39 - 0.09\theta$	$1.48 - 0.23\theta$	$4.18 + 1.45\theta$	$2.34 - 0.04\theta$	$1.37 - 0.14\theta$
	12	$5.02 + 0.92\theta$	$2.65 - 0.28\theta$	$1.90 - 0.72\theta$	$4.74 + 1.19\theta$	$2.52 - 0.15\theta$	$1.51 - 0.32\theta$	$4.65 + 1.29\theta$	$2.48 - 0.11\theta$	$1.41 - 0.23\theta$
Depth First	1	$1.67 + 1.02\theta$	$1.67 + 1.02\theta$	$1.67 + 1.02\theta$	$1.64 + 1.05\theta$	$1.64 + 1.05\theta$	$1.64 + 1.05\theta$	$1.65 + 1.04\theta$	$1.65 + 1.04\theta$	$1.65 + 1.04\theta$
	2	$1.99 + 1.12\theta$	$1.99 + 1.12\theta$	$1.99 + 1.12\theta$	$1.94 + 1.17\theta$	$1.94 + 1.17\theta$	$1.94 + 1.17\theta$	$1.92 + 1.19\theta$	$1.92 + 1.19\theta$	$1.92 + 1.19\theta$
	3	$2.30 + 1.24\theta$	$2.30 + 1.24\theta$	$2.30 + 1.24\theta$	$2.21 + 1.32\theta$	$2.21 + 1.32\theta$	$2.21 + 1.32\theta$	$2.20 + 1.34\theta$	$2.20 + 1.34\theta$	$2.20 + 1.34\theta$
	4	$2.57 + 1.40\theta$	$2.57 + 1.40\theta$	$2.57 + 1.40\theta$	$2.49 + 1.48\theta$	$2.49 + 1.48\theta$	$2.49 + 1.48\theta$	$2.50 + 1.47\theta$	$2.50 + 1.47\theta$	$2.50 + 1.47\theta$
	5	$2.97 + 1.47\theta$	$2.97 + 1.47\theta$	$2.97 + 1.47\theta$	$2.86 + 1.58\theta$	$2.86 + 1.58\theta$	$2.86 + 1.58\theta$	$2.86 + 1.58\theta$	$2.86 + 1.58\theta$	$2.86 + 1.58\theta$
	6	$3.37 + 1.50\theta$	$3.37 + 1.50\theta$	$3.37 + 1.50\theta$	$3.19 + 1.68\theta$	$3.19 + 1.68\theta$	$3.19 + 1.68\theta$	$3.15 + 1.73\theta$	$3.15 + 1.73\theta$	$3.15 + 1.73\theta$
	7	$3.69 + 1.61\theta$	$3.69 + 1.61\theta$	$3.69 + 1.61\theta$	$3.54 + 1.76\theta$	$3.54 + 1.76\theta$	$3.54 + 1.76\theta$	$3.48 + 1.82\theta$	$3.48 + 1.82\theta$	$3.48 + 1.82\theta$
	8	$4.15 + 1.57\theta$	$4.15 + 1.57\theta$	$4.15 + 1.57\theta$	$3.86 + 1.85\theta$	$3.86 + 1.85\theta$	$3.86 + 1.85\theta$	$3.75 + 1.96\theta$	$3.75 + 1.96\theta$	$3.75 + 1.96\theta$
	9	$4.42 + 1.71\theta$	$4.42 + 1.71\theta$	$4.42 + 1.71\theta$	$4.19 + 1.95\theta$	$4.19 + 1.95\theta$	$4.19 + 1.95\theta$	$4.13 + 2.01\theta$	$4.13 + 2.01\theta$	$4.13 + 2.01\theta$
	10	$4.73 + 1.82\theta$	$4.73 + 1.82\theta$	$4.73 + 1.82\theta$	$4.59 + 1.95\theta$	$4.59 + 1.95\theta$	$4.59 + 1.95\theta$	$4.46 + 2.09\theta$	$4.46 + 2.09\theta$	$4.46 + 2.09\theta$
	11	$5.09 + 1.86\theta$	$5.09 + 1.86\theta$	$5.09 + 1.86\theta$	$4.86 + 2.09\theta$	$4.86 + 2.09\theta$	$4.86 + 2.09\theta$	$4.75 + 2.19\theta$	$4.75 + 2.19\theta$	$4.75 + 2.19\theta$
	12	$5.45 + 1.90\theta$	$5.45 + 1.90\theta$	$5.45 + 1.90\theta$	$5.19 + 2.16\theta$	$5.19 + 2.16\theta$	$5.19 + 2.16\theta$	$5.10 + 2.25\theta$	$5.10 + 2.25\theta$	$5.10 + 2.25\theta$

Table A.9: Normalised Cycle Times for the Random-BBO, RSCS and RSCS-NN Strategies for AS/R Systems.

		$L \cdot W \cdot H = 10000$			$L \cdot W \cdot H = 50000$			$L \cdot W \cdot H = 100000$		
	H	γ_1	γ_2	γ_3	γ_1	γ_2	γ_3	γ_1	γ_2	γ_3
Random-BBO	1	$1.28+1.41\theta$	$1.28+1.41\theta$	$1.28+1.41\theta$	$1.25+1.44\theta$	$1.25+1.44\theta$	$1.25+1.44\theta$	$1.25+1.44\theta$	$1.25+1.44\theta$	$1.25+1.44\theta$
	2	$1.41+2.45\theta$	$1.41+2.45\theta$	$1.41+2.45\theta$	$1.31+2.55\theta$	$1.31+2.55\theta$	$1.31+2.55\theta$	$1.28+2.58\theta$	$1.28+2.58\theta$	$1.28+2.58\theta$
	3	$1.57+3.33\theta$	$1.57+3.33\theta$	$1.57+3.33\theta$	$1.38+3.52\theta$	$1.38+3.52\theta$	$1.38+3.52\theta$	$1.33+3.56\theta$	$1.33+3.56\theta$	$1.33+3.56\theta$
	4	$1.73+4.10\theta$	$1.73+4.10\theta$	$1.73+4.10\theta$	$1.46+4.37\theta$	$1.46+4.37\theta$	$1.46+4.37\theta$	$1.40+4.42\theta$	$1.40+4.42\theta$	$1.40+4.42\theta$
	5	$1.95+4.73\theta$	$1.95+4.73\theta$	$1.95+4.73\theta$	$1.56+5.12\theta$	$1.56+5.12\theta$	$1.56+5.12\theta$	$1.47+5.21\theta$	$1.47+5.21\theta$	$1.47+5.21\theta$
	6	$2.20+5.29\theta$	$2.20+5.29\theta$	$2.20+5.29\theta$	$1.67+5.82\theta$	$1.67+5.82\theta$	$1.67+5.82\theta$	$1.54+5.95\theta$	$1.54+5.95\theta$	$1.54+5.95\theta$
	7	$2.44+5.81\theta$	$2.44+5.81\theta$	$2.44+5.81\theta$	$1.80+6.45\theta$	$1.80+6.45\theta$	$1.80+6.45\theta$	$1.63+6.62\theta$	$1.63+6.62\theta$	$1.63+6.62\theta$
	8	$2.76+6.22\theta$	$2.76+6.22\theta$	$2.76+6.22\theta$	$1.93+7.05\theta$	$1.93+7.05\theta$	$1.93+7.05\theta$	$1.71+7.27\theta$	$1.71+7.27\theta$	$1.71+7.27\theta$
	9	$3.00+6.68\theta$	$3.00+6.68\theta$	$3.00+6.68\theta$	$2.06+7.62\theta$	$2.06+7.62\theta$	$2.06+7.62\theta$	$1.82+7.86\theta$	$1.82+7.86\theta$	$1.82+7.86\theta$
	10	$3.28+7.09\theta$	$3.28+7.09\theta$	$3.28+7.09\theta$	$2.23+8.14\theta$	$2.23+8.14\theta$	$2.23+8.14\theta$	$1.93+8.44\theta$	$1.93+8.44\theta$	$1.93+8.44\theta$
	11	$3.61+7.43\theta$	$3.61+7.43\theta$	$3.61+7.43\theta$	$2.37+8.66\theta$	$2.37+8.66\theta$	$2.37+8.66\theta$	$2.04+9.00\theta$	$2.04+9.00\theta$	$2.04+9.00\theta$
	12	$3.96+7.73\theta$	$3.96+7.73\theta$	$3.96+7.73\theta$	$2.54+9.15\theta$	$2.54+9.15\theta$	$2.54+9.15\theta$	$2.17+9.52\theta$	$2.17+9.52\theta$	$2.17+9.52\theta$
RSCS	1	$1.67+1.02\theta$	$1.67+1.02\theta$	$1.67+1.02\theta$	$1.64+1.05\theta$	$1.64+1.05\theta$	$1.64+1.05\theta$	$1.65+1.04\theta$	$1.65+1.04\theta$	$1.65+1.04\theta$
	2	$2.08+1.18\theta$	$2.08+1.18\theta$	$2.08+1.18\theta$	$2.02+1.24\theta$	$2.02+1.24\theta$	$2.02+1.24\theta$	$2.00+1.26\theta$	$2.00+1.26\theta$	$2.00+1.26\theta$
	3	$2.46+1.31\theta$	$2.46+1.31\theta$	$2.46+1.31\theta$	$2.37+1.40\theta$	$2.37+1.40\theta$	$2.37+1.40\theta$	$2.35+1.41\theta$	$2.35+1.41\theta$	$2.35+1.41\theta$
	4	$2.82+1.43\theta$	$2.82+1.43\theta$	$2.82+1.43\theta$	$2.73+1.52\theta$	$2.73+1.52\theta$	$2.73+1.52\theta$	$2.74+1.51\theta$	$2.74+1.51\theta$	$2.74+1.51\theta$
	5	$3.25+1.45\theta$	$3.25+1.45\theta$	$3.25+1.45\theta$	$3.12+1.58\theta$	$3.12+1.58\theta$	$3.12+1.58\theta$	$3.12+1.58\theta$	$3.12+1.58\theta$	$3.12+1.58\theta$
	6	$3.70+1.44\theta$	$3.70+1.44\theta$	$3.70+1.44\theta$	$3.50+1.64\theta$	$3.50+1.64\theta$	$3.50+1.64\theta$	$3.45+1.69\theta$	$3.45+1.69\theta$	$3.45+1.69\theta$
	7	$4.07+1.48\theta$	$4.07+1.48\theta$	$4.07+1.48\theta$	$3.90+1.65\theta$	$3.90+1.65\theta$	$3.90+1.65\theta$	$3.83+1.73\theta$	$3.83+1.73\theta$	$3.83+1.73\theta$
	8	$4.61+1.36\theta$	$4.61+1.36\theta$	$4.61+1.36\theta$	$4.28+1.68\theta$	$4.28+1.68\theta$	$4.28+1.68\theta$	$4.15+1.81\theta$	$4.15+1.81\theta$	$4.15+1.81\theta$
	9	$4.91+1.45\theta$	$4.91+1.45\theta$	$4.91+1.45\theta$	$4.63+1.73\theta$	$4.63+1.73\theta$	$4.63+1.73\theta$	$4.57+1.79\theta$	$4.57+1.79\theta$	$4.57+1.79\theta$
	10	$5.25+1.50\theta$	$5.25+1.50\theta$	$5.25+1.50\theta$	$5.09+1.66\theta$	$5.09+1.66\theta$	$5.09+1.66\theta$	$4.94+1.81\theta$	$4.94+1.81\theta$	$4.94+1.81\theta$
	11	$5.66+1.47\theta$	$5.66+1.47\theta$	$5.66+1.47\theta$	$5.40+1.74\theta$	$5.40+1.74\theta$	$5.40+1.74\theta$	$5.28+1.86\theta$	$5.28+1.86\theta$	$5.28+1.86\theta$
	12	$6.09+1.43\theta$	$6.09+1.43\theta$	$6.09+1.43\theta$	$5.79+1.73\theta$	$5.79+1.73\theta$	$5.79+1.73\theta$	$5.69+1.83\theta$	$5.69+1.83\theta$	$5.69+1.83\theta$
RSCS-NN	1	$1.28+1.41\theta$	$1.28+1.41\theta$	$1.28+1.41\theta$	$1.25+1.44\theta$	$1.25+1.44\theta$	$1.25+1.44\theta$	$1.25+1.44\theta$	$1.25+1.44\theta$	$1.25+1.44\theta$
	2	$1.37+1.88\theta$	$1.37+1.88\theta$	$1.37+1.88\theta$	$1.29+1.96\theta$	$1.29+1.96\theta$	$1.29+1.96\theta$	$1.27+1.99\theta$	$1.27+1.99\theta$	$1.27+1.99\theta$
	3	$1.47+2.30\theta$	$1.47+2.30\theta$	$1.47+2.30\theta$	$1.33+2.43\theta$	$1.33+2.43\theta$	$1.33+2.43\theta$	$1.30+2.47\theta$	$1.30+2.47\theta$	$1.30+2.47\theta$
	4	$1.57+2.67\theta$	$1.57+2.67\theta$	$1.57+2.67\theta$	$1.39+2.86\theta$	$1.39+2.86\theta$	$1.39+2.86\theta$	$1.35+2.90\theta$	$1.35+2.90\theta$	$1.35+2.90\theta$
	5	$1.72+2.98\theta$	$1.72+2.98\theta$	$1.72+2.98\theta$	$1.46+3.24\theta$	$1.46+3.24\theta$	$1.46+3.24\theta$	$1.40+3.30\theta$	$1.40+3.30\theta$	$1.40+3.30\theta$
	6	$1.89+3.24\theta$	$1.89+3.24\theta$	$1.89+3.24\theta$	$1.53+3.60\theta$	$1.53+3.60\theta$	$1.53+3.60\theta$	$1.44+3.69\theta$	$1.44+3.69\theta$	$1.44+3.69\theta$
	7	$2.05+3.51\theta$	$2.05+3.51\theta$	$2.05+3.51\theta$	$1.61+3.94\theta$	$1.61+3.94\theta$	$1.61+3.94\theta$	$1.50+4.05\theta$	$1.50+4.05\theta$	$1.50+4.05\theta$
	8	$2.27+3.69\theta$	$2.27+3.69\theta$	$2.27+3.69\theta$	$1.70+4.26\theta$	$1.70+4.26\theta$	$1.70+4.26\theta$	$1.55+4.41\theta$	$1.55+4.41\theta$	$1.55+4.41\theta$
	9	$2.42+3.94\theta$	$2.42+3.94\theta$	$2.42+3.94\theta$	$1.79+4.57\theta$	$1.79+4.57\theta$	$1.79+4.57\theta$	$1.63+4.73\theta$	$1.63+4.73\theta$	$1.63+4.73\theta$
	10	$2.61+4.14\theta$	$2.61+4.14\theta$	$2.61+4.14\theta$	$1.91+4.85\theta$	$1.91+4.85\theta$	$1.91+4.85\theta$	$1.70+5.05\theta$	$1.70+5.05\theta$	$1.70+5.05\theta$
	11	$2.83+4.31\theta$	$2.83+4.31\theta$	$2.83+4.31\theta$	$2.00+5.14\theta$	$2.00+5.14\theta$	$2.00+5.14\theta$	$1.77+5.36\theta$	$1.77+5.36\theta$	$1.77+5.36\theta$
	12	$3.06+4.46\theta$	$3.06+4.46\theta$	$3.06+4.46\theta$	$2.11+5.41\theta$	$2.11+5.41\theta$	$2.11+5.41\theta$	$1.86+5.66\theta$	$1.86+5.66\theta$	$1.86+5.66\theta$

Table A.10: Normalised Cycle Times for the RSLS, RSLS-NN and Stack First Strategies for AS/R Systems.

		$L \cdot W \cdot H = 10000$			$L \cdot W \cdot H = 50000$			$L \cdot W \cdot H = 100000$		
	H	γ_1	γ_2	γ_3	γ_1	γ_2	γ_3	γ_1	γ_2	γ_3
RSLS	1	$1.67 + 1.02\theta$	$1.67 + 1.02\theta$	$1.67 + 1.02\theta$	$1.64 + 1.05\theta$	$1.64 + 1.05\theta$	$1.64 + 1.05\theta$	$1.65 + 1.04\theta$	$1.65 + 1.04\theta$	$1.65 + 1.04\theta$
	2	$2.06 + 1.16\theta$	$2.06 + 1.16\theta$	$2.06 + 1.16\theta$	$2.00 + 1.22\theta$	$2.00 + 1.22\theta$	$2.00 + 1.22\theta$	$1.98 + 1.24\theta$	$1.98 + 1.24\theta$	$1.98 + 1.24\theta$
	3	$2.42 + 1.29\theta$	$2.42 + 1.29\theta$	$2.42 + 1.29\theta$	$2.33 + 1.38\theta$	$2.33 + 1.38\theta$	$2.33 + 1.38\theta$	$2.32 + 1.39\theta$	$2.32 + 1.39\theta$	$2.32 + 1.39\theta$
	4	$2.76 + 1.42\theta$	$2.76 + 1.42\theta$	$2.76 + 1.42\theta$	$2.67 + 1.50\theta$	$2.67 + 1.50\theta$	$2.67 + 1.50\theta$	$2.68 + 1.49\theta$	$2.68 + 1.49\theta$	$2.68 + 1.49\theta$
	5	$3.17 + 1.45\theta$	$3.17 + 1.45\theta$	$3.17 + 1.45\theta$	$3.05 + 1.57\theta$	$3.05 + 1.57\theta$	$3.05 + 1.57\theta$	$3.04 + 1.58\theta$	$3.04 + 1.58\theta$	$3.04 + 1.58\theta$
	6	$3.60 + 1.45\theta$	$3.60 + 1.45\theta$	$3.60 + 1.45\theta$	$3.41 + 1.64\theta$	$3.41 + 1.64\theta$	$3.41 + 1.64\theta$	$3.36 + 1.70\theta$	$3.36 + 1.70\theta$	$3.36 + 1.70\theta$
	7	$3.96 + 1.52\theta$	$3.96 + 1.52\theta$	$3.96 + 1.52\theta$	$3.79 + 1.68\theta$	$3.79 + 1.68\theta$	$3.79 + 1.68\theta$	$3.72 + 1.75\theta$	$3.72 + 1.75\theta$	$3.72 + 1.75\theta$
	8	$4.47 + 1.41\theta$	$4.47 + 1.41\theta$	$4.47 + 1.41\theta$	$4.16 + 1.72\theta$	$4.16 + 1.72\theta$	$4.16 + 1.72\theta$	$4.03 + 1.85\theta$	$4.03 + 1.85\theta$	$4.03 + 1.85\theta$
	9	$4.75 + 1.53\theta$	$4.75 + 1.53\theta$	$4.75 + 1.53\theta$	$4.49 + 1.79\theta$	$4.49 + 1.79\theta$	$4.49 + 1.79\theta$	$4.43 + 1.85\theta$	$4.43 + 1.85\theta$	$4.43 + 1.85\theta$
	10	$5.08 + 1.60\theta$	$5.08 + 1.60\theta$	$5.08 + 1.60\theta$	$4.93 + 1.75\theta$	$4.93 + 1.75\theta$	$4.93 + 1.75\theta$	$4.78 + 1.90\theta$	$4.78 + 1.90\theta$	$4.78 + 1.90\theta$
	11	$5.48 + 1.59\theta$	$5.48 + 1.59\theta$	$5.48 + 1.59\theta$	$5.23 + 1.84\theta$	$5.23 + 1.84\theta$	$5.23 + 1.84\theta$	$5.11 + 1.96\theta$	$5.11 + 1.96\theta$	$5.11 + 1.96\theta$
	12	$5.88 + 1.57\theta$	$5.88 + 1.57\theta$	$5.88 + 1.57\theta$	$5.59 + 1.86\theta$	$5.59 + 1.86\theta$	$5.59 + 1.86\theta$	$5.50 + 1.96\theta$	$5.50 + 1.96\theta$	$5.50 + 1.96\theta$
RSLS-NN	1	$1.28 + 1.41\theta$	$1.28 + 1.41\theta$	$1.28 + 1.41\theta$	$1.25 + 1.44\theta$	$1.25 + 1.44\theta$	$1.25 + 1.44\theta$	$1.25 + 1.44\theta$	$1.25 + 1.44\theta$	$1.25 + 1.44\theta$
	2	$1.37 + 1.85\theta$	$1.37 + 1.85\theta$	$1.37 + 1.85\theta$	$1.29 + 1.93\theta$	$1.29 + 1.93\theta$	$1.29 + 1.93\theta$	$1.27 + 1.95\theta$	$1.27 + 1.95\theta$	$1.27 + 1.95\theta$
	3	$1.46 + 2.25\theta$	$1.46 + 2.25\theta$	$1.46 + 2.25\theta$	$1.33 + 2.38\theta$	$1.33 + 2.38\theta$	$1.33 + 2.38\theta$	$1.30 + 2.41\theta$	$1.30 + 2.41\theta$	$1.30 + 2.41\theta$
	4	$1.55 + 2.62\theta$	$1.55 + 2.62\theta$	$1.55 + 2.62\theta$	$1.37 + 2.80\theta$	$1.37 + 2.80\theta$	$1.37 + 2.80\theta$	$1.34 + 2.83\theta$	$1.34 + 2.83\theta$	$1.34 + 2.83\theta$
	5	$1.69 + 2.93\theta$	$1.69 + 2.93\theta$	$1.69 + 2.93\theta$	$1.44 + 3.18\theta$	$1.44 + 3.18\theta$	$1.44 + 3.18\theta$	$1.39 + 3.23\theta$	$1.39 + 3.23\theta$	$1.39 + 3.23\theta$
	6	$1.84 + 3.21\theta$	$1.84 + 3.21\theta$	$1.84 + 3.21\theta$	$1.51 + 3.55\theta$	$1.51 + 3.55\theta$	$1.51 + 3.55\theta$	$1.42 + 3.63\theta$	$1.42 + 3.63\theta$	$1.42 + 3.63\theta$
	7	$1.98 + 3.49\theta$	$1.98 + 3.49\theta$	$1.98 + 3.49\theta$	$1.58 + 3.89\theta$	$1.58 + 3.89\theta$	$1.58 + 3.89\theta$	$1.48 + 3.99\theta$	$1.48 + 3.99\theta$	$1.48 + 3.99\theta$
	8	$2.18 + 3.70\theta$	$2.18 + 3.70\theta$	$2.18 + 3.70\theta$	$1.66 + 4.22\theta$	$1.66 + 4.22\theta$	$1.66 + 4.22\theta$	$1.52 + 4.35\theta$	$1.52 + 4.35\theta$	$1.52 + 4.35\theta$
	9	$2.31 + 3.97\theta$	$2.31 + 3.97\theta$	$2.31 + 3.97\theta$	$1.74 + 4.54\theta$	$1.74 + 4.54\theta$	$1.74 + 4.54\theta$	$1.59 + 4.69\theta$	$1.59 + 4.69\theta$	$1.59 + 4.69\theta$
	10	$2.47 + 4.20\theta$	$2.47 + 4.20\theta$	$2.47 + 4.20\theta$	$1.84 + 4.84\theta$	$1.84 + 4.84\theta$	$1.84 + 4.84\theta$	$1.66 + 5.02\theta$	$1.66 + 5.02\theta$	$1.66 + 5.02\theta$
	11	$2.67 + 4.40\theta$	$2.67 + 4.40\theta$	$2.67 + 4.40\theta$	$1.92 + 5.15\theta$	$1.92 + 5.15\theta$	$1.92 + 5.15\theta$	$1.72 + 5.35\theta$	$1.72 + 5.35\theta$	$1.72 + 5.35\theta$
	12	$2.87 + 4.58\theta$	$2.87 + 4.58\theta$	$2.87 + 4.58\theta$	$2.02 + 5.44\theta$	$2.02 + 5.44\theta$	$2.02 + 5.44\theta$	$1.79 + 5.66\theta$	$1.79 + 5.66\theta$	$1.79 + 5.66\theta$
Stack First	1	$1.67 + 1.02\theta$	$1.67 + 1.02\theta$	$1.67 + 1.02\theta$	$1.64 + 1.05\theta$	$1.64 + 1.05\theta$	$1.64 + 1.05\theta$	$1.65 + 1.04\theta$	$1.65 + 1.04\theta$	$1.65 + 1.04\theta$
	2	$2.14 + 1.22\theta$	$2.14 + 1.22\theta$	$2.14 + 1.22\theta$	$2.08 + 1.28\theta$	$2.08 + 1.28\theta$	$2.08 + 1.28\theta$	$2.06 + 1.31\theta$	$2.06 + 1.31\theta$	$2.06 + 1.31\theta$
	3	$2.59 + 1.37\theta$	$2.59 + 1.37\theta$	$2.59 + 1.37\theta$	$2.49 + 1.47\theta$	$2.49 + 1.47\theta$	$2.49 + 1.47\theta$	$2.47 + 1.49\theta$	$2.47 + 1.49\theta$	$2.47 + 1.49\theta$
	4	$3.01 + 1.50\theta$	$3.01 + 1.50\theta$	$3.01 + 1.50\theta$	$2.91 + 1.60\theta$	$2.91 + 1.60\theta$	$2.91 + 1.60\theta$	$2.92 + 1.59\theta$	$2.92 + 1.59\theta$	$2.92 + 1.59\theta$
	5	$3.51 + 1.51\theta$	$3.51 + 1.51\theta$	$3.51 + 1.51\theta$	$3.37 + 1.65\theta$	$3.37 + 1.65\theta$	$3.37 + 1.65\theta$	$3.37 + 1.66\theta$	$3.37 + 1.66\theta$	$3.37 + 1.66\theta$
	6	$4.04 + 1.46\theta$	$4.04 + 1.46\theta$	$4.04 + 1.46\theta$	$3.81 + 1.69\theta$	$3.81 + 1.69\theta$	$3.81 + 1.69\theta$	$3.76 + 1.75\theta$	$3.76 + 1.75\theta$	$3.76 + 1.75\theta$
	7	$4.48 + 1.48\theta$	$4.48 + 1.48\theta$	$4.48 + 1.48\theta$	$4.28 + 1.68\theta$	$4.28 + 1.68\theta$	$4.28 + 1.68\theta$	$4.20 + 1.76\theta$	$4.20 + 1.76\theta$	$4.20 + 1.76\theta$
	8	$5.10 + 1.30\theta$	$5.10 + 1.30\theta$	$5.10 + 1.30\theta$	$4.74 + 1.67\theta$	$4.74 + 1.67\theta$	$4.74 + 1.67\theta$	$4.59 + 1.81\theta$	$4.59 + 1.81\theta$	$4.59 + 1.81\theta$
	9	$5.46 + 1.37\theta$	$5.46 + 1.37\theta$	$5.46 + 1.37\theta$	$5.15 + 1.68\theta$	$5.15 + 1.68\theta$	$5.15 + 1.68\theta$	$5.07 + 1.76\theta$	$5.07 + 1.76\theta$	$5.07 + 1.76\theta$
	10	$5.87 + 1.38\theta$	$5.87 + 1.38\theta$	$5.87 + 1.38\theta$	$5.69 + 1.56\theta$	$5.69 + 1.56\theta$	$5.69 + 1.56\theta$	$5.51 + 1.74\theta$	$5.51 + 1.74\theta$	$5.51 + 1.74\theta$
	11	$6.36 + 1.30\theta$	$6.36 + 1.30\theta$	$6.36 + 1.30\theta$	$6.05 + 1.60\theta$	$6.05 + 1.60\theta$	$6.05 + 1.60\theta$	$5.91 + 1.74\theta$	$5.91 + 1.74\theta$	$5.91 + 1.74\theta$
	12	$6.85 + 1.20\theta$	$6.85 + 1.20\theta$	$6.85 + 1.20\theta$	$6.51 + 1.54\theta$	$6.51 + 1.54\theta$	$6.51 + 1.54\theta$	$6.39 + 1.66\theta$	$6.39 + 1.66\theta$	$6.39 + 1.66\theta$

Table A.11: Normalised Cycle Times for the Homogeneous Strategy for AS/R Systems.

H	$L \cdot W \cdot H = 10000$			$L \cdot W \cdot H = 50000$			$L \cdot W \cdot H = 100000$		
	γ_1	γ_2	γ_3	γ_1	γ_2	γ_3	γ_1	γ_2	γ_3
Homogeneous									
1	$1.67 + 1.02\theta$	$1.67 + 1.02\theta$	$1.67 + 1.02\theta$	$1.64 + 1.05\theta$	$1.64 + 1.05\theta$	$1.64 + 1.05\theta$	$1.65 + 1.04\theta$	$1.65 + 1.04\theta$	$1.65 + 1.04\theta$
2	$2.67 + 1.14\theta$	$2.67 + 1.14\theta$	$2.67 + 1.14\theta$	$2.60 + 1.21\theta$	$2.60 + 1.21\theta$	$2.60 + 1.21\theta$	$2.57 + 1.23\theta$	$2.57 + 1.23\theta$	$2.57 + 1.23\theta$
3	$3.49 + 1.29\theta$	$3.49 + 1.29\theta$	$3.49 + 1.29\theta$	$3.37 + 1.41\theta$	$3.37 + 1.41\theta$	$3.37 + 1.41\theta$	$3.35 + 1.44\theta$	$3.35 + 1.44\theta$	$3.35 + 1.44\theta$
4	$4.21 + 1.46\theta$	$4.21 + 1.46\theta$	$4.21 + 1.46\theta$	$4.08 + 1.59\theta$	$4.08 + 1.59\theta$	$4.08 + 1.59\theta$	$4.10 + 1.57\theta$	$4.10 + 1.57\theta$	$4.10 + 1.57\theta$
5	$5.00 + 1.48\theta$	$5.00 + 1.48\theta$	$5.00 + 1.48\theta$	$4.82 + 1.66\theta$	$4.82 + 1.66\theta$	$4.82 + 1.66\theta$	$4.81 + 1.68\theta$	$4.81 + 1.68\theta$	$4.81 + 1.68\theta$
6	$5.82 + 1.43\theta$	$5.82 + 1.43\theta$	$5.82 + 1.43\theta$	$5.52 + 1.74\theta$	$5.52 + 1.74\theta$	$5.52 + 1.74\theta$	$5.44 + 1.82\theta$	$5.44 + 1.82\theta$	$5.44 + 1.82\theta$
7	$6.50 + 1.48\theta$	$6.50 + 1.48\theta$	$6.50 + 1.48\theta$	$6.24 + 1.74\theta$	$6.24 + 1.74\theta$	$6.24 + 1.74\theta$	$6.13 + 1.85\theta$	$6.13 + 1.85\theta$	$6.13 + 1.85\theta$
8	$7.44 + 1.23\theta$	$7.44 + 1.23\theta$	$7.44 + 1.23\theta$	$6.94 + 1.74\theta$	$6.94 + 1.74\theta$	$6.94 + 1.74\theta$	$6.74 + 1.94\theta$	$6.74 + 1.94\theta$	$6.74 + 1.94\theta$
9	$8.00 + 1.34\theta$	$8.00 + 1.34\theta$	$8.00 + 1.34\theta$	$7.58 + 1.77\theta$	$7.58 + 1.77\theta$	$7.58 + 1.77\theta$	$7.47 + 1.88\theta$	$7.47 + 1.88\theta$	$7.47 + 1.88\theta$
10	$8.63 + 1.36\theta$	$8.63 + 1.36\theta$	$8.63 + 1.36\theta$	$8.38 + 1.61\theta$	$8.38 + 1.61\theta$	$8.38 + 1.61\theta$	$8.14 + 1.86\theta$	$8.14 + 1.86\theta$	$8.14 + 1.86\theta$
11	$9.37 + 1.25\theta$	$9.37 + 1.25\theta$	$9.37 + 1.25\theta$	$8.95 + 1.67\theta$	$8.95 + 1.67\theta$	$8.95 + 1.67\theta$	$8.75 + 1.87\theta$	$8.75 + 1.87\theta$	$8.75 + 1.87\theta$
12	$10.12 + 1.12\theta$	$10.12 + 1.12\theta$	$10.12 + 1.12\theta$	$9.64 + 1.60\theta$	$9.64 + 1.60\theta$	$9.64 + 1.60\theta$	$9.47 + 1.77\theta$	$9.47 + 1.77\theta$	$9.47 + 1.77\theta$

Table A.12: Normalised Cycle Times for the AS-LFR Strategy for RCS/R Systems.

	AS-LFR								
	$L \cdot W \cdot H = 10000$			$L \cdot W \cdot H = 50000$			$L \cdot W \cdot H = 100000$		
H	γ_1	γ_2	γ_3	γ_1	γ_2	γ_3	γ_1	γ_2	γ_3
1	$1.07 + 1.80\theta$	$1.07 + 1.80\theta$	$1.07 + 1.80\theta$	$0.87 + 2.00\theta$	$0.87 + 2.00\theta$	$0.87 + 2.00\theta$	$0.81 + 2.06\theta$	$0.81 + 2.06\theta$	$0.81 + 2.06\theta$
2	$1.20 + 1.62\theta$	$1.20 + 1.62\theta$	$1.20 + 1.62\theta$	$0.94 + 1.87\theta$	$0.94 + 1.87\theta$	$0.94 + 1.87\theta$	$0.87 + 1.95\theta$	$0.87 + 1.95\theta$	$0.87 + 1.95\theta$
3	$2.07 + 3.11\theta$	$1.45 + 1.65\theta$	$1.30 + 1.30\theta$	$1.40 + 3.77\theta$	$1.08 + 2.02\theta$	$1.00 + 1.59\theta$	$1.21 + 3.96\theta$	$0.97 + 2.13\theta$	$0.91 + 1.69\theta$
4	$2.66 + 3.49\theta$	$1.65 + 1.61\theta$	$1.38 + 1.11\theta$	$1.73 + 4.42\theta$	$1.19 + 2.07\theta$	$1.05 + 1.44\theta$	$1.46 + 4.70\theta$	$1.06 + 2.20\theta$	$0.95 + 1.54\theta$
5	$3.30 + 3.74\theta$	$1.88 + 1.55\theta$	$1.47 + 0.93\theta$	$2.10 + 4.95\theta$	$1.32 + 2.10\theta$	$1.10 + 1.29\theta$	$1.73 + 5.31\theta$	$1.15 + 2.27\theta$	$0.99 + 1.40\theta$
6	$3.99 + 3.87\theta$	$2.11 + 1.47\theta$	$1.57 + 0.73\theta$	$2.50 + 5.36\theta$	$1.46 + 2.12\theta$	$1.16 + 1.14\theta$	$2.03 + 5.82\theta$	$1.26 + 2.32\theta$	$1.04 + 1.26\theta$
7	$4.73 + 3.88\theta$	$2.37 + 1.37\theta$	$1.66 + 0.57\theta$	$2.93 + 5.68\theta$	$1.63 + 2.11\theta$	$1.24 + 0.99\theta$	$2.37 + 6.24\theta$	$1.39 + 2.35\theta$	$1.09 + 1.13\theta$
8	$5.42 + 3.88\theta$	$2.60 + 1.28\theta$	$1.73 + 0.44\theta$	$3.40 + 5.91\theta$	$1.80 + 2.08\theta$	$1.32 + 0.85\theta$	$2.73 + 6.57\theta$	$1.53 + 2.35\theta$	$1.17 + 1.00\theta$
9	$6.21 + 3.74\theta$	$2.85 + 1.17\theta$	$1.78 + 0.33\theta$	$3.89 + 6.06\theta$	$1.98 + 2.04\theta$	$1.39 + 0.73\theta$	$3.11 + 6.84\theta$	$1.68 + 2.35\theta$	$1.24 + 0.88\theta$
10	$6.99 + 3.56\theta$	$3.09 + 1.06\theta$	$1.83 + 0.23\theta$	$4.36 + 6.20\theta$	$2.14 + 2.01\theta$	$1.44 + 0.62\theta$	$3.51 + 7.04\theta$	$1.82 + 2.33\theta$	$1.30 + 0.77\theta$
11	$7.77 + 3.36\theta$	$3.33 + 0.95\theta$	$1.88 + 0.15\theta$	$4.88 + 6.25\theta$	$2.31 + 1.97\theta$	$1.48 + 0.54\theta$	$3.92 + 7.21\theta$	$1.96 + 2.32\theta$	$1.34 + 0.68\theta$
12	$8.58 + 3.09\theta$	$3.57 + 0.82\theta$	$1.92 + 0.06\theta$	$5.38 + 6.28\theta$	$2.47 + 1.93\theta$	$1.52 + 0.47\theta$	$4.31 + 7.35\theta$	$2.09 + 2.30\theta$	$1.38 + 0.61\theta$
13	$9.41 + 3.91\theta$	$3.74 + 1.01\theta$	$1.89 + 0.04\theta$	$5.83 + 7.49\theta$	$2.51 + 2.24\theta$	$1.43 + 0.50\theta$	$4.64 + 8.68\theta$	$2.09 + 2.66\theta$	$1.27 + 0.66\theta$
14	$10.25 + 3.89\theta$	$3.98 + 0.96\theta$	$1.92 - 0.03\theta$	$6.39 + 7.76\theta$	$2.67 + 2.27\theta$	$1.46 + 0.43\theta$	$5.05 + 9.10\theta$	$2.21 + 2.73\theta$	$1.29 + 0.60\theta$
15	$11.16 + 3.81\theta$	$4.23 + 0.89\theta$	$1.96 - 0.10\theta$	$6.93 + 8.03\theta$	$2.83 + 2.30\theta$	$1.49 + 0.37\theta$	$5.50 + 9.46\theta$	$2.35 + 2.78\theta$	$1.32 + 0.54\theta$
16	$12.07 + 3.71\theta$	$4.49 + 0.82\theta$	$2.00 - 0.17\theta$	$7.51 + 8.27\theta$	$2.99 + 2.32\theta$	$1.51 + 0.32\theta$	$5.94 + 9.83\theta$	$2.47 + 2.84\theta$	$1.34 + 0.49\theta$
17	$13.06 + 3.53\theta$	$4.77 + 0.73\theta$	$2.04 - 0.23\theta$	$8.12 + 8.47\theta$	$3.17 + 2.33\theta$	$1.54 + 0.26\theta$	$6.44 + 10.15\theta$	$2.61 + 2.88\theta$	$1.36 + 0.44\theta$
18	$13.89 + 3.50\theta$	$5.00 + 0.68\theta$	$2.06 - 0.28\theta$	$8.70 + 8.68\theta$	$3.33 + 2.35\theta$	$1.56 + 0.22\theta$	$6.89 + 10.50\theta$	$2.74 + 2.94\theta$	$1.38 + 0.40\theta$
19	$14.79 + 3.40\theta$	$5.25 + 0.63\theta$	$2.09 - 0.33\theta$	$9.31 + 8.87\theta$	$3.51 + 2.37\theta$	$1.59 + 0.17\theta$	$7.37 + 10.82\theta$	$2.88 + 3.00\theta$	$1.40 + 0.35\theta$
20	$15.66 + 3.32\theta$	$5.49 + 0.58\theta$	$2.11 - 0.38\theta$	$9.95 + 9.03\theta$	$3.68 + 2.38\theta$	$1.61 + 0.12\theta$	$7.82 + 11.17\theta$	$3.01 + 3.06\theta$	$1.42 + 0.32\theta$
21	$16.79 + 2.98\theta$	$5.81 + 0.45\theta$	$2.16 - 0.44\theta$	$10.54 + 9.23\theta$	$3.85 + 2.40\theta$	$1.64 + 0.08\theta$	$8.33 + 11.44\theta$	$3.15 + 3.10\theta$	$1.44 + 0.28\theta$
22	$17.77 + 2.79\theta$	$6.07 + 0.37\theta$	$2.19 - 0.49\theta$	$11.23 + 9.34\theta$	$4.04 + 2.40\theta$	$1.66 + 0.04\theta$	$8.87 + 11.69\theta$	$3.30 + 3.14\theta$	$1.46 + 0.24\theta$
23	$18.49 + 2.86\theta$	$6.26 + 0.37\theta$	$2.20 - 0.51\theta$	$11.85 + 9.50\theta$	$4.22 + 2.42\theta$	$1.68 + 0.00\theta$	$9.39 + 11.96\theta$	$3.45 + 3.19\theta$	$1.48 + 0.20\theta$
24	$19.74 + 2.39\theta$	$6.61 + 0.21\theta$	$2.24 - 0.57\theta$	$12.52 + 9.61\theta$	$4.40 + 2.42\theta$	$1.71 - 0.03\theta$	$9.92 + 12.22\theta$	$3.60 + 3.23\theta$	$1.50 + 0.17\theta$

Table A.13: Normalised Cycle Times for the AutoStore for RCS/R Systems.

		$L \cdot W \cdot H = 10000$			$L \cdot W \cdot H = 50000$			$L \cdot W \cdot H = 100000$		
	H	γ_1	γ_2	γ_3	γ_1	γ_2	γ_3	γ_1	γ_2	γ_3
AutoStore	1	$1.07 + 1.80\theta$	$1.07 + 1.80\theta$	$1.07 + 1.80\theta$	$0.87 + 2.00\theta$	$0.87 + 2.00\theta$	$0.87 + 2.00\theta$	$0.81 + 2.06\theta$	$0.81 + 2.06\theta$	$0.81 + 2.06\theta$
	2	$1.20 + 1.62\theta$	$1.20 + 1.62\theta$	$1.20 + 1.62\theta$	$0.94 + 1.87\theta$	$0.94 + 1.87\theta$	$0.94 + 1.87\theta$	$0.87 + 1.95\theta$	$0.87 + 1.95\theta$	$0.87 + 1.95\theta$
	3	$2.07 + 3.11\theta$	$1.69 + 2.21\theta$	$1.54 + 1.86\theta$	$1.40 + 3.77\theta$	$1.20 + 2.70\theta$	$1.13 + 2.28\theta$	$1.21 + 3.96\theta$	$1.06 + 2.84\theta$	$1.01 + 2.40\theta$
	4	$2.66 + 3.49\theta$	$2.03 + 2.31\theta$	$1.78 + 1.85\theta$	$1.73 + 4.42\theta$	$1.39 + 2.95\theta$	$1.26 + 2.37\theta$	$1.46 + 4.70\theta$	$1.21 + 3.13\theta$	$1.11 + 2.52\theta$
	5	$3.30 + 3.74\theta$	$2.39 + 2.35\theta$	$2.02 + 1.81\theta$	$2.10 + 4.95\theta$	$1.60 + 3.14\theta$	$1.41 + 2.44\theta$	$1.73 + 5.31\theta$	$1.36 + 3.38\theta$	$1.22 + 2.63\theta$
	6	$3.99 + 3.87\theta$	$2.76 + 2.35\theta$	$2.28 + 1.76\theta$	$2.50 + 5.36\theta$	$1.82 + 3.29\theta$	$1.55 + 2.48\theta$	$2.03 + 5.82\theta$	$1.53 + 3.58\theta$	$1.33 + 2.70\theta$
	7	$4.73 + 3.88\theta$	$3.17 + 2.28\theta$	$2.54 + 1.67\theta$	$2.93 + 5.68\theta$	$2.06 + 3.39\theta$	$1.71 + 2.50\theta$	$2.37 + 6.24\theta$	$1.71 + 3.73\theta$	$1.45 + 2.76\theta$
	8	$5.42 + 3.88\theta$	$3.55 + 2.22\theta$	$2.79 + 1.59\theta$	$3.40 + 5.91\theta$	$2.31 + 3.45\theta$	$1.88 + 2.50\theta$	$2.73 + 6.57\theta$	$1.91 + 3.85\theta$	$1.58 + 2.80\theta$
	9	$6.21 + 3.74\theta$	$3.98 + 2.08\theta$	$3.07 + 1.46\theta$	$3.89 + 6.06\theta$	$2.58 + 3.48\theta$	$2.05 + 2.49\theta$	$3.11 + 6.84\theta$	$2.11 + 3.94\theta$	$1.71 + 2.82\theta$
	10	$6.99 + 3.56\theta$	$4.41 + 1.92\theta$	$3.36 + 1.32\theta$	$4.36 + 6.20\theta$	$2.84 + 3.49\theta$	$2.22 + 2.46\theta$	$3.51 + 7.04\theta$	$2.33 + 4.00\theta$	$1.85 + 2.83\theta$
	11	$7.77 + 3.36\theta$	$4.83 + 1.76\theta$	$3.64 + 1.18\theta$	$4.88 + 6.25\theta$	$3.13 + 3.46\theta$	$2.41 + 2.42\theta$	$3.92 + 7.21\theta$	$2.56 + 4.03\theta$	$1.99 + 2.83\theta$
	12	$8.58 + 3.09\theta$	$5.26 + 1.57\theta$	$3.93 + 1.02\theta$	$5.38 + 6.28\theta$	$3.42 + 3.42\theta$	$2.59 + 2.36\theta$	$4.31 + 7.35\theta$	$2.79 + 4.05\theta$	$2.14 + 2.81\theta$
	13	$9.41 + 3.91\theta$	$5.65 + 1.99\theta$	$4.16 + 1.27\theta$	$5.83 + 7.49\theta$	$3.61 + 4.03\theta$	$2.73 + 2.71\theta$	$4.64 + 8.68\theta$	$2.93 + 4.72\theta$	$2.24 + 3.19\theta$
	14	$10.25 + 3.89\theta$	$6.09 + 1.94\theta$	$4.44 + 1.21\theta$	$6.39 + 7.76\theta$	$3.90 + 4.14\theta$	$2.91 + 2.75\theta$	$5.05 + 9.10\theta$	$3.14 + 4.90\theta$	$2.38 + 3.28\theta$
	15	$11.16 + 3.81\theta$	$6.56 + 1.87\theta$	$4.75 + 1.13\theta$	$6.93 + 8.03\theta$	$4.19 + 4.24\theta$	$3.10 + 2.79\theta$	$5.50 + 9.46\theta$	$3.38 + 5.05\theta$	$2.54 + 3.35\theta$
	16	$12.07 + 3.71\theta$	$7.04 + 1.78\theta$	$5.05 + 1.06\theta$	$7.51 + 8.27\theta$	$4.49 + 4.33\theta$	$3.29 + 2.82\theta$	$5.94 + 9.83\theta$	$3.61 + 5.21\theta$	$2.69 + 3.43\theta$
	17	$13.06 + 3.53\theta$	$7.56 + 1.65\theta$	$5.38 + 0.95\theta$	$8.12 + 8.47\theta$	$4.81 + 4.40\theta$	$3.50 + 2.84\theta$	$6.44 + 10.15\theta$	$3.87 + 5.34\theta$	$2.85 + 3.49\theta$
	18	$13.89 + 3.50\theta$	$7.99 + 1.61\theta$	$5.65 + 0.90\theta$	$8.70 + 8.68\theta$	$5.12 + 4.49\theta$	$3.69 + 2.88\theta$	$6.89 + 10.50\theta$	$4.11 + 5.49\theta$	$3.01 + 3.56\theta$
	19	$14.79 + 3.40\theta$	$8.45 + 1.53\theta$	$5.95 + 0.84\theta$	$9.31 + 8.87\theta$	$5.43 + 4.56\theta$	$3.90 + 2.90\theta$	$7.37 + 10.82\theta$	$4.36 + 5.63\theta$	$3.17 + 3.63\theta$
	20	$15.66 + 3.32\theta$	$8.90 + 1.47\theta$	$6.23 + 0.78\theta$	$9.95 + 9.03\theta$	$5.77 + 4.61\theta$	$4.11 + 2.92\theta$	$7.82 + 11.17\theta$	$4.59 + 5.79\theta$	$3.32 + 3.71\theta$
	21	$16.79 + 2.98\theta$	$9.49 + 1.26\theta$	$6.61 + 0.63\theta$	$10.54 + 9.23\theta$	$6.07 + 4.69\theta$	$4.30 + 2.95\theta$	$8.33 + 11.44\theta$	$4.86 + 5.90\theta$	$3.49 + 3.77\theta$
	22	$17.77 + 2.79\theta$	$10.00 + 1.14\theta$	$6.93 + 0.54\theta$	$11.23 + 9.34\theta$	$6.43 + 4.72\theta$	$4.53 + 2.95\theta$	$8.87 + 11.69\theta$	$5.14 + 6.01\theta$	$3.67 + 3.82\theta$
	23	$18.49 + 2.86\theta$	$10.36 + 1.16\theta$	$7.16 + 0.54\theta$	$11.85 + 9.50\theta$	$6.76 + 4.78\theta$	$4.74 + 2.97\theta$	$9.39 + 11.96\theta$	$5.41 + 6.12\theta$	$3.84 + 3.87\theta$
	24	$19.74 + 2.39\theta$	$11.02 + 0.89\theta$	$7.58 + 0.35\theta$	$12.52 + 9.61\theta$	$7.10 + 4.81\theta$	$4.96 + 2.98\theta$	$9.92 + 12.22\theta$	$5.69 + 6.23\theta$	$4.01 + 3.93\theta$

Table A.14: Normalised Cycle Times for the CBS-1 Strategy for RCS/R Systems.

		$L \cdot W \cdot H = 10000$			$L \cdot W \cdot H = 50000$			$L \cdot W \cdot H = 100000$		
	H	γ_1	γ_2	γ_3	γ_1	γ_2	γ_3	γ_1	γ_2	γ_3
CBS-1	1	$1.05 + 1.82\theta$	$1.01 + 1.86\theta$	$1.00 + 1.87\theta$	$0.88 + 1.99\theta$	$0.84 + 2.03\theta$	$0.83 + 2.04\theta$	$0.83 + 2.04\theta$	$0.79 + 2.08\theta$	$0.78 + 2.09\theta$
	2	$1.52 + 2.70\theta$	$1.48 + 2.74\theta$	$1.48 + 2.74\theta$	$1.12 + 3.10\theta$	$1.09 + 3.13\theta$	$1.08 + 3.14\theta$	$1.01 + 3.21\theta$	$0.98 + 3.24\theta$	$0.97 + 3.25\theta$
	3	$2.07 + 3.40\theta$	$2.04 + 3.43\theta$	$2.03 + 3.44\theta$	$1.42 + 4.04\theta$	$1.39 + 4.08\theta$	$1.38 + 4.09\theta$	$1.24 + 4.23\theta$	$1.20 + 4.27\theta$	$1.19 + 4.28\theta$
	4	$2.69 + 3.94\theta$	$2.66 + 3.97\theta$	$2.65 + 3.98\theta$	$1.77 + 4.86\theta$	$1.73 + 4.90\theta$	$1.72 + 4.91\theta$	$1.49 + 5.14\theta$	$1.46 + 5.17\theta$	$1.45 + 5.18\theta$
	5	$3.35 + 4.37\theta$	$3.32 + 4.40\theta$	$3.32 + 4.41\theta$	$2.14 + 5.58\theta$	$2.11 + 5.61\theta$	$2.10 + 5.62\theta$	$1.77 + 5.95\theta$	$1.74 + 5.98\theta$	$1.73 + 5.99\theta$
	6	$4.05 + 4.71\theta$	$4.02 + 4.74\theta$	$4.01 + 4.75\theta$	$2.55 + 6.21\theta$	$2.51 + 6.24\theta$	$2.50 + 6.25\theta$	$2.08 + 6.67\theta$	$2.05 + 6.71\theta$	$2.04 + 6.72\theta$
	7	$4.80 + 4.94\theta$	$4.78 + 4.97\theta$	$4.77 + 4.97\theta$	$2.97 + 6.77\theta$	$2.94 + 6.80\theta$	$2.93 + 6.81\theta$	$2.41 + 7.33\theta$	$2.38 + 7.37\theta$	$2.37 + 7.38\theta$
	8	$5.52 + 5.17\theta$	$5.49 + 5.19\theta$	$5.49 + 5.20\theta$	$3.43 + 7.25\theta$	$3.40 + 7.28\theta$	$3.39 + 7.29\theta$	$2.76 + 7.92\theta$	$2.73 + 7.95\theta$	$2.72 + 7.96\theta$
	9	$6.35 + 5.24\theta$	$6.32 + 5.27\theta$	$6.31 + 5.28\theta$	$3.92 + 7.67\theta$	$3.89 + 7.71\theta$	$3.88 + 7.71\theta$	$3.13 + 8.46\theta$	$3.09 + 8.50\theta$	$3.08 + 8.51\theta$
	10	$7.19 + 5.28\theta$	$7.16 + 5.30\theta$	$7.16 + 5.31\theta$	$4.39 + 8.07\theta$	$4.36 + 8.10\theta$	$4.35 + 8.11\theta$	$3.52 + 8.95\theta$	$3.48 + 8.98\theta$	$3.47 + 8.99\theta$
	11	$8.02 + 5.29\theta$	$8.00 + 5.31\theta$	$7.99 + 5.32\theta$	$4.93 + 8.38\theta$	$4.90 + 8.41\theta$	$4.89 + 8.42\theta$	$3.92 + 9.39\theta$	$3.88 + 9.43\theta$	$3.87 + 9.44\theta$
	12	$8.90 + 5.23\theta$	$8.88 + 5.25\theta$	$8.87 + 5.26\theta$	$5.46 + 8.67\theta$	$5.43 + 8.70\theta$	$5.42 + 8.71\theta$	$4.32 + 9.81\theta$	$4.29 + 9.84\theta$	$4.28 + 9.85\theta$
	13	$9.74 + 5.19\theta$	$9.72 + 5.21\theta$	$9.71 + 5.22\theta$	$6.00 + 8.94\theta$	$5.97 + 8.97\theta$	$5.96 + 8.98\theta$	$4.76 + 10.18\theta$	$4.72 + 10.21\theta$	$4.71 + 10.22\theta$
	14	$10.62 + 5.10\theta$	$10.59 + 5.12\theta$	$10.59 + 5.13\theta$	$6.57 + 9.14\theta$	$6.54 + 9.17\theta$	$6.53 + 9.18\theta$	$5.18 + 10.53\theta$	$5.15 + 10.57\theta$	$5.14 + 10.58\theta$
	15	$11.56 + 4.92\theta$	$11.53 + 4.94\theta$	$11.53 + 4.95\theta$	$7.13 + 9.35\theta$	$7.10 + 9.38\theta$	$7.09 + 9.38\theta$	$5.65 + 10.83\theta$	$5.62 + 10.86\theta$	$5.61 + 10.87\theta$
	16	$12.50 + 4.73\theta$	$12.48 + 4.75\theta$	$12.47 + 4.76\theta$	$7.73 + 9.50\theta$	$7.70 + 9.53\theta$	$7.69 + 9.53\theta$	$6.10 + 11.12\theta$	$6.07 + 11.16\theta$	$6.06 + 11.16\theta$
	17	$13.53 + 4.43\theta$	$13.51 + 4.46\theta$	$13.50 + 4.46\theta$	$8.36 + 9.60\theta$	$8.33 + 9.63\theta$	$8.32 + 9.64\theta$	$6.61 + 11.35\theta$	$6.58 + 11.38\theta$	$6.57 + 11.39\theta$
	18	$14.40 + 4.29\theta$	$14.38 + 4.31\theta$	$14.37 + 4.32\theta$	$8.97 + 9.72\theta$	$8.94 + 9.75\theta$	$8.93 + 9.75\theta$	$7.08 + 11.60\theta$	$7.05 + 11.64\theta$	$7.04 + 11.65\theta$
	19	$15.35 + 4.05\theta$	$15.32 + 4.08\theta$	$15.32 + 4.08\theta$	$9.61 + 9.79\theta$	$9.58 + 9.82\theta$	$9.57 + 9.83\theta$	$7.58 + 11.82\theta$	$7.55 + 11.85\theta$	$7.54 + 11.86\theta$
	20	$16.25 + 3.85\theta$	$16.23 + 3.87\theta$	$16.23 + 3.88\theta$	$10.27 + 9.84\theta$	$10.24 + 9.87\theta$	$10.23 + 9.88\theta$	$8.05 + 12.06\theta$	$8.02 + 12.09\theta$	$8.01 + 12.10\theta$
	21	$17.43 + 3.37\theta$	$17.41 + 3.39\theta$	$17.40 + 3.39\theta$	$10.88 + 9.92\theta$	$10.85 + 9.95\theta$	$10.84 + 9.95\theta$	$8.58 + 12.21\theta$	$8.55 + 12.25\theta$	$8.54 + 12.25\theta$
	22	$18.47 + 3.02\theta$	$18.44 + 3.04\theta$	$18.44 + 3.05\theta$	$11.59 + 9.89\theta$	$11.56 + 9.92\theta$	$11.55 + 9.93\theta$	$9.14 + 12.34\theta$	$9.11 + 12.37\theta$	$9.10 + 12.38\theta$
	23	$19.23 + 2.93\theta$	$19.21 + 2.96\theta$	$19.20 + 2.96\theta$	$12.25 + 9.92\theta$	$12.22 + 9.94\theta$	$12.21 + 9.95\theta$	$9.68 + 12.48\theta$	$9.65 + 12.52\theta$	$9.64 + 12.52\theta$
	24	$20.53 + 2.31\theta$	$20.50 + 2.33\theta$	$20.50 + 2.33\theta$	$12.95 + 9.88\theta$	$12.92 + 9.91\theta$	$12.91 + 9.92\theta$	$10.23 + 12.60\theta$	$10.20 + 12.63\theta$	$10.19 + 12.64\theta$

Table A.15: Normalised Cycle Times for the CBS-3-BBO Strategy for RCS/R Systems.

		$L \cdot W \cdot H = 10000$			$L \cdot W \cdot H = 50000$			$L \cdot W \cdot H = 100000$		
	H	γ_1	γ_2	γ_3	γ_1	γ_2	γ_3	γ_1	γ_2	γ_3
CBS-3-BBO	1	$1.07 + 1.80\theta$	$1.07 + 1.80\theta$	$1.07 + 1.80\theta$	$0.87 + 2.00\theta$	$0.87 + 2.00\theta$	$0.87 + 2.00\theta$	$0.81 + 2.06\theta$	$0.81 + 2.06\theta$	$0.81 + 2.06\theta$
	2	$1.20 + 1.62\theta$	$1.20 + 1.62\theta$	$1.20 + 1.62\theta$	$0.94 + 1.87\theta$	$0.94 + 1.87\theta$	$0.94 + 1.87\theta$	$0.87 + 1.95\theta$	$0.87 + 1.95\theta$	$0.87 + 1.95\theta$
	3	$1.96 + 2.51\theta$	$1.57 + 1.44\theta$	$1.44 + 1.25\theta$	$1.43 + 3.04\theta$	$1.24 + 1.77\theta$	$1.15 + 1.54\theta$	$1.28 + 3.19\theta$	$1.15 + 1.86\theta$	$1.06 + 1.63\theta$
	4	$2.56 + 2.87\theta$	$1.93 + 1.62\theta$	$1.76 + 1.28\theta$	$1.81 + 3.62\theta$	$1.46 + 2.08\theta$	$1.36 + 1.69\theta$	$1.59 + 3.85\theta$	$1.32 + 2.22\theta$	$1.24 + 1.80\theta$
	5	$3.16 + 3.17\theta$	$2.61 + 2.03\theta$	$2.51 + 1.61\theta$	$2.16 + 4.17\theta$	$1.84 + 2.80\theta$	$1.80 + 2.33\theta$	$1.85 + 4.48\theta$	$1.60 + 3.04\theta$	$1.58 + 2.55\theta$
	6	$3.94 + 3.35\theta$	$3.96 + 2.36\theta$	$3.02 + 1.68\theta$	$2.61 + 4.68\theta$	$2.83 + 3.95\theta$	$2.45 + 2.70\theta$	$2.20 + 5.09\theta$	$2.34 + 4.43\theta$	$2.28 + 3.26\theta$
	7	$5.57 + 3.10\theta$	$4.41 + 2.17\theta$	$3.47 + 1.52\theta$	$4.01 + 4.84\theta$	$3.74 + 4.19\theta$	$2.73 + 2.76\theta$	$3.48 + 5.39\theta$	$3.50 + 5.13\theta$	$2.56 + 3.27\theta$
	8	$6.32 + 3.01\theta$	$4.89 + 2.00\theta$	$4.12 + 1.57\theta$	$4.59 + 4.98\theta$	$4.13 + 4.09\theta$	$3.13 + 2.78\theta$	$3.98 + 5.64\theta$	$3.88 + 5.08\theta$	$2.82 + 3.33\theta$
	9	$7.18 + 2.78\theta$	$6.24 + 2.04\theta$	$4.83 + 1.42\theta$	$5.20 + 5.06\theta$	$4.58 + 3.98\theta$	$4.07 + 3.31\theta$	$4.48 + 5.83\theta$	$4.22 + 5.02\theta$	$3.74 + 4.20\theta$
	10	$8.25 + 2.56\theta$	$7.08 + 1.76\theta$	$5.38 + 1.16\theta$	$5.81 + 5.11\theta$	$5.99 + 4.76\theta$	$4.01 + 3.00\theta$	$5.03 + 5.96\theta$	$5.41 + 6.00\theta$	$4.05 + 4.05\theta$
	11	$9.25 + 2.23\theta$	$7.68 + 1.40\theta$	$6.06 + 0.95\theta$	$6.57 + 5.08\theta$	$6.51 + 4.47\theta$	$4.26 + 2.72\theta$	$5.63 + 6.04\theta$	$5.92 + 5.88\theta$	$3.35 + 2.02\theta$
	12	$10.17 + 1.84\theta$	$8.55 + 1.04\theta$	$6.90 + 0.67\theta$	$7.23 + 4.99\theta$	$7.68 + 3.72\theta$	$4.63 + 2.48\theta$	$6.18 + 6.07\theta$	$7.26 + 5.03\theta$	$4.90 + 2.79\theta$
	13	$11.92 + 1.80\theta$	$9.62 + 1.29\theta$	$7.33 + 0.92\theta$	$8.92 + 5.07\theta$	$8.75 + 4.29\theta$	$5.07 + 2.91\theta$	$7.84 + 6.21\theta$	$8.40 + 5.67\theta$	$5.54 + 3.09\theta$
	14	$13.27 + 1.35\theta$	$10.57 + 1.05\theta$	$7.96 + 0.79\theta$	$10.13 + 4.78\theta$	$9.91 + 4.02\theta$	$5.53 + 2.91\theta$	$8.90 + 6.07\theta$	$9.58 + 5.48\theta$	$6.20 + 2.94\theta$
	15	$14.75 + 0.76\theta$	$11.59 + 0.73\theta$	$8.63 + 0.61\theta$	$11.38 + 4.44\theta$	$11.10 + 3.71\theta$	$5.98 + 2.91\theta$	$10.13 + 5.75\theta$	$10.93 + 5.10\theta$	$6.95 + 2.68\theta$
	16	$16.28 + 0.11\theta$	$12.63 + 0.38\theta$	$9.30 + 0.42\theta$	$12.76 + 3.97\theta$	$12.41 + 3.28\theta$	$6.46 + 2.88\theta$	$11.39 + 5.40\theta$	$12.31 + 4.69\theta$	$7.72 + 2.41\theta$
	17	$17.97 - 0.71\theta$	$13.75 - 0.06\theta$	$10.02 + 0.19\theta$	$14.26 + 3.36\theta$	$13.82 + 2.73\theta$	$6.96 + 2.82\theta$	$12.84 + 4.85\theta$	$13.90 + 4.05\theta$	$8.59 + 2.02\theta$
	18	$19.50 - 1.36\theta$	$14.73 - 0.36\theta$	$10.62 + 0.06\theta$	$15.78 + 2.73\theta$	$15.24 + 2.16\theta$	$7.45 + 2.78\theta$	$14.27 + 4.32\theta$	$15.46 + 3.43\theta$	$9.44 + 1.65\theta$
	19	$21.16 - 2.16\theta$	$15.77 - 0.73\theta$	$11.25 - 0.10\theta$	$17.42 + 1.98\theta$	$16.76 + 1.49\theta$	$7.94 + 2.72\theta$	$15.84 + 3.64\theta$	$17.16 + 2.65\theta$	$10.36 + 1.20\theta$
	20	$22.82 - 2.96\theta$	$16.79 - 1.08\theta$	$11.86 - 0.24\theta$	$19.17 + 1.10\theta$	$18.38 + 0.70\theta$	$8.46 + 2.64\theta$	$17.40 + 2.96\theta$	$18.87 + 1.87\theta$	$11.28 + 0.76\theta$
	21	$24.93 - 4.22\theta$	$18.10 - 1.73\theta$	$12.65 - 0.56\theta$	$20.90 + 0.24\theta$	$19.97 - 0.05\theta$	$8.94 + 2.60\theta$	$19.20 + 2.04\theta$	$20.82 + 0.83\theta$	$12.33 + 0.18\theta$
	22	$26.85 - 5.29\theta$	$19.24 - 2.22\theta$	$13.31 - 0.77\theta$	$22.90 - 0.88\theta$	$21.79 - 1.05\theta$	$9.49 + 2.48\theta$	$21.14 + 0.97\theta$	$22.92 - 0.37\theta$	$13.46 - 0.48\theta$
	23	$28.42 - 6.01\theta$	$20.11 - 2.44\theta$	$13.78 - 0.78\theta$	$24.85 - 1.97\theta$	$23.56 - 2.00\theta$	$9.99 + 2.40\theta$	$23.09 - 0.11\theta$	$25.04 - 1.58\theta$	$14.59 - 1.14\theta$
	24	$30.87 - 7.62\theta$	$21.57 - 3.24\theta$	$14.62 - 1.16\theta$	$26.97 - 3.22\theta$	$25.48 - 3.10\theta$	$10.52 + 2.30\theta$	$25.17 - 1.32\theta$	$27.28 - 2.93\theta$	$15.78 - 1.87\theta$

Table A.16: Normalised Cycle Times for the CBS-3-RBP Strategy for RCS/R Systems.

		$L \cdot W \cdot H = 10000$			$L \cdot W \cdot H = 50000$			$L \cdot W \cdot H = 100000$		
	H	γ_1	γ_2	γ_3	γ_1	γ_2	γ_3	γ_1	γ_2	γ_3
CBS-3-RBP	1	$1.07 + 1.80\theta$	$1.07 + 1.80\theta$	$1.07 + 1.80\theta$	$0.87 + 2.00\theta$	$0.87 + 2.00\theta$	$0.87 + 2.00\theta$	$0.81 + 2.06\theta$	$0.81 + 2.06\theta$	$0.81 + 2.06\theta$
	2	$1.46 + 1.69\theta$	$1.27 + 1.53\theta$	$1.22 + 1.48\theta$	$1.18 + 1.97\theta$	$1.01 + 1.79\theta$	$0.96 + 1.74\theta$	$1.10 + 2.05\theta$	$0.94 + 1.87\theta$	$0.89 + 1.81\theta$
	3	$1.75 + 1.87\theta$	$1.46 + 1.32\theta$	$1.38 + 1.16\theta$	$1.35 + 2.27\theta$	$1.16 + 1.62\theta$	$1.11 + 1.44\theta$	$1.24 + 2.38\theta$	$1.07 + 1.70\theta$	$1.03 + 1.52\theta$
	4	$2.41 + 1.61\theta$	$1.73 + 1.00\theta$	$1.50 + 0.92\theta$	$1.98 + 2.04\theta$	$1.43 + 1.31\theta$	$1.21 + 1.21\theta$	$1.85 + 2.17\theta$	$1.34 + 1.40\theta$	$1.12 + 1.30\theta$
	5	$2.66 + 1.79\theta$	$1.78 + 0.95\theta$	$1.52 + 0.78\theta$	$2.03 + 2.42\theta$	$1.41 + 1.32\theta$	$1.17 + 1.13\theta$	$1.85 + 2.60\theta$	$1.30 + 1.43\theta$	$1.07 + 1.23\theta$
	6	$3.21 + 1.68\theta$	$2.00 + 0.76\theta$	$1.61 + 0.58\theta$	$2.58 + 2.31\theta$	$1.63 + 1.13\theta$	$1.29 + 0.90\theta$	$2.38 + 2.51\theta$	$1.51 + 1.24\theta$	$1.19 + 1.00\theta$
	7	$3.75 + 1.54\theta$	$2.17 + 0.66\theta$	$1.69 + 0.41\theta$	$3.05 + 2.24\theta$	$1.77 + 1.07\theta$	$1.36 + 0.74\theta$	$2.83 + 2.46\theta$	$1.64 + 1.20\theta$	$1.25 + 0.85\theta$
	8	$3.99 + 1.69\theta$	$2.27 + 0.59\theta$	$1.68 + 0.33\theta$	$3.15 + 2.52\theta$	$1.83 + 1.02\theta$	$1.34 + 0.67\theta$	$2.88 + 2.80\theta$	$1.69 + 1.16\theta$	$1.26 + 0.75\theta$
	9	$4.65 + 1.37\theta$	$2.46 + 0.44\theta$	$1.70 + 0.24\theta$	$3.77 + 2.25\theta$	$2.00 + 0.89\theta$	$1.39 + 0.58\theta$	$2.57 + 3.06\theta$	$1.85 + 1.04\theta$	$1.23 + 0.71\theta$
	10	$4.95 + 1.45\theta$	$2.61 + 0.37\theta$	$1.73 + 0.13\theta$	$3.89 + 2.52\theta$	$2.10 + 0.88\theta$	$1.32 + 0.55\theta$	$3.52 + 2.89\theta$	$1.93 + 1.06\theta$	$1.20 + 0.67\theta$
	11	$5.52 + 1.25\theta$	$2.76 + 0.25\theta$	$1.81 - 0.01\theta$	$4.43 + 2.34\theta$	$2.23 + 0.78\theta$	$1.45 + 0.36\theta$	$4.07 + 2.69\theta$	$2.06 + 0.96\theta$	$1.32 + 0.48\theta$
	12	$6.07 + 1.06\theta$	$2.95 + 0.16\theta$	$1.85 - 0.11\theta$	$4.90 + 2.22\theta$	$2.39 + 0.72\theta$	$1.48 + 0.28\theta$	$4.52 + 2.61\theta$	$2.20 + 0.91\theta$	$1.35 + 0.39\theta$
	13	$6.56 + 0.92\theta$	$3.15 + 0.05\theta$	$1.87 - 0.18\theta$	$5.32 + 2.16\theta$	$2.56 + 0.64\theta$	$1.49 + 0.21\theta$	$4.90 + 2.57\theta$	$2.36 + 0.84\theta$	$1.36 + 0.33\theta$
	14	$7.04 + 0.80\theta$	$3.33 - 0.03\theta$	$1.90 - 0.26\theta$	$5.71 + 2.12\theta$	$2.71 + 0.59\theta$	$1.52 + 0.14\theta$	$5.27 + 2.58\theta$	$2.50 + 0.80\theta$	$1.38 + 0.25\theta$
	15	$7.53 + 0.65\theta$	$3.53 - 0.13\theta$	$1.93 - 0.34\theta$	$6.11 + 2.07\theta$	$2.87 + 0.54\theta$	$1.54 + 0.06\theta$	$5.66 + 2.57\theta$	$2.64 + 0.76\theta$	$1.41 + 0.18\theta$
	16	$8.03 + 0.50\theta$	$3.74 - 0.22\theta$	$1.96 - 0.41\theta$	$6.51 + 2.02\theta$	$3.04 + 0.48\theta$	$1.57 - 0.00\theta$	$6.04 + 2.56\theta$	$2.79 + 0.73\theta$	$1.43 + 0.11\theta$
	17	$8.56 + 0.32\theta$	$3.96 - 0.32\theta$	$1.99 - 0.48\theta$	$6.92 + 1.95\theta$	$3.21 + 0.43\theta$	$1.60 - 0.07\theta$	$6.45 + 2.54\theta$	$2.95 + 0.69\theta$	$1.45 + 0.04\theta$
	18	$9.03 + 0.18\theta$	$4.18 - 0.40\theta$	$2.00 - 0.54\theta$	$7.32 + 1.89\theta$	$3.39 + 0.38\theta$	$1.62 - 0.13\theta$	$6.85 + 2.52\theta$	$3.12 + 0.65\theta$	$1.47 - 0.02\theta$
	19	$9.53 + 0.03\theta$	$4.40 - 0.49\theta$	$2.02 - 0.59\theta$	$7.74 + 1.82\theta$	$3.58 + 0.33\theta$	$1.65 - 0.19\theta$	$7.26 + 2.49\theta$	$3.29 + 0.62\theta$	$1.49 - 0.07\theta$
	20	$10.02 - 0.12\theta$	$4.63 - 0.58\theta$	$2.04 - 0.64\theta$	$8.16 + 1.74\theta$	$3.78 + 0.28\theta$	$1.67 - 0.24\theta$	$7.66 + 2.47\theta$	$3.46 + 0.59\theta$	$1.51 - 0.12\theta$
	21	$10.59 - 0.35\theta$	$4.90 - 0.70\theta$	$2.07 - 0.70\theta$	$8.57 + 1.67\theta$	$3.98 + 0.23\theta$	$1.69 - 0.28\theta$	$8.10 + 2.43\theta$	$3.65 + 0.56\theta$	$1.54 - 0.18\theta$
	22	$11.12 - 0.54\theta$	$5.16 - 0.79\theta$	$2.09 - 0.75\theta$	$9.01 + 1.57\theta$	$4.19 + 0.18\theta$	$1.71 - 0.33\theta$	$8.54 + 2.38\theta$	$3.84 + 0.53\theta$	$1.55 - 0.22\theta$
	23	$11.56 - 0.64\theta$	$5.39 - 0.85\theta$	$2.09 - 0.78\theta$	$9.43 + 1.49\theta$	$4.41 + 0.13\theta$	$1.73 - 0.37\theta$	$8.98 + 2.33\theta$	$4.04 + 0.50\theta$	$1.56 - 0.26\theta$
	24	$12.17 - 0.91\theta$	$5.70 - 0.99\theta$	$2.12 - 0.84\theta$	$9.87 + 1.39\theta$	$4.63 + 0.08\theta$	$1.74 - 0.41\theta$	$9.43 + 2.28\theta$	$4.25 + 0.47\theta$	$1.58 - 0.30\theta$

Table A.17: Normalised Cycle Times for the Depth First Strategy for RCS/R Systems.

		$L \cdot W \cdot H = 10000$			$L \cdot W \cdot H = 50000$			$L \cdot W \cdot H = 100000$		
	H	γ_1	γ_2	γ_3	γ_1	γ_2	γ_3	γ_1	γ_2	γ_3
Depth First	1	$1.34 + 1.53\theta$	$1.34 + 1.53\theta$	$1.34 + 1.53\theta$	$1.17 + 1.70\theta$	$1.17 + 1.70\theta$	$1.17 + 1.70\theta$	$1.12 + 1.75\theta$	$1.12 + 1.75\theta$	$1.12 + 1.75\theta$
	2	$1.77 + 1.62\theta$	$1.77 + 1.62\theta$	$1.77 + 1.62\theta$	$1.51 + 1.89\theta$	$1.51 + 1.89\theta$	$1.51 + 1.89\theta$	$1.43 + 1.97\theta$	$1.43 + 1.97\theta$	$1.43 + 1.97\theta$
	3	$2.20 + 1.71\theta$	$2.20 + 1.71\theta$	$2.20 + 1.71\theta$	$1.84 + 2.07\theta$	$1.84 + 2.07\theta$	$1.84 + 2.07\theta$	$1.74 + 2.17\theta$	$1.74 + 2.17\theta$	$1.74 + 2.17\theta$
	4	$2.64 + 1.79\theta$	$2.64 + 1.79\theta$	$2.64 + 1.79\theta$	$2.19 + 2.24\theta$	$2.19 + 2.24\theta$	$2.19 + 2.24\theta$	$2.05 + 2.37\theta$	$2.05 + 2.37\theta$	$2.05 + 2.37\theta$
	5	$3.15 + 1.85\theta$	$3.15 + 1.85\theta$	$3.15 + 1.85\theta$	$2.59 + 2.41\theta$	$2.59 + 2.41\theta$	$2.59 + 2.41\theta$	$2.43 + 2.57\theta$	$2.43 + 2.57\theta$	$2.43 + 2.57\theta$
	6	$3.64 + 1.89\theta$	$3.64 + 1.89\theta$	$3.64 + 1.89\theta$	$2.99 + 2.54\theta$	$2.99 + 2.54\theta$	$2.99 + 2.54\theta$	$2.79 + 2.74\theta$	$2.79 + 2.74\theta$	$2.79 + 2.74\theta$
	7	$4.13 + 1.90\theta$	$4.13 + 1.90\theta$	$4.13 + 1.90\theta$	$3.38 + 2.65\theta$	$3.38 + 2.65\theta$	$3.38 + 2.65\theta$	$3.14 + 2.89\theta$	$3.14 + 2.89\theta$	$3.14 + 2.89\theta$
	8	$4.60 + 1.91\theta$	$4.60 + 1.91\theta$	$4.60 + 1.91\theta$	$3.77 + 2.75\theta$	$3.77 + 2.75\theta$	$3.77 + 2.75\theta$	$3.50 + 3.02\theta$	$3.50 + 3.02\theta$	$3.50 + 3.02\theta$
	9	$5.14 + 1.88\theta$	$5.14 + 1.88\theta$	$5.14 + 1.88\theta$	$4.19 + 2.83\theta$	$4.19 + 2.83\theta$	$4.19 + 2.83\theta$	$3.88 + 3.14\theta$	$3.88 + 3.14\theta$	$3.88 + 3.14\theta$
	10	$5.67 + 1.83\theta$	$5.67 + 1.83\theta$	$5.67 + 1.83\theta$	$4.60 + 2.90\theta$	$4.60 + 2.90\theta$	$4.60 + 2.90\theta$	$4.26 + 3.24\theta$	$4.26 + 3.24\theta$	$4.26 + 3.24\theta$
	11	$6.18 + 1.78\theta$	$6.18 + 1.78\theta$	$6.18 + 1.78\theta$	$5.02 + 2.94\theta$	$5.02 + 2.94\theta$	$5.02 + 2.94\theta$	$4.64 + 3.32\theta$	$4.64 + 3.32\theta$	$4.64 + 3.32\theta$
	12	$6.70 + 1.72\theta$	$6.70 + 1.72\theta$	$6.70 + 1.72\theta$	$5.44 + 2.99\theta$	$5.44 + 2.99\theta$	$5.44 + 2.99\theta$	$5.01 + 3.41\theta$	$5.01 + 3.41\theta$	$5.01 + 3.41\theta$
	13	$7.23 + 1.65\theta$	$7.23 + 1.65\theta$	$7.23 + 1.65\theta$	$5.87 + 3.02\theta$	$5.87 + 3.02\theta$	$5.87 + 3.02\theta$	$5.41 + 3.47\theta$	$5.41 + 3.47\theta$	$5.41 + 3.47\theta$
	14	$7.76 + 1.58\theta$	$7.76 + 1.58\theta$	$7.76 + 1.58\theta$	$6.31 + 3.03\theta$	$6.31 + 3.03\theta$	$6.31 + 3.03\theta$	$5.80 + 3.54\theta$	$5.80 + 3.54\theta$	$5.80 + 3.54\theta$
	15	$8.30 + 1.48\theta$	$8.30 + 1.48\theta$	$8.30 + 1.48\theta$	$6.73 + 3.05\theta$	$6.73 + 3.05\theta$	$6.73 + 3.05\theta$	$6.20 + 3.58\theta$	$6.20 + 3.58\theta$	$6.20 + 3.58\theta$
	16	$8.84 + 1.38\theta$	$8.84 + 1.38\theta$	$8.84 + 1.38\theta$	$7.17 + 3.06\theta$	$7.17 + 3.06\theta$	$7.17 + 3.06\theta$	$6.59 + 3.63\theta$	$6.59 + 3.63\theta$	$6.59 + 3.63\theta$
	17	$9.43 + 1.24\theta$	$9.43 + 1.24\theta$	$9.43 + 1.24\theta$	$7.62 + 3.04\theta$	$7.62 + 3.04\theta$	$7.62 + 3.04\theta$	$7.01 + 3.65\theta$	$7.01 + 3.65\theta$	$7.01 + 3.65\theta$
	18	$9.95 + 1.15\theta$	$9.95 + 1.15\theta$	$9.95 + 1.15\theta$	$8.07 + 3.03\theta$	$8.07 + 3.03\theta$	$8.07 + 3.03\theta$	$7.41 + 3.69\theta$	$7.41 + 3.69\theta$	$7.41 + 3.69\theta$
	19	$10.48 + 1.04\theta$	$10.48 + 1.04\theta$	$10.48 + 1.04\theta$	$8.51 + 3.01\theta$	$8.51 + 3.01\theta$	$8.51 + 3.01\theta$	$7.81 + 3.71\theta$	$7.81 + 3.71\theta$	$7.81 + 3.71\theta$
	20	$11.00 + 0.95\theta$	$11.00 + 0.95\theta$	$11.00 + 0.95\theta$	$8.97 + 2.99\theta$	$8.97 + 2.99\theta$	$8.97 + 2.99\theta$	$8.20 + 3.75\theta$	$8.20 + 3.75\theta$	$8.20 + 3.75\theta$
	21	$11.63 + 0.75\theta$	$11.63 + 0.75\theta$	$11.63 + 0.75\theta$	$9.41 + 2.96\theta$	$9.41 + 2.96\theta$	$9.41 + 2.96\theta$	$8.63 + 3.75\theta$	$8.63 + 3.75\theta$	$8.63 + 3.75\theta$
	22	$12.19 + 0.60\theta$	$12.19 + 0.60\theta$	$12.19 + 0.60\theta$	$9.89 + 2.91\theta$	$9.89 + 2.91\theta$	$9.89 + 2.91\theta$	$9.05 + 3.74\theta$	$9.05 + 3.74\theta$	$9.05 + 3.74\theta$
	23	$12.66 + 0.56\theta$	$12.66 + 0.56\theta$	$12.66 + 0.56\theta$	$10.34 + 2.88\theta$	$10.34 + 2.88\theta$	$10.34 + 2.88\theta$	$9.47 + 3.75\theta$	$9.47 + 3.75\theta$	$9.47 + 3.75\theta$
	24	$13.31 + 0.32\theta$	$13.31 + 0.32\theta$	$13.31 + 0.32\theta$	$10.79 + 2.84\theta$	$10.79 + 2.84\theta$	$10.79 + 2.84\theta$	$9.88 + 3.75\theta$	$9.88 + 3.75\theta$	$9.88 + 3.75\theta$

Table A.18: Normalised Cycle Times for the Random-BBO Strategy for RCS/R Systems.

		$L \cdot W \cdot H = 10000$			$L \cdot W \cdot H = 50000$			$L \cdot W \cdot H = 100000$		
	H	γ_1	γ_2	γ_3	γ_1	γ_2	γ_3	γ_1	γ_2	γ_3
Random-BBO	1	$1.07 + 1.80\theta$	$1.07 + 1.80\theta$	$1.07 + 1.80\theta$	$0.87 + 2.00\theta$	$0.87 + 2.00\theta$	$0.87 + 2.00\theta$	$0.81 + 2.06\theta$	$0.81 + 2.06\theta$	$0.81 + 2.06\theta$
	2	$1.56 + 2.66\theta$	$1.56 + 2.66\theta$	$1.56 + 2.66\theta$	$1.13 + 3.09\theta$	$1.13 + 3.09\theta$	$1.13 + 3.09\theta$	$1.00 + 3.22\theta$	$1.00 + 3.22\theta$	$1.00 + 3.22\theta$
	3	$2.13 + 3.34\theta$	$2.13 + 3.34\theta$	$2.13 + 3.34\theta$	$1.43 + 4.03\theta$	$1.43 + 4.03\theta$	$1.43 + 4.03\theta$	$1.23 + 4.23\theta$	$1.23 + 4.23\theta$	$1.23 + 4.23\theta$
	4	$2.76 + 3.87\theta$	$2.76 + 3.87\theta$	$2.76 + 3.87\theta$	$1.78 + 4.85\theta$	$1.78 + 4.85\theta$	$1.78 + 4.85\theta$	$1.49 + 5.14\theta$	$1.49 + 5.14\theta$	$1.49 + 5.14\theta$
	5	$3.43 + 4.30\theta$	$3.43 + 4.30\theta$	$3.43 + 4.30\theta$	$2.17 + 5.56\theta$	$2.17 + 5.56\theta$	$2.17 + 5.56\theta$	$1.78 + 5.94\theta$	$1.78 + 5.94\theta$	$1.78 + 5.94\theta$
	6	$4.13 + 4.63\theta$	$4.13 + 4.63\theta$	$4.13 + 4.63\theta$	$2.57 + 6.18\theta$	$2.57 + 6.18\theta$	$2.57 + 6.18\theta$	$2.09 + 6.66\theta$	$2.09 + 6.66\theta$	$2.09 + 6.66\theta$
	7	$4.89 + 4.85\theta$	$4.89 + 4.85\theta$	$4.89 + 4.85\theta$	$3.01 + 6.74\theta$	$3.01 + 6.74\theta$	$3.01 + 6.74\theta$	$2.43 + 7.32\theta$	$2.43 + 7.32\theta$	$2.43 + 7.32\theta$
	8	$5.61 + 5.07\theta$	$5.61 + 5.07\theta$	$5.61 + 5.07\theta$	$3.47 + 7.22\theta$	$3.47 + 7.22\theta$	$3.47 + 7.22\theta$	$2.78 + 7.90\theta$	$2.78 + 7.90\theta$	$2.78 + 7.90\theta$
	9	$6.45 + 5.15\theta$	$6.45 + 5.15\theta$	$6.45 + 5.15\theta$	$3.96 + 7.63\theta$	$3.96 + 7.63\theta$	$3.96 + 7.63\theta$	$3.15 + 8.44\theta$	$3.15 + 8.44\theta$	$3.15 + 8.44\theta$
	10	$7.29 + 5.17\theta$	$7.29 + 5.17\theta$	$7.29 + 5.17\theta$	$4.44 + 8.03\theta$	$4.44 + 8.03\theta$	$4.44 + 8.03\theta$	$3.54 + 8.93\theta$	$3.54 + 8.93\theta$	$3.54 + 8.93\theta$
	11	$8.13 + 5.18\theta$	$8.13 + 5.18\theta$	$8.13 + 5.18\theta$	$4.98 + 8.33\theta$	$4.98 + 8.33\theta$	$4.98 + 8.33\theta$	$3.94 + 9.37\theta$	$3.94 + 9.37\theta$	$3.94 + 9.37\theta$
	12	$9.02 + 5.12\theta$	$9.02 + 5.12\theta$	$9.02 + 5.12\theta$	$5.51 + 8.62\theta$	$5.51 + 8.62\theta$	$5.51 + 8.62\theta$	$4.35 + 9.78\theta$	$4.35 + 9.78\theta$	$4.35 + 9.78\theta$
	13	$9.86 + 5.07\theta$	$9.86 + 5.07\theta$	$9.86 + 5.07\theta$	$6.05 + 8.88\theta$	$6.05 + 8.88\theta$	$6.05 + 8.88\theta$	$4.79 + 10.14\theta$	$4.79 + 10.14\theta$	$4.79 + 10.14\theta$
	14	$10.73 + 4.98\theta$	$10.73 + 4.98\theta$	$10.73 + 4.98\theta$	$6.63 + 9.09\theta$	$6.63 + 9.09\theta$	$6.63 + 9.09\theta$	$5.21 + 10.50\theta$	$5.21 + 10.50\theta$	$5.21 + 10.50\theta$
	15	$11.68 + 4.80\theta$	$11.68 + 4.80\theta$	$11.68 + 4.80\theta$	$7.19 + 9.29\theta$	$7.19 + 9.29\theta$	$7.19 + 9.29\theta$	$5.69 + 10.79\theta$	$5.69 + 10.79\theta$	$5.69 + 10.79\theta$
	16	$12.62 + 4.60\theta$	$12.62 + 4.60\theta$	$12.62 + 4.60\theta$	$7.79 + 9.44\theta$	$7.79 + 9.44\theta$	$7.79 + 9.44\theta$	$6.14 + 11.09\theta$	$6.14 + 11.09\theta$	$6.14 + 11.09\theta$
	17	$13.66 + 4.31\theta$	$13.66 + 4.31\theta$	$13.66 + 4.31\theta$	$8.43 + 9.54\theta$	$8.43 + 9.54\theta$	$8.43 + 9.54\theta$	$6.65 + 11.31\theta$	$6.65 + 11.31\theta$	$6.65 + 11.31\theta$
	18	$14.53 + 4.16\theta$	$14.53 + 4.16\theta$	$14.53 + 4.16\theta$	$9.04 + 9.65\theta$	$9.04 + 9.65\theta$	$9.04 + 9.65\theta$	$7.12 + 11.56\theta$	$7.12 + 11.56\theta$	$7.12 + 11.56\theta$
	19	$15.48 + 3.92\theta$	$15.48 + 3.92\theta$	$15.48 + 3.92\theta$	$9.67 + 9.73\theta$	$9.67 + 9.73\theta$	$9.67 + 9.73\theta$	$7.62 + 11.78\theta$	$7.62 + 11.78\theta$	$7.62 + 11.78\theta$
	20	$16.38 + 3.72\theta$	$16.38 + 3.72\theta$	$16.38 + 3.72\theta$	$10.33 + 9.77\theta$	$10.33 + 9.77\theta$	$10.33 + 9.77\theta$	$8.09 + 12.01\theta$	$8.09 + 12.01\theta$	$8.09 + 12.01\theta$
	21	$17.57 + 3.23\theta$	$17.57 + 3.23\theta$	$17.57 + 3.23\theta$	$10.95 + 9.85\theta$	$10.95 + 9.85\theta$	$10.95 + 9.85\theta$	$8.63 + 12.17\theta$	$8.63 + 12.17\theta$	$8.63 + 12.17\theta$
	22	$18.60 + 2.88\theta$	$18.60 + 2.88\theta$	$18.60 + 2.88\theta$	$11.66 + 9.82\theta$	$11.66 + 9.82\theta$	$11.66 + 9.82\theta$	$9.19 + 12.29\theta$	$9.19 + 12.29\theta$	$9.19 + 12.29\theta$
	23	$19.36 + 2.80\theta$	$19.36 + 2.80\theta$	$19.36 + 2.80\theta$	$12.32 + 9.84\theta$	$12.32 + 9.84\theta$	$12.32 + 9.84\theta$	$9.73 + 12.44\theta$	$9.73 + 12.44\theta$	$9.73 + 12.44\theta$
	24	$20.67 + 2.17\theta$	$20.67 + 2.17\theta$	$20.67 + 2.17\theta$	$13.02 + 9.81\theta$	$13.02 + 9.81\theta$	$13.02 + 9.81\theta$	$10.28 + 12.55\theta$	$10.28 + 12.55\theta$	$10.28 + 12.55\theta$

Table A.19: Normalised Cycle Times for the RSCS for RCS/R Systems.

RSCS H	$L \cdot W \cdot H = 10000$			$L \cdot W \cdot H = 50000$			$L \cdot W \cdot H = 100000$		
	γ_1	γ_2	γ_3	γ_1	γ_2	γ_3	γ_1	γ_2	γ_3
1	$1.34 + 1.53\theta$	$1.34 + 1.53\theta$	$1.34 + 1.53\theta$	$1.17 + 1.70\theta$	$1.17 + 1.70\theta$	$1.17 + 1.70\theta$	$1.12 + 1.75\theta$	$1.12 + 1.75\theta$	$1.12 + 1.75\theta$
2	$1.86 + 1.70\theta$	$1.86 + 1.70\theta$	$1.86 + 1.70\theta$	$1.58 + 1.98\theta$	$1.58 + 1.98\theta$	$1.58 + 1.98\theta$	$1.50 + 2.06\theta$	$1.50 + 2.06\theta$	$1.50 + 2.06\theta$
3	$2.39 + 1.82\theta$	$2.39 + 1.82\theta$	$2.39 + 1.82\theta$	$2.00 + 2.21\theta$	$2.00 + 2.21\theta$	$2.00 + 2.21\theta$	$1.89 + 2.32\theta$	$1.89 + 2.32\theta$	$1.89 + 2.32\theta$
4	$2.93 + 1.89\theta$	$2.93 + 1.89\theta$	$2.93 + 1.89\theta$	$2.43 + 2.39\theta$	$2.43 + 2.39\theta$	$2.43 + 2.39\theta$	$2.28 + 2.54\theta$	$2.28 + 2.54\theta$	$2.28 + 2.54\theta$
5	$3.48 + 1.92\theta$	$3.48 + 1.92\theta$	$3.48 + 1.92\theta$	$2.87 + 2.53\theta$	$2.87 + 2.53\theta$	$2.87 + 2.53\theta$	$2.68 + 2.72\theta$	$2.68 + 2.72\theta$	$2.68 + 2.72\theta$
6	$4.03 + 1.93\theta$	$4.03 + 1.93\theta$	$4.03 + 1.93\theta$	$3.31 + 2.65\theta$	$3.31 + 2.65\theta$	$3.31 + 2.65\theta$	$3.09 + 2.87\theta$	$3.09 + 2.87\theta$	$3.09 + 2.87\theta$
7	$4.60 + 1.89\theta$	$4.60 + 1.89\theta$	$4.60 + 1.89\theta$	$3.76 + 2.73\theta$	$3.76 + 2.73\theta$	$3.76 + 2.73\theta$	$3.50 + 2.99\theta$	$3.50 + 2.99\theta$	$3.50 + 2.99\theta$
8	$5.15 + 1.85\theta$	$5.15 + 1.85\theta$	$5.15 + 1.85\theta$	$4.22 + 2.79\theta$	$4.22 + 2.79\theta$	$4.22 + 2.79\theta$	$3.92 + 3.09\theta$	$3.92 + 3.09\theta$	$3.92 + 3.09\theta$
9	$5.75 + 1.76\theta$	$5.75 + 1.76\theta$	$5.75 + 1.76\theta$	$4.68 + 2.82\theta$	$4.68 + 2.82\theta$	$4.68 + 2.82\theta$	$4.34 + 3.17\theta$	$4.34 + 3.17\theta$	$4.34 + 3.17\theta$
10	$6.34 + 1.66\theta$	$6.34 + 1.66\theta$	$6.34 + 1.66\theta$	$5.15 + 2.85\theta$	$5.15 + 2.85\theta$	$5.15 + 2.85\theta$	$4.77 + 3.23\theta$	$4.77 + 3.23\theta$	$4.77 + 3.23\theta$
11	$6.93 + 1.54\theta$	$6.93 + 1.54\theta$	$6.93 + 1.54\theta$	$5.63 + 2.84\theta$	$5.63 + 2.84\theta$	$5.63 + 2.84\theta$	$5.20 + 3.27\theta$	$5.20 + 3.27\theta$	$5.20 + 3.27\theta$
12	$7.53 + 1.40\theta$	$7.53 + 1.40\theta$	$7.53 + 1.40\theta$	$6.11 + 2.83\theta$	$6.11 + 2.83\theta$	$6.11 + 2.83\theta$	$5.63 + 3.30\theta$	$5.63 + 3.30\theta$	$5.63 + 3.30\theta$
13	$8.12 + 1.27\theta$	$8.12 + 1.27\theta$	$8.12 + 1.27\theta$	$6.59 + 2.80\theta$	$6.59 + 2.80\theta$	$6.59 + 2.80\theta$	$6.08 + 3.32\theta$	$6.08 + 3.32\theta$	$6.08 + 3.32\theta$
14	$8.71 + 1.13\theta$	$8.71 + 1.13\theta$	$8.71 + 1.13\theta$	$7.08 + 2.76\theta$	$7.08 + 2.76\theta$	$7.08 + 2.76\theta$	$6.51 + 3.32\theta$	$6.51 + 3.32\theta$	$6.51 + 3.32\theta$
15	$9.33 + 0.95\theta$	$9.33 + 0.95\theta$	$9.33 + 0.95\theta$	$7.57 + 2.71\theta$	$7.57 + 2.71\theta$	$7.57 + 2.71\theta$	$6.97 + 3.31\theta$	$6.97 + 3.31\theta$	$6.97 + 3.31\theta$
16	$9.95 + 0.76\theta$	$9.95 + 0.76\theta$	$9.95 + 0.76\theta$	$8.06 + 2.65\theta$	$8.06 + 2.65\theta$	$8.06 + 2.65\theta$	$7.42 + 3.29\theta$	$7.42 + 3.29\theta$	$7.42 + 3.29\theta$
17	$10.60 + 0.54\theta$	$10.60 + 0.54\theta$	$10.60 + 0.54\theta$	$8.57 + 2.56\theta$	$8.57 + 2.56\theta$	$8.57 + 2.56\theta$	$7.88 + 3.25\theta$	$7.88 + 3.25\theta$	$7.88 + 3.25\theta$
18	$11.18 + 0.37\theta$	$11.18 + 0.37\theta$	$11.18 + 0.37\theta$	$9.07 + 2.48\theta$	$9.07 + 2.48\theta$	$9.07 + 2.48\theta$	$8.33 + 3.22\theta$	$8.33 + 3.22\theta$	$8.33 + 3.22\theta$
19	$11.79 + 0.18\theta$	$11.79 + 0.18\theta$	$11.79 + 0.18\theta$	$9.58 + 2.39\theta$	$9.58 + 2.39\theta$	$9.58 + 2.39\theta$	$8.79 + 3.18\theta$	$8.79 + 3.18\theta$	$8.79 + 3.18\theta$
20	$12.39 - 0.01\theta$	$12.39 - 0.01\theta$	$12.39 - 0.01\theta$	$10.10 + 2.28\theta$	$10.10 + 2.28\theta$	$10.10 + 2.28\theta$	$9.24 + 3.14\theta$	$9.24 + 3.14\theta$	$9.24 + 3.14\theta$
21	$13.09 - 0.30\theta$	$13.09 - 0.30\theta$	$13.09 - 0.30\theta$	$10.60 + 2.19\theta$	$10.60 + 2.19\theta$	$10.60 + 2.19\theta$	$9.71 + 3.08\theta$	$9.71 + 3.08\theta$	$9.71 + 3.08\theta$
22	$13.73 - 0.53\theta$	$13.73 - 0.53\theta$	$13.73 - 0.53\theta$	$11.13 + 2.06\theta$	$11.13 + 2.06\theta$	$11.13 + 2.06\theta$	$10.20 + 3.00\theta$	$10.20 + 3.00\theta$	$10.20 + 3.00\theta$
23	$14.26 - 0.67\theta$	$14.26 - 0.67\theta$	$14.26 - 0.67\theta$	$11.64 + 1.95\theta$	$11.64 + 1.95\theta$	$11.64 + 1.95\theta$	$10.67 + 2.93\theta$	$10.67 + 2.93\theta$	$10.67 + 2.93\theta$
24	$15.00 - 1.01\theta$	$15.00 - 1.01\theta$	$15.00 - 1.01\theta$	$12.17 + 1.82\theta$	$12.17 + 1.82\theta$	$12.17 + 1.82\theta$	$11.14 + 2.85\theta$	$11.14 + 2.85\theta$	$11.14 + 2.85\theta$

Table A.20: Normalised Cycle Times for the RSCS-NN for RCS/R Systems.

		$L \cdot W \cdot H = 10000$			$L \cdot W \cdot H = 50000$			$L \cdot W \cdot H = 100000$		
	H	γ_1	γ_2	γ_3	γ_1	γ_2	γ_3	γ_1	γ_2	γ_3
RSCS-NN	1	$1.07 + 1.80\theta$	$1.07 + 1.80\theta$	$1.07 + 1.80\theta$	$0.87 + 2.00\theta$	$0.87 + 2.00\theta$	$0.87 + 2.00\theta$	$0.81 + 2.06\theta$	$0.81 + 2.06\theta$	$0.81 + 2.06\theta$
	2	$1.40 + 2.17\theta$	$1.40 + 2.17\theta$	$1.40 + 2.17\theta$	$1.04 + 2.52\theta$	$1.04 + 2.52\theta$	$1.04 + 2.52\theta$	$0.94 + 2.62\theta$	$0.94 + 2.62\theta$	$0.94 + 2.62\theta$
	3	$1.75 + 2.46\theta$	$1.75 + 2.46\theta$	$1.75 + 2.46\theta$	$1.24 + 2.97\theta$	$1.24 + 2.97\theta$	$1.24 + 2.97\theta$	$1.09 + 3.12\theta$	$1.09 + 3.12\theta$	$1.09 + 3.12\theta$
	4	$2.14 + 2.68\theta$	$2.14 + 2.68\theta$	$2.14 + 2.68\theta$	$1.45 + 3.37\theta$	$1.45 + 3.37\theta$	$1.45 + 3.37\theta$	$1.25 + 3.57\theta$	$1.25 + 3.57\theta$	$1.25 + 3.57\theta$
	5	$2.54 + 2.87\theta$	$2.54 + 2.87\theta$	$2.54 + 2.87\theta$	$1.68 + 3.72\theta$	$1.68 + 3.72\theta$	$1.68 + 3.72\theta$	$1.42 + 3.98\theta$	$1.42 + 3.98\theta$	$1.42 + 3.98\theta$
	6	$2.95 + 3.01\theta$	$2.95 + 3.01\theta$	$2.95 + 3.01\theta$	$1.92 + 4.03\theta$	$1.92 + 4.03\theta$	$1.92 + 4.03\theta$	$1.61 + 4.35\theta$	$1.61 + 4.35\theta$	$1.61 + 4.35\theta$
	7	$3.40 + 3.09\theta$	$3.40 + 3.09\theta$	$3.40 + 3.09\theta$	$2.18 + 4.31\theta$	$2.18 + 4.31\theta$	$2.18 + 4.31\theta$	$1.81 + 4.69\theta$	$1.81 + 4.69\theta$	$1.81 + 4.69\theta$
	8	$3.82 + 3.19\theta$	$3.82 + 3.19\theta$	$3.82 + 3.19\theta$	$2.45 + 4.55\theta$	$2.45 + 4.55\theta$	$2.45 + 4.55\theta$	$2.02 + 4.99\theta$	$2.02 + 4.99\theta$	$2.02 + 4.99\theta$
	9	$4.31 + 3.20\theta$	$4.31 + 3.20\theta$	$4.31 + 3.20\theta$	$2.74 + 4.77\theta$	$2.74 + 4.77\theta$	$2.74 + 4.77\theta$	$2.23 + 5.28\theta$	$2.23 + 5.28\theta$	$2.23 + 5.28\theta$
	10	$4.81 + 3.19\theta$	$4.81 + 3.19\theta$	$4.81 + 3.19\theta$	$3.02 + 4.97\theta$	$3.02 + 4.97\theta$	$3.02 + 4.97\theta$	$2.46 + 5.54\theta$	$2.46 + 5.54\theta$	$2.46 + 5.54\theta$
	11	$5.30 + 3.17\theta$	$5.30 + 3.17\theta$	$5.30 + 3.17\theta$	$3.34 + 5.13\theta$	$3.34 + 5.13\theta$	$3.34 + 5.13\theta$	$2.70 + 5.77\theta$	$2.70 + 5.77\theta$	$2.70 + 5.77\theta$
	12	$5.81 + 3.12\theta$	$5.81 + 3.12\theta$	$5.81 + 3.12\theta$	$3.65 + 5.28\theta$	$3.65 + 5.28\theta$	$3.65 + 5.28\theta$	$2.94 + 6.00\theta$	$2.94 + 6.00\theta$	$2.94 + 6.00\theta$
	13	$6.31 + 3.09\theta$	$6.31 + 3.09\theta$	$6.31 + 3.09\theta$	$3.97 + 5.42\theta$	$3.97 + 5.42\theta$	$3.97 + 5.42\theta$	$3.19 + 6.20\theta$	$3.19 + 6.20\theta$	$3.19 + 6.20\theta$
	14	$6.81 + 3.02\theta$	$6.81 + 3.02\theta$	$6.81 + 3.02\theta$	$4.30 + 5.53\theta$	$4.30 + 5.53\theta$	$4.30 + 5.53\theta$	$3.44 + 6.40\theta$	$3.44 + 6.40\theta$	$3.44 + 6.40\theta$
	15	$7.37 + 2.91\theta$	$7.37 + 2.91\theta$	$7.37 + 2.91\theta$	$4.63 + 5.64\theta$	$4.63 + 5.64\theta$	$4.63 + 5.64\theta$	$3.72 + 6.56\theta$	$3.72 + 6.56\theta$	$3.72 + 6.56\theta$
	16	$7.92 + 2.79\theta$	$7.92 + 2.79\theta$	$7.92 + 2.79\theta$	$4.98 + 5.73\theta$	$4.98 + 5.73\theta$	$4.98 + 5.73\theta$	$3.98 + 6.73\theta$	$3.98 + 6.73\theta$	$3.98 + 6.73\theta$
	17	$8.52 + 2.62\theta$	$8.52 + 2.62\theta$	$8.52 + 2.62\theta$	$5.35 + 5.78\theta$	$5.35 + 5.78\theta$	$5.35 + 5.78\theta$	$4.28 + 6.85\theta$	$4.28 + 6.85\theta$	$4.28 + 6.85\theta$
	18	$9.02 + 2.53\theta$	$9.02 + 2.53\theta$	$9.02 + 2.53\theta$	$5.71 + 5.85\theta$	$5.71 + 5.85\theta$	$5.71 + 5.85\theta$	$4.55 + 7.00\theta$	$4.55 + 7.00\theta$	$4.55 + 7.00\theta$
	19	$9.58 + 2.39\theta$	$9.58 + 2.39\theta$	$9.58 + 2.39\theta$	$6.08 + 5.89\theta$	$6.08 + 5.89\theta$	$6.08 + 5.89\theta$	$4.84 + 7.13\theta$	$4.84 + 7.13\theta$	$4.84 + 7.13\theta$
	20	$10.11 + 2.27\theta$	$10.11 + 2.27\theta$	$10.11 + 2.27\theta$	$6.46 + 5.92\theta$	$6.46 + 5.92\theta$	$6.46 + 5.92\theta$	$5.12 + 7.27\theta$	$5.12 + 7.27\theta$	$5.12 + 7.27\theta$
	21	$10.79 + 2.00\theta$	$10.79 + 2.00\theta$	$10.79 + 2.00\theta$	$6.82 + 5.97\theta$	$6.82 + 5.97\theta$	$6.82 + 5.97\theta$	$5.43 + 7.36\theta$	$5.43 + 7.36\theta$	$5.43 + 7.36\theta$
	22	$11.39 + 1.80\theta$	$11.39 + 1.80\theta$	$11.39 + 1.80\theta$	$7.23 + 5.96\theta$	$7.23 + 5.96\theta$	$7.23 + 5.96\theta$	$5.76 + 7.44\theta$	$5.76 + 7.44\theta$	$5.76 + 7.44\theta$
	23	$11.83 + 1.76\theta$	$11.83 + 1.76\theta$	$11.83 + 1.76\theta$	$7.61 + 5.98\theta$	$7.61 + 5.98\theta$	$7.61 + 5.98\theta$	$6.07 + 7.53\theta$	$6.07 + 7.53\theta$	$6.07 + 7.53\theta$
	24	$12.58 + 1.41\theta$	$12.58 + 1.41\theta$	$12.58 + 1.41\theta$	$8.02 + 5.97\theta$	$8.02 + 5.97\theta$	$8.02 + 5.97\theta$	$6.39 + 7.60\theta$	$6.39 + 7.60\theta$	$6.39 + 7.60\theta$

Table A.21: Normalised Cycle Times for the RSLS for RCS/R Systems.

		$L \cdot W \cdot H = 10000$			$L \cdot W \cdot H = 50000$			$L \cdot W \cdot H = 100000$		
	H	γ_1	γ_2	γ_3	γ_1	γ_2	γ_3	γ_1	γ_2	γ_3
RSLS	1	$1.34 + 1.53\theta$	$1.34 + 1.53\theta$	$1.34 + 1.53\theta$	$1.17 + 1.70\theta$	$1.17 + 1.70\theta$	$1.17 + 1.70\theta$	$1.12 + 1.75\theta$	$1.12 + 1.75\theta$	$1.12 + 1.75\theta$
	2	$1.84 + 1.68\theta$	$1.84 + 1.68\theta$	$1.84 + 1.68\theta$	$1.56 + 1.96\theta$	$1.56 + 1.96\theta$	$1.56 + 1.96\theta$	$1.48 + 2.03\theta$	$1.48 + 2.03\theta$	$1.48 + 2.03\theta$
	3	$2.34 + 1.79\theta$	$2.34 + 1.79\theta$	$2.34 + 1.79\theta$	$1.96 + 2.17\theta$	$1.96 + 2.17\theta$	$1.96 + 2.17\theta$	$1.85 + 2.28\theta$	$1.85 + 2.28\theta$	$1.85 + 2.28\theta$
	4	$2.86 + 1.86\theta$	$2.86 + 1.86\theta$	$2.86 + 1.86\theta$	$2.37 + 2.35\theta$	$2.37 + 2.35\theta$	$2.37 + 2.35\theta$	$2.23 + 2.49\theta$	$2.23 + 2.49\theta$	$2.23 + 2.49\theta$
	5	$3.38 + 1.90\theta$	$3.38 + 1.90\theta$	$3.38 + 1.90\theta$	$2.79 + 2.49\theta$	$2.79 + 2.49\theta$	$2.79 + 2.49\theta$	$2.61 + 2.68\theta$	$2.61 + 2.68\theta$	$2.61 + 2.68\theta$
	6	$3.91 + 1.91\theta$	$3.91 + 1.91\theta$	$3.91 + 1.91\theta$	$3.21 + 2.61\theta$	$3.21 + 2.61\theta$	$3.21 + 2.61\theta$	$3.00 + 2.83\theta$	$3.00 + 2.83\theta$	$3.00 + 2.83\theta$
	7	$4.46 + 1.89\theta$	$4.46 + 1.89\theta$	$4.46 + 1.89\theta$	$3.64 + 2.70\theta$	$3.64 + 2.70\theta$	$3.64 + 2.70\theta$	$3.39 + 2.96\theta$	$3.39 + 2.96\theta$	$3.39 + 2.96\theta$
	8	$4.99 + 1.87\theta$	$4.99 + 1.87\theta$	$4.99 + 1.87\theta$	$4.08 + 2.77\theta$	$4.08 + 2.77\theta$	$4.08 + 2.77\theta$	$3.79 + 3.06\theta$	$3.79 + 3.06\theta$	$3.79 + 3.06\theta$
	9	$5.55 + 1.79\theta$	$5.55 + 1.79\theta$	$5.55 + 1.79\theta$	$4.53 + 2.82\theta$	$4.53 + 2.82\theta$	$4.53 + 2.82\theta$	$4.19 + 3.16\theta$	$4.19 + 3.16\theta$	$4.19 + 3.16\theta$
	10	$6.12 + 1.71\theta$	$6.12 + 1.71\theta$	$6.12 + 1.71\theta$	$4.97 + 2.86\theta$	$4.97 + 2.86\theta$	$4.97 + 2.86\theta$	$4.60 + 3.23\theta$	$4.60 + 3.23\theta$	$4.60 + 3.23\theta$
	11	$6.69 + 1.62\theta$	$6.69 + 1.62\theta$	$6.69 + 1.62\theta$	$5.43 + 2.87\theta$	$5.43 + 2.87\theta$	$5.43 + 2.87\theta$	$5.02 + 3.28\theta$	$5.02 + 3.28\theta$	$5.02 + 3.28\theta$
	12	$7.26 + 1.50\theta$	$7.26 + 1.50\theta$	$7.26 + 1.50\theta$	$5.89 + 2.87\theta$	$5.89 + 2.87\theta$	$5.89 + 2.87\theta$	$5.43 + 3.33\theta$	$5.43 + 3.33\theta$	$5.43 + 3.33\theta$
	13	$7.82 + 1.40\theta$	$7.82 + 1.40\theta$	$7.82 + 1.40\theta$	$6.35 + 2.87\theta$	$6.35 + 2.87\theta$	$6.35 + 2.87\theta$	$5.86 + 3.36\theta$	$5.86 + 3.36\theta$	$5.86 + 3.36\theta$
	14	$8.39 + 1.27\theta$	$8.39 + 1.27\theta$	$8.39 + 1.27\theta$	$6.82 + 2.85\theta$	$6.82 + 2.85\theta$	$6.82 + 2.85\theta$	$6.27 + 3.39\theta$	$6.27 + 3.39\theta$	$6.27 + 3.39\theta$
	15	$8.98 + 1.12\theta$	$8.98 + 1.12\theta$	$8.98 + 1.12\theta$	$7.29 + 2.82\theta$	$7.29 + 2.82\theta$	$7.29 + 2.82\theta$	$6.71 + 3.39\theta$	$6.71 + 3.39\theta$	$6.71 + 3.39\theta$
	16	$9.58 + 0.96\theta$	$9.58 + 0.96\theta$	$9.58 + 0.96\theta$	$7.76 + 2.78\theta$	$7.76 + 2.78\theta$	$7.76 + 2.78\theta$	$7.14 + 3.40\theta$	$7.14 + 3.40\theta$	$7.14 + 3.40\theta$
	17	$10.20 + 0.77\theta$	$10.20 + 0.77\theta$	$10.20 + 0.77\theta$	$8.25 + 2.72\theta$	$8.25 + 2.72\theta$	$8.25 + 2.72\theta$	$7.58 + 3.38\theta$	$7.58 + 3.38\theta$	$7.58 + 3.38\theta$
	18	$10.76 + 0.63\theta$	$10.76 + 0.63\theta$	$10.76 + 0.63\theta$	$8.73 + 2.66\theta$	$8.73 + 2.66\theta$	$8.73 + 2.66\theta$	$8.02 + 3.38\theta$	$8.02 + 3.38\theta$	$8.02 + 3.38\theta$
	19	$11.34 + 0.47\theta$	$11.34 + 0.47\theta$	$11.34 + 0.47\theta$	$9.21 + 2.60\theta$	$9.21 + 2.60\theta$	$9.21 + 2.60\theta$	$8.46 + 3.36\theta$	$8.46 + 3.36\theta$	$8.46 + 3.36\theta$
	20	$11.91 + 0.32\theta$	$11.91 + 0.32\theta$	$11.91 + 0.32\theta$	$9.71 + 2.52\theta$	$9.71 + 2.52\theta$	$9.71 + 2.52\theta$	$8.88 + 3.34\theta$	$8.88 + 3.34\theta$	$8.88 + 3.34\theta$
	21	$12.58 + 0.06\theta$	$12.58 + 0.06\theta$	$12.58 + 0.06\theta$	$10.18 + 2.46\theta$	$10.18 + 2.46\theta$	$10.18 + 2.46\theta$	$9.34 + 3.30\theta$	$9.34 + 3.30\theta$	$9.34 + 3.30\theta$
	22	$13.19 - 0.14\theta$	$13.19 - 0.14\theta$	$13.19 - 0.14\theta$	$10.70 + 2.35\theta$	$10.70 + 2.35\theta$	$10.70 + 2.35\theta$	$9.80 + 3.25\theta$	$9.80 + 3.25\theta$	$9.80 + 3.25\theta$
	23	$13.70 - 0.24\theta$	$13.70 - 0.24\theta$	$13.70 - 0.24\theta$	$11.19 + 2.27\theta$	$11.19 + 2.27\theta$	$11.19 + 2.27\theta$	$10.25 + 3.21\theta$	$10.25 + 3.21\theta$	$10.25 + 3.21\theta$
	24	$14.41 - 0.55\theta$	$14.41 - 0.55\theta$	$14.41 - 0.55\theta$	$11.69 + 2.17\theta$	$11.69 + 2.17\theta$	$11.69 + 2.17\theta$	$10.70 + 3.16\theta$	$10.70 + 3.16\theta$	$10.70 + 3.16\theta$

Table A.22: Normalised Cycle Times for the RSLS-NN for RCS/R Systems.

		$L \cdot W \cdot H = 10000$			$L \cdot W \cdot H = 50000$			$L \cdot W \cdot H = 100000$		
	H	γ_1	γ_2	γ_3	γ_1	γ_2	γ_3	γ_1	γ_2	γ_3
RSLS-NN	1	$1.07 + 1.80\theta$	$1.07 + 1.80\theta$	$1.07 + 1.80\theta$	$0.87 + 2.00\theta$	$0.87 + 2.00\theta$	$0.87 + 2.00\theta$	$0.81 + 2.06\theta$	$0.81 + 2.06\theta$	$0.81 + 2.06\theta$
	2	$1.38 + 2.13\theta$	$1.38 + 2.13\theta$	$1.38 + 2.13\theta$	$1.04 + 2.48\theta$	$1.04 + 2.48\theta$	$1.04 + 2.48\theta$	$0.94 + 2.58\theta$	$0.94 + 2.58\theta$	$0.94 + 2.58\theta$
	3	$1.72 + 2.41\theta$	$1.72 + 2.41\theta$	$1.72 + 2.41\theta$	$1.22 + 2.91\theta$	$1.22 + 2.91\theta$	$1.22 + 2.91\theta$	$1.08 + 3.06\theta$	$1.08 + 3.06\theta$	$1.08 + 3.06\theta$
	4	$2.09 + 2.63\theta$	$2.09 + 2.63\theta$	$2.09 + 2.63\theta$	$1.43 + 3.30\theta$	$1.43 + 3.30\theta$	$1.43 + 3.30\theta$	$1.23 + 3.49\theta$	$1.23 + 3.49\theta$	$1.23 + 3.49\theta$
	5	$2.47 + 2.81\theta$	$2.47 + 2.81\theta$	$2.47 + 2.81\theta$	$1.65 + 3.64\theta$	$1.65 + 3.64\theta$	$1.65 + 3.64\theta$	$1.39 + 3.89\theta$	$1.39 + 3.89\theta$	$1.39 + 3.89\theta$
	6	$2.86 + 2.96\theta$	$2.86 + 2.96\theta$	$2.86 + 2.96\theta$	$1.88 + 3.95\theta$	$1.88 + 3.95\theta$	$1.88 + 3.95\theta$	$1.57 + 4.25\theta$	$1.57 + 4.25\theta$	$1.57 + 4.25\theta$
	7	$3.29 + 3.06\theta$	$3.29 + 3.06\theta$	$3.29 + 3.06\theta$	$2.12 + 4.23\theta$	$2.12 + 4.23\theta$	$2.12 + 4.23\theta$	$1.76 + 4.59\theta$	$1.76 + 4.59\theta$	$1.76 + 4.59\theta$
	8	$3.69 + 3.17\theta$	$3.69 + 3.17\theta$	$3.69 + 3.17\theta$	$2.38 + 4.48\theta$	$2.38 + 4.48\theta$	$2.38 + 4.48\theta$	$1.96 + 4.90\theta$	$1.96 + 4.90\theta$	$1.96 + 4.90\theta$
	9	$4.15 + 3.20\theta$	$4.15 + 3.20\theta$	$4.15 + 3.20\theta$	$2.65 + 4.70\theta$	$2.65 + 4.70\theta$	$2.65 + 4.70\theta$	$2.16 + 5.19\theta$	$2.16 + 5.19\theta$	$2.16 + 5.19\theta$
	10	$4.62 + 3.21\theta$	$4.62 + 3.21\theta$	$4.62 + 3.21\theta$	$2.91 + 4.92\theta$	$2.91 + 4.92\theta$	$2.91 + 4.92\theta$	$2.38 + 5.45\theta$	$2.38 + 5.45\theta$	$2.38 + 5.45\theta$
	11	$5.08 + 3.22\theta$	$5.08 + 3.22\theta$	$5.08 + 3.22\theta$	$3.21 + 5.09\theta$	$3.21 + 5.09\theta$	$3.21 + 5.09\theta$	$2.60 + 5.70\theta$	$2.60 + 5.70\theta$	$2.60 + 5.70\theta$
	12	$5.56 + 3.20\theta$	$5.56 + 3.20\theta$	$5.56 + 3.20\theta$	$3.51 + 5.26\theta$	$3.51 + 5.26\theta$	$3.51 + 5.26\theta$	$2.83 + 5.94\theta$	$2.83 + 5.94\theta$	$2.83 + 5.94\theta$
	13	$6.03 + 3.19\theta$	$6.03 + 3.19\theta$	$6.03 + 3.19\theta$	$3.80 + 5.41\theta$	$3.80 + 5.41\theta$	$3.80 + 5.41\theta$	$3.07 + 6.15\theta$	$3.07 + 6.15\theta$	$3.07 + 6.15\theta$
	14	$6.50 + 3.16\theta$	$6.50 + 3.16\theta$	$6.50 + 3.16\theta$	$4.12 + 5.54\theta$	$4.12 + 5.54\theta$	$4.12 + 5.54\theta$	$3.30 + 6.36\theta$	$3.30 + 6.36\theta$	$3.30 + 6.36\theta$
	15	$7.02 + 3.09\theta$	$7.02 + 3.09\theta$	$7.02 + 3.09\theta$	$4.43 + 5.68\theta$	$4.43 + 5.68\theta$	$4.43 + 5.68\theta$	$3.56 + 6.54\theta$	$3.56 + 6.54\theta$	$3.56 + 6.54\theta$
	16	$7.54 + 3.00\theta$	$7.54 + 3.00\theta$	$7.54 + 3.00\theta$	$4.76 + 5.78\theta$	$4.76 + 5.78\theta$	$4.76 + 5.78\theta$	$3.81 + 6.73\theta$	$3.81 + 6.73\theta$	$3.81 + 6.73\theta$
	17	$8.10 + 2.87\theta$	$8.10 + 2.87\theta$	$8.10 + 2.87\theta$	$5.10 + 5.86\theta$	$5.10 + 5.86\theta$	$5.10 + 5.86\theta$	$4.09 + 6.88\theta$	$4.09 + 6.88\theta$	$4.09 + 6.88\theta$
	18	$8.57 + 2.82\theta$	$8.57 + 2.82\theta$	$8.57 + 2.82\theta$	$5.44 + 5.95\theta$	$5.44 + 5.95\theta$	$5.44 + 5.95\theta$	$4.35 + 7.05\theta$	$4.35 + 7.05\theta$	$4.35 + 7.05\theta$
	19	$9.09 + 2.73\theta$	$9.09 + 2.73\theta$	$9.09 + 2.73\theta$	$5.78 + 6.03\theta$	$5.78 + 6.03\theta$	$5.78 + 6.03\theta$	$4.62 + 7.19\theta$	$4.62 + 7.19\theta$	$4.62 + 7.19\theta$
	20	$9.58 + 2.65\theta$	$9.58 + 2.65\theta$	$9.58 + 2.65\theta$	$6.14 + 6.09\theta$	$6.14 + 6.09\theta$	$6.14 + 6.09\theta$	$4.87 + 7.36\theta$	$4.87 + 7.36\theta$	$4.87 + 7.36\theta$
	21	$10.22 + 2.42\theta$	$10.22 + 2.42\theta$	$10.22 + 2.42\theta$	$6.48 + 6.16\theta$	$6.48 + 6.16\theta$	$6.48 + 6.16\theta$	$5.16 + 7.48\theta$	$5.16 + 7.48\theta$	$5.16 + 7.48\theta$
	22	$10.78 + 2.27\theta$	$10.78 + 2.27\theta$	$10.78 + 2.27\theta$	$6.86 + 6.19\theta$	$6.86 + 6.19\theta$	$6.86 + 6.19\theta$	$5.47 + 7.58\theta$	$5.47 + 7.58\theta$	$5.47 + 7.58\theta$
	23	$11.18 + 2.27\theta$	$11.18 + 2.27\theta$	$11.18 + 2.27\theta$	$7.22 + 6.24\theta$	$7.22 + 6.24\theta$	$7.22 + 6.24\theta$	$5.76 + 7.70\theta$	$5.76 + 7.70\theta$	$5.76 + 7.70\theta$
	24	$11.89 + 1.97\theta$	$11.89 + 1.97\theta$	$11.89 + 1.97\theta$	$7.60 + 6.26\theta$	$7.60 + 6.26\theta$	$7.60 + 6.26\theta$	$6.06 + 7.80\theta$	$6.06 + 7.80\theta$	$6.06 + 7.80\theta$

Table A.23: Normalised Cycle Times for the Stack First Strategy for RCS/R Systems.

		$L \cdot W \cdot H = 10000$			$L \cdot W \cdot H = 50000$			$L \cdot W \cdot H = 100000$		
	H	γ_1	γ_2	γ_3	γ_1	γ_2	γ_3	γ_1	γ_2	γ_3
Stack First	1	$1.34 + 1.53\theta$	$1.34 + 1.53\theta$	$1.34 + 1.53\theta$	$1.17 + 1.70\theta$	$1.17 + 1.70\theta$	$1.17 + 1.70\theta$	$1.12 + 1.75\theta$	$1.12 + 1.75\theta$	$1.12 + 1.75\theta$
	2	$1.93 + 1.75\theta$	$1.93 + 1.75\theta$	$1.93 + 1.75\theta$	$1.64 + 2.05\theta$	$1.64 + 2.05\theta$	$1.64 + 2.05\theta$	$1.56 + 2.13\theta$	$1.56 + 2.13\theta$	$1.56 + 2.13\theta$
	3	$2.54 + 1.91\theta$	$2.54 + 1.91\theta$	$2.54 + 1.91\theta$	$2.13 + 2.32\theta$	$2.13 + 2.32\theta$	$2.13 + 2.32\theta$	$2.01 + 2.44\theta$	$2.01 + 2.44\theta$	$2.01 + 2.44\theta$
	4	$3.16 + 1.99\theta$	$3.16 + 1.99\theta$	$3.16 + 1.99\theta$	$2.62 + 2.54\theta$	$2.62 + 2.54\theta$	$2.62 + 2.54\theta$	$2.46 + 2.70\theta$	$2.46 + 2.70\theta$	$2.46 + 2.70\theta$
	5	$3.80 + 2.03\theta$	$3.80 + 2.03\theta$	$3.80 + 2.03\theta$	$3.13 + 2.70\theta$	$3.13 + 2.70\theta$	$3.13 + 2.70\theta$	$2.93 + 2.90\theta$	$2.93 + 2.90\theta$	$2.93 + 2.90\theta$
	6	$4.44 + 2.02\theta$	$4.44 + 2.02\theta$	$4.44 + 2.02\theta$	$3.65 + 2.82\theta$	$3.65 + 2.82\theta$	$3.65 + 2.82\theta$	$3.40 + 3.07\theta$	$3.40 + 3.07\theta$	$3.40 + 3.07\theta$
	7	$5.11 + 1.97\theta$	$5.11 + 1.97\theta$	$5.11 + 1.97\theta$	$4.17 + 2.90\theta$	$4.17 + 2.90\theta$	$4.17 + 2.90\theta$	$3.88 + 3.19\theta$	$3.88 + 3.19\theta$	$3.88 + 3.19\theta$
	8	$5.75 + 1.90\theta$	$5.75 + 1.90\theta$	$5.75 + 1.90\theta$	$4.71 + 2.95\theta$	$4.71 + 2.95\theta$	$4.71 + 2.95\theta$	$4.37 + 3.28\theta$	$4.37 + 3.28\theta$	$4.37 + 3.28\theta$
	9	$6.44 + 1.77\theta$	$6.44 + 1.77\theta$	$6.44 + 1.77\theta$	$5.25 + 2.96\theta$	$5.25 + 2.96\theta$	$5.25 + 2.96\theta$	$4.86 + 3.35\theta$	$4.86 + 3.35\theta$	$4.86 + 3.35\theta$
	10	$7.14 + 1.62\theta$	$7.14 + 1.62\theta$	$7.14 + 1.62\theta$	$5.79 + 2.96\theta$	$5.79 + 2.96\theta$	$5.79 + 2.96\theta$	$5.37 + 3.39\theta$	$5.37 + 3.39\theta$	$5.37 + 3.39\theta$
	11	$7.83 + 1.46\theta$	$7.83 + 1.46\theta$	$7.83 + 1.46\theta$	$6.36 + 2.92\theta$	$6.36 + 2.92\theta$	$6.36 + 2.92\theta$	$5.87 + 3.41\theta$	$5.87 + 3.41\theta$	$5.87 + 3.41\theta$
	12	$8.53 + 1.26\theta$	$8.53 + 1.26\theta$	$8.53 + 1.26\theta$	$6.92 + 2.87\theta$	$6.92 + 2.87\theta$	$6.92 + 2.87\theta$	$6.38 + 3.41\theta$	$6.38 + 3.41\theta$	$6.38 + 3.41\theta$
	13	$9.22 + 1.07\theta$	$9.22 + 1.07\theta$	$9.22 + 1.07\theta$	$7.48 + 2.81\theta$	$7.48 + 2.81\theta$	$7.48 + 2.81\theta$	$6.90 + 3.39\theta$	$6.90 + 3.39\theta$	$6.90 + 3.39\theta$
	14	$9.92 + 0.85\theta$	$9.92 + 0.85\theta$	$9.92 + 0.85\theta$	$8.06 + 2.71\theta$	$8.06 + 2.71\theta$	$8.06 + 2.71\theta$	$7.41 + 3.36\theta$	$7.41 + 3.36\theta$	$7.41 + 3.36\theta$
	15	$10.64 + 0.60\theta$	$10.64 + 0.60\theta$	$10.64 + 0.60\theta$	$8.63 + 2.62\theta$	$8.63 + 2.62\theta$	$8.63 + 2.62\theta$	$7.95 + 3.30\theta$	$7.95 + 3.30\theta$	$7.95 + 3.30\theta$
	16	$11.37 + 0.34\theta$	$11.37 + 0.34\theta$	$11.37 + 0.34\theta$	$9.21 + 2.50\theta$	$9.21 + 2.50\theta$	$9.21 + 2.50\theta$	$8.47 + 3.24\theta$	$8.47 + 3.24\theta$	$8.47 + 3.24\theta$
	17	$12.13 + 0.04\theta$	$12.13 + 0.04\theta$	$12.13 + 0.04\theta$	$9.81 + 2.35\theta$	$9.81 + 2.35\theta$	$9.81 + 2.35\theta$	$9.02 + 3.14\theta$	$9.02 + 3.14\theta$	$9.02 + 3.14\theta$
	18	$12.82 - 0.20\theta$	$12.82 - 0.20\theta$	$12.82 - 0.20\theta$	$10.40 + 2.22\theta$	$10.40 + 2.22\theta$	$10.40 + 2.22\theta$	$9.55 + 3.06\theta$	$9.55 + 3.06\theta$	$9.55 + 3.06\theta$
	19	$13.53 - 0.48\theta$	$13.53 - 0.48\theta$	$13.53 - 0.48\theta$	$11.00 + 2.06\theta$	$11.00 + 2.06\theta$	$11.00 + 2.06\theta$	$10.09 + 2.97\theta$	$10.09 + 2.97\theta$	$10.09 + 2.97\theta$
	20	$14.23 - 0.74\theta$	$14.23 - 0.74\theta$	$14.23 - 0.74\theta$	$11.60 + 1.89\theta$	$11.60 + 1.89\theta$	$11.60 + 1.89\theta$	$10.62 + 2.87\theta$	$10.62 + 2.87\theta$	$10.62 + 2.87\theta$
	21	$15.05 - 1.14\theta$	$15.05 - 1.14\theta$	$15.05 - 1.14\theta$	$12.19 + 1.73\theta$	$12.19 + 1.73\theta$	$12.19 + 1.73\theta$	$11.17 + 2.75\theta$	$11.17 + 2.75\theta$	$11.17 + 2.75\theta$
	22	$15.80 - 1.46\theta$	$15.80 - 1.46\theta$	$15.80 - 1.46\theta$	$12.81 + 1.53\theta$	$12.81 + 1.53\theta$	$12.81 + 1.53\theta$	$11.74 + 2.61\theta$	$11.74 + 2.61\theta$	$11.74 + 2.61\theta$
	23	$16.43 - 1.67\theta$	$16.43 - 1.67\theta$	$16.43 - 1.67\theta$	$13.41 + 1.35\theta$	$13.41 + 1.35\theta$	$13.41 + 1.35\theta$	$12.29 + 2.47\theta$	$12.29 + 2.47\theta$	$12.29 + 2.47\theta$
	24	$17.30 - 2.12\theta$	$17.30 - 2.12\theta$	$17.30 - 2.12\theta$	$14.03 + 1.14\theta$	$14.03 + 1.14\theta$	$14.03 + 1.14\theta$	$12.85 + 2.33\theta$	$12.85 + 2.33\theta$	$12.85 + 2.33\theta$